



**TOXICOLOGICAL REVIEW**

**OF**

**TRICHLOROETHYLENE**

**CHAPTER 5**

(CAS No. 79-01-6)

**In Support of Summary Information on the  
Integrated Risk Information System (IRIS)**

*September 2011*

## 5. DOSE-RESPONSE ASSESSMENT

### 5.1. DOSE-RESPONSE ANALYSES FOR NONCANCER ENDPOINTS

Because of the large number of noncancer health effects associated with TCE exposure and the large number of studies reporting on these effects, a screening process, described below, was used to reduce the number of endpoints and studies to those that would best inform the selection of the critical effects for the inhalation RfC and oral RfD.<sup>16</sup> The screening process helped identify the more sensitive endpoints for different types of effects within each health effect domain (e.g., different target systems) and provided information on the exposure levels that could contribute to the most sensitive effects, used for the RfC and RfD, as well as to additional noncancer effects as exposure increases. These more sensitive endpoints were also used to investigate the impacts of pharmacokinetic uncertainty and variability.

The general process used to derive the RfD and RfC was as follows (see Figure 5-1):

- (1) Consider all studies described in Chapter 4 that reported adverse noncancer health effects or markers for such effects and provide quantitative dose-response data<sup>17</sup>.
- (2) Consider for each study/endpoint possible points of departure (PODs) on the basis of applied dose, with the order of preference being first a BMD<sup>18</sup> derived from empirical modeling of the dose-response data, then a NOAEL, and lastly a LOAEL.
- (3) Adjust each POD by endpoint/study-specific “uncertainty factors” (UFs), accounting for uncertainties and adjustments in the extrapolation from the study conditions to conditions of human exposure, to derive candidate RfCs (cRfCs) or RfDs (cRfDs) intended to be protective for each endpoint (individually) on the basis of applied dose.
- (4) Array the cRfCs and cRfDs across the following health effect domains: (1) neurotoxic effects; (2) systemic (body weight) and organ toxicity (kidney, liver) effects; (3) immunotoxic effects; (4) reproductive effects; and (5) developmental effects.
- (5) Select as candidate critical effects those endpoints with the lowest cRfCs or cRfDs for each species (where appropriate), within each of these effect domains, taking into account the confidence in each estimate. When there are alternative estimates available for a particular endpoint, preference is given to studies whose design characteristics (e.g., species, statistical power, exposure level(s) and duration, endpoint measures) are better suited for determining the most sensitive human health effects of chronic TCE exposure.

---

<sup>16</sup>In U.S. EPA noncancer health assessments, the RfC (RfD) is an estimate (with uncertainty spanning perhaps an order of magnitude) of a continuous inhalation (daily oral) exposure to the human population (including sensitive subgroups) that is likely to be without an appreciable risk of deleterious effects during a lifetime. It can be derived from a NOAEL, LOAEL, or benchmark concentration (dose), with uncertainty factors generally applied to reflect limitations of the data used.

<sup>17</sup>Adequate dose-response data comprise, at a minimum, one exposure group and an appropriate control group, from which one can derive a LOAEL (or a NOAEL, if evidence of the effect is available from some other comparable study).

<sup>18</sup>More precisely, it is the BMDL, i.e., the (one-sided) 95% lower confidence bound on the dose corresponding to the benchmark response for the effect that is used as the POD.

- (6) For each candidate critical effect selected in step 5, use, to the extent possible, the PBPK model developed in Section 3.5 to calculate an internal dose POD (idPOD) for plausible internal dose-metrics that were selected on the basis of what is understood about the role of different TCE metabolites in toxicity and the mode of action for toxicity. Effects within the same health effect domain were generally assumed to have the same relevant internal dose-metrics; thus, screening for the effects with the lowest cRfCs and cRfDs for each species within health effect domains on the basis of applied dose should capture the same endpoints which would have the lowest candidate reference values on the basis of an appropriate dose-metric.
- (7) For each idPOD for each candidate critical effect, use the PBPK model to estimate interspecies and within-human pharmacokinetic variability (or just within-human variability for human-based PODs). The results of this calculation are 99<sup>th</sup> percentile estimates of the human equivalent concentration and human equivalent dose (HEC<sub>99</sub> and HED<sub>99</sub>) for each candidate critical effect.<sup>19</sup>
- (8) Adjust each HEC<sub>99</sub> or HED<sub>99</sub> by endpoint-/study-specific UFs (which, due to the use of the PBPK model, may differ from the UFs used in step 3) to derive a PBPK model-based candidate RfCs (p-cRfC) and RfD (p-cRfD) for each candidate critical effect.
- (9) Characterize the uncertainties in the cRfCs, cRfDs, p-cRfCs, and p-cRfDs, with the inclusion of quantitative uncertainty analyses of pharmacokinetic uncertainty and variability as derived from the Bayesian population analysis using the PBPK model.
- (10) Evaluate the most sensitive cRfCs, p-cRfCs, cRfDs, and p-cRfDs, taking into account the confidence in the estimates, to arrive at an RfC and RfD for TCE. Except for candidate critical effects for which the PBPK model could not be used, the candidate reference values considered in the final selection process were those based on the most plausible internal dose-metric on the basis of the metabolism and mode-of-action considerations for each candidate critical effect.

---

<sup>19</sup>The choice of the 99<sup>th</sup> percentile is discussed in Section 5.1.3.2.

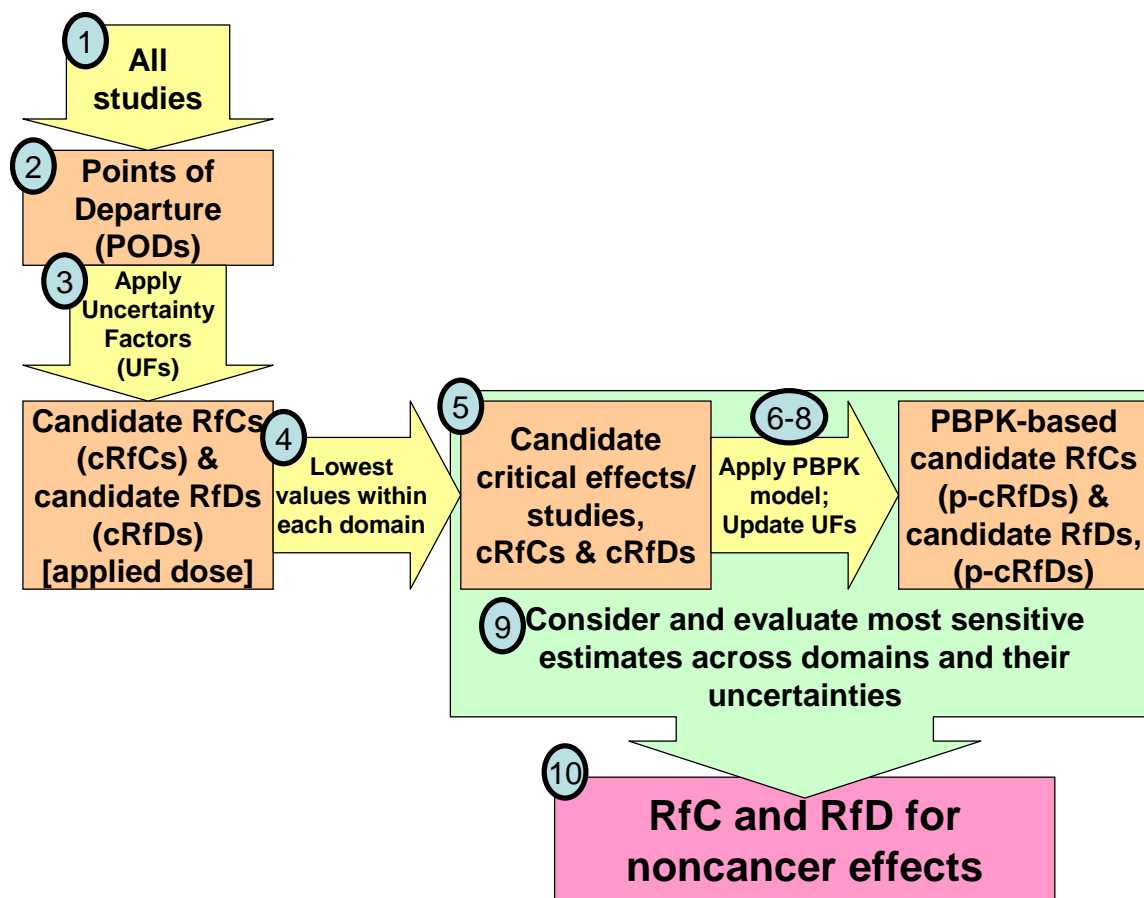


**Figure 5-1. Flow-chart of the process used to derive the RfD and RfC for noncancer effects.**

In contrast to the approach used in most previous assessments, in which the RfC and RfD are each based on a single critical effect, the final RfC and RfD for TCE were based on multiple critical effects that resulted in very similar candidate RfC and RfD values at the low end of the full range of values. This approach was taken here as it was considered to provide more robust estimates of the RfC and RfD and because it highlights the multiple effects that are yielding very similar candidate values. This approach is also consistent with recommendations from *A Review of the Reference Dose and Reference Concentration Process* (U.S. EPA, 2002b), which proposes that reference values be based on consideration of all relevant and appropriate endpoints carried through to the derivation of sample (or “candidate”) reference values. The results of this process are summarized in the sections below, with technical details presented in Appendix F.

### **5.1.1. Modeling Approaches and UFs for Developing Candidate Reference Values Based on Applied Dose**

This section summarizes the general methodology used with all of the TCE studies and endpoints for developing cRfCs and cRfDs on the basis of applied dose. A detailed discussion of

the application of these approaches to the studies and endpoints for each health effect domain follows in the next section (see Section 5.1.2).

Standard adjustments<sup>20</sup> were made to the applied doses to obtain continuous inhalation exposures and daily average oral doses over the study exposure period (see Appendix F for details), except for effects for which there was sufficient evidence that the effect was more closely associated with administered exposure level (e.g., changes in visual function). The PODs based on applied dose in the following sections and in Appendix F are presented in terms of the adjusted doses (except where noted).

As described above, wherever possible,<sup>21</sup> BMD modeling was conducted to obtain benchmark dose lower bounds (BMDLs) to serve as PODs for the cRfCs and cRfDs. Note that not all quantitative dose-response data are amenable to BMD modeling. For example, while nonnumerical data (e.g., data presented in line or bar graphs rather than in tabular form) were considered for developing LOAELs or NOAELs, they were not used for BMD modeling. In addition, sometimes, the available models used do not provide an adequate fit to the data. For the BMD modeling for this assessment, the EPA's BenchMark Dose Software (BMDS), which is freely available at [www.epa.gov/ncea/bmnds](http://www.epa.gov/ncea/bmnds), was used. For dichotomous responses, the log-logistic, multistage, and Weibull models were fitted. This subset of BMDS dichotomous models was used to reduce modeling demands, and these particular models were selected because, as a group, they have been found to be capable of describing the great majority of dose-response data sets, and specifically for some TCE data sets ([Filipsson and Victorin, 2003](#)). For continuous responses, the distinct models available in BMDS—the power, polynomial, and Hill models—were fitted. For some reproductive and developmental data sets, two nested models (the nested logistic and the Rai and Van Ryzin models in BMDS<sup>22</sup>) were fitted to examine and account for potential intralitter correlations. Models with unconstrained power parameters <1 were considered when the dose-response relationship appeared supralinear, but these models often yield very low BMDL estimates and there was no situation in which an unconstrained model with a power parameter <1 was selected for the data sets modeled here. In most cases, a constrained model or the Hill model provided an adequate fit to such a dose-response relationship. In a few cases, the highest dose group was dropped to obtain an improved fit to the lower dose groups. See Appendix F for further details on model fitting and parameter constraints.

---

<sup>20</sup>Discontinuous exposures (e.g., gavage exposures once a day, 5 days/week, or inhalation exposures for 5 days/week, 6 hours/day) were adjusted to the continuous exposure yielding the same cumulative exposure. For inhalation studies, these adjustments are equivalent to those recommended by U.S. EPA ([1994a](#)) for deriving a human equivalent concentration for a Category 3 gas for which the blood:air partition coefficient in laboratory animals is greater than that in humans (The posterior population median estimate for the TCE blood:air partition coefficient was 14 in the mouse [Table 3-37], 19 in the rat [Table 3-38], and 9.2 in the human [Table 3-39]).

<sup>21</sup>An exception was for the systemic effect of decreased body weight, which was observed in multiple chronic studies. Dose-response data were available, but the resources were not invested into modeling these data because the endpoint appeared a priori to be less sensitive than others and was not expected to be a critical effect.

<sup>22</sup>The BMDS v1.4 module for the National Center for Toxicological Research model failed with the TCE data sets.

After fitting these models to the data sets, the following procedure for model selection was applied. First, models were rejected if the  $p$ -value for goodness of fit was  $<0.10$ .<sup>23</sup> Second, models were rejected if they did not appear to adequately fit the low-dose region of the dose-response relationship, based on an examination of graphical displays of the data and scaled residuals. If the BMDL estimates from the remaining models were “sufficiently close” (with a criterion of within twofold for “sufficiently close”), then the model with the lowest Akaike’s Information Criteria (AIC) was selected.<sup>24</sup> If the BMDL estimates from the remaining models are not sufficiently close, some model dependence is assumed. With no clear biological or statistical basis to choose among them, the lowest BMDL was chosen as a reasonable conservative estimate, unless the lowest BMDL appeared to be an outlier, in which case, further judgments were made. Additionally, for continuous models, constant variance models were used for model parsimony unless the  $p$ -value for the test of homogenous variance was  $<0.10$ , in which case the modeled variance models were considered.

For BMR selection, statistical and biological considerations were taken into account. For dichotomous responses, our general approach was to use 10% extra risk as the BMR for borderline or minimally adverse effects and either 5 or 1% extra risk for adverse effects, with 1% reserved for the most severe effects. For continuous responses, the preferred approach for defining the BMR is to use a preestablished cut-point for the minimal level of change in the endpoint at which the effect is generally considered to become biologically significant (e.g., there is substantial precedence for using a 10% change in weight for organ and body weights and a 5% change in weight for fetal weight). In the absence of a well-established cut-point, a BMR of 1 (control) SD change from the control mean, or 0.5 SD for effects considered to be more serious, was generally selected. For one neurological effect (traverse time), a doubling (i.e., twofold change) was selected because the control SD appeared unusually small.

After the PODs were determined for each study/endpoint, UFs were applied to obtain the cRfCs and cRfDs. UFs are used to address differences between study conditions and conditions of human environmental exposure ([U.S. EPA, 2002b](#)). These include:

- (a) *Extrapolating from laboratory animals to humans:* If a POD is derived from experimental animal data, it is divided by an UF to reflect pharmacokinetic and pharmacodynamic differences that may make humans more sensitive than laboratory animals. For oral exposures, the standard value for the interspecies UF is 10, which breaks down (approximately) to a factor of 3 for pharmacokinetic differences (which is removed if the PBPK model is used) and a factor of 3 for pharmacodynamic

---

<sup>23</sup>In a few cases in which none of the models fit the data with  $p > 0.10$ , linear models were selected on the basis of an adequate visual fit overall.

<sup>24</sup>Akaike’s Information Criteria—a measure of information loss from a dose-response model that can be used to compare a set of models. Among a specified set of models, the model with the lowest AIC is considered the “best.” If two or more models share the lowest AIC, an average of the BMDLs could be used, but averaging was not used in this assessment because for the one occasion in which models shared the lowest AIC, a selection was made based on visual fit.

differences. For inhalation exposures, ppm equivalence across species is generally assumed or other cross-species scaling is performed, in accordance with U.S. EPA (1994a) inhalation dosimetry guidance, in which case, residual pharmacokinetic differences are considered to be negligible, and the standard value used for the interspecies UF is 3, which is ascribed to pharmacodynamic differences. These standard values were used for all of the cRfCs and cRfDs based on laboratory animal data in this assessment.

- (b) *Human (intraspecies) variability*: RfCs and RfDs apply to the human population, including sensitive subgroups, but studies rarely examine sensitive humans. Sensitive humans could be adversely affected at lower exposures than a general study population; consequently, PODs from general-population studies are divided by an UF to address sensitive humans. Similarly, the animals used in most laboratory animal studies are considered to be “typical” or “average” responders, and the human (intraspecies) variability UF is also applied to PODs from such studies to address sensitive subgroups. The standard value for the human variability UF is 10, which breaks down (approximately) to a factor of 3 for pharmacokinetic variability (which is removed if the PBPK model is used) and a factor of 3 for pharmacodynamic variability. This standard value was used for all of the PODs in this assessment with the exception of the PODs for a few immunological effects that were based on data from a sensitive (autoimmune-prone) mouse strain; for those PODs, an UF of 3 was used for human variability.
- (c) *Uncertainty in extrapolating from subchronic to chronic exposures*:<sup>25</sup> RfCs and RfDs apply to lifetime exposure, but sometimes the best (or only) available data come from less-than-lifetime studies. Lifetime exposure can induce effects that may not be apparent or as large in magnitude in a shorter study; consequently, a dose that elicits a specific level of response from a lifetime exposure may be less than the dose eliciting the same level of response from a shorter exposure period. Thus, PODs based on subchronic exposure data are generally divided by a subchronic-to-chronic UF, which has a standard value of 10. If there is evidence suggesting that exposure for longer time periods does not increase the magnitude of an effect, a lower value of 3 or one might be used. For some reproductive and developmental effects, chronic exposure is that which covers a specific window of exposure that is relevant for eliciting the effect, and subchronic exposure would correspond to an exposure that is notably less than the full window of exposure.
- (d) *Uncertainty in extrapolating from LOAELs to NOAELs*: PODs are intended to be estimates of exposure levels without appreciable risk under the study conditions so that, after the application of appropriate UFs for interspecies extrapolation, human variability, and/or duration extrapolation, the absence of appreciable risk is conveyed to the RfC or RfD exposure level to address sensitive humans with lifetime exposure. Under the NOAEL/LOAEL approach to determining a POD, however, adverse effects are sometimes observed at all study doses. If the POD is a LOAEL, then it is divided by an UF to better estimate a NOAEL. The standard value for the LOAEL-to-NOAEL UF is 10, although a value of 3 is sometimes used if the effect is considered minimally adverse at the response level observed at the LOAEL or is an

---

<sup>25</sup>Rodent studies exceeding 90 days of exposure are considered chronic, and rodent studies with 4 weeks to 90 days of exposure are considered subchronic (see [http://www.epa.gov/iris/help\\_gloss.htm](http://www.epa.gov/iris/help_gloss.htm)).

early marker for an adverse effect. For one POD in this assessment, a value of 30 was used for the LOAEL-to-NOAEL UF because the incidence rate for the adverse effect was  $\geq 90\%$  at the LOAEL.

- (e) *Additional database uncertainties*: A database UF of 1, 3, or 10 is used to reflect the potential for deriving an underprotective toxicity value as a result of an incomplete characterization of the chemical's toxicity. No database UF was used in this assessment. See Section 5.1.4.1 for additional discussion of the uncertainties associated with the overall database for TCE.

(Note that UF values of "3" actually represent  $\sqrt{10}$ , and, when 2 such values are multiplied together, the result is 10 rather than 9.)

### **5.1.2. Candidate Critical Effects by Effect Domain**

A large number of endpoints and studies were considered within each of the five health effect domains. A comprehensive list of all endpoints/studies that were considered for developing cRfCs and cRfDs is shown in Tables 5-1–5-5. These tables also summarize the PODs for the various study endpoints, the UFs applied, and the resulting cRfCs or cRfDs. Inhalation and oral studies are presented together so that the extent of the available data, as well as concordance, or lack thereof, in the responses across routes of exposure, is evident. In addition, the PBPK model developed in Section 3.5 will be applied to each candidate critical effect to develop an idPOD; and subsequent extrapolation of the idPOD to pharmacokinetically sensitive humans is performed for both inhalation and oral human exposures, regardless of the route of exposure in the original study.

The sections below discuss the cRfCs and cRfDs developed from the effects and studies identified in the hazard characterization (see Chapter 4) that were suitable for the derivation of reference values (i.e., that provided quantitative dose-response data). Because the general approach for applying UFs was discussed above, the sections below only discuss the selection of particular UFs when there are study characteristics that require additional judgment as to the appropriate UF values and possible deviations from the standard values usually assigned.

#### **5.1.2.1. Candidate Critical Neurological Effects on the Basis of Applied Dose**

As summarized in Section 4.11.1.1, both human and experimental animal studies have associated TCE exposure with effects on several neurological domains. The strongest neurological evidence of hazard is for changes in trigeminal nerve function or morphology and impairment of vestibular function. There is also evidence for effects on motor function; changes in auditory, visual, and cognitive function or performance; structural or functional changes in the brain; and neurochemical and molecular changes. Studies with numerical dose-response information are summarized in Table 5-1, with their corresponding cRfCs or cRfDs shown in Table 5-2. Because impairment of vestibular function occurs at higher exposures, such changes were not considered candidate critical effects; however, the other neurological effect domains are

represented. For trigeminal nerve effects, cRfC estimates based on two human studies are in a similar range of 0.4–0.5 ppm ([Mhiri et al., 2004](#); [Ruijten et al., 1991](#)). There remains some uncertainty as to the exposure characterization, as shown by the use of an alternative POD for Mhiri et al. (2004) based on urinary TCA resulting in a fivefold smaller cRfC. However, the overall confidence in these estimates is increased by the fact that they are based on humans exposed under chronic or nearly chronic conditions. Other human studies (e.g., [Barret et al., 1984](#)), while indicative of hazard, did not have adequate exposure information for quantitative estimates of an inhalation POD. A cRfD of 0.2 mg/kg/day was developed from the only oral study demonstrating trigeminal nerve changes, a subchronic study in rats ([Barret et al., 1992](#)). This estimate required multiple extrapolations with a composite UF of 10,000.<sup>26</sup>

For auditory effects, a high confidence cRfC of about 0.7 ppm was developed based on BMD modeling of data from Crofton and Zhao ([1997](#)); and cRfCs developed from two other auditory studies ([Albee et al., 2006](#); [Rebert et al., 1991](#)) were within about fourfold. No oral data were available for auditory effects. For psychomotor effects, the available human studies (e.g., [Rasmussen et al., 1993a](#); [Rasmussen et al., 1993b](#); [Rasmussen et al., 1993d](#)) did not have adequate exposure information for quantitative estimates of an inhalation POD. However, a relatively high confidence cRfC of 0.5 ppm was developed from a study in rats ([Waseem et al., 2001](#)). Two cRfDs within a narrow range of 0.7–1.7 mg/kg/day were developed based on two oral studies reporting psychomotor effects ([Nunes et al., 2001](#); [Moser et al., 1995](#)), although varying in degree of confidence.

---

<sup>26</sup>U.S. EPA's report on the RfC and RfD processes ([U.S. EPA, 2002b](#)) recommends not deriving reference values with a composite UF of >3,000; however, composite UFs exceeding 3,000 are considered here because the derivation of the cRfCs and cRfDs is part of a screening process and the subsequent application of the PBPK model for candidate critical effects will reduce the values of some of the individual UFs.

**Table 5-1. Summary of studies of neurological effects suitable for dose-response assessment**

Effect type Study reference	Species, strain (if applicable), sex, number used for dose-response assessment	Exposure(s) used for dose-response assessment	Endpoint(s) used for dose-response assessment	Chapter 4 Section/Table
<b>Trigeminal nerve effects</b>				<b>Section 4.3.1</b>
Mhiri et al. ( <a href="#">2004</a> )	Human phosphate industry workers (23 exposed, 23 controls)	Inhalation: Exposure ranged from 50 to 150 ppm, for 6 hrs/d for at least 2 yrs	Increased TSEP latency.	Table 4-20
Ruijten et al. ( <a href="#">1991</a> )	Human mail printing workers (31 exposed, 28 controls)	Inhalation: Mean cumulative exposure: 704 ppm × yrs; mean exposure duration: 16 yrs	Increased latency in masseter reflex.	Table 4-20
Barret et al. ( <a href="#">1992</a> )	Rat, Sprague-Dawley, female, 7/group	Oral: 0 and 2,500 mg/kg; 1 dose/d, 5 d/wk, 10 wks	Increased internode length and fiber diameter in class A fibers of the trigeminal nerve observed with TCE treatment; changes in fatty acid composition.	Table 4-21
<b>Auditory effects</b>				<b>Section 4.3.2</b>
Rebert et al. ( <a href="#">1991</a> )	Rat, Long-Evans, male, 10/group	Inhalation: 0, 1,600, and 3,200 ppm; 12 hrs/d, 12 wks	Significant decreases in BAER amplitude and an increase in latency of appearance of the initial peak (P1).	Table 4-23
Albee et al. ( <a href="#">2006</a> )	Rat, F344, male and female, 10/sex/group	Inhalation: 0, 250, 800, and 2,500 ppm; 6 hrs/d, 5 d/wk, 13 wks	Mild frequency specific hearing deficits; focal loss of cochlear hair cells.	Table 4-23
Crofton and Zhao ( <a href="#">1997</a> )	Rat, Long-Evans, male, 8–10/group	Inhalation: 0, 800, 1,600, 2,400, and 3,200 ppm; 6 hrs/d, 5 d/wk, 13 wks	Increased auditory thresholds as measured by BAERs for the 16 kHz tone.	Table 4-23

**Table. 5-1 Summary of studies of neurological effects suitable for dose-response assessment (continued)**

<b>Effect type</b> Study reference	<b>Species, strain (if applicable), sex, number used for dose-response assessment</b>	<b>Exposure(s) used for dose-response assessment</b>	<b>Endpoint(s) used for dose-response assessment</b>	<b>Chapter 4 Section/Table</b>
<b>Psychomotor effects</b>				<b>Section 4.3.6</b>
Waseem et al. ( <a href="#">2001</a> )	Rat, Wistar, male, 8/group	Inhalation: 0 and 376 ppm for up to 180 d; 4 hrs/d, 5 d/wk	Changes in locomotor activity.	Table 4-31
Nunes et al. ( <a href="#">2001</a> )	Rat, Sprague-Dawley, male, 10/group	Oral: 0 and 2,000 mg/kg/d; 7 d	Increased foot splay.	Table 4-30
Moser et al. ( <a href="#">1995</a> )	Rat, F344, female, 8/dose	Oral: 0, 150, 500, 1,500, and 5,000 mg/kg, 1 dose	Neuro-muscular impairment.	Table 4-30
		0, 50, 150, 500, and 1,500 mg/kg/d, 14 d	Increased rearing activity.	Table 4-30
<b>Visual function effects</b>				<b>Section 4.3.4</b>
Blain et al. ( <a href="#">1994</a> )	Rabbit, New Zealand albino, male, 6–8/group	Inhalation: 0, 350, 700 ppm; 4 hrs/d, 4 d/wk, 12 wks	Weekly ERGs and OPs.	Table 4-26
<b>Cognitive effects</b>				<b>Sections 4.3.5 and 4.3.6</b>
Kulig et al. ( <a href="#">1987</a> )	Rat, Wistar, male, 8/dose	Inhalation: 0, 500, 1,000, and 1,500 ppm; 16 hrs/d, 5 d/wk, 18 wks	Increased time in two-choice visual discrimination test.	Table 4-31
Isaacson et al. ( <a href="#">1990</a> )	Rat, Sprague-Dawley, male weanlings, 12/dose	Oral: (1) 0 mg/kg/d, 8 wks (2) 47 mg/kg/d, 4 wks + 0 mg/kg/d, 4 wks (3) 47 mg/kg/d, 4 wks + 0 mg/kg/d, 2 wks + 24 mg/kg/d, 2 wks	Demyelination of hippocampus	Table 4-28
<b>Mood and sleep disorders</b>				<b>Section 4.3.7</b>
Albee et al. ( <a href="#">2006</a> )	Rat, F344, male and female, 10/sex/group	Inhalation: 0, 250, 800, and 2,500 ppm; 6 hrs/d, 5 d/wk, 13 wks	Increased handling reactivity.	Table 4-33

**Table. 5-1 Summary of studies of neurological effects suitable for dose-response assessment (continued)**

Effect type Study reference	Species, strain (if applicable), sex, number used for dose-response assessment	Exposure(s) used for dose-response assessment	Endpoint(s) used for dose-response assessment	Chapter 4 Section/Table
Arito et al. ( <a href="#">1994</a> )	Rat, Wistar, male, 5/group	Inhalation: 0, 50, 100, and 300 ppm; 8 hrs/d, 5 d/wk, for 6 wks	Significant decreases in wakefulness.	Table 4-33
<b>Other neurological effects</b>				<b>Section 4.3.9</b>
Kjellstrand et al. ( <a href="#">1987</a> )	Rat, Sprague-Dawley, female	0 and 300 ppm, 24 hrs/d, 24 d	Sciatic nerve regeneration was inhibited.	Table 4-36
	Mouse, NMRI, male	0, 150, or 300 ppm, 24 hrs/d, 24 d	Sciatic nerve regeneration was inhibited.	Table 4-36
Gash et al. ( <a href="#">2008</a> )	Rat, F344, male, 9/group	Oral: 0 and 1,000 mg/kg; 5 d/wk, 6 wks	Degeneration of dopamine-containing neurons in substantia nigra.	Table 4-35

**Table 5-2. Neurological effects in studies suitable for dose-response assessment, and corresponding cRfCs and cRfDs**

Effect type Supporting studies <sup>a</sup>	Species	POD type	POD <sup>b</sup>	UF <sub>S</sub>	UF <sub>A</sub>	UF <sub>H</sub>	UF <sub>L</sub>	UF <sub>D</sub>	UF <sup>c</sup>	cRfC (ppm)	cRfD (mg/kg/d)	Effect; comments
<b>Trigeminal nerve effects</b>												
Mhiri et al. (2004)	Human	LOAEL	40	1	1	10	10	1	100	0.40		Abnormal TSEPs; preferred POD based on middle of reported range of 50–150 ppm.
	Human	LOAEL	6	1	1	10	10	1	100	0.06		Alternate POD based on U-TCA and Ikeda et al. (1972).
Ruijten et al. (1991)	Human	LOAEL	14	1	1	10	3	1	30	0.47		Trigeminal nerve effects; POD based on mean cumulative exposure and mean duration, UF <sub>L</sub> = 3 due to early marker effect and minimal degree of change.
Barret et al. (1992)	Rat	LOAEL	1,800	10	10	10	10	1	10,000 <sup>d</sup>		0.18	Morphological changes; uncertain adversity; some effects consistent with demyelination.
<b>Auditory effects</b>												
Rebert et al. (1991)	Rat	NOAEL	800	10	3	10	1	1	300	2.7		
Albee et al. (2006)	Rat	NOAEL	140	10	3	10	1	1	300	0.47		
Crofton and Zhao (1997)	Rat	BMDL	274	10	3	10	1	1	300	0.91		Preferred, due to better dose-response data, amenable to BMD modeling. BMR = 10 dB absolute change.
<b>Psychomotor effects</b>												
Waseem et al. (2001)	Rat	LOAEL	45	1	3	10	3	1		0.45		Changes in locomotor activity; transient, minimal degree of adversity; no effect reported in same study for oral exposures (210 mg/kg/d).
Nunes et al. (2001)	Rat	LOAEL	2,000	10	10	10	3	1	3,000		0.67	↑ Foot splaying; minimal adversity.

**Table 5-2. Neurological effects in studies suitable for dose-response assessment, and corresponding cRfCs and cRfDs (continued)**

Effect type Supporting studies <sup>a</sup>	Species	POD type	POD <sup>b</sup>	UF <sub>S</sub>	UF <sub>A</sub>	UF <sub>H</sub>	UF <sub>L</sub>	UF <sub>D</sub>	UF <sup>c</sup>	cRfC (ppm)	cRfD (mg/kg/d)	Effect; comments
<b>Psychomotor effects (continued)</b>												
Moser et al. (1995)	Rat	BMDL	248	3	10	10	1	1	300		0.83	↑ # rears (standing on hindlimbs); BMR = 1 SD change.
	Rat	NOAEL	500	3	10	10	1	1	300		1.7	↑ Severity score for neuromuscular changes.
<b>Visual function effects</b>												
Blain et al. (1994)	Rabbit	LOAEL	350	10	3	10	10	1	3,000	0.12		POD not adjusted to continuous exposure because visual effects more closely associated with administered exposure.
<b>Cognitive effects</b>												
Kulig et al. (1987)	Rat	NOAEL	500	1	3	10	1	1	30	17		↑ time in 2-choice visual discrimination test; test involves multiple systems but largely visual so not adjusted to continuous exposure.
Isaacson et al. (1990)	Rat	LOAEL	47	10	10	10	10	1	10,000 <sup>d</sup>		0.0047	Demyelination in hippocampus.
<b>Mood and sleep disorders</b>												
Albee et al. (2006)	Rat	NOAEL	140	10	3	10	1	1	300	0.47		Hyperactivity.
Arito et al. (1994)	Rat	LOAEL	12	3	3	10	10	1	1,000	0.012		Changes in wakefulness.
<b>Other neurological effects</b>												
Kjellstrand et al. (1987)	Rat	LOAEL	300	10	3	10	10	1	3,000	0.10		↓ regeneration of sciatic nerve.
	Mouse	LOAEL	150	10	3	10	10	1	3,000	0.050		↓ regeneration of sciatic nerve.
Gash et al. (2008)	Rat	LOAEL	710	10	10	10	10	1	10,000 <sup>d</sup>		0.071	Degeneration of dopaminergic neurons.

<sup>a</sup>Shaded studies/endpoints were selected as candidate critical effects/studies.

<sup>b</sup>Adjusted to continuous exposure unless otherwise noted. For inhalation studies, adjustments yield a POD that is a HEC as recommended for a Category 3 gas in U.S. EPA (1994a) in the absence of PBPK modeling. Same units as cRfC (ppm) or cRfD (mg/kg/day).

<sup>c</sup>Product of individual UFs.

<sup>d</sup>EPA's report on the RfC and RfD processes (U.S. EPA, 2002b) recommends not deriving reference values with a composite UF of >3,000; however, composite UFs exceeding 3,000 are considered here because the derivation of the cRfCs and cRfDs is part of a screening process and the subsequent application of the PBPK model for candidate critical effects will reduce the values of some of the individual UFs.

UF<sub>S</sub> = subchronic-to-chronic UF; UF<sub>A</sub> = interspecies UF; UF<sub>H</sub> = human variability UF; UF<sub>L</sub> = LOAEL-to-NOAEL UF; UF<sub>D</sub> = database UF

For the other neurological effects, the estimated cRfCs and cRfDs were more uncertain, as there were fewer studies available for any particular endpoint, and the PODs from several studies required more adjustment to arrive at a cRfC or cRfD. However, the endpoints in these studies also tended to be indicative of more sensitive effects and, therefore, they need to be considered. The lower cRfCs fall in the range 0.01–0.1 ppm and were based on effects on visual function in rabbits ([Blain et al., 1994](#)), wakefulness in rats ([Arito et al., 1994](#)), and regeneration of the sciatic nerve in mice and rats ([Kjellstrand et al., 1987](#)). Of these, altered wakefulness ([Arito et al., 1994](#)) has both the lowest POD and the lowest cRfC. There is relatively high confidence in this study, as it shows a clear dose-response trend, with effects persisting postexposure. For the subchronic-to-chronic UF, a value of 3 was used because, even though it was just a 6-week study, there was no evidence of a greater impact on wakefulness following 6 weeks of exposure than there was following 2 weeks of exposure at the LOAEL, although there was an effect of repeated exposure on the postexposure period impacts of higher exposure levels. The cRfDs, in the range 0.005–0.07, were based on demyelination in the hippocampus ([Isaacson et al., 1990](#)) and degeneration of dopaminergic neurons ([Gash et al., 2008](#)), both in rats. In both of these cases, adjusting for study design characteristics led to a composite uncertainty factor of 10,000,<sup>27</sup> so the confidence in these cRfDs is lower. However, no other studies of these effects are available.

In summary, although there is high confidence both in the hazard and in the cRfCs and cRfDs for trigeminal nerve, auditory, or psychomotor effects, the available data suggest that the more sensitive indicators of TCE neurotoxicity are changes in wakefulness, regeneration of the sciatic nerve, demyelination in the hippocampus, and degeneration of dopaminergic neurons. Therefore, these more sensitive effects are considered the candidate critical effects for neurotoxicity, albeit with more uncertainty in the corresponding cRfCs and cRfDs. Of these more sensitive effects, for the reasons discussed above, there is greater confidence in the changes in wakefulness reported by Arito et al. ([1994](#)). In addition, trigeminal nerve effects are considered a candidate critical effect because this is the only type of neurological effect for which human data are available, and the POD for this effect is similar to that from the most sensitive rodent study ([Arito et al., 1994](#), for changes in wakefulness). Between the two human studies of trigeminal nerve effects, Ruijten et al. ([1991](#)) is preferred for deriving noncancer reference values because its exposure characterization is considered more reliable.

#### **5.1.2.2. Candidate Critical Kidney Effects on the Basis of Applied Dose**

As summarized in Section 4.11.1.2, multiple lines of evidence support TCE nephrotoxicity in the form of tubular toxicity, mediated predominantly through the GSH

---

<sup>27</sup>U.S. EPA's report on the RfC and RfD processes ([U.S. EPA, 2002b](#)) recommends not deriving reference values with a composite UF of >3,000; however, composite UFs exceeding 3,000 are considered here because the derivation of the cRfCs and cRfDs is part of a screening process and the subsequent application of the PBPK model for candidate critical effects will reduce the values of some of the individual UFs.

conjugation product DCVC. Available human studies, while providing evidence of hazard, did not have adequate exposure information for quantitative estimates of PODs. Several studies in rodents, some of chronic duration, have shown histological changes, nephropathy, or increased kidney/body weight ratios. Studies with numerical dose-response information are summarized in Table 5-3, with their corresponding cRfCs or cRfDs shown in Table 5-4.

The cRfCs developed from three suitable inhalation studies, one reporting meganucleocytosis in rats ([Maltoni et al., 1986](#)), and two others reporting increased kidney weights in mice ([Kjellstrand et al., 1983a](#)) and rats ([Woolhiser et al., 2006](#)),<sup>28</sup> are in a narrow range of 0.5–1.3 ppm. All three utilized BMD modeling and, thus, take into account statistical limitations of the Woolhiser et al. (2006) and Kjellstrand et al. (1983a) studies, such as variability in responses or the use of low numbers of animals in the experiment. The response used for kidney weight increases was the organ weight as a percentage of body weight, to account for any commensurate decreases in body weight, although the results did not generally differ much when absolute weights were used instead. Although the two studies reporting kidney weight changes were subchronic, longer-term experiments by Kjellstrand et al. (1983a) did not report increased severity, so no subchronic-to-chronic UF was used in the derivation of the cRfC. The high response level of 73% at the lowest dose for meganucleocytosis in the chronic study of Maltoni et al. (1986) implies more uncertainty in the low-dose extrapolation. However, it is the only inhalation study that includes histopathological analysis, and it uses relatively high numbers of animals per dose group.

---

<sup>28</sup>Woolhiser et al. (2006) is an Organisation for Economic Co-operation and Development guideline immunotoxicity study performed by the Dow Chemical Company, certified by Dow as conforming to Good Laboratory Practices as published by the U.S. EPA for the Toxic Substances Control Act.

**Table 5-3. Summary of studies of kidney, liver, and body weight effects suitable for dose-response assessment**

Effect type Study reference	Species, strain (if applicable), sex, number used for dose-response assessment	Exposure(s) used for dose-response assessment	Endpoint(s) used for dose-response assessment	Chapter 4 Section/Table
<b>Histological changes in kidney</b>				<b>Section 4.4.4</b>
Maltoni et al. ( <a href="#">1986</a> )	Rat, Sprague-Dawley, M, 116–124/group	Inhalation: 0, 100, 300, and 600 ppm, 7 hrs/d, 5 d/wk, 104 wks exposure, observed for lifespan	Meganeucleocytosis	Table 4-49, Table 4-43
NTP ( <a href="#">1990</a> )	Rat, F344/N, male and female, 48–50/group	Oral: 0, 500, and 1,000 mg/kg/d, 5 d/wk, 103 wks	Cytomegaly and karyomegaly	Table 4-45, Table 4-44
NCI ( <a href="#">1976</a> )	Mouse, B6C3F <sub>1</sub> , female, 20–50/group	Oral: 0, 869, and 1,739 mg/kg/d, 5 d/wk, TWA during exposure period (78 wks), observed for 90 wks	Toxic nephrosis	Table 4-46, Table 4-44
NTP ( <a href="#">1988</a> )	Rat, Marshall, F, 44–50/group	Oral: 0, 500, and 1,000 mg/kg/d, 5 d/wk, 104 wks	Toxic nephropathy	Table 4-47, Table 4-44
<b>↑ kidney/body weight ratio</b>				<b>Section 4.4.4</b>
Kjellstrand et al. ( <a href="#">1983a</a> )	Mouse, NMRI, M, 10–20/group	Inhalation: 0 (air), 37, 75, 150, 225, 300, 450, 900, 1,800, and 3,600 ppm; continuous and intermittent exposures for 30–120 d	Increased kidney/body weight ratio	Table 4-43
Woolhiser et al. ( <a href="#">2006</a> )	Rat, Sprague-Dawley, F, 16/group	Inhalation: 0, 100, 300, and 1,000 ppm, 6 hr/d, 5 d/wk, for 4 wks	Increased kidney/body weight ratio	Table 4-43

**Table 5-3. Summary of studies of kidney, liver, and body weight effects suitable for dose-response assessment (continued)**

Effect type Study reference	Species, strain (if applicable), sex, number used for dose-response assessment	Exposure(s) used for dose-response assessment	Endpoint(s) used for dose-response assessment	Chapter 4 Section/Table
<b>↑ liver/body weight ratio</b>				<b>Section 4.5.4.1</b>
Kjellstrand et al. ( <a href="#">1983a</a> )	Mouse, NMRI, M, 10–20/group	Inhalation: 0 (air), 37, 75, 150, 225, 300, 450, 900, 1,800, and 3,600 ppm; continuous and intermittent exposures for 30–120 d	Increased liver/body weight ratio	Table 4-59
Woolhiser et al. ( <a href="#">2006</a> )	Rat, Sprague-Dawley, F, 16/group	Inhalation: 0, 100, 300, and 1,000 ppm, 6 hr/d, 5 d/wk, for 4 wks	Increased liver/body weight ratio	Table 4-59
Buben and O'Flaherty ( <a href="#">1985</a> )	Mouse, Swiss-Cox, 12–15/group	Oral: 0, 100, 200, 400, 800, 1,600, 2,400, and 3,200 mg/kg/d, 5 d/wk for 6 wks	Increased liver/body weight ratio	Table 4-58
<b>Decreased body weight</b>				
NTP ( <a href="#">1990</a> )	Mouse, B6C3F <sub>1</sub> , M, 48–50/group	Oral: 0 and 1,000 mg/kg/d, 5 d/wk, 103 wks	Decreased body weight.	NA
NCI ( <a href="#">1976</a> )	Rat, Osborne-Mendel, M and F, 20–50/group	Oral: 0, 549, and 1,097 mg/kg/d, 5 d/wk, TWA during exposure period (78 wks), observed at 110 wks	Decreased body weight.	NA

**Table 5-4. Kidney, liver, and body weight effects in studies suitable for dose-response assessment, and corresponding cRfCs and cRfDs**

Effect type Supporting studies <sup>a</sup>	Species	POD type	POD <sup>b</sup>	UF <sub>S</sub>	UF <sub>A</sub>	UF <sub>H</sub>	UF <sub>L</sub>	UF <sub>D</sub>	UF <sup>c</sup>	cRfC (ppm)	cRfD (mg/kg/d)	Effect; comments
<b>Histological changes in kidney</b>												
Maltoni ( <a href="#">1986</a> )	Rat	BMDL	40.2	1	3	10	1	1	30	1.3		meganucleocytosis; BMR = 10% extra risk
Maltoni ( <a href="#">1986</a> )	Rat	BMDL	34	1	10	10	1	1	100		0.34	meganucleocytosis; BMR = 10% extra risk
NTP ( <a href="#">1990</a> )	Rat	LOAEL	360	1	10	10	10	1	1,000		0.36	cytomegaly and karyomegaly; considered minimally adverse, but UF <sub>L</sub> = 10 due to high response rate (≥98%) at LOAEL; also in mice, but use NCI (1976) for that species
NCI ( <a href="#">1976</a> )	Mouse	LOAEL	620	1	10	10	30	1	3,000		0.21	toxic nephrosis; UF <sub>L</sub> = 30 due to >90% response at LOAEL for severe effect
NTP ( <a href="#">1988</a> )	Rat	BMDL	9.45	1	10	10	1	1	100		0.0945	toxic nephropathy; female Marshall (most sensitive sex/strain); BMR = 5% extra risk
<b>↑ kidney/body weight ratio</b>												
Kjellstrand et al. ( <a href="#">1983a</a> )	Mouse	BMDL	34.7	1	3	10	1	1	30	1.2		BMR = 10% increase; 30 d, but 120 d @ 120 ppm not more severe so UF <sub>S</sub> = 1; results are for males, which were slightly more sensitive, and yielded better fit to variance model
Woolhiser et al. ( <a href="#">2006</a> )	Rat	BMDL	15.7	1	3	10	1	1	30	0.52		BMR = 10% increase; UF <sub>S</sub> = 1 based on Kjellstrand et al. (1983a) result
<b>↑ liver/body weight ratio</b>												
Kjellstrand et al. ( <a href="#">1983a</a> )	Mouse	BMDL	21.6	1	3	10	1	1	30	0.72		BMR = 10% increase; UF <sub>S</sub> = 1 based on not more severe at 4 months
Woolhiser et al. ( <a href="#">2006</a> )	Rat	BMDL	25.2	1	3	10	1	1	30	0.84		BMR = 10% increase; UF <sub>S</sub> = 1 based on Kjellstrand et al. (1983a) result
Buben and O'Flaherty ( <a href="#">1985</a> )	Mouse	BMDL	81.5	1	10	10	1	1	100		0.82	BMR = 10% increase; UF <sub>S</sub> = 1 based on Kjellstrand et al. (1983a) result

**Table 5-4. Kidney, liver, and body weight effects in studies suitable for dose-response assessment, and corresponding cRfCs and cRfDs (continued)**

Effect type Supporting studies	Species	POD type	POD <sup>a</sup>	UF <sub>S</sub>	UF <sub>A</sub>	UF <sub>H</sub>	UF <sub>L</sub>	UF <sub>D</sub>	UF <sup>b</sup>	cRfC (ppm)	cRfD (mg/kg/d)	Effect; comments
<b>Histological changes in kidney</b>												
NTP ( <a href="#">1990</a> )	Mouse	LOAEL	710	1	10	10	10	1	1,000		0.71	
NCI ( <a href="#">1976</a> )	Rat	LOAEL	360	1	10	10	10	1	1,000		0.36	Reflects several, but not all, strains/sexes.

<sup>a</sup>Shaded studies/endpoints were selected as candidate critical effects/studies.

<sup>b</sup>Adjusted to continuous exposure unless otherwise noted. For inhalation studies, adjustments yield a POD that is a HEC as recommended for a Category 3 gas in U.S. EPA ([1994a](#)) in the absence of PBPK modeling. Same units as cRfC (ppm) or cRfD (mg/kg/day).

<sup>c</sup>Product of individual UFs.

UF<sub>S</sub> = subchronic-to-chronic UF; UF<sub>A</sub> = interspecies UF; UF<sub>H</sub> = human variability UF; UF<sub>L</sub> = LOAEL-to-NOAEL UF; UF<sub>D</sub> = database UF

The suitable oral studies give cRfDs within a narrow range of 0.09–0.4 mg/kg/day, as shown in Table 5-4, although the degree of confidence in the cRfDs varies considerably. For cRfDs based on NTP ([NTP, 1990](#)) and NCI ([NCI, 1976](#)) chronic studies in rodents, extremely high response rates of >90% precluded BMD modeling. An UF of 10 was applied for extrapolation from a LOAEL to a NOAEL in the NTP ([1990](#)) study because the effect (cytomegaly and karyomegaly), although minimally adverse, was observed at such a high incidence. An UF of 30 was applied for extrapolation from a LOAEL to a NOAEL in the NCI ([1976](#)) study because of the high incidence of a clearly adverse effect (toxic nephrosis). There is more confidence in the cRfDs based on meganucleocytosis reported in Maltoni et al. ([1986](#)) and toxic nephropathy NTP ([1988](#)), as BMD modeling was used to estimate BMDLs. Because these two oral studies measured somewhat different endpoints, but both were sensitive markers of nephrotoxic responses, they were considered to have similarly strong weight from a hazard perspective. For meganucleocytosis, a BMR of 10% extra risk was selected because the effect was considered to be minimally adverse. For toxic nephropathy, a BMR of 5% extra risk was used because toxic nephropathy is a severe toxic effect. This BMR required substantial extrapolation below the observed responses (about 60%); however, the response level seemed warranted for this type of effect and the ratio of the BMD to the BMDL was not large (1.56). Thus, from a dose-response extrapolation perspective, there is more confidence in Maltoni et al. ([1986](#)). However, the effect observed in NTP ([1988](#)) is more severe and therefore also merits consideration.

In summary, there is high confidence in the hazard and moderate confidence in the cRfCs and cRfDs for histopathological and weight changes in the kidney. These effects are considered to be candidate critical effects for several reasons. First, they appear to be the most sensitive indicators of toxicity that are available for the kidney. In addition, as discussed in Section 3.5, some pharmacokinetic data indicate substantially more production of GSH-conjugates thought to mediate TCE kidney effects in humans relative to rats and mice, although there is uncertainty in these data due to possible analytic errors. As discussed above, several studies are considered reliable for developing cRfCs and cRfDs for these endpoints. For histopathological changes, in general, the most sensitive were selected as candidate critical studies. These include the only available inhalation study ([Maltoni et al., 1986](#)), the Maltoni et al. ([1986](#)) and NTP ([1988](#)) oral studies in rats, and the NCI ([1976](#)) oral study in mice. For oral studies in rats, Maltoni et al. ([1986](#)) was considered in addition to NTP ([1988](#)), despite its having a higher cRfD, because of the much greater degree of low-dose extrapolation necessary for NTP ([1988](#)) and the excessive mortality present in that study. While the NCI ([1976](#)) study has even greater uncertainty, as discussed above, with a high response incidence at the POD that necessitates greater low-dose extrapolation, it is included to add a second species to the set of candidate critical effects. For kidney weight changes, both available studies were chosen as candidate critical studies.

### 5.1.2.3. Candidate Critical Liver Effects on the Basis of Applied Dose

As summarized in Section 4.11.1.3, while there is only limited epidemiologic evidence of TCE hepatotoxicity, TCE clearly leads to liver toxicity in laboratory animals, likely through its oxidative metabolites. Available human studies contribute to the overall weight of evidence of hazard, but did not have adequate exposure information for quantitative estimates of PODs. In rodent studies, TCE causes a wide array of hepatotoxic endpoints: increased liver weight, small transient increases in DNA synthesis, changes in ploidy, cytomegaly, increased nuclear size, and proliferation of peroxisomes. Increased liver weight (hepatomegaly, or specifically increased liver/body weight ratio) has been the most studied endpoint across a range of studies in both sexes of rats and mice, with a variety of exposure routes and durations. Hepatomegaly was selected as the critical liver effect for multiple reasons. First, it has been consistently reported in multiple studies in rats and mice following both inhalation and oral routes of exposure. In addition, it appears to accompany the other hepatic effects at the doses tested, and hence constitutes a hepatotoxicity marker of similar sensitivity to the other effects. Finally, in several studies, there are good dose-response data for BMD modeling.

As shown in Table 5-4, cRfCs for hepatomegaly developed from the two most suitable subchronic inhalation studies ([Woolhiser et al., 2006](#); [Kjellstrand et al., 1983a](#)), while in different species (rats and mice, respectively), are both based on similar PODs derived from BMD modeling, have the same composite UF of 30, and result in similar cRfC estimates of about 0.8 ppm. The cRfD for hepatomegaly developed from the oral study of Buben and O'Flaherty ([1985](#)) in mice also was based on a POD derived from BMD modeling and resulted in a cRfD estimate of 0.8 mg/kg/day. Among the studies reporting liver weight changes (reviewed in Section 4.5 and Appendix E), this study had by far the most extensive dose-response data. The response used in each case was the liver weight as a percentage of body weight, to account for any commensurate decreases in body weight, although the results did not generally differ much when absolute weights were used instead.

There is high confidence in all of these candidate reference values. BMD modeling takes into account statistical limitations such as variability in response or low numbers of animals and standardizes the response rate at the POD. Although the studies were subchronic, hepatomegaly occurs rapidly with TCE exposure, and the degree of hepatomegaly does not increase with chronic exposure ([Kjellstrand et al., 1983a](#)), so no subchronic-to-chronic UF was used.

In summary, there is high confidence both in the hazard and the cRfCs and cRfDs for hepatomegaly. Hepatomegaly also appears to be the most sensitive indicator of toxicity that is available for the liver and is therefore considered a candidate critical effect. As discussed above, several studies are considered reliable for developing cRfCs and cRfDs for this endpoint, and, since they all indicated similar sensitivity but represented different species and/or routes of exposure, they were all considered candidate critical studies.

#### **5.1.2.4. Candidate Critical Body Weight Effects on the Basis of Applied Dose**

The chronic oral bioassays, NCI (1976) and NTP (1990), reported decreased body weight with TCE exposure, as shown in Table 5-4. However, the lowest doses in these studies were quite high, even on an adjusted basis (see PODs in Table 5-4). These were not considered critical effects because they are not likely to be the most sensitive noncancer endpoints, and were not considered candidate critical effects.

#### **5.1.2.5. Candidate Critical Immunological Effects on the Basis of Applied Dose**

As summarized in Section 4.11.1.4, the human and experimental animal studies of TCE and immune-related effects provide strong evidence for a role of TCE in autoimmune disease and in a specific type of generalized hypersensitivity syndrome, while there are fewer data pertaining to immunosuppressive effects. Available human studies, while providing evidence of hazard, did not have adequate exposure information for quantitative estimates of PODs. Several studies in rodents were available on autoimmune and immunosuppressive effects that were adequate for deriving cRfCs and cRfDs. Studies with numerical dose-response information are summarized in Table 5-5, with their corresponding cRfCs or cRfDs summarized in Table 5-6.

For decreased thymus weights, a cRfD from the only suitable study (Keil et al., 2009) is 0.00035 mg/kg/day based on results from nonautoimmune-prone B6C3F<sub>1</sub> mice, with a composite UF of 1,000 for a POD that is a LOAEL (the dose-response relationship is sufficiently supralinear that attempts at BMD modeling did not result in adequate fits to these data). Thymus weights were not significantly affected in autoimmune prone mice in the same study, consistent with the results reported by Kaneko et al. (2000) in autoimmune-prone mice. In addition, Keil et al. (2009) and Peden-Adams et al. (2008) reported that for several immunotoxicity endpoints associated with TCE, the autoimmune-prone strain appeared to be less sensitive than the nonautoimmune prone B6C3F<sub>1</sub> strain. In rats, Woolhiser et al. (2006) reported no significant change in thymus weights in the Sprague-Dawley strain. These data are consistent with normal mice being sensitive to this effect as compared to autoimmune-prone mice or Sprague-Dawley rats, so the results of Keil et al. (2009) are not necessarily discordant with the other studies.

**Table 5-5. Summary of studies of immunological effects suitable for dose-response assessment**

Effect type Study reference	Species, strain (if applicable), sex, number used for dose-response assessment	Exposure(s) used for dose-response assessment	Endpoint(s) used for dose-response assessment	Chapter 4 Section/Table
↓ thymus weight				<b>Section 4.6.2.3</b>
Keil et al. ( <a href="#">2009</a> )	Mouse, B6C3F <sub>1</sub> , Female, 10/group	Oral: 0, 1,400, or 14,000 ppb TCE (0, 0.35, or 3.5 mg/kg/d), 27 wks	Decreased thymus weights; decrease in thymus cellularity	Table 4-78
<b>Autoimmunity</b>				<b>Section 4.6.2.3</b>
Kaneko et al. ( <a href="#">2000</a> )	5/group	Inhalation: 0, 500, 1,000, or 2,000 ppm TCE, 4 hrs/d, 6 d/wk, 8 wks	Liver inflammation, splenomegaly and hyperplasia of lymphatic follicles	Table 4-78
Keil et al. ( <a href="#">2009</a> )	Mouse, B6C3F <sub>1</sub> , Female, 10/group	Oral: 0, 1,400, or 14,000 ppb TCE (0, 0.35, or 3.5 mg/kg/d), 27 wks	Increased anti-dsDNA and anti-ssDNA antibodies	Table 4-78
Griffin et al. ( <a href="#">2000b</a> )	Mouse, MRL +/+, Female, 8/group	Oral: 0, 21, 100, or 400 mg/kg/d, 32 wks	Various signs of autoimmune hepatitis (serology, ex vivo assays of cultured splenocytes, clinical and histopathologic findings)	Table 4-78
Cai et al. ( <a href="#">2008</a> )	Mouse, MRL +/+, Female, 5/group	Oral: 0 or 60 mg/kg/d, 48 wks	Hepatic necrosis; hepatocyte proliferation; leukocyte infiltrate in the liver, lungs, and kidneys	Table 4-78

**Table 5-5. Summary of studies of immunological effects suitable for dose-response assessment (continued)**

Effect type Study reference	Species, strain (if applicable), sex, number used for dose-response assessment	Exposure(s) used for dose-response assessment	Endpoint(s) used for dose-response assessment	Chapter 4 Section/Table
<b>Immunosuppression</b>				<b>Section 4.6.2.1</b>
Woolhiser et al. ( <a href="#">2006</a> )	Rat, Sprague-Dawley, female, 16/group	Inhalation: 0, 100, 300, or 1,000 ppm, 6 hrs/d, 5 d/wk, 4 wks	Decreased PFC assay response	Table 4-76
Sanders et al. ( <a href="#">1982b</a> )	Mouse, CD-1, Female, 7–25/group	Oral: 0, 0.1, 1.0, 2.5, or 5.0 mg/mL (0, 18, 217, 393, or 660 mg/kg/d, from Tucker et al., 1982), 4 or 6 mo	Decreased humoral immunity, cell-mediated immunity, and bone marrow stem cell colonization	Table 4-76

**Table 5-6. Immunological effects in studies suitable for dose-response assessment, and corresponding cRfCs and cRfDs**

Effect type Supporting studies <sup>a</sup>	Species	POD type	POD <sup>b</sup>	UF <sub>S</sub>	UF <sub>A</sub>	UF <sub>H</sub>	UF <sub>L</sub>	UF <sub>D</sub>	UF <sup>c</sup>	cRfC (ppm)	cRfD (mg/kg/d)	Effect; comments
<b>↓ thymus weight</b>												
Keil et al. (2009)	Mouse	LOAEL	0.35	1	10	10	10	1	1,000		0.00035	↓ thymus weight; corresponding decrease in total thymic cellularity reported at 10 × higher dose
<b>Autoimmunity</b>												
Kaneko et al., (2000)	Mouse (MRL- lpr/lpr)	LOAEL	70	10	3	3	10	1	1,000	0.070		Changes in immunoreactive organs—liver (incl. sporadic necrosis in hepatic lobules), spleen; UF <sub>H</sub> = 3 due to autoimmune-prone mouse
Keil et al. (2009)	Mouse	LOAEL	0.35	1	10	10	3	1	300		0.0012	↑ anti-dsDNA and anti-ssDNA Abs (early markers for autoimmune disease) (B6C3F <sub>1</sub> mouse); UF <sub>L</sub> = 3 due to early marker
Griffin et al. (2000b)	Mouse (MRL+/+)	BMDL	13.4	1	10	3	1	1	30		0.45	Various signs of autoimmune hepatitis; BMR = 10% extra risk for > minimal effects
Cai et al. (2008)	Mouse (MRL+/+)	LOAEL	60	1	10	3	10	1	300		0.20	Inflammation in liver, kidney, lungs, and pancreas indicative of autoimmune disease; hepatic necrosis; UF <sub>H</sub> = 3 due to autoimmune-prone mouse
<b>Immunosuppression</b>												
Woolhiser et al. (2006)	Rat	BMDL	31.2	10	3	10	1	1	300	0.10		↓ PFC response; BMR = 1 SD change
Sanders et al. (1982b)	Mouse	NOAEL	190	1	10	10	1	1	100		1.9	↓ humoral response to SRBC; largely transient during exposure
Sanders et al. (1982b)	Mouse	LOAEL	18	1	10	10	10	1	1,000		0.018	↓ cell-mediated response to SRBC (largely transient during exposure) and ↓ stem cell bone marrow recolonization (sustained); females more sensitive; UF <sub>L</sub> = 10 since multiple immunotoxicity effects were observed

<sup>a</sup>Shaded studies/endpoints were selected as candidate critical effects/studies.

<sup>b</sup>Adjusted to continuous exposure unless otherwise noted. For inhalation studies, adjustments yield a POD that is a HEC as recommended for a Category 3 gas in U.S. EPA (1994a) in the absence of PBPK modeling. Same units as cRfC (ppm) or cRfD (mg/kg/day).

<sup>c</sup>Product of individual UFs.

UF<sub>S</sub> = subchronic-to-chronic UF; UF<sub>A</sub> = interspecies UF; UF<sub>H</sub> = human variability UF; UF<sub>L</sub> = LOAEL-to-NOAEL UF; UF<sub>D</sub> = database UF

For autoimmune effects, the cRfC from the only suitable inhalation study ([Kaneko et al., 2000](#)) is 0.07 ppm. This study reported changes in immunoreactive organs (i.e., liver and spleen) in autoimmune-prone mice. BMD modeling was not feasible, so a LOAEL was used as the POD. The standard value of 10 was used for the LOAEL-to-NOAEL UF because the inflammation was reported to include sporadic necrosis in the hepatic lobules at the LOAEL, so this was considered an adverse effect. A value of 3 was used for the human (intraspecies) variability UF because the effect was induced in autoimmune-prone mice, a sensitive mouse strain for such an effect. The cRfDs from the oral studies ([Keil et al., 2009](#); [Cai et al., 2008](#); [Griffin et al., 2000b](#)) spanned over a 100-fold range from 0.001 to 0.5 mg/kg/day. Each of the studies used different markers for autoimmune effects, which may explain the over 100-fold range of PODs (0.4–60 mg/kg/day). The most sensitive endpoint, reported by Keil et al. ([2009](#)), was increases in anti-dsDNA and anti-ssDNA antibodies in B6C3F<sub>1</sub> mice exposed to the lowest tested dose of 0.35 mg/kg/day. These markers of autoimmune responsiveness were not accompanied by evidence of inflammation or kidney disease in a similar dose- and time-dependent manner. In accordance with the interpretation of these measures as an early, subclinical or pre-clinical marker of disease, a LOAEL-to-NOAEL UF of 3 was used, and the resulting cRfD was 0.001 mg/kg/day. The results of Keil et al. ([2009](#)) are not discordant with the higher PODs and cRfDs derived from the other oral studies that examined leukocyte infiltration and tissue damage in autoimmune-prone mice ([Cai et al., 2008](#); [Griffin et al., 2000a](#)). Cai et al. ([2008](#)) noted that the autoimmune nephritis together with multi-organ involvement and an increased level of antinuclear antibodies observed in their study suggested the induction of autoimmune disease.

For immunosuppressive effects, the only suitable inhalation study ([Woolhiser et al., 2006](#)) gave a cRfC of 0.08 ppm. The cRfDs from the only suitable oral study ([Sanders et al., 1982b](#)) ranged from 0.06 to 2 mg/kg/day, based on different markers for immunosuppression. Woolhiser et al. ([2006](#)) reported decreased PFC response in rats. Data from Woolhiser et al. ([2006](#)) were amenable to BMD modeling, but there is notable uncertainty in the modeling. First, it is unclear what should constitute the cut-point for characterizing the change as minimally biologically significant, so a BMR of 1 control SD change was used. In addition, the dose-response relationship is supralinear, and the highest exposure group was dropped to improve the fit to the low-dose data points. Nonetheless, the uncertainty in the BMD modeling is no greater than the uncertainty inherent in the use of a LOAEL or NOAEL. The more sensitive endpoints reported by Sanders et al. ([1982b](#)), both of which were in female mice exposed to a LOAEL of 18 mg/kg/day TCE in drinking water for 4 months, were decreased cell-mediated response to SRBC and decreased stem cell bone recolonization, a sign of impaired bone marrow function. The cRfD based on these endpoints is 0.02 mg/kg/day, with a LOAEL-to-NOAEL UF of 10 for the multiple effects of decreased cell-mediated response to SRBC and decreased stem cell bone recolonization.

In summary, there is high qualitative confidence for TCE immunotoxicity and moderate confidence in the cRfCs and cRfDs that can be derived from the available studies. Decreased thymus weight reported at relatively low exposures in nonautoimmune-prone mice is a clear indicator of immunotoxicity ([Keil et al., 2009](#)), and is therefore considered a candidate critical effect. A number of studies have also reported changes in markers of immunotoxicity at relatively low exposures. Therefore, among markers for autoimmune effects, the more sensitive measures of autoimmune changes in liver and spleen ([Kaneko et al., 2000](#)) and increased anti-dsDNA and anti-ssDNA antibodies ([Keil et al., 2009](#)) are considered the candidate critical effects. Similarly, for markers of immunosuppression, the more sensitive measures of decreased PFC response ([Woolhiser et al., 2006](#)), decreased stem cell bone marrow recolonization, and decreased cell-mediated response to SRBC [both from Sanders et al. ([1982b](#))] are considered the candidate critical effects.

#### **5.1.2.6. Candidate Critical Respiratory Tract Effects on the Basis of Applied Dose**

As summarized in Section 4.11.1.5, available data are suggestive of TCE causing respiratory tract toxicity, based primarily on short-term studies in mice and rats. However, these studies are generally at high inhalation exposures and over durations of <2 weeks. Thus, these were not considered critical effects because such data are not necessarily indicators of longer-term effects at lower exposure and are not likely to be the most sensitive noncancer endpoints for chronic exposures. Therefore, cRfCs and cRfDs were not developed for them.

#### **5.1.2.7. Candidate Critical Reproductive Effects on the Basis of Applied Dose**

As summarized in Section 4.11.1.6, both human and experimental animal studies have associated TCE exposure with adverse reproductive effects. The strongest evidence of hazard is for effects on sperm and male reproductive outcomes, with evidence from multiple human studies and several experimental animal studies. There is also substantial evidence for effects on the male reproductive tract and male serum hormone levels, as well as evidence for effects on male reproductive behavior. There are fewer data and more limited support for effects on female reproduction. Studies with numerical dose-response information are summarized in Table 5-7, with their corresponding cRfCs or cRfDs summarized in Table 5-8.

**Table 5-7. Summary of studies of reproductive effects suitable for dose-response assessment**

Effect type Study reference	Species, strain (if applicable), sex, number used for dose-response assessment	Exposure(s) used for dose-response assessment	Endpoint(s) used for dose-response assessment	Chapter 4 Section/Table
<b>Effects on sperm, male reproductive outcomes</b>				<b>Sections 4.8.1.1–4.8.1.2</b>
Chia et al. ( <a href="#">1996</a> )	Human, 85 men (37 low exposure, 48 high exposure)	Inhalation: Mean personal air TCE: 29.6 ppm; Mean U-TCA: 22.4 mg/g creatinine	Decreased normal sperm morphology and hyperzoospermia.	Table 4-85
Land et al. ( <a href="#">1981</a> )	Mouse, C57BlxC3H (F1), M, 5 or 10/group	Inhalation: 0, 200, 2,000 ppm, 4 hrs/d, 5 d exposure, 23 d rest	Increased percent morphologically abnormal epididymal sperm.	Table 4-86
Kan et al. ( <a href="#">2007</a> )	Mouse, CD-1, male, 4/group	Inhalation: 0 or 1,000 ppm, 6 hrs/d, 5 d/wk, 4 wks	Abnormalities of the head and tail in sperm located in the epididymal lumen.	Table 4-86
Xu et al. ( <a href="#">2004</a> )	Mouse, CD-1, male, 4–27/group	Inhalation: 0 or 1,000 ppm, 6 hrs/d, 5 d/wk, 6 wks	Decreased in vitro sperm-oocyte binding and in vivo fertilization.	Table 4-86
Kumar et al. ( <a href="#">2000b</a> )	Rat, Wistar, male, 12–13/group	Inhalation: 0 or 376 ppm, 4 hrs/d, 5 d/wk, 2–10 wks exposed, 2–8 wks unexposed.	Multiple sperm effects; pre- and postimplantation losses.	Table 4-86
Kumar et al. ( <a href="#">2001b</a> )	Rat, Wistar, male, 6/group	Inhalation: 0 or 376 ppm, 4 hrs/d, 5 d/wk, 12 and 24 wks	Multiple sperm effects, increasing severity from 12 to 24 wks exposure.	Table 4-86

**Table 5-7. Summary of studies of reproductive effects suitable for dose-response assessment (continued)**

Effect type Study reference	Species, strain (if applicable), sex, number used for dose-response assessment	Exposure(s) used for dose-response assessment	Endpoint(s) used for dose-response assessment	Chapter 4 Section/Table
George et al. ( <a href="#">1985</a> )	Mouse, CD-1, male and female, 20 pairs/treatment group; 40 controls/sex	Oral: 0, 173, 362, or 737 mg/kg/d, Breeders exposed 1 wk pre mating, then for 13 wks; pregnant females exposed throughout gestation (i.e., 18 wks total)	Decreased sperm motility in F0 and F1 males.	Table 4-87
DuTeaux et al. ( <a href="#">2004a</a> )	Rat, Sprague-Dawley, male, 3/group, or Simonson albino (UC Davis), male, 3/group	Oral: 0, 143, or 270 mg/kg/d, 14 d	Decreased ability of sperm to fertilize oocytes collected from untreated females. Oxidative damage to sperm membrane in head and mid-piece.	Table 4-87
<b>Male reproductive tract effects</b>				<b>Section 4.8.1.2</b>
Forkert et al. ( <a href="#">2002</a> )	Mouse, CD-1, male, 6/group	Inhalation: 0 or 1,000 ppm, 6 hrs/d, 5 d/wk, 19 d over 4 wks	Sloughing of epididymal epithelial cells.	Table 4-86
Kan et al. ( <a href="#">2007</a> )	Mouse, CD-1, male, 4/group	Inhalation: 0 or 1,000 ppm, 6 hrs/d, 5 d/wk, 1–4 wks	Degeneration and sloughing of epididymal epithelial cells (more severe by 4 wks). Vesiculation in cytoplasm, disintegration of basolateral cell membranes, sloughing of epithelial cells.	Table 4-86
Kumar et al. ( <a href="#">2000b</a> )	Rat, Wistar, male, 12–13/group	Inhalation: 0 or 376 ppm, 4 hrs/d, 5 d/wk, 2–10 wks exposed, 2–8 wks unexposed	Smaller, necrotic spermatogenic tubules.	Table 4-86
Kumar et al. ( <a href="#">2001b</a> )	Rat, Wistar, male, 6/group	Inhalation: 0 or 376 ppm, 4 hrs/d, 5 d/wk, 12 and 24 wks	Decreased testes weight, numbers of spermatogenic cells and spermatids, testes atrophy, smaller tubules devoid of spermatocytes and spermatids, hyperplastic Leydig cells, altered testicular enzyme markers. Increasing severity from 12 to 24 wks of exposure.	Table 4-86

**Table 5-7. Summary of studies of reproductive effects suitable for dose-response assessment (continued)**

Effect type Study reference	Species, strain (if applicable), sex, number used for dose-response assessment	Exposure(s) used for dose-response assessment	Endpoint(s) used for dose-response assessment	Chapter 4 Section/Table
George et al. (1985)	Mouse, CD-1, male and female, 20 pairs/treatment group; 40 controls/sex	Oral: 0, 173, 362, or 737 mg/kg/d, Breeders exposed 1 wk pre mating, then for 13 wks; pregnant females exposed throughout gestation (i.e., 18 wks total)	Decreased testes and seminal vesicle weights in F0.	Table 4-87
George et al. (1986)	Rat, F334, males and female, 20 pairs/treatment group, 40 controls/sex	Oral: 0, 72, 186, or 389 mg/kg/d (estimated), Breeders exposed 1 wk pre mating, then for 13 wks; pregnant females exposed throughout gestation (i.e., 18 wks total)	Increased testes and epididymis weights in F0.	Table 4-87
<b>Female maternal weight gain</b>				<b>Section 4.8.3.2</b>
Carney et al. (2006)	Rat, Sprague-Dawley, females, 27 dams/group	Inhalation: 0, 50, 150, or 600 ppm, 6 hrs/d; GDs 6–20	Decreased body weight gain on GDs 6–9.	Table 4-96
Schwetz et al. (1975)	Rat, Sprague-Dawley, female, 20–35/group	Inhalation: 0 or 300 ppm, 7 hrs/d; GDs 6–15	Decreased body weight gain on GDs 6–9.	Table 4-96
Narotsky et al. (1995)	Rat, F344, females, 8–12 dams/group	Oral: 0, 10.1, 32, 101, 320, 475, 633, 844, or 1,125 mg/kg/d, GDs 6–15	Decreased body weight gain on GDs 6–8 and 6–20.	Table 4-98
Manson et al. (1984)	Rat, Long-Evans, female, 23–25/group	Oral: 0, 10, 100, or 1,000 mg/kg/d, 6 wks: 2 wks pre mating, 1 wk mating period, GDs 1–21	Decreased gestation body weight gain.	Table 4-87

**Table 5-7. Summary of studies of reproductive effects suitable for dose-response assessment (continued)**

Effect type Study reference	Species, strain (if applicable), sex, number used for dose-response assessment	Exposure(s) used for dose-response assessment	Endpoint(s) used for dose-response assessment	Chapter 4 Section/Table
George et al. ( <a href="#">1986</a> )	Rat, F334, males and female, 20 pairs/treatment group, 40 controls/sex	Oral: 0, 72, 186, or 389 mg/kg/d (estimated), Breeders exposed 1 wk pre mating, then for 13 wks; pregnant females exposed throughout gestation (i.e., 18 wks total)	Decreased term and postpartum dam body weight in F0 and F1.	Table 4-87
<b>Female reproductive outcomes</b>				<b>Section 4.8.3.2</b>
Narotsky et al. ( <a href="#">1995</a> )	Rat, F344, females, 8–12 dams/group	Oral: 0, 10.1, 32, 101, 320, 475, 633, 844, or 1,125 mg/kg/d, GDs 6–15	Delayed parturition.	Table 4-98
<b>Reproductive behavior</b>				<b>Section 4.8.1.2</b>
Zenick et al. ( <a href="#">1984</a> )	Rat, Long-Evans, male, 10/group	Oral: 0, 10, 100, or 1,000 mg/kg/d, 5 d/wk, 6 wks exposure, 4 wks recovery	Impaired copulatory performance.	Table 4-87
George et al. ( <a href="#">1986</a> )	Rat, F334, males and female, 20 pairs/treatment group, 40 controls/sex	Oral: 0, 72, 186, or 389 mg/kg/d (estimated), Breeders exposed 1 wk pre mating, then for 13 wks; pregnant females exposed throughout gestation (i.e., 18 wks total)	Decreased F0 mating in cross-over mating trials.	Table 4-87

**Table 5-7. Summary of studies of reproductive effects suitable for dose-response assessment (continued)**

Effect type Study reference	Species, strain (if applicable), sex, number used for dose-response assessment	Exposure(s) used for dose-response assessment	Endpoint(s) used for dose-response assessment	Chapter 4 Section/Table
<b>Reproductive effects from exposure to both sexes</b>				<b>Section 4.8.1.2</b>
George et al. ( <a href="#">1986</a> )	Rat, F334, males and female, 20 pairs/treatment group, 40 controls/sex	Oral: 0, 72, 186, or 389 mg/kg/d (estimated), Breeders exposed 1 wk pre mating, then for 13 wks; pregnant females exposed throughout gestation (i.e., 18 wks total)	Decreased F0 litters/pair and live F1 pups/litter.	Table 4-87

**Table 5-8. Reproductive effects in studies suitable for dose-response assessment, and corresponding cRfCs and cRfDs**

Effect type Supporting studies <sup>a</sup>	Species	POD type	POD <sup>b</sup>	UF <sub>S</sub>	UF <sub>A</sub>	UF <sub>H</sub>	UF <sub>L</sub>	UF <sub>D</sub>	UF <sup>c</sup>	cRfC (ppm)	cRfD (mg/kg/d)	Effect; comments
<b>Effects on sperm, male reproductive outcomes</b>												
Chia et al. (1996)	Human	BMDL	1.43	10	1	10	1	1	100	0.014		Hyperzoospermia; exposure estimates based on U-TCA from Ikeda et al. (1972); BMR = 10% extra risk
Land et al. (1981)	Mouse	BMDL	46.9	10	3	10	1	1	300	0.16		↑ abnormal sperm; BMR = 0.5 SD
Kan et al. (2007)	Mouse	LOAEL	180	10	3	10	10	1	3,000	0.060		↑ abnormal sperm; Land et al. (1981) cRfC preferred due to BMD modeling
Xu et al. (2004)	Mouse	LOAEL	180	10	3	10	10	1	3,000	0.060		↓ fertilization
Kumar et al. (2001b; 2000b)	Rat	LOAEL	45	10	3	10	10	1	3,000	0.015		Multiple sperm effects, increasing severity from 12 to 24 wks
Kumar et al. (2000b)	Rat	LOAEL	45	1	3	10	10	1	300	0.15		Pre- and postimplantation losses; UF <sub>S</sub> = 1 due to exposure covered time period for sperm development; higher response for preimplantation losses
George et al. (1985)	Mouse	NOAEL	362	1	10	10	1	1	100		3.6	↓ sperm motility
DuTeaux et al., (2004a)	Rat	LOAEL	141	10	10	10	10	1	10,000 <sup>d</sup>		0.014	↓ ability of sperm to fertilize in vitro
<b>Male reproductive tract effects</b>												
Forkert et al. (2002), Kan et al. (2007)	Mouse	LOAEL	180	10	3	10	10	1	3,000	0.060		Effects on epididymis epithelium
Kumar et al. (2001b; 2000b)	Rat	LOAEL	45	10	3	10	10	1	3,000	0.015		Testes effects, altered testicular enzyme markers, increasing severity from 12 to 24 wks
George et al. (1985)	Mouse	NOAEL	362	1	10	10	1	1	100		3.6	↓ testis/seminal vesicle weights
George et al. (1986)	Rat	NOAEL	186	1	10	10	1	1	100		1.9	↑ testis/epididymis weights

**Table 5-8. Reproductive effects in studies suitable for dose-response assessment, and corresponding cRfCs and cRfDs (continued)**

Effect type Supporting studies <sup>a</sup>	Species	POD type	POD <sup>b</sup>	UF <sub>S</sub>	UF <sub>A</sub>	UF <sub>H</sub>	UF <sub>L</sub>	UF <sub>D</sub>	UF <sup>c</sup>	cRfC (ppm)	cRfD (mg/kg/d)	Effect; comments
<b>Female maternal weight gain</b>												
Carney et al. (2006)	Rat	BMDL	10.5	1	3	10	1	1	30	0.35		↓ Body weight gain; BMR = 10% decrease
Schwetz et al. (1975)	Rat	LOAEL	88	1	3	10	10	1	300	0.29		↓ maternal body weight; Carney et al. (2006) cRfC preferred due to BMD modeling
Narotsky et al. (1995)	Rat	BMDL	108	1	10	10	1	1	100		1.1	↓ Body weight gain; BMR = 10% decrease
Manson et al. (1984)	Rat	NOAEL	100	1	10	10	1	1	100		1.0	↓ Body weight gain; Narotsky et al. (1995) preferred due to BMD modeling (different strain)
George et al. (1986)	Rat	NOAEL	186	1	10	10	1	1	100		1.9	↓ postpartum body weight; Narotsky et al. (1995) cRfD preferred due to BMD modeling
<b>Female reproductive outcomes</b>												
Narotsky et al. (1995)	Rat	LOAEL	475	1	10	10	10	1	1,000		0.48	Delayed parturition
Reproductive behavior												
Zenick et al. (1984)	Rat	NOAEL	100	1	10	10	1	1	100		1.0	↓ copulatory performance in males
George et al. (1986)	Rat	LOAEL	389	1	10	10	10	1	1,000		0.39	↓ mating (both sexes exposed)
<b>Reproductive effects from exposure to both sexes</b>												
George et al. (1986)	Rat	BMDL	179	1	10	10	1	1	100		1.8	↓ number of litters/pair; BMR = 0.5 SD
	Rat	BMDL	152	1	10	10	1	1	100		1.5	↓ live pups/litter; BMR = 0.5 SD

<sup>a</sup>Shaded studies/endpoints were selected as candidate critical effects/studies.

<sup>b</sup>Adjusted to continuous exposure unless otherwise noted. For inhalation studies, adjustments yield a POD that is a HEC as recommended for a Category 3 gas in U.S. EPA (1994a) in the absence of PBPK modeling. Same units as cRfC (ppm) or cRfD (mg/kg/day).

<sup>c</sup>Product of individual UFs.

<sup>d</sup>EPA's report on the RfC and RfD processes (U.S. EPA, 2002b) recommends not deriving reference values with a composite UF of >3,000; however, composite UFs exceeding 3,000 are considered here because the derivation of the cRfCs and cRfDs is part of a screening process and the subsequent application of the PBPK model for candidate critical effects will reduce the values of some of the individual UFs.

UF<sub>S</sub> = subchronic-to-chronic UF; UF<sub>A</sub> = interspecies UF; UF<sub>H</sub> = human variability UF; UF<sub>L</sub> = LOAEL-to-NOAEL UF; UF<sub>D</sub> = database UF

#### 5.1.2.7.1. Male reproductive effects (effects on sperm and reproductive tract)

A number of available studies have reported functional and structural changes in sperm and male reproductive organs and effects on male reproductive outcomes following TCE exposure (see Table 5-8). A cRfC of 0.014 ppm was derived based on hyperzoospermia reported in the available human study ([Chia et al., 1996](#)), but there is substantial uncertainty in this estimate due to multiple issues.<sup>29</sup> Among the rodent inhalation studies, the cRfC of 0.2 ppm based on increased abnormal sperm in the mouse reported by Land et al. ([1981](#)) is considered relatively reliable because it is based on BMD modeling rather than a LOAEL or NOAEL. However, increased sperm abnormalities do not appear to be the most sensitive effect, as Kumar et al. ([2001b](#); [2000b](#)) reported a similar POD to be a LOAEL for reported multiple effects on sperm and testes, as well as altered testicular enzyme markers, in the rat. Although there are greater uncertainties associated with the cRfC of 0.02 ppm for this effect and a composite UF of 3,000 was applied to the POD, the uncertainties are generally typical of those encountered in RfC derivations.

Standard values of 3, 10, and 10 were used for the interspecies UF, the human variability UF, and the LOAEL-to-NOAEL UF, respectively. In addition, although the study would have qualified as a chronic exposure study based on its duration of 24 weeks (i.e., >10% of lifetime), statistically significant decreases in testicular weight and in sperm count and motility were already observed from subchronic exposure (12 weeks) to the same TCE exposure concentration and these effects became more severe after 24 weeks of exposure. Moreover, several testicular enzyme markers associated with spermatogenesis and germ cell maturation had significantly altered activities after 12 weeks of exposure, with more severe alterations at 24 weeks, and histological changes were also observed in the testes at 12 weeks, with the testes being severely deteriorated by 24 weeks. Thus, since the single exposure level used was already a LOAEL from subchronic exposure, and the testes were even more seriously affected by longer exposures, a subchronic-to-chronic UF of 10 was applied.<sup>30</sup> Note that for the cRfC derived for pre- and postimplantation losses reported by Kumar et al. ([2000b](#)), the subchronic-to-chronic UF was not applied because the exposure covered the time period for sperm development. This cRfC was

---

<sup>29</sup>Mean exposure estimates for the exposure groups were limited because they were defined in terms of ranges and because they were based on mean urinary TCA (mg/g creatinine). There is substantial uncertainty in the conversion of urinary TCA to TCE exposure level (see discussion of Mhiri et al. ([2004](#)), for neurotoxicity, above). In addition, there was uncertainty about the adversity of the effect being measured. While rodent evidence supports effects of TCE on sperm, and hyperzoospermia has reportedly been associated with infertility, the adversity of the hyperzoospermia (i.e., high sperm density) outcome measured in the Chia et al. ([1996](#)) study is unclear. Furthermore, the cut-point used to define hyperzoospermia in this study (i.e., >120 million sperm per mL ejaculate) is lower than some other reported cut-points, such as 200 and 250 million sperm/mL. A BMR of 10% extra risk was used on the assumption that this is a minimally adverse effect, but biological significance of this effect level is unclear.

<sup>30</sup>Alternatively, the value of the LOAEL-to-NOAEL UF could have been increased above 10 to reflect the extreme severity of the effects at the LOAEL after 24 weeks; however, the comparison of the 12- and 24-week results gives such a clear depiction of the progression of the effects, it was more compelling to frame the issue as a subchronic-to-chronic extrapolation issue.

0.2 ppm, similar to that derived from Land et al. (1981) based on BMD modeling of increases in abnormal sperm.

At a higher inhalation POD, Xu et al. (2004) reported decreased fertilization following exposure in male mice, and Forkert et al. (2002) and Kan et al. (2007) reported effects on the epididymal epithelium in male mice. Kan et al. (2007) reported degenerative effects on the epididymis as early as 1 week into exposure that became more severe at 4 weeks of exposure when the study ended; increases in abnormal sperm were also observed. As with the cRfC developed from the Kumar et al. (2001b; 2000b) studies, a composite UF of 3,000 was applied to these data, but the uncertainties are again typical of those encountered in RfC derivations. Standard values of 3 for the interspecies UF, 10 for the human variability UF, 10 for the LOAEL-to-NOAEL UF, and 10 for the subchronic-to-chronic UF were applied to each of the study PODs.

Among the oral studies, cRfDs derived for decreased sperm motility and changes in reproductive organ weights in rodents reported by George et al. (1986; 1985) were relatively high (2–4 mg/kg/day), and these effects were not considered candidate critical effects. The remaining available oral study of male reproductive effects is DuTeaux et al. (2004a), which reported decreased ability of sperm from TCE-exposed rats to fertilize eggs in vitro. This effect occurred in the absence of changes in combined testes/epididymes weight, sperm concentration or motility, or histological changes in the testes or epididymes. DuTeaux et al. (2004a) hypothesized that the effect is due to oxidative damage to the sperm. A LOAEL was used as the POD, and the standard UF values of 10 were used for each of the UFs, i.e., the subchronic-to-chronic UF (14-day study; substantially less than the 70-day time period for sperm development), the interspecies UF for oral exposures, the human variability UF, and the LOAEL-to-NOAEL UF. The resulting composite UF was 10,000,<sup>31</sup> and this yielded a cRfD of 0.01 mg/kg/day. The excessive magnitude of the composite UF, however, highlights the uncertainty in this estimate.

In summary, there is high qualitative confidence for TCE male reproductive tract toxicity and lower confidence in the cRfCs and cRfDs that can be derived from the available studies. Relatively high PODs are derived from several studies reporting less sensitive endpoints (George et al., 1986; George et al., 1985; 1981), and correspondingly higher cRfCs and cRfDs suggest that they are not likely to be critical effects. The studies reporting more sensitive endpoints also tend to have greater uncertainty. For the human study by Chia et al. (1996), as discussed above, there are uncertainties in the characterization of exposure and the adversity of the effect measured in the study. For the Kumar et al. (2001b; 2000a; 2000b), Forkert et al. (2002), and Kan et al. (2007) studies, the severity of the sperm and testes effects appears to be continuing to

---

<sup>31</sup>U.S. EPA's report on the RfC and RfD processes (U.S. EPA, 2002b) recommends not deriving reference values with a composite UF of >3,000; however, composite UFs exceeding 3,000 are considered here because the derivation of the cRfCs and cRfDs is part of a screening process and the subsequent application of the PBPK model for candidate critical effects will reduce the values of some of the individual UFs.

increase with duration even at the end of the study, so it is plausible that a lower exposure for a longer duration may elicit similar effects. For the DuTeaux et al. (2004a) study, there is also duration- and low-dose extrapolation uncertainty due to the short duration of the study in comparison to the time period for sperm development as well as the lack of a NOAEL at the tested doses. Overall, even though there are limitations in the quantitative assessment, there remains sufficient evidence to consider these to be candidate critical effects.

#### 5.1.2.7.2. Other reproductive effects

With respect to female reproductive effects, several studies reporting decreased maternal weight gain were suitable for deriving candidate reference values (see Table 5-8). The cRfCs from the two inhalation studies (Carney et al., 2006; Schwetz et al., 1975) yielded virtually the same estimate (0.3–0.4 ppm), although the Carney et al. (2006) result is preferred due to the use of BMD modeling, which obviates the need for the 10-fold LOAEL-to-NOAEL UF used for Schwetz et al. (1975) (the other UFs, with a product of 30, were the same). The cRfDs for this endpoint from the three oral studies were within twofold of each other (1.1–1.9 mg/kg/day), with the same composite UFs of 100. The most sensitive estimate of Narotsky et al. (1995) is preferred due to the use of BMD modeling and the apparent greater sensitivity of the rat strain used.

With respect to other reproductive effects, the most reliable cRfD estimates of about 2 mg/kg/day, derived from BMD modeling with composite UFs of 100, are based on decreased litters/pair and decreased live pups/litter in rats reported in the continuous breeding study of George et al. (1986). Both of these effects were considered severe adverse effects, so a BMR of a 0.5 control SD shift from the control mean was used. Somewhat lower cRfDs of 0.4–1 mg/kg/day were derived based on delayed parturition in females (Narotsky et al., 1995), decreased copulatory performance in males (Zenick et al., 1984), and decreased mating for both exposed males and females in cross-over mating trials (George et al., 1986), all with composite UFs of 100 or 1,000, depending on whether a LOAEL or NOAEL was used.

In summary, there is moderate confidence both in the hazard and the cRfCs and cRfDs for reproductive effects other than the male reproductive effects discussed previously. While there are multiple studies suggesting decreased maternal body weight with TCE exposure, this systemic change may not be indicative of more sensitive reproductive effects. None of the estimates developed from other reproductive effects is particularly uncertain or unreliable. Therefore, delayed parturition (Narotsky et al., 1995) and decreased mating (George et al., 1986), which yielded the lowest cRfDs, were considered candidate critical effects. These effects were also included so that candidate critical reproductive effects from oral studies would not include only that reported by DuTeaux et al. (2004a), from which deriving the cRfD entailed a higher degree of uncertainty.

#### 5.1.2.8. Candidate Critical Developmental Effects on the Basis of Applied Dose

As summarized in Section 4.11.1.7, both human and experimental animal studies have associated TCE exposure with adverse developmental effects. Weakly suggestive epidemiologic data and fairly consistent experimental animal data support TCE exposure posing a hazard for increased prenatal or postnatal mortality and decreased pre- or postnatal growth. In addition, congenital malformations following maternal TCE exposure have been reported in a number of epidemiologic and experimental animal studies. There is also some support for TCE effects on neurological and immunological development. Available human studies, while indicative of hazard, did not have adequate exposure information for quantitative estimates of PODs, so only experimental animal studies are considered here. Studies with numerical dose-response information are summarized in Table 5-9, with their corresponding cRfCs or cRfDs summarized in Table 5-10.

For pre- and postnatal mortality and growth, a cRfC of 0.06 ppm for resorptions, decreased fetal weight, and variations in skeletal development indicative of delays in ossification was developed based on the single available (rat) inhalation study considered ([Healy et al., 1982](#)) and utilizing the composite UF of 300 for an inhalation POD that is a LOAEL. The cRfDs for pre- and postnatal mortality derived from oral studies were within about a 10-fold range of 0.4–5 mg/kg/day, depending on the study and specific endpoint assessed. Of these, the estimate based on Narotsky et al. ([1995](#)) rat data was both the most sensitive and most reliable cRfD. The dose response for increased full-litter resorptions from this study is based on BMD modeling. Because of the severe nature of this effect, a BMR of 1% extra risk was used. The ratio of the resulting BMD to the BMDL was 5.7, which is on the high side, but given the severity of the effect and the low background response, a judgment was made to use 1% extra risk. Alternatively, a 10% extra risk could have been used, in which case the POD would have been considered more analogous to a LOAEL than a NOAEL, and a LOAEL-to-NOAEL UF of 10 would have been applied, ultimately resulting in the same cRfD estimate. The cRfDs for altered pre- and postnatal growth developed from the oral studies ranged about 10-fold from 0.8 to 8 mg/kg/day, all utilizing the composite UFs for the corresponding type of POD. The cRfDs for decreased fetal weight, both of which were based on NOAELs, were consistent, being about twofold apart ([Narotsky et al., 1995](#); [George et al., 1985](#)). The cRfD based on postnatal growth at 21 days, reported in George et al. ([1986](#)), was lower and is preferred because it was based on BMD modeling. A BMR of 5% decrease in weight was used for postnatal growth at 21 days because decreases in weight gain so early in life were considered similar to effects on fetal weight.

**Table 5-9. Summary of studies of developmental effects suitable for dose-response assessment**

Effect type Study reference	Species, strain (if applicable), sex, number used for dose-response assessment	Exposure(s) used for dose-response assessment	Endpoint(s) used for dose-response assessment	Chapter 4 Section/Table
<b>Pre- and postnatal mortality</b>				<b>Section 4.8.1.2 and 4.8.3.2</b>
George et al. ( <a href="#">1985</a> )	Mouse, CD-1, male and female, 20 pairs/treatment group; 40 controls/sex	Oral: 0, 173, 362, or 737 mg/kg/d, Breeders exposed 1 wk pre mating, then for 13 wks; pregnant females exposed throughout gestation (i.e., 18 wks total)	Increase perinatal mortality (PNDs 0–21)	Table 4-87
Narotsky et al. ( <a href="#">1995</a> )	Rat, F344, females, 8–12 dams/group	Oral: 0, 10.1, 32, 101, 320, 475, 633, 844, or 1,125 mg/kg/d, GDs 6–15	Increased resorptions, prenatal loss, and postnatal mortality	Table 4-98
Manson et al. ( <a href="#">1984</a> )	Rat, Long-Evans, female, 23–25/group	Oral: 0, 10, 100, or 1,000 mg/kg/d, 6 wks: 2 wks pre mating, 1 wk mating period, GDs 1–21	Increased neonatal deaths on PNDs 1, 10, and 14.	Table 4-87
Healy et al. ( <a href="#">1982</a> )	Rat, Wistar, females, 31–32 dams/group	Inhalation: 0 or 100 ppm, 4 hrs/d; GDs 8–21	Increased resorptions.	Table 4-96
<b>Pre- and postnatal growth</b>				<b>Section 4.8.3.2</b>
Healy et al. ( <a href="#">1982</a> )	Rat, Wistar, females, 31–32 dams/group	Inhalation: 0 or 100 ppm, 4 hrs/d; GDs 8–21	Decreased fetal weight, increased bipartite, or absent skeletal ossification centers	Table 4-96

**Table 5-9. Summary of studies of developmental effects suitable for dose-response assessment (continued)**

Effect type Study reference	Species, strain (if applicable), sex, number used for dose-response assessment	Exposure(s) used for dose-response assessment	Endpoint(s) used for dose-response assessment	Chapter 4 Section/Table
Narotsky et al. (1995)	Rat, F344, females, 8–12 dams/group	Oral: 0, 10.1, 32, 101, 320, 475, 633, 844, or 1,125 mg/kg/d, GDs 6–15	Decreased pup body weight on PNDs 1 and 6.	Table 4-98
George et al. (1985)	Mouse, CD-1, male and female, 20 pairs/treatment group; 40 controls/sex	Oral: 0, 173, 362, or 737 mg/kg/d, Breeders exposed 1 wk pre mating, then for 13 wks; pregnant females exposed throughout gestation (i.e., 18 wks total)	Decreased live birth weights, PND 4 pup body weights.	Table 4-87
George et al. (1986)	Rat, F334, males and female, 20 pairs/treatment group, 40 controls/sex	Oral: 0, 72, 186, or 389 mg/kg/d (estimated), Breeders exposed 1 wk pre mating, then for 13 wks; pregnant females exposed throughout gestation (i.e., 18 wks total)	Decreased F1 body weight on PNDs 4–80.	Table 4-87
<b>Congenital defects</b>				<b>Section 4.8.3.2</b>
Narotsky et al. (1995)	Rat, F344, females, 8–12 dams/group	Oral: 0, 10.1, 32, 101, 320, 475, 633, 844, or 1,125 mg/kg/d, GDs 6–15	Increased incidence of eye defects.	Table 4-98
Johnson et al. (2003)	Rat, Sprague-Dawley, female, 9–13/group, 55 in control group	Oral: 0, 0.00045, 0.048, 0.218, or 129 mg/kg/d, GDs 0–22	Increased percentage of abnormal hearts; increased percentage of litters with abnormal hearts.	Table 4-98

**Table 5-9. Summary of studies of developmental effects suitable for dose-response assessment (continued)**

Effect type Study reference	Species, strain (if applicable), sex, number used for dose-response assessment	Exposure(s) used for dose-response assessment	Endpoint(s) used for dose-response assessment	Chapter 4 Section/Table
<b>Developmental neurotoxicity</b>				<b>Sections 4.3.8.2 and 4.8.3.2</b>
George et al. ( <a href="#">1986</a> )	Rat, F334, males and female, 20 pairs/treatment group, 40 controls/sex	Oral: 0, 72, 186, or 389 mg/kg/d (estimated), Breeders exposed 1 wk pre mating, then for 13 wks; pregnant females exposed throughout gestation (i.e., 18 wks total)	Decreased locomotor, as assessed by increased time required for pups to cross the first grid in open-field testing.	Tables 4-34 and 4-98
Fredriksson et al. ( <a href="#">1993</a> )	Mouse, NMRI, male pups, 12 pups from 3 to 4 different litters/group	Oral: 0, 50, or 290 mg/kg/d, PNDs 10–16	Decreased rearing activity on PND 60.	Tables 4-34 and 4-98
Taylor et al. ( <a href="#">1985</a> )	Rat, Sprague-Dawley, females, no. dams/group not reported	Oral: 0, 312, 625, or 1,250 mg/L (0, 45, 80, or 140 mg/kg/d estimated), dams (and pups) exposed from 14 d prior to mating until end of lactation	Increased exploratory behavior in 60- and 90-d-old male rats (offspring).	Tables 4-34 and 4-98
Isaacson and Taylor ( <a href="#">1989</a> )	Rat, Sprague-Dawley, females, 6 dams/group	Oral: 0, 4.0, or 8.1 mg/d (0, 15, or 32 mg/kg/d estimated) <sup>a</sup> , dams (and pups) exposed from 14 d prior to mating until end of lactation.	Decreased myelinated fibers in the stratum lacunosum-moleculare of pups; decreased myelin in the hippocampus.	Tables 4-34 and 4-98

**Table 5-9. Summary of studies of developmental effects suitable for dose-response assessment (continued)**

Effect type Study reference	Species, strain (if applicable), sex, number used for dose-response assessment	Exposure(s) used for dose-response assessment	Endpoint(s) used for dose-response assessment	Chapter 4 Section/Table
<b>Developmental immunotoxicity</b>				<b>Section 4.8.3.2</b>
Peden-Adams et al. (2006)	Mouse, B6C3F <sub>1</sub> , dams and both sexes offspring, 5 dams/group; 5–7 pups/group at 3 wks; 4–5 pups/sex/group at 8 wks	Oral: 0, 1,400, or 14,000 ppb in water (0, 0.37, or 3.7 mg/kg/d estimated), parental mice and/or offspring exposed during mating, and from GDs 0 through 3 or 8 wks of age	Suppressed PFC responses in males and in females. Delayed hypersensitivity response increased at 8 wks of age in females. Splenic cell population decreased in 3-wk-old pups. Increased thymic T-cells at 8 wks of age. Delayed hypersensitivity response increased at 8 wks of age in males and females	Table 4-98

<sup>a</sup>The Isaacson and Taylor (1989) and Taylor et al. (1985) studies report different doses despite identical study designs and administered concentrations, both studies taking TCE degradation into account. Taylor et al. (1985) report total consumption of 646, 1,102, and 1,991 mg TCE for rats exposed to 312, 625, and 1,250 mg TCE/L drinking water, respectively. Dividing by the 56 days of exposure and the average 250 g per rat for female Sprague-Dawley rats of those ages yields estimated doses of roughly 45, 80, and 140 mg/kg/day, respectively. Isaacson and Taylor (1989) report average doses of TCE of 4.0 and 8.1 mg/day corresponding to exposures of 312 and 625 mg TCE/L drinking water, respectively. Dividing by the average 250 g per rat yields estimated doses of 16 and 32 mg/kg/day, respectively. Thus, the estimated doses for Taylor et al. (1985) are nearly 3 times higher than those for Isaacson and Taylor (1989), for reasons unknown.

**Table 5-10. Developmental effects in studies suitable for dose-response assessment, and corresponding cRfCs and cRfDs**

Effect type Supporting studies <sup>a</sup>	Species	POD type	POD <sup>b</sup>	UF <sub>S</sub>	UF <sub>A</sub>	UF <sub>H</sub>	UF <sub>L</sub>	UF <sub>D</sub>	UF <sup>c</sup>	cRfC (ppm)	cRfD (mg/kg/d)	Effect; comments
<b>Pre- and postnatal mortality</b>												
George et al. (1985)	Mouse	NOAEL	362	1	10	10	1	1	100		3.6	↑ perinatal mortality
Narotsky et al. (1995)	Rat	LOAEL	475	1	10	10	10	1	1,000		0.48	Postnatal mortality; Manson et al. (1984) cRfD preferred for same endpoint due to NOAEL vs. LOAEL
Manson et al. (1984)	Rat	NOAEL	100	1	10	10	1	1	100		1.0	↑ neonatal death
Healy et al. (1982)	Rat	LOAEL	17	1	3	10	10	1	300	0.057		Resorptions
Narotsky et al. (1995)	Rat	BMDL	469	1	10	10	1	1	100		4.7	Prenatal loss; BMR = 1% extra risk
Narotsky et al. (1995)	Rat	BMDL	32.2	1	10	10	1	1	100		0.32	Resorptions; BMR = 1% extra risk
<b>Pre- and postnatal growth</b>												
Healy et al. (1982)	Rat	LOAEL	17	1	3	10	10	1	300	0.057		↓ fetal weight; skeletal effects
Narotsky et al. (1995)	Rat	NOAEL	844	1	10	10	1	1	100		8.4	↓ fetal weight
George et al. (1985)	Mouse	NOAEL	362	1	10	10	1	1	100		3.6	↓ fetal weight
George et al. (1986)	Rat	BMDL	79.7	1	10	10	1	1	100		0.80	↓ Body weight at d21; BMR = 5% decrease
<b>Congenital defects</b>												
Narotsky et al. (1995)	Rat	BMDL	60	1	10	10	1	1	100		0.60	Eye defects; low BMR (1%), but severe effect and low background. rate (<1%)
Johnson et al. (2003)	Rat	BMDL	0.0146	1	10	10	1	1	100		0.00015	Heart malformations (litters); BMR = 10% extra risk (only ~1/10 from each litter affected); highest-dose group (1,000-fold higher than next highest) dropped for model fit.
Johnson et al. (2003)	Rat	BMDL	0.0207	1	10	10	1	1	100		0.00021	Heart malformations (pups); BMR = 1% extra risk; preferred due to accounting for intralitter effects via nested model and pups being the unit of measure; highest-dose group (1,000-fold higher than next highest) dropped for model fit

**Table 5-10. Developmental effects in studies suitable for dose-response assessment, and corresponding cRfCs and cRfDs (continued)**

Effect type Supporting studies <sup>a</sup>	Species	POD type	POD <sup>b</sup>	UF <sub>S</sub>	UF <sub>A</sub>	UF <sub>H</sub>	UF <sub>L</sub>	UF <sub>D</sub>	UF <sup>c</sup>	cRfC (ppm)	cRfD (mg/kg/d)	Effect; comments
<b>Developmental neurotoxicity</b>												
George et al. (1986)	Rat	BMDL	72.6	1	10	10	1	1	100		0.73	↓ locomotor activity; BMR = doubling of traverse time; results from females (males similar with BMDL = 92)
Fredriksson et al. (1993)	Mouse	LOAEL	50	3	10	10	10	1	3,000		0.017	↓ rearing postexposure; pup gavage dose; no effect at tested doses on locomotion behavior; UF <sub>S</sub> = 3 because exposure only during PNDs 10–16
Taylor et al. (1985)	Rat	LOAEL	45	1	10	10	10	1	1,000		0.045	↑ exploration postexposure; estimated dam dose; less sensitive than Isaacson and Taylor (1989), but included because exposure is preweaning, so can utilize PBPK model
Isaacson and Taylor (1989)	Rat	LOAEL	16	1	10	10	10	1	1,000		0.016	↓ myelination in hippocampus; estimated dam dose
<b>Developmental immunotoxicity</b>												
Peden-Adams et al. (2006)	Mouse	LOAEL	0.37	1	10	10	10	1	1,000		0.00037	↓ PFC, ↑ DTH; POD is estimated dam dose (exposure throughout gestation and lactation + to 3 or 8 wks of age); UF LOAEL = 10 since multiple immunotoxicity effects

<sup>a</sup>Shaded studies/endpoints were selected as candidate critical effects/studies.

<sup>b</sup>Adjusted to continuous exposure unless otherwise noted. For inhalation studies, adjustments yield a POD that is a HEC as recommended for a Category 3 gas in U.S. EPA (1994a) in the absence of PBPK modeling. Same units as cRfC (ppm) or cRfD (mg/kg/day).

<sup>c</sup>Product of individual UFs.

UF<sub>S</sub> = subchronic-to-chronic UF; UF<sub>A</sub> = interspecies UF; UF<sub>H</sub> = human variability UF; UF<sub>L</sub> = LOAEL-to-NOAEL UF; UF<sub>D</sub> = database UF

For congenital defects, there is relatively high confidence in the cRfD for eye defects in rats reported in Narotsky et al. (1995), derived using a composite UF of 100 for BMD modeling in a study of duration that encompasses the full window of eye development. However, the most sensitive developmental effect by far was heart malformations in the rat reported by Johnson et al. (2003), yielding a cRfD estimate of 0.0002 mg/kg/day, also with a composite UF of 100. As discussed in detail in Section 4.8 and summarized in Section 4.11.1.7, although this study has important limitations, the overall weight of evidence supports an effect of TCE on cardiac development, and this is the only study of heart malformations available for conducting dose-response analysis. Individual data were kindly provided by Dr. Johnson ([personal communication from Paula Johnson, University of Arizona, to Susan Makris, EPA, 25 August 2008](#)), and, for analyses for which the pup was the unit of measure, BMD modeling was done using nested models because accounting for the intralitter correlation improved model fit. For these latter analyses, a 1% extra risk of a pup having a heart malformation was used as the BMR because of the severity of the effect, since, for example, some of the types of malformations observed could have been fatal. The ratio of the resulting BMD to the BMDL was about three.

For developmental neurotoxicity, the cRfD estimates based on the four oral studies span a wide range from 0.02 to 0.8 mg/kg/day. The most reliable estimate, with a composite UF of 100, is based on BMD modeling of decreased locomotor activity in rats reported in George et al. (1986), although a nonstandard BMR of a twofold change was selected because the control SD appeared unusually small. The cRfDs developed for decreased rearing postexposure in mice ([Fredriksson et al., 1993](#)), increased exploration postexposure in rats ([Taylor et al., 1985](#)), and decreased myelination in the hippocampus of rats ([Isaacson and Taylor, 1989](#)), while being >10-fold lower, are all within a 3-fold range of 0.02–0.05 mg/kg/day. Importantly, there is some evidence from adult neurotoxicity studies of TCE causing demyelination, so there is additional biological support for the latter effect. There is greater uncertainty in the Fredriksson et al. (1993), the cRfD for which utilized a subchronic-to-chronic UF of 3 rather than 1, because exposure during PND 10–16 does not cover the full developmental window ([Rice and Barone, 2000](#)). The cRfDs derived from Taylor et al. (1985) and ([Isaacson and Taylor, 1989](#)) used the composite UF of 1,000 for a POD that is a LOAEL. While there is greater uncertainty in these endpoints, none of the uncertainties is particularly high, and they also appear to be more sensitive indicators of developmental neurotoxicity than that from George et al. (1986).

A cRfD of 0.0004 mg/kg/day was developed from the study ([Peden-Adams et al., 2006](#)) that reported developmental immunotoxicity. The main effects observed were significantly decreased PFC response and increased delayed-type hypersensitivity. The data on these effects were kindly provided by Dr. Peden-Adams ([personal communication from Margie Peden-Adams, Medical University of South Carolina, to Jennifer Jinot, EPA, 26 August 2008](#)); however, the dose-response relationships were sufficiently supralinear that attempts at BMD modeling did not result in adequate fits to these data. Thus, the LOAEL was used as the POD.

A LOAEL-to-NOAEL UF of 10 was used for the multiple effects of decreased PFC response and increased delayed-type hypersensitivity at the same dose. While there is uncertainty in this estimate, it is notable that decreased PFC response was also observed in an immunotoxicity study in adult animals ([Woolhiser et al., 2006](#)), lending biological plausibility to the effect.

In summary, there is moderate-to-high confidence both in the hazard and the cRfCs and cRfDs for developmental effects of TCE. It is also noteworthy that the PODs for the more sensitive developmental effects were similar to or, in most cases, lower than the PODs for the more sensitive reproductive effects, suggesting that developmental effects are not a result of paternal or maternal toxicity. Among inhalation studies, cRfCs were only developed for effects in rats reported in Healy et al. ([1982](#)), so the effects of resorptions, decreased fetal weight, and delayed skeletal ossification were considered candidate critical developmental effects. Because resorptions were also reported in oral studies, the most sensitive (rat) oral study (and most reliable for dose-response analysis) of Narotsky et al. ([1995](#)) was also selected as a candidate critical study for this effect. The confidence in the oral studies and candidate reference values developed for more sensitive endpoints is more moderate, but still sufficient for consideration as candidate critical effects. The most sensitive endpoints by far are the increased fetal heart malformations in rats reported by Johnson et al. ([2003](#)) and the developmental immunotoxicity in mice reported by Peden-Adams et al. ([2006](#)), and these are both considered candidate critical effects. Neurodevelopmental effects are a distinct type among developmental effects. Thus, the next most sensitive endpoints of decreased rearing postexposure in mice ([Fredriksson et al., 1993](#)), increased exploration postexposure in rats ([Taylor et al., 1985](#)), and decreased myelination in the hippocampus of rats ([Isaacson and Taylor, 1989](#)) are also considered candidate critical effects.

#### **5.1.2.9. Summary of cRfCs, cRfDs, and Candidate Critical Effects**

An overall summary of the cRfCs, cRfDs, and candidate critical effects across the health effect domains is shown in Tables 5-11 and 5-12. These tables present, for each type of noncancer effect, the relative ranges of the cRfC and cRfD developed for the different endpoints. The candidate critical effects selected above for each effect domain are shown in bold. As discussed above, these effects were generally selected to represent the most sensitive endpoints, across species where possible. From these candidate critical effects, candidate reference values based on internal dose-metrics from the PBPK model (p-cRfCs and p-cRfDs) were developed where possible. Effects within the same health effect domain were generally assumed to have the same relevant internal dose-metrics; thus, screening for the effects with the lowest cRfCs and cRfDs for each species within health effect domains on the basis of applied dose should capture the same endpoints which would have the lowest candidate reference values on the basis of an appropriate dose-metric. Application of the PBPK model is discussed in the next section.

**Table 5-11. Ranges of cRfCs based on applied dose for various noncancer effects associated with inhalation TCE exposure<sup>a</sup>**

cRfC range (ppm)	Neurological	Systemic/organ-specific	Immunological	Reproductive	Developmental
10–100	Impaired visual discrimination (rat)				
1–10		<b>Kidney meganucleocytosis (rat)</b> <b>↑ kidney weight (mouse)</b>			
0.1–1	Ototoxicity (rat) Hyperactivity (rat) Changes in locomotor activity (rat) <b>Trigeminal nerve effects (human)</b> Impaired visual function (rabbit) <b>↓ regeneration of sciatic nerve (rat)</b>	<b>↑ liver weight (rat)</b> <b>↑ liver weight (mouse)</b> <b>↑ kidney weight (rat)</b>	<b>↓ PFC response (rat)</b>	<b>↓ maternal body weight gain (rat)</b> <b>↑ abnormal sperm (mouse)</b> <b>pre/postimplantation losses (male rat exp)</b>	
0.01–0.1	<b>↓ regeneration of sciatic nerve (mouse)</b> <b>Disturbed wakefulness (rat)</b>		<b>Autoimmune changes (MRL—lpr/lpr mouse)</b>	<b>Effects on epididymis epithelium (mouse)</b> <b>↓ fertilization (male mouse exp)</b> <b>Testes and sperm effects (rat)</b> <b>Hyperzoospermia (human)</b>	<b>Resorptions (female rat)</b> <b>↓ fetal weight (rat)</b> <b>Skeletal effects (rat)</b>

<sup>a</sup>Endpoints in **bold** were selected as candidate critical effects (see Sections 5.1.2.1–5.1.2.8).

**Table 5-12. Ranges of cRfDs based on applied dose for various noncancer effects associated with oral TCE exposure<sup>a</sup>**

cRfD range (mg/kg/d)	Neurological	Systemic/organ-specific	Immunological	Reproductive	Developmental
1–10	↑ neuromuscular changes (rat)	↓ Body weight (mouse)	↓ humoral response to SRBC (mouse)	↓ testis/seminal vesicle weight (mouse) ↓ sperm motility (mouse) ↑ testis/epididymis weight (rat) ↓ litters/pair (rat) ↓ live pups/litter (rat) ↓ Body weight gain (rat) ↓ copulatory performance (rat)	↓ fetal weight (rat) Prenatal loss (rat) ↓ fetal weight (mouse) ↑ neonatal mortality (mouse, rat)
0.1–1	↑ number rears (rat) ↑ foot splaying (rat) Trigeminal nerve effect (rat)	↑ <b>liver weight (mouse)</b> ↓ Body weight (mouse) ↓ Body weight (rat) <b>Toxic nephropathy</b> (other rat strains/sexes and <b>mouse</b> ) <b>Meganucleocytosis (male Sprague-Dawley rat)</b>	Signs of autoimmune hepatitis (MRL +/- mouse) Inflammation in various tissues (MRL +/- mouse)	<b>Delayed parturition (rat)</b> ↓ <b>mating (rat)</b>	↓ Body weight at PND 21 (rat) ↓ locomotor activity (rat) Eye defects (rat) <b>Resorptions (rat)</b>
0.01–0.1	<b>Degeneration of dopaminergic neurons (rat)</b>	<b>Toxic nephropathy (female Marshall rat)</b>	↓ <b>cell-mediated response to SRBC (mouse)</b> ↓ <b>stem cell bone marrow recolonization (mouse)</b>	↓ <b>ability of sperm to fertilize (rat)</b>	↑ <b>exploration (postexposure) (rat)</b> ↓ <b>rearing (postexposure) (mouse)</b> ↓ <b>myelination in hippocampus (rat)</b>
0.001–0.01	<b>Demyelination in hippocampus (rat)</b>		↑ <b>anti-dsDNA and anti-ssDNA Abs (early marker for autoimmune disease) (mouse)</b>		
10 <sup>-4</sup> –0.001			↓ <b>thymus weight (mouse)</b>		<b>Immunotoxicity (↓ PFC, ↑ DTH) (B6C3F<sub>1</sub> mouse)</b> <b>Heart malformations (rat)</b>

<sup>a</sup>Endpoints in **bold** were selected as candidate critical effects (see Sections 5.1.2.1–5.1.2.8).

### 5.1.3. Application of PBPK Model to Inter- and Intraspecies Extrapolation for Candidate Critical Effects

For the candidate critical effects, the use of PBPK modeling of internal doses could justify, where appropriate, replacement of the UFs for pharmacokinetic inter- and intraspecies extrapolation. For more details on PBPK modeling used to estimate levels of dose-metrics corresponding to different exposure scenarios in rodents and humans, as well as a qualitative discussion of the uncertainties and limitations of the model, see Section 3.5.

Quantitative analyses of the PBPK modeling uncertainties and their implications for dose-response assessment, utilizing the results of the Bayesian analysis of the PBPK model, are discussed separately in Section 5.1.4.

#### 5.1.3.1. Selection of Dose-metrics for Different Endpoints

One area of scientific uncertainty in noncancer dose-response assessment is the appropriate scaling between rodent and human doses for equivalent responses. As discussed above, the interspecies UF of 10 is usually thought of as a product of two factors of (approximately) three each for pharmacokinetics ( $UF_{A-pk}$ ) and pharmacodynamics ( $UF_{A-pd}$ ). In this assessment, EPA's cross-species scaling methodology, grounded in general principles of allometric variation of biologic processes, is used for describing pharmacokinetic equivalence (U.S. EPA, [1992](#), [2011a](#), [2005b](#); [Allen and Fisher, 1993](#); [Crump et al., 1989](#); [Allen et al., 1987](#)). Briefly, in the absence of adequate information to the contrary, the methodology determines pharmacokinetic equivalence across species through equal average lifetime concentrations or AUCs of the toxicant. Thus, in cases where the PBPK model can predict internal concentrations of the active moiety, equivalent daily AUCs are assumed to address cross-species pharmacokinetics, and the interspecies UF is reduced to 3 to account for the remaining pharmacodynamic factor.

In the absence of directly estimated AUCs, the cross-species scaling methodology assumes that, unless there is evidence to the contrary (U.S. EPA, [1992](#), [2011a](#), [2005b](#)):

- (1) The production of the active moiety(ies) is proportional to dose
- (2) The clearance of the active moiety(ies) scales allometrically by body weight to the  $3/4$  power; and
- (3) The tissue distribution is equal across species.

Under these assumptions, for oral exposures, pharmacokinetic equivalence of AUCs between animals to humans is expressed on the basis of  $mg/kg^{3/4}/day$ , not  $mg/kg/day$  ("body-weight scaling"). For inhalation exposures, pharmacokinetic equivalence would be on the basis of equivalent air concentrations, since the alveolar ventilation rate (which determines dose, for a

constant air concentration) scales approximately by body weight to the  $3/4$  power, cancelling out the assumed scaling dependence of clearance.

However, when one or more metabolites are thought to be the toxicologically active compound(s), it is often the case that a PBPK model can predict the rate of production of the active moiety(ies) (i.e., the rate of metabolism) but cannot predict AUCs due to lack of data to inform clearance. In this case, assumption (1) above can be replaced by the PBPK model, while the other two cross-species scaling methodology assumptions are retained. The resulting pharmacokinetic equivalence can therefore be expressed on the basis of rate of metabolism/kg $^{3/4}$ /day.<sup>32</sup> Thus, in cases where the PBPK model can predict the rate of production of the active metabolite(s), equivalent daily amounts metabolized through the appropriate pathway per unit body weight to the  $3/4$  power are assumed to address cross-species pharmacokinetics, and the interspecies UF is reduced to 3 to account for the remaining pharmacodynamic factor.

In addition, in some cases when AUCs cannot be estimated, there are data to replace assumption (2), above, that the clearance of the active moiety(ies) scales allometrically by body weight to the  $3/4$  power. Often, this is considered for toxicity associated with local (in situ) production of “reactive” metabolites whose concentrations cannot be directly measured in the target tissue. In such a case, an alternative approach of scaling the rate of local metabolism by target tissue mass, rather than body weight to the  $3/4$  power, is appropriate if the metabolites are sufficiently reactive *and* are cleared by “spontaneous” deactivation (i.e., changes in chemical structure without the need of biological influences). In particular, use of this alternative scaling approach requires evidence that: (1) the active moiety or moieties do not leave the target tissue in appreciable quantities (i.e., are cleared primarily by in situ transformation to other chemical species and/or binding to/reactions with cellular components), and (2) the clearance of the active moieties from the target tissue is governed by biochemical reactions whose rates are independent of body weight (e.g., purely chemical reactions). If these conditions are met, equivalent daily amounts metabolized through the appropriate pathway per unit target tissue mass are assumed to address cross-species pharmacokinetics, and the interspecies UF is reduced to 3 to account for the remaining pharmacodynamic factor.

---

<sup>32</sup>Consider a circulating stable metabolite  $X$ . Under a one-compartment model, at steady-state, the production of  $X$  will be equal to the clearance of  $X$ , so that

$$R_{met} = V_d \times BW \times C_X \times k_{cl}$$

where  $R_{met}$  = rate of production of  $X$  (mg/time),  $V_d$  = fractional volume of distribution,  $BW$  = body weight,  $C_X$  = concentration of  $X$  and  $k_{cl}$  = clearance of  $X$  in units of 1/time. Then, for the concentration  $C_X$  to be equivalent between experimental animals ( $A$ ) and humans ( $H$ ):

$$C_X = [R_{met}/BW \times k_{cl} \times V_d]_H = [R_{met}/BW \times k_{cl} \times V_d]_A$$

Under the cross-species scaling methodology, it is assumed that  $V_d$  is the same across species, so  $[R_{met}/BW \times k_{cl}]_H = [R_{met}/BW \times k_{cl}]_A$ . Next, under the cross-species scaling methodology,  $k_{cl}$  (with units of 1/time) is assumed to scale according to  $BW^{1/4}$  (U.S. EPA, 2005b; U.S. EPA, 2011a), leading to:

$$R_{met(H)}/BW_H^{3/4} = R_{met(A)}/BW_A^{3/4}$$

Finally, there is the case where local metabolism, rather than systemically delivered metabolite(s), is thought to be involved in toxicity, but there are inadequate data to determine either the rate of local metabolism or its clearance. In this case, assumption (1) above can be replaced by the assumption that local metabolism will be proportional to blood concentration. Because tissue blood flow approximately scales allometrically by body weight to the  $\frac{3}{4}$  power, combining this with assumptions (2) and (3) above will lead to the AUC of the parent compound in blood as an appropriate surrogate for local metabolism. Thus, in this case, equivalent daily AUCs of the parent compound are assumed to address cross-species pharmacokinetics, and the interspecies UF is reduced to 3 to account for the remaining pharmacodynamic factor.

To summarize, the internal dose-metric for addressing cross-species pharmacokinetics is based on the Agency's cross-species scaling methodology. The preferred dose-metric under this methodology is equivalent daily AUC of the active moiety (parent compound or metabolite). For metabolites, in cases where the rate of production, but not the rate of clearance, of the active moiety can be estimated, the preferred dose-metric is the rate of metabolism (through the appropriate pathway) scaled by body weight to the  $\frac{3}{4}$  power. If there are sufficient data to consider the active metabolite moiety(ies) "reactive" and cleared through nonbiological processes, then the preferred dose-metric is the rate of metabolism (through the appropriate pathway) scaled by the tissue mass. Finally, if local metabolism is thought to be involved, but cannot be estimated with the available data, then the AUC of the parent compound in blood is considered an appropriate surrogate and thus the preferred dose-metric.

These dose-metrics were then also used in addressing the pharmacokinetic component,  $UF_{H-pk}$ , of the UF for human (intraspecies) variability. Because all of the dose-metrics used for TCE were for adults, and the dose-metrics are not very sensitive to the plausible range of adult body weight, for convenience the body weight  $\frac{3}{4}$  scaling used for interspecies extrapolation was retained for characterization of human variability. However, it should be emphasized that this intraspecies characterization is of pharmacokinetics only, and not pharmacodynamics.

In general, an attempt was made to use tissue-specific dose-metrics representing particular pathways or metabolites identified from available data on the role of metabolism in toxicity for each endpoint (discussed in more detail below). The selection was limited to dose-metrics for which uncertainty and variability could be adequately characterized by the PBPK model (see Section 3.5). For most endpoints, sufficient information on the role of metabolites or mode of action was not available to identify likely relevant dose-metrics, and more "upstream" metrics representing either parent compound or total metabolism had to be used. The "primary" or "preferred" dose-metric referred to in subsequent tables has the greater biological support for its involvement in toxicity, whereas "alternative" dose-metrics are those that may also be plausibly involved (discussed further below). A discussion of the dose-metrics selected for particular noncancer endpoints follows.

#### 5.1.3.1.1. Kidney toxicity (meganucleocytosis, increased kidney weight, toxic nephropathy)

As discussed in Sections 4.4.6–4.4.7, there is sufficient evidence to conclude that TCE-induced kidney toxicity is caused predominantly by GSH conjugation metabolites either produced in situ in or delivered systemically to the kidney. As discussed in Section 3.3.3.2, bioactivation of DCVG, DCVC, and *N*-acetyl-S-(1,2-dichlorovinyl)-L-cysteine (NAcDCVC) within the kidney, either by beta-lyase, flavin mono-oxygenase (FMO), or CYP, produces reactive species, any or all of which may cause nephrotoxicity. Therefore, multiple lines of evidence support the conclusion that renal bioactivation of DCVC is the preferred basis for internal dose extrapolations for TCE-induced kidney toxicity. However, uncertainties remain as to the relative contribution from each bioactivation pathway; and quantitative clearance data necessary to calculate the concentration of each species are lacking. Moreover, the estimates of the amount bioactivated are indirect, derived from the difference between overall GSH conjugation flux and NAcDCVC excretion (see Section 3.5.7.3.1).

Under the cross-species scaling methodology, the rate of renal bioactivation of DCVC would be scaled by body weight to the  $\frac{3}{4}$  power. However, it is necessary to consider whether there are adequate data to support use of the alternative scaling by target tissue mass. For the beta-lyase pathway, Dekant et al. (1988) reported in trapping experiments that the postulated reactive metabolites decompose to stable (unreactive) metabolites in the presence of water. Moreover, the necessity of a chemical trapping mechanism to detect the reactive metabolites suggests a very rapid reaction such that it is unlikely that the reactive metabolites leave the site of production. Therefore, these data support the conclusion that, for this bioactivation pathway, clearance is chemical in nature and hence species-independent. If this were the only bioactivation pathway, then scaling by kidney weight would be supported. With respect to the FMO bioactivation pathway, Sausen and Elfarra (1991) reported that after direct dosing of the postulated reactive sulfoxide (DCVC sulfoxide), the sulfoxide was detected as an excretion product in bile. These data suggest that reactivity in the tissue to which the sulfoxide was delivered (the liver, in this case) is insufficient to rule out a significant role for enzymatic or other biologically mediated systemic clearance. Therefore, according to the criteria outlined above, for this bioactivation pathway, the data support scaling the rate of metabolism by body weight to the  $\frac{3}{4}$  power. For P450-mediated bioactivation producing NAcDCVC sulfoxide, the only relevant data on clearance are from a study of the structural analogue to DCVC, fluoromethyl-2,2-difluoro-1-(trifluoromethyl)vinyl ether (FDVE) (Sheffels et al., 2004), which reported that the postulated reactive sulfoxide was detected in urine. This suggests that the sulfoxide is sufficiently stable to be excreted by the kidney and supports the scaling of the rate of metabolism by body weight to the  $\frac{3}{4}$  power.

Therefore, because the contributions to TCE-induced nephrotoxicity from each possible bioactivation pathway are not clear, and the scaling by body weight to the  $\frac{3}{4}$  power is supported

for two of the identified three bioactivation pathways, it is decided here to scale the DCVC bioactivation rate by body weight to the  $\frac{3}{4}$  power. The primary internal dose-metric for TCE-induced kidney toxicity is thus, the weekly rate of DCVC bioactivation per unit body weight to the  $\frac{3}{4}$  power (**ABioactDCVCBW34 [mg/kg<sup>3/4</sup>/week]**). However, it should be noted that due to the larger relative kidney weight in rats as compared to humans, scaling by kidney weight instead of body weight to the  $\frac{3}{4}$  power would only change the quantitative interspecies extrapolation by about twofold,<sup>33</sup> so the sensitivity of the results to the scaling choice is relatively small. In addition, quantitative estimates for this dose-metric are only available in rats and humans, and not in mice. Accordingly, this metric was only used for extrapolating results from rat toxicity studies.

An alternative dose-metric that also involves the GSH conjugation pathway is the amount of GSH conjugation scaled by the  $\frac{3}{4}$  power of body weight (**AMetGSHBW34 [mg/kg<sup>3/4</sup>/week]**). This dose-metric uses the total flux of GSH conjugation as the toxicologically-relevant dose, and, thus, incorporates any direct contributions from DCVG and DCVC, which are not addressed in the DCVC bioactivation metric. The rationale for scaling by body weight to the  $\frac{3}{4}$  power rather than target tissue mass is the same as above. Because of the lack of availability of the DCVC bioactivation dose-metric in mice, the GSH conjugation metric is used as the primary dose-metric for the nephrotoxicity endpoint in studies of mice.

Another alternative dose-metric is the total amount of TCE metabolism (oxidation and GSH conjugation together) scaled by the  $\frac{3}{4}$  power of body weight (**TotMetabBW34 [mg/kg<sup>3/4</sup>/week]**). This dose-metric uses the total flux of TCE metabolism as the toxicologically relevant dose, and, thus, incorporates the possible involvement of oxidative metabolites, acting either additively or interactively, in addition to GSH conjugation metabolites in nephrotoxicity (see Section 4.4.6). However, this dose-metric is given less weight than those involving GSH conjugation because, as discussed in Sections 4.4.6, the weight of evidence supports the conclusion that GSH conjugation metabolites play a predominant role in nephrotoxicity. The rationale for scaling by body weight to the  $\frac{3}{4}$  power rather than target tissue mass is the same as above.

#### **5.1.3.1.2. Liver weight increases (hepatomegaly)**

As discussed in Section 4.5.6, there is substantial evidence that oxidative metabolism is involved in TCE hepatotoxicity, based primarily on similarities in noncancer effects with a number of oxidative metabolites of TCE (e.g., CH, TCA, and DCA). While TCA is a stable, circulating metabolite, CH and DCA are relatively short-lived, although enzymatically cleared (see Section 3.3.3.1). As discussed in Section 4.5.6.2.1, there is substantial evidence that TCA

---

<sup>33</sup>The range of the difference is 2.1–2.4-fold using the posterior medians for the relative kidney weight in rats and humans from the PBPK model described in Section 3.5 (see Table 3-38), and body weights of 0.3–0.4 kg for rats and 60–70 kg for humans.

alone does not adequately account for the hepatomegaly induced by TCE; therefore, unlike in previous dose-response analyses ([Clewell and Andersen, 2004](#); [Barton and Clewell, 2000](#)), the AUC of TCA in plasma or in liver were not considered as dose-metrics. However, there are inadequate data across species to quantify the dosimetry of CH and DCA, and other intermediates of oxidative metabolism (such as TCE-oxide or dichloroacetylchloride) may be involved in hepatomegaly. Thus, due to uncertainties as to the active moiety(ies), but given the strong evidence associating TCE liver effects with oxidative metabolism in the liver, hepatic oxidative metabolism is the preferred basis for internal dose extrapolations of TCE-induced liver weight increases.

Under the cross-species scaling methodology, the rate of hepatic oxidative metabolism would be scaled by body weight to the  $3/4$  power. However, it is necessary to consider whether there are adequate data to support use of the alternative scaling by target tissue mass. Several of the oxidative metabolites are stable and systemically available, and several of those that are cleared rapidly are metabolized enzymatically, so, according to the criteria discussed above, there are insufficient data to support the conclusions that the active moiety or moieties do not leave the target tissue in appreciable quantities and are cleared by mechanisms whose rates are independent of body weight.

Therefore, the primary internal dose-metric for TCE-induced liver weight changes is selected to be the weekly rate of hepatic oxidation per unit body weight to the  $3/4$  power (AMetLiv1BW $^{3/4}$  [mg/kg $^{3/4}$ /week]). The use of this dose-metric is also supported by the analysis in Section 4.5.6.2.1 showing much more consistency in the dose-response relationships for TCE-induced hepatomegaly across studies and routes of exposure using this metric and the total oxidative metabolism dose-metric (discussed below) as compared to the AUC of TCE in blood. It should be noted that due to the larger relative liver weight in mice as compared to humans, scaling by liver weight instead of body weight to the  $3/4$  power would only change the quantitative interspecies extrapolation by about fourfold,<sup>34</sup> so the sensitivity of the results to the scaling choice is relatively modest.

It is also known that the lung has substantial capacity for oxidative metabolism, with some proportion of the oxidative metabolites produced there entering systemic circulation. Thus, it is possible that extrahepatic oxidative metabolism can contribute to TCE-induced hepatomegaly. Therefore, the total amount of oxidative metabolism of TCE scaled by the  $3/4$  power of body weight (**TotOxMetabBW $^{3/4}$  [mg/kg $^{3/4}$ /week]**) was selected as an alternative dose-metric (the rationale for the body weight to the  $3/4$  power scaling is analogous to that for hepatic oxidative metabolism, above).

---

<sup>34</sup>The range of the difference is 3.5–3.9-fold using the posterior medians for the relative liver weight in mice and humans from the PBPK model described in Section 3.5 (see Table 3-37), and body weights of 0.03–0.04 kg for mice and 60–70 kg for humans.

#### **5.1.3.1.3. Developmental toxicity—heart malformations**

As discussed in Section 4.8.3.2.1, several studies have reported that the prenatal exposure to TCE oxidative metabolites TCA or DCA also induces heart malformations, suggesting that oxidative metabolism is involved in TCE-induced heart malformations. However, there are inadequate data across species to quantify the dosimetry of DCA, and it is unclear if other products of TCE oxidative metabolism are involved. Therefore, the total amount of oxidative metabolism of TCE scaled by the  $3/4$  power of body weight (TotOxMetabBW $^{3/4}$  [mg/kg $^{3/4}$ /week]) was selected as the primary dose-metric. The rationale for the scaling by body weight to the  $3/4$  power is analogous to that for hepatic oxidative metabolism, above.

An alternative dose-metric that is considered here is the AUC of TCE in (maternal) blood (AUCCBld [mg-hour/L/day]). The placenta is a highly perfused tissue, and TCE is known to cross the placenta to the fetus, with rats showing similar (within twofold) maternal and fetal blood TCE concentrations (see Section 3.2). This dose-metric accounts for the possible roles either of local metabolism or of TCE itself.

#### **5.1.3.1.4. Reproductive toxicity—decreased ability of sperm to fertilize oocytes**

The decreased ability of sperm to fertilize oocytes observed by DuTeaux et al. (2004a) occurred in the absence of changes in combined testes/epididymes weight, sperm concentration or motility, or histological changes in the testes or epididymes. However, there was evidence of oxidative damage to the sperm, and DuTeaux et al. (2003) previously reported the ability of the rat epididymis and efferent ducts to metabolize TCE oxidatively. Based on this evidence, DuTeaux et al. (2004a) hypothesized that the decreased ability to fertilize is due to oxidative damage to the sperm from local metabolism. Thus, the primary dose-metric for this endpoint is selected to be the AUC of TCE in blood (AUCCBld [mg-hour/L/day]), based on the assumption that in situ oxidation of systemically-delivered TCE (the flow rate of which scales as body weight to the  $3/4$  power) is the determinant of toxicity.

Because metabolites causing oxidative damage may be delivered systemically to the target tissue, an alternative dose-metric that is considered here is total oxidative metabolism of TCE scaled by the  $3/4$  power of body weight (TotOxMetabBW $^{3/4}$  [mg/kg $^{3/4}$ /day]). The rationale for the scaling by body weight to the  $3/4$  power is analogous to that for hepatic oxidative metabolism, above. Because oxidative metabolites make up the majority of TCE metabolism, total metabolism gives very similar results (within 1.2-fold) to total oxidative metabolism and is therefore not included as a dose-metric.

#### **5.1.3.1.5. Other reproductive and developmental effects and neurological effects and immunologic effects**

For all other candidate critical endpoints listed in Tables 5-11 and 5-12, including developmental effects other than heart malformations and reproductive effects other than

decreased ability of sperm to fertilize, there is insufficient information for site-specific determinations of an appropriate dose-metric. While TCE metabolites and/or metabolizing enzymes have been reported in some of these tissues (e.g., male reproductive tract), their general roles in toxicity in the respective tissues have not been established. The choice of total metabolism as the primary dose-metric is based on the observation that, in general, TCE toxicity is associated with metabolism rather than the parent compound. It is acknowledged that there is no compelling evidence that definitively establishes one metric as more plausible than the other in any particular case. Nonetheless, as a general inference in the absence of specific data, total metabolism is viewed as more likely to be involved in toxicity than the concentration of TCE itself.

Therefore, given that the majority of the toxic and carcinogenic responses in many tissues to TCE appears to be associated with metabolism, the primary dose-metric is selected to be total metabolism of TCE scaled by the  $3/4$  power of body weight (TotMetabBW $^{3/4}$  [mg/kg $^{3/4}$ /day]). The rationale for the scaling by body weight to the  $3/4$  power is analogous to that for the other metabolism dose-metrics, above. Because oxidative metabolites make up the majority of TCE metabolism, total oxidative metabolism gives very similar results (within 1.2-fold) to total metabolism and is therefore not included as a dose-metric.

An alternative dose-metric that is considered here is the AUC of TCE in blood (AUCCBld [mg-hour/L/day]). This dose-metric would account for the possible role of local metabolism, which is determined by TCE delivered in blood via systemic circulation to the target tissue (the flow rate of which scales as body weight to the  $3/4$  power), and the possible role of TCE itself. This dose-metric would also be most applicable to tissues that have similar tissue:blood partition coefficients across and within species.

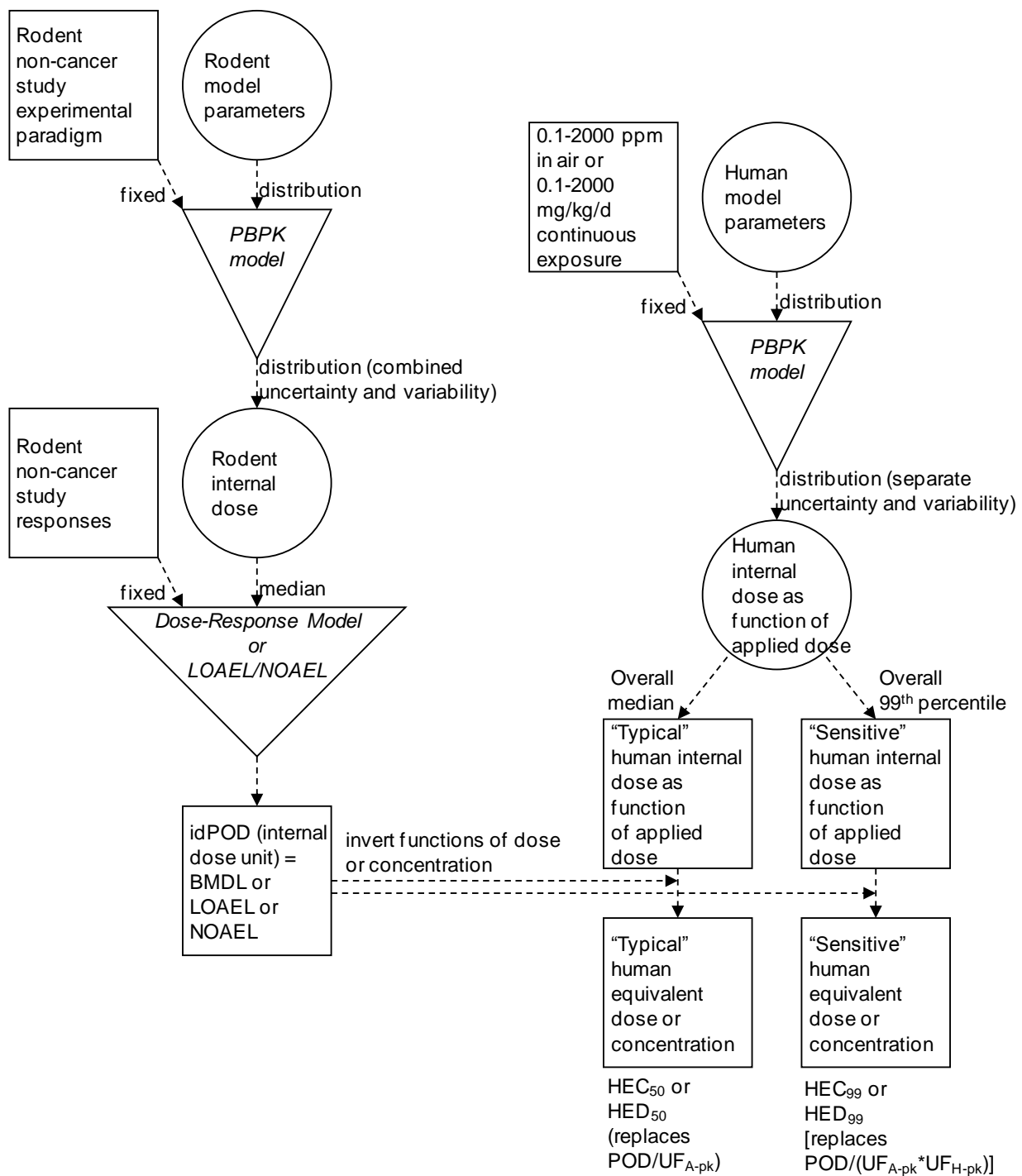
Because the PBPK model described in Section 3.5 did not include a fetal compartment, the maternal internal dose-metric is taken as a surrogate for developmental effects in which exposure was before or during pregnancy ([Johnson et al., 2003](#); [Narotsky et al., 1995](#); [Fredriksson et al., 1993](#); [Taylor et al., 1985](#)). This was considered reasonable because TCE and the major circulating metabolites (TCA and TCOH) appear to cross the placenta (see Sections 3.2, 3.3, and 4.10 ([Fisher et al., 1989](#); [Ghantous et al., 1986](#))), and maternal metabolizing capacity is generally greater than that of the fetus (see Section 4.10). In the cases where exposure continues after birth ([Peden-Adams et al., 2006](#); [Isaacson and Taylor, 1989](#)), no PBPK model-based internal dose was used. Because of the complicated fetus/neonate dosing that includes transplacental, lactational, and direct (if dosing continues postweaning) exposure, the maternal internal dose is no more accurate a surrogate than applied dose in this case.

### 5.1.3.2. Methods for Inter- and Intraspecies Extrapolation Using Internal Doses<sup>35</sup>

As shown in Figures 5-2 and 5-3, the general approach taken to use the internal dose-metrics in deriving HECs and HEDs was to first apply the rodent PBPK model to get rodent values for the dose-metrics corresponding to the applied doses in a study reporting noncancer effects. The idPOD is then obtained either directly from the internal dose corresponding to the applied dose LOAEL or NOAEL, or by dose-response modeling of responses with respect to the internal doses to derive a BMDL in terms of internal dose. Separately, the human PBPK model is run for a range of continuous exposures from  $10^{-1}$  to  $2 \times 10^3$  ppm or mg/kg/day to obtain the relationship between human exposure and internal dose for the same dose-metric used for the rodent. The human equivalent exposure (HEC or HED) corresponding to the idPOD is derived by interpolation. It should be noted that median values of dose-metrics were used for rodents, whereas both median and 99<sup>th</sup> percentile values were used for humans. As discussed in Section 3.5, the rodent population model characterizes study-to-study variation, while, within a study, animals with the same sex/species/strain combination were assumed to be identical pharmacokinetically and represented by the group average (typically the only data reported). Therefore, use of median dose-metric values can be interpreted as assuming that the animals in the noncancer toxicity study were all “typical” animals and the idPOD is for a rodent that is pharmacokinetically “typical.” In practice, the use of median or mean internal doses for rodents did not make much difference except when the uncertainty in the rodent dose-metric was high. The impact of the uncertainty in the rodent PBPK dose-metrics is analyzed quantitatively in Section 5.1.4.2.

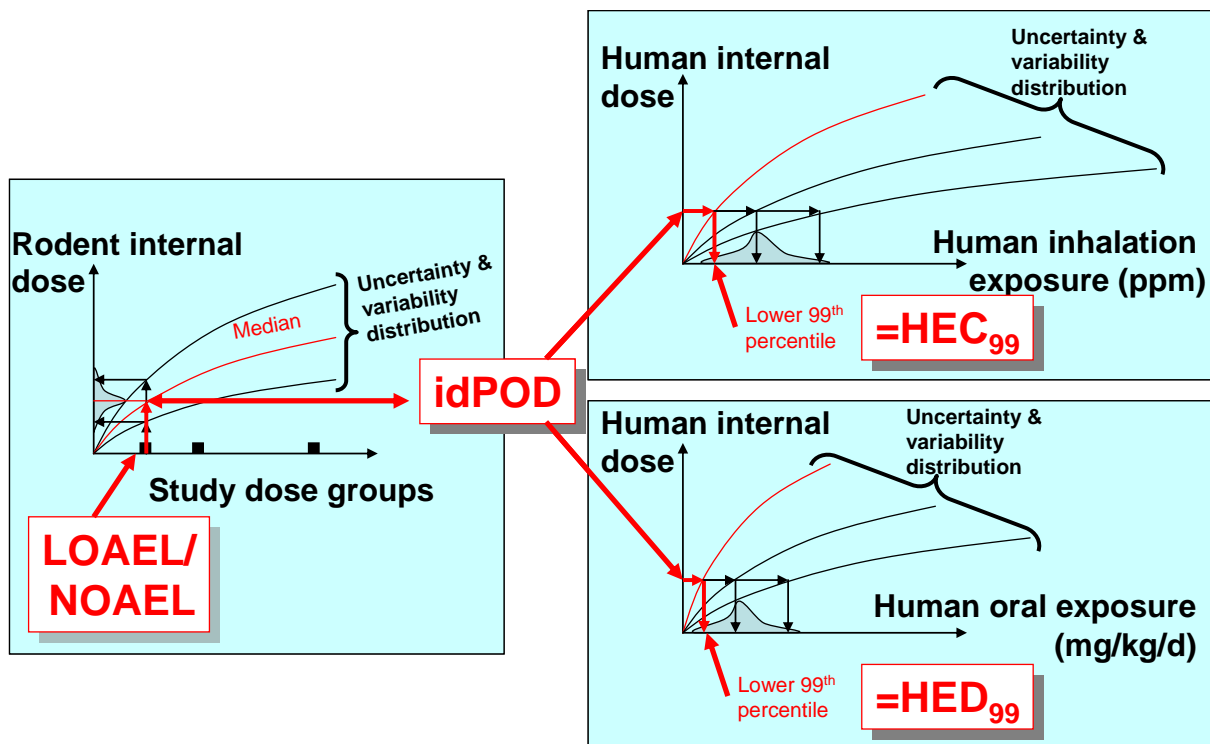
---

<sup>35</sup>An alternative approach (e.g., Clewell et al., 1995) applies the UFs to the internal dose prior to using the human PBPK model to derive a human exposure level. As noted by Barton and Clewell (2000) for previous TCE PBPK models, because the human PBPK model for TCE is linear for all the dose metrics over very broad dose and concentration ranges, essentially identical results would be obtained using this alternative approach. Specifically, for all the primary dose metrics, the difference in the two approaches is less than two-fold, with the results from the critical studies differing by <0.1%. For some studies using AUCBld as an alternative dose metric, the difference ranged from three- to -sevenfold. Overall, use of the alternative approach would not significantly change the noncancer dose-response assessment of TCE, and the derived RfC and RfD would be identical.



Square nodes indicate point values, circle nodes indicate distributions, and the inverted triangle indicates a (deterministic) functional relationship.

**Figure 5-2. Flow-chart for dose-response analyses of rodent noncancer effects using PBPK model-based dose-metrics.**



In the case where BMD modeling is performed, the applied dose values are replaced by the corresponding median internal dose estimate, and the idPOD is the modeled BMDL in internal dose units.

**Figure 5-3. Schematic of combined interspecies, intraspecies, and route-to-route extrapolation from a rodent study LOAEL or NOAEL.**

The human population model characterizes individual-to-individual variation, in addition to its uncertainty. The “median” value for the HEC or HED was calculated as a point of comparison but was not actually used for derivation of candidate reference values. Because the RfC and RfD are intended to characterize the dose below which a sensitive individual would likely not experience adverse effects, the overall 99<sup>th</sup> percentile of the combined uncertainty and variability distribution was used for deriving the HEC and HED (denoted HEC<sub>99</sub> and HED<sub>99</sub>) from each idPOD.<sup>36</sup> As shown in Figures 5-2 and 5-3, the HEC<sub>99</sub> or HED<sub>99</sub> replaces the quantity  $POD/(UF_{A-pk} \times UF_{H-pk})$  in the calculation of the RfC or RfD (i.e., the pharmacokinetic components of the UFs representing interspecies extrapolation and human interindividual variability).

As calculated, the extrapolated HEC<sub>99</sub> and HED<sub>99</sub> can be interpreted as being the dose or exposure for which there is 99% likelihood that a randomly selected individual will have an internal dose less than or equal to the idPOD derived from the rodent study. By contrast, the HEC<sub>50</sub> and HED<sub>50</sub> can be interpreted as being the dose or exposure for which there is 50% likelihood that a randomly selected individual will have an internal dose less than or equal to the idPOD derived from the rodent study. Values of HEC<sub>99</sub> or HED<sub>99</sub> are shown for each study and dose-metric considered in Tables 5-13 through 5-18. In addition, values of HEC<sub>50</sub> or HED<sub>50</sub> are shown for comparison, to give a sense of the difference between the median and the 99% confidence bound for combined uncertainty and variability. The separate contributions of uncertainty and variability in the human PBPK model are analyzed quantitatively, along with the uncertainty in the rodent PBPK dose-metrics as mentioned above, in Section 5.1.4.2.

---

<sup>36</sup>While for uncertainty, a 95<sup>th</sup> percentile is often selected by convention, there is no explicit guidance on the selection of the percentile for human toxicokinetic variability. Ideally, all sources of uncertainty and variability would be included, and percentile selected that is more in line with the levels of risk at which cancer dose-response is typically characterized (e.g., 10<sup>-6</sup> to 10<sup>-4</sup>) along with a level of confidence. However, only toxicokinetic uncertainty and variability is assessed quantitatively. Because the distribution here incorporates both uncertainty and variability simultaneously, a percentile higher than the 95<sup>th</sup> (a conventional choice for uncertainty *only*) was selected. However, percentiles greater than the 99<sup>th</sup> percentile are likely to be progressively less reliable due to the unknown shape of the tail of the input uncertainty and variability distributions for the PBPK model parameters (which were largely assumed to be normal or lognormal), and the fact that only 42 individuals were incorporated in the PBPK model for characterization of uncertainty and inter-individual variability (see Section 3.5). This concern is somewhat ameliorated because the candidate reference values also incorporate use of UFs to account for inter- and intraspecies toxicodynamic sensitivity.

**Table 5-13. cRfCs and cRfDs (based on applied dose) and p-cRfCs and p-cRfDs (based on PBPK modeled internal dose-metrics) for candidate critical neurological effects**

Effect type Candidate critical studies <sup>a</sup>	Species	POD type	HEC <sub>50</sub> or HED <sub>50</sub>	POD, HEC <sub>99</sub> , or HED <sub>99</sub> <sup>b</sup>	UF <sub>S</sub>	UF <sub>A</sub>	UF <sub>H</sub>	UF <sub>L</sub>	UF <sub>D</sub>	UF <sup>c</sup>	cRfC or p-cRfC (ppm)	cRfD or p-cRfD (mg/kg/d)	Candidate critical effect; comments [dose-metric]
<b>Trigeminal nerve effects</b>													
Ruijten et al. (1991)	Human	LOAEL		14	1	1	10	3	1	30	0.47		Trigeminal nerve effects
		HEC	14	5.3	1	1	3	3	1	10	0.53		[TotMetabBW34]
		HEC	14	8.3	1	1	3	3	1	10	0.83		[AUCCBld]
		HED	7.4	7.3	1	1	3	3	1	10		0.73	[TotMetabBW34] (route-to-route)
		HED	59	14	1	1	3	3	1	10		1.4	[AUCCBld] (route-to-route)
<b>Cognitive effects</b>													
Isaacson et al. (1990)	Rat	LOAEL		47	10	10	10	10	1	10,000 <sup>d</sup>		0.0047	demyelination in hippocampus
		HED	9.4	9.2	10	3	3	10	1	1,000		0.0092	[TotMetabBW34]
		HED	31	4.3	10	3	3	10	1	1,000		0.0043	[AUCCBld]
		HEC	18	7.1	10	3	3	10	1	1,000	0.0071		[TotMetabBW34] (route-to-route)
		HEC	3.8	2.3	10	3	3	10	1	1,000	0.0023		[AUCCBld] (route-to-route)
<b>Mood and sleep disorders</b>													
Arito et al. (1994)	Rat	LOAEL		12	3	3	10	10	1	1,000	0.012		Changes in wakefulness
		HEC	13	4.8	3	3	3	10	1	300	0.016		[TotMetabBW34]
		HEC	15	9.0	3	3	3	10	1	300	0.030		[AUCCBld]
		HED	6.6	6.5	3	3	3	10	1	300		0.022	[TotMetabBW34] (route-to-route)
		HED	65	15	3	3	3	10	1	300		0.051	[AUCCBld] (route-to-route)

**Table 5-13. cRfCs and cRfDs (based on applied dose) and p-cRfCs and p-cRfDs (based on PBPK modeled internal dose-metrics) for candidate critical neurological effects (continued)**

Effect type Candidate critical studies <sup>a</sup>	Species	POD type	HEC <sub>50</sub> or HED <sub>50</sub>	POD, HEC <sub>99</sub> , or HED <sub>99</sub> <sup>b</sup>	UF <sub>S</sub>	UF <sub>A</sub>	UF <sub>H</sub>	UF <sub>L</sub>	UF <sub>D</sub>	UF <sup>c</sup>	cRfC or p-cRfC (ppm)	cRfD or p-cRfD (mg/kg/d)	Candidate critical effect; comments [dose-metric]
<b>Other neurological effects</b>													
Kjellstrand et al. (1987)	Rat	LOAEL		300	10	3	10	10	1	3,000	0.10		↓ regeneration of sciatic nerve
		HEC	274	93	10	3	3	10	1	1,000	0.093		[TotMetabBW34]
		HEC	487	257	10	3	3	10	1	1,000	0.26		[AUCCBld]
		HED	110	97	10	3	3	10	1	1,000		0.097	[TotMetabBW34] (route-to-route)
		HED	436	142	10	3	3	10	1	1,000		0.14	[AUCCBld] (route-to-route)
	Mouse	LOAEL		150	10	3	10	10	1	3,000	0.050		↓ regeneration of sciatic nerve
		HEC	378	120	10	3	3	10	1	1,000	0.12		[TotMetabBW34]
		HEC	198	108	10	3	3	10	1	1,000	0.11		[AUCCBld]
		HED	145	120	10	3	3	10	1	1,000		0.12	[TotMetabBW34] (route-to-route)
		HED	237	76	10	3	3	10	1	1,000		0.076	[AUCCBld] (route-to-route)
Gash et al. (2008)	Rat	LOAEL		710	10	10	10	10	1	10,000 <sup>d</sup>		0.071	degeneration of dopaminergic neurons
		HED	56	53	10	3	3	10	1	1,000		0.053	[TotMetabBW34]
		HED	571	192	10	3	3	10	1	1,000		0.19	[AUCCBld]
		HEC	126	47	10	3	3	10	1	1,000	0.047		[TotMetabBW34] (route-to-route)
		HEC	679	363	10	3	3	10	1	1,000	0.36		[AUCCBld] (route-to-route)

<sup>a</sup>Shaded rows represent the p-cRfC or p-cRfD using the preferred PBPK model dose-metric.

<sup>b</sup>Applied dose POD adjusted to continuous exposure unless otherwise noted. POD, HEC<sub>99</sub>, and HED<sub>99</sub> have same units as cRfC (ppm) or cRfD (mg/kg/day).

<sup>c</sup>Product of individual UFs, rounded to 3, 10, 30, 100, 300, 1,000, 3,000, or 10,000 [see Footnote d below].

<sup>d</sup>EPA's report on the RfC and RfD processes (U.S. EPA, 2002b) recommends not deriving reference values with a composite UF of >3,000; however, composite UFs exceeding 3,000 are considered here because the derivation of the cRfCs and cRfDs is part of a screening process and the application of the PBPK model for candidate critical effects reduces the values of some of the individual UFs for the p-cRfCs and p-cRfDs.

UF<sub>S</sub> = subchronic-to-chronic UF; UF<sub>A</sub> = interspecies UF; UF<sub>H</sub> = human variability UF; UF<sub>L</sub> = LOAEL-to-NOAEL UF; UF<sub>D</sub> = database UF

**Table 5-14. cRfCs and cRfDs (based on applied dose) and p-cRfCs and p-cRfDs (based on PBPK modeled internal dose-metrics) for candidate critical kidney effects**

Effect type Candidate critical studies <sup>a</sup>	Species	POD type	HEC <sub>50</sub> or HED <sub>50</sub>	POD, HEC <sub>99</sub> , or HED <sub>99</sub> <sup>b</sup>	UF <sub>S</sub>	UF <sub>A</sub>	UF <sub>H</sub>	UF <sub>L</sub>	UF <sub>D</sub>	UF <sup>c</sup>	cRfC or p-cRfC (ppm)	cRfD or p-cRfD (mg/kg/d)	Candidate critical effect; comments [dose-metric]
<b>Histological changes in kidney</b>													
Maltoni (1986) (inhalation)	Rat	BMDL		40.2	1	3	10	1	1	30	1.3		meganucleocytosis; BMR = 10%
		HEC	0.28	0.038	1	3	3	1	1	10	0.0038		[ABioactDCVCBW34]
		HEC	0.45	0.058	1	3	3	1	1	10	0.0058		[AMetGSHBW34]
		HEC	39	15.3	1	3	3	1	1	10	1.5		[TotMetabBW34]
		HED	0.22	0.023	1	3	3	1	1	10		0.0023	[ABioactDCVCBW34] (route-to-route)
		HED	0.35	0.036	1	3	3	1	1	10		0.0036	[AMetGSHBW34] (route-to-route)
		HED	19	19	1	3	3	1	1	10		1.9	[TotMetabBW34] (route-to-route)
NCI (1976)	Mouse	LOAEL		620	1	10	10	30	1	3,000		0.21	toxic nephrosis
		HED	2.9	0.30	1	3	3	30	1	300		0.00101	[AMetGSHBW34]
		HED	51	48	1	3	3	30	1	300		0.160	[TotMetabBW34]
		HEC	3.9	0.50	1	3	3	30	1	300	0.00165		[AMetGSHBW34] (route-to-route)
		HEC	113	42	1	3	3	30	1	300	0.140		[TotMetabBW34] (route-to-route)

**Table 5-14. cRfCs and cRfDs (based on applied dose) and p-cRfCs and p-cRfDs (based on PBPK modeled internal dose-metrics) for candidate critical kidney effects (continued)**

Effect type Candidate critical studies <sup>a</sup>	Species	POD type	HEC <sub>50</sub> or HED <sub>50</sub>	POD, HEC <sub>99</sub> , or HED <sub>99</sub> <sup>b</sup>	UF <sub>S</sub>	UF <sub>A</sub>	UF <sub>H</sub>	UF <sub>L</sub>	UF <sub>D</sub>	UF <sup>c</sup>	cRfC or p-cRfC (ppm)	cRfD or p-cRfD (mg/kg/d)	Candidate critical effect; comments [dose-metric]
<b>Histological changes in kidney</b>													
NTP (1988)	Rat	BMDL		9.45	1	10	10	1	1	100		0.0945	Toxic nephropathy; BMR = 5%; female Marshall (most sensitive sex/strain)
		HED	0.033	0.0034	1	3	3	1	1	10		0.00034	[ABioactDCVCBW34]
		HED	0.053	0.0053	1	3	3	1	1	10		0.00053	[AMetGSHBW34]
		HED	0.75	0.74	1	3	3	1	1	10		0.074	[TotMetabBW34]
		HEC	0.042	0.0056	1	3	3	1	1	10	0.00056		[ABioactDCVCBW34] (route-to-route)
		HEC	0.067	0.0087	1	3	3	1	1	10	0.00087		[AMetGSHBW34] (route-to-route)
		HEC	1.4	0.51	1	3	3	1	1	10	0.051		[TotMetabBW34] (route-to-route)
Maltoni (1986) (oral)	Rat	BMDL		34	1	10	10	1	1	100		0.34	meganucleocytosis; BMR = 10%
		HED	0.15	0.015	1	3	3	1	1	10		0.0015	[ABioactDCVCBW34]
		HED	0.25	0.025	1	3	3	1	1	10		0.0025	[AMetGSHBW34]
		HED	11	11	1	3	3	1	1	10		0.11	[TotMetabBW34]
		HEC	0.19	0.025	1	3	3	1	1	10	0.0025		[ABioactDCVCBW34] (route-to-route)
		HEC	0.31	0.041	1	3	3	1	1	10	0.0041		[AMetGSHBW34] (route-to-route)
		HEC	22	8.5	1	3	3	1	1	10	0.85		[TotMetabBW34] (route-to-route)

**Table 5-14. cRfCs and cRfDs (based on applied dose) and p-cRfCs and p-cRfDs (based on PBPK modeled internal dose-metrics) for candidate critical kidney effects (continued)**

Effect type Candidate critical studies <sup>a</sup>	Species	POD type	HEC <sub>50</sub> or HED <sub>50</sub>	POD, HEC <sub>99</sub> , or HED <sub>99</sub> <sup>b</sup>	UF <sub>S</sub>	UF <sub>A</sub>	UF <sub>H</sub>	UF <sub>L</sub>	UF <sub>D</sub>	UF <sup>c</sup>	cRfC or p-cRfC (ppm)	cRfD or p-cRfD (mg/kg/d)	Candidate critical effect; comments [dose-metric]
<b>↑ Kidney/body weight ratio</b>													
Kjellstrand et al. (1983b)	Mouse	BMDL		34.7	1	3	10	1	1	30	1.2		BMR = 10%
		HEC	0.88	0.12	1	3	3	1	1	10	0.012		[AMetGSHBW34]
		HEC	52	21	1	3	3	1	1	10	2.1		[TotMetabBW34]
		HED	0.69	0.070	1	3	3	1	1	10		0.0070	[AMetGSHBW34] (route-to-route)
		HED	25	25	1	3	3	1	1	10		2.5	[TotMetabBW34] (route-to-route)
Woolhiser et al. (2006)	Rat	BMDL		15.7	1	3	10	1	1	30	0.52		BMR = 10%
		HEC	0.099	0.013	1	3	3	1	1	10	0.0013		[ABioactDCVCBW34]
		HEC	0.17	0.022	1	3	3	1	1	10	0.0022		[AMetGSHBW34]
		HEC	29	11	1	3	3	1	1	10	1.1		[TotMetabBW34]
		HED	0.078	0.0079	1	3	3	1	1	10		0.00079	[ABioactDCVCBW34] (route-to-route)
		HED	0.13	0.013	1	3	3	1	1	10		0.0013	[AMetGSHBW34] (route-to-route)
		HED	14	14	1	3	3	1	1	10		1.4	[TotMetabBW34] (route-to-route)

<sup>a</sup>Shaded rows represent the p-cRfC or p-cRfD using the preferred PBPK model dose-metric.

<sup>b</sup>Applied dose POD adjusted to continuous exposure unless otherwise noted. POD, HEC<sub>99</sub>, and HED<sub>99</sub> have same units as cRfC or cRfD.

<sup>c</sup>Product of individual UFs, rounded to 3, 10, 30, 100, 300, 1,000, or 3,000.

UF<sub>S</sub> = subchronic-to-chronic UF; UF<sub>A</sub> = interspecies UF; UF<sub>H</sub> = human variability UF; UF<sub>L</sub> = LOAEL-to-NOAEL UF; UF<sub>D</sub> = database UF

**Table 5-15. cRfCs and cRfDs (based on applied dose) and p-cRfCs and p-cRfDs (based on PBPK modeled internal dose-metrics) for candidate critical liver effects**

Effect type Candidate critical studies <sup>a</sup>	Species	POD type	HEC <sub>50</sub> or HED <sub>50</sub>	POD, HEC <sub>99</sub> , or HED <sub>99</sub> <sup>b</sup>	UF <sub>S</sub>	UF <sub>A</sub>	UF <sub>H</sub>	UF <sub>L</sub>	UF <sub>D</sub>	UF <sup>c</sup>	cRfC or p-cRfC (ppm)	cRfD or p-cRfD (mg/kg/d)	Candidate critical effect; comments [dose-metric]
<b>↑ Liver/body weight ratio</b>													
Kjellstrand et al. (1983b)	Mouse	BMDL		21.6	1	3	10	1	1	30	0.72		BMR = 10% increase
		HEC	25	9.1	1	3	3	1	1	10	0.91		[AMetLiv1BW34]
		HEC	75	24.9	1	3	3	1	1	10	2.5		[TotOxMetabBW34]
		HED	9.0	7.9	1	3	3	1	1	10		0.79	[AMetLiv1BW34] (route-to-route)
		HED	32	25.7	1	3	3	13	1	10		2.6	[TotOxMetabBW34] (route-to-route)
Woolhiser et al. (2006)	Rat	BMDL		25	1	3	10	1	1	30	0.83		BMR = 10% increase
		HEC	53	19	1	3	3	1	1	10	1.9		[AMetLiv1BW34]
		HEC	46	16	1	3	3	1	1	10	1.6		[TotOxMetabBW34]
		HED	19	16	1	3	3	1	1	10		1.6	[AMetLiv1BW34] (route-to-route)
		HED	20	17	1	3	3	1	1	10		1.7	[TotOxMetabBW34] (route-to-route)
Buben and O'Flaherty (1985)	Mouse	BMDL		82	1	10	10	1	1	100		0.82	BMR = 10% increase
		HED	12	10	1	3	3	1	1	10		1.0	[AMetLiv1BW34]
		HED	15	13	1	3	3	1	1	10		1.3	[TotOxMetabBW34]
		HEC	32	11	1	3	3	1	1	10	1.1		[AMetLiv1BW34] (route-to-route)
		HEC	34	11	1	3	3	1	1	10	1.1		[TotOxMetabBW34] (route-to-route)

<sup>a</sup>Shaded rows represent the p-cRfC or p-cRfD using the preferred PBPK model dose-metric.

<sup>b</sup>Applied dose POD adjusted to continuous exposure unless otherwise noted. POD, HEC<sub>99</sub>, and HED<sub>99</sub> have same units as cRfC (ppm) or cRfD (mg/kg/day).

<sup>c</sup>Product of individual UFs, rounded to 3, 10, 30, 100, 300, 1,000, or 3,000.

UF<sub>S</sub> = subchronic-to-chronic UF; UF<sub>A</sub> = interspecies UF; UF<sub>H</sub> = human variability UF; UF<sub>L</sub> = LOAEL-to-NOAEL UF; UF<sub>D</sub> = database UF

**Table 5-16. cRfCs and cRfDs (based on applied dose) and p-cRfCs and p-cRfDs (based on PBPK modeled internal dose-metrics) for candidate critical immunological effects**

Effect type Candidate critical studies <sup>a</sup>	Species	POD type	HEC <sub>50</sub> or HED <sub>50</sub>	POD, HEC <sub>99</sub> , or HED <sub>99</sub> <sup>b</sup>	UF <sub>S</sub>	UF <sub>A</sub>	UF <sub>H</sub>	UF <sub>L</sub>	UF <sub>D</sub>	UF <sup>c</sup>	cRfC or p-cRfC (ppm)	cRfD or p-cRfD (mg/kg/d)	Candidate critical effect; comments [dose-metric]
<b>↓ Thymus weight</b>													
Keil et al. (2009)	Mouse	LOAEL		0.35	1	10	10	10	1	1,000		0.00035	↓ thymus weight
		HED	0.049	0.048	1	3	3	10	1	100		0.00048	[TotMetabBW34]
		HED	0.20	0.016	1	3	3	10	1	100		0.00016	[AUCCBId]
		HEC	0.092	0.033	1	3	3	10	1	100	0.00033		[TotMetabBW34] (route-to-route)
		HEC	0.014	0.0082	1	3	3	10	1	100	0.000082		[AUCCBId] (route-to-route)
<b>Autoimmunity</b>													
Kaneko et al. (2000)	Mouse	LOAEL		70	10	3	3	10	1	1,000	0.070		Changes in immunoreactive organs - liver (including sporadic necrosis in hepatic lobules), spleen; UF <sub>H</sub> = 3 due to autoimmune-prone mouse
		HED	97	37	10	3	1	10	1	300	0.12		[TotMetabBW34]
		HEC	121	69	10	3	1	10	1	300	0.23		[AUCCBId]
		HED	44	42	10	3	1	10	1	300		0.14	[TotMetabBW34] (route-to-route)
		HED	181	57	10	3	1	10	1	300		0.19	[AUCCBId] (route-to-route)
Keil et al. (2009)	Mouse	LOAEL		0.35	1	10	10	3	1	300		0.0012	↑ anti-dsDNA and anti-ssDNA Abs (early markers for autoimmune disease)
		HED	0.049	0.048	1	3	3	3	1	30		0.0016	[TotMetabBW34]
		HED	0.20	0.016	1	3	3	3	1	30		0.00053	[AUCCBId]
		HEC	0.092	0.033	1	3	3	3	1	30	0.0011		[TotMetabBW34] (route-to-route)
		HEC	0.014	0.0082	1	3	3	3	1	30	0.00027		[AUCCBId] (route-to-route)

**Table 5-16. cRfCs and cRfDs (based on applied dose) and p-cRfCs and p-cRfDs (based on PBPK modeled internal dose-metrics) for candidate critical immunological effects (continued)**

Effect type Candidate critical studies <sup>a</sup>	Species	POD type	HEC <sub>50</sub> or HED <sub>50</sub>	POD, HEC <sub>99</sub> , or HED <sub>99</sub> <sup>b</sup>	UF <sub>S</sub>	UF <sub>A</sub>	UF <sub>H</sub>	UF <sub>L</sub>	UF <sub>D</sub>	UF <sup>c</sup>	cRfC or p-cRfC (ppm)	cRfD or p-cRfD (mg/kg/d)	Candidate critical effect; comments [dose-metric]
<b>Immunosuppression</b>													
Woolhiser et al. (2006)	Rat	BMDL		24.9	10	3	10	1	1	300	0.083		↓ PFC response; BMR = 1 SD change; dropped highest dose
		HEC	29	11	10	3	3	1	1	100	0.11		[TotMetabBW34]; all does groups
		HEC	263	140	10	3	3	1	1	100	1.4		[AUCCBld]; all does groups
		HED	14	14	10	3	3	1	1	100		0.14	[TotMetabBW34] (route-to-route); all does groups
		HED	282	91	10	3	3	1	1	100		0.91	[AUCCBld] (route-to-route); all does groups
Sanders et al. (1982b)	Mouse	LOAEL		18	1	10	10	10	1	1000		0.018	↓ stem cell bone marrow recolonization (sustained); ↓ cell-mediated response to SRBC (largely transient during exposure); females more sensitive
		HED	2.5	2.5	1	3	3	10	1	100		0.025	[TotMetabBW34]
		HED	8.8	0.84	1	3	3	10	1	100		0.0084	[AUCCBld]
		HEC	4.8	1.7	1	3	3	10	1	100	0.017		[TotMetabBW34] (route-to-route)
		HEC	0.73	0.43	1	3	3	10	1	100	0.0043		[AUCCBld] (route-to-route)

<sup>a</sup>Shaded rows represent the p-cRfC or p-cRfD using the preferred PBPK model dose-metric.

<sup>b</sup>Applied dose POD adjusted to continuous exposure unless otherwise noted. POD, HEC<sub>99</sub>, and HED<sub>99</sub> have same units as cRfC (ppm) or cRfD (mg/kg/day).

<sup>c</sup>Product of individual UFs, rounded to 3, 10, 30, 100, 300, 1,000, or 3,000.

UF<sub>S</sub> = subchronic-to-chronic UF; UF<sub>A</sub> = interspecies UF; UF<sub>H</sub> = human variability UF; UF<sub>L</sub> = LOAEL-to-NOAEL UF; UF<sub>D</sub> = database UF

**Table 5-17. cRfCs and cRfDs (based on applied dose) and p-cRfCs and p-cRfDs (based on PBPK modeled internal dose-metrics) for candidate critical reproductive effects**

Effect type Candidate critical studies <sup>a</sup>	Species	POD type	HEC <sub>50</sub> or HED <sub>50</sub>	POD, HEC <sub>99</sub> , or HED <sub>99</sub> <sup>b</sup>	UF <sub>S</sub>	UF <sub>A</sub>	UF <sub>H</sub>	UF <sub>L</sub>	UF <sub>D</sub>	UF <sup>c</sup>	cRfC or p-cRfC (ppm)	cRfD or p-cRfD (mg/kg/d)	Candidate critical effect; comments [dose-metric]
<b>Effects on sperm, male reproductive outcomes</b>													
Chia et al. (1996)	Human	BMDL		1.4	10	1	10	1	1	100	0.014		Hyperzoospermia; BMR = 10% extra risk
		HEC	1.4	0.50	10	1	3	1	1	30	0.0017		[TotMetabBW34]
		HEC	1.4	0.83	10	1	3	1	1	30	0.0028		[AUCCBld]
		HED	0.74	0.73	10	1	3	1	1	30		0.024	[TotMetabBW34] (route-to-route)
		HED	15	1.6	10	1	3	1	1	30		0.053	[AUCCBld] (route-to-route)
Xu et al. (2004)	Mouse	LOAEL		180	10	3	10	10	1	3,000	0.060		↓ fertilization
		HEC	190	67	10	3	3	10	1	1,000	0.067		[TotMetabBW34]
		HEC	321	170	10	3	3	10	1	1,000	0.17		[AUCCBld]
		HED	80	73	10	3	3	10	1	1,000		0.073	[TotMetabBW34] (route-to-route)
		HED	324	104	10	3	3	10	1	1,000		0.10	[AUCCBld] (route-to-route)
Kumar et al. (2000b); (2001b)	Rat	LOAEL		45	10	3	10	10	1	3,000	0.015		Multiple sperm effects, increasing severity from 12 to 24 wks
		HEC	32	13	10	3	3	10	1	1,000	0.013		[TotMetabBW34]
		HEC	91	53	10	3	3	10	1	1,000	0.053		[AUCCBld]
		HED	16	16	10	3	3	10	1	1,000		0.016	[TotMetabBW34] (route-to-route)
		HED	157	49	10	3	3	10	1	1,000		0.049	[AUCCBld] (route-to-route)

**Table 5-17. cRfCs and cRfDs (based on applied dose) and p-cRfCs and p-cRfDs (based on PBPK modeled internal dose-metrics) for candidate critical reproductive effects (continued)**

Effect type Candidate critical studies <sup>a</sup>	Species	POD type	HEC <sub>50</sub> or HED <sub>50</sub>	POD, HEC <sub>99</sub> , or HED <sub>99</sub> <sup>b</sup>	UF <sub>S</sub>	UF <sub>A</sub>	UF <sub>H</sub>	UF <sub>L</sub>	UF <sub>D</sub>	UF <sup>c</sup>	cRfC or p-cRfC (ppm)	cRfD or p-cRfD (mg/kg/d)	Candidate critical effect; comments [dose-metric]
DuTeaux et al. (2004a)	Rat	LOAEL		141	10	10	10	10	1	10,000 <sup>d</sup>		0.014	↓ ability of sperm to fertilize in vitro
		HED	66	16	10	3	3	10	1	1,000		0.016	[AUCCBld]
		HED	65	42	10	3	3	10	1	1,000		0.042	[TotOxMetabBW34]
		HEC	16	9.3	10	3	3	10	1	1,000	0.0093		[AUCCBld] (route-to-route)
		HEC	160	43	10	3	3	10	1	1,000	0.043		[TotOxMetabBW34] (route-to-route)
<b>Male reproductive tract effects</b>													
Forkert et al. (2002); Kan et al. (2007)	Mouse	LOAEL		180	10	3	10	10	1	3,000	0.060		Effects on epididymis epithelium
		HEC	190	67	10	3	3	10	1	1,000	0.067		[TotMetabBW34]
		HEC	321	170	10	3	3	10	1	1,000	0.17		[AUCCBld]
		HED	80	73	10	3	3	10	1	1,000		0.073	[TotMetabBW34] (route-to-route)
		HED	324	104	10	3	3	10	1	1,000		0.10	[AUCCBld] (route-to-route)
Kumar et al. (2000b, 2001b)	Rat	LOAEL		45	10	3	10	10	1	3,000	0.015		Testes effects, testicular enzyme markers, increasing severity from 12 to 24 wks
		HEC	32	13	10	3	3	10	1	1,000	0.013		[TotMetabBW34]
		HEC	91	53	10	3	3	10	1	1,000	0.053		[AUCCBld]
		HED	16	16	10	3	3	10	1	1,000		0.016	[TotMetabBW34] (route-to-route)
		HED	157	49	10	3	3	10	1	1,000		0.049	[AUCCBld] (route-to-route)
<b>Female reproductive outcomes</b>													
Narotsky et al. (1995)	Rat	LOAEL		475	1	10	10	10	1	1,000		0.48	Delayed parturition
		HED	47	44	1	3	3	10	1	100		0.44	[TotMetabBW34]
		HED	350	114	1	3	3	10	1	100		1.1	[AUCCBld]
		HEC	98	37	1	3	3	10	1	100	0.37		[TotMetabBW34] (route-to-route)
		HEC	363	190	1	3	3	10	1	100	1.9		[AUCCBld] (route-to-route)

**Table 5-17. cRfCs and cRfDs (based on applied dose) and p-cRfCs and p-cRfDs (based on PBPK modeled internal dose-metrics) for candidate critical reproductive effects (continued)**

Effect type Candidate critical studies <sup>a</sup>	Species	POD type	HEC <sub>50</sub> or HED <sub>50</sub>	POD, HEC <sub>99</sub> , or HED <sub>99</sub> <sup>b</sup>	UF <sub>S</sub>	UF <sub>A</sub>	UF <sub>H</sub>	UF <sub>L</sub>	UF <sub>D</sub>	UF <sup>c</sup>	cRfC or p-cRfC (ppm)	cRfD or p-cRfD (mg/kg/d)	Candidate critical effect; comments [dose-metric]
<b>Reproductive behavior</b>													
George et al. (1986)	Rat	LOAEL		389	1	10	10	10	1	1,000		0.39	↓ mating (both sexes exposed)
		HED	85	77	1	3	3	10	1	100		0.77	[TotMetabBW34]
		HED	167	52	1	3	3	10	1	100		0.52	[AUCCBld]
		HEC	204	71	1	3	3	10	1	100	0.71		[TotMetabBW34] (route-to-route)
		HEC	103	60	1	3	3	10	1	100	0.60		[AUCCBld] (route-to-route)

<sup>a</sup>Shaded rows represent the p-cRfC or p-cRfD using the preferred PBPK model dose-metric.

<sup>b</sup>Applied dose POD adjusted to continuous exposure unless otherwise noted. POD, HEC<sub>99</sub>, and HED<sub>99</sub> have same units as cRfC (ppm) or cRfD (mg/kg/day).

<sup>c</sup>Product of individual UFs, rounded to 3, 10, 30, 100, 300, 1,000, 3,000, or 10,000 (see footnote [d] below).

<sup>d</sup>EPA's report on the RfC and RfD processes ([U.S. EPA, 2002b](https://www.epa.gov/assessing-and-managing-chemical-hazard/screening-critical-effects)) recommends not deriving reference values with a composite UF of >3,000; however, composite UFs exceeding 3,000 are considered here because the derivation of the cRfCs and cRfDs is part of a screening process and the application of the PBPK model for candidate critical effects reduces the values of some of the individual UFs for the p-cRfCs and p-cRfDs.

UF<sub>S</sub> = subchronic-to-chronic UF; UF<sub>A</sub> = interspecies UF; UF<sub>H</sub> = human variability UF; UF<sub>L</sub> = LOAEL-to-NOAEL UF; UF<sub>D</sub> = database UF

**Table 5-18. cRfCs and cRfDs (based on applied dose) and p-cRfCs and p-cRfDs (based on PBPK modeled internal dose-metrics) for candidate critical developmental effects**

Effect type Candidate critical studies <sup>a</sup>	Species	POD type	HEC <sub>50</sub> or HED <sub>50</sub>	POD, HEC <sub>99</sub> , or HED <sub>99</sub> <sup>b</sup>	UF <sub>S</sub>	UF <sub>A</sub>	UF <sub>H</sub>	UF <sub>L</sub>	UF <sub>D</sub>	UF <sup>c</sup>	cRfC or p-cRfC (ppm)	cRfD or p-cRfD (mg/kg/d)	Candidate critical effect; comments [dose-metric]
<b>Pre- and postnatal mortality</b>													
Healy et al. (1982)	Rat	LOAEL		17	1	3	10	10	1	300	0.057		Resorptions
		HEC	16	6.2	1	3	3	10	1	100	0.062		[TotMetabBW34]
		HEC	23	14	1	3	3	10	1	100	0.14		[AUCCBld]
		HED	8.7	8.5	1	3	3	10	1	100		0.085	[TotMetabBW34] (route-to-route)
		HED	73	20	1	3	3	10	1	100		0.20	[AUCCBld] (route-to-route)
Narotsky et al. (1995)	Rat	BMDL		32.2	1	10	10	1	1	100		0.32	Resorptions; BMR = 1% extra risk
		HED	29	28	1	3	3	1	1	10		2.8	[TotMetabBW34]
		HED	95	29	1	3	3	1	1	10		2.9	[AUCCBld]
		HEC	57	23	1	3	3	1	1	10	2.3		[TotMetabBW34] (route-to-route)
		HEC	40	24	1	3	3	1	1	10	2.4		[AUCCBld] (route-to-route)
<b>Pre- and postnatal growth</b>													
Healy et al. (1982)	Rat	LOAEL		17	1	3	10	10	1	300	0.057		↓ fetal weight; skeletal effects
		HEC	16	6.2	1	3	3	10	1	100	0.062		[TotMetabBW34]
		HEC	23	14	1	3	3	10	1	100	0.14		[AUCCBld]
		HED	8.7	8.5	1	3	3	10	1	100		0.085	[TotMetabBW34] (route-to-route)
		HED	73	20	1	3	3	10	1	100		0.20	[AUCCBld] (route-to-route)

**Table 5-18. cRfCs and cRfDs (based on applied dose) and p-cRfCs and p-cRfDs (based on PBPK modeled internal dose-metrics) for candidate critical developmental effects (continued)**

Effect type Candidate critical studies <sup>a</sup>	Species	POD type	HEC <sub>50</sub> or HED <sub>50</sub>	POD, HEC <sub>99</sub> , or HED <sub>99</sub> <sup>b</sup>	UF <sub>S</sub>	UF <sub>A</sub>	UF <sub>H</sub>	UF <sub>L</sub>	UF <sub>D</sub>	UF <sup>c</sup>	cRfC or p-cRfC (ppm)	cRfD or p-cRfD (mg/kg/d)	Candidate critical effect; comments [dose-metric]
<b>Congenital defects</b>													
Johnson et al. (2003)	Rat	BMDL		0.0207	1	10	10	1	1	100		0.00021	Heart malformations (pups); BMR = 1% extra risk; highest-dose group (1,000-fold higher than next highest) dropped to improve model fit
		HED	0.0058	0.0052	1	3	3	1	1	10		0.00052	[TotOxMetabBW34]
		HED	0.019	0.0017	1	3	3	1	1	10		0.00017	[AUCCBld]
		HEC	0.012	0.0037	1	3	3	1	1	10	0.00037		[TotOxMetabBW34] (route-to-route)
		HEC	0.0016	0.00093	1	3	3	1	1	10	0.000093		[AUCCBld] (route-to-route)
<b>Developmental neurotoxicity</b>													
Fredriksson et al. (1993)	Mouse	LOAEL		50	3	10	10	10	1	3,000		0.017	↓ rearing postexposure; pup gavage dose
		HED	4.2	4.1	3	3	3	10	1	300		0.014	[TotMetabBW34]
		HED	27	3.5	3	3	3	10	1	300		0.012	[AUCCBld]
		HEC	8.0	3.0	3	3	3	10	1	300	0.010		[TotMetabBW34] (route-to-route)
		HEC	3.1	1.8	3	3	3	10	1	300	0.0061		[AUCCBld] (route-to-route)
Taylor et al. (1985)	Rat	LOAEL		45	1	10	10	10	1	1,000		0.045	↑ exploration postexposure; estimated dam dose
		HED	11	11	1	3	3	10	1	100		0.11	[TotMetabBW34]
		HED	30	4.1	1	3	3	10	1	100		0.041	[AUCCBld]
		HEC	22	8.4	1	3	3	10	1	100	0.084		[TotMetabBW34] (route-to-route)
		HEC	3.7	2.2	1	3	3	10	1	100	0.022		[AUCCBld] (route-to-route)
Isaacson and Taylor (1989)	Rat	LOAEL		16	1	10	10	10	1	1,000		0.016	↓ myelination in hippocampus; estimated dam dose

**Table 5-18. cRfCs and cRfDs (based on applied dose) and p-cRfCs and p-cRfDs (based on PBPK modeled internal dose-metrics) for candidate critical developmental effects (continued)**

Effect type Candidate critical studies <sup>a</sup>	Species	POD type	HEC <sub>50</sub> or HED <sub>50</sub>	POD, HEC <sub>99</sub> , or HED <sub>99</sub> <sup>b</sup>	UF <sub>S</sub>	UF <sub>A</sub>	UF <sub>H</sub>	UF <sub>L</sub>	UF <sub>D</sub>	UF <sup>c</sup>	cRfC or p-cRfC (ppm)	cRfD or p-cRfD (mg/kg/d)	Candidate critical effect; comments [dose-metric]
<b>Developmental immunotoxicity</b>													
Peden-Adams et al. (2006)	Mouse	LOAEL		0.37	1	10	10	10	1	1,000		0.00037	↓ PFC, ↑ DTH; POD is estimated dam dose (exposure throughout gestation and lactation + to 3 or 8 wks of age)

<sup>a</sup>Shaded rows represent the p-cRfC or p-cRfD using the preferred PBPK model dose-metric or, in the cases where the PBPK model was not used, the cRfD or cRfC based on applied dose.

<sup>b</sup>Applied dose POD adjusted to continuous exposure unless otherwise noted. POD, HEC<sub>99</sub>, and HED<sub>99</sub> have same units as cRfC (ppm) or cRfD (mg/kg/day).

<sup>c</sup>Product of individual UFs, rounded to 3, 10, 30, 100, 300, 1,000, or 3,000.

UF<sub>S</sub> = subchronic-to-chronic UF; UF<sub>A</sub> = interspecies UF; UF<sub>H</sub> = human variability UF; UF<sub>L</sub> = LOAEL-to-NOAEL UF; UF<sub>D</sub> = database UF

Because they are derived from rodent internal dose estimates, the HEC and HED are derived in the same manner independent of the route of administration of the original rodent study. Therefore, a route-to-route extrapolation from an oral (inhalation) study in rodents to a HEC (HED) in humans is straight-forward. As shown in Tables 5-13–5-18, route-to-route extrapolation was performed for a number of endpoints with low cRfCs and cRfDs to derive p-cRfDs and p-cRfCs.

#### **5.1.3.3. Results and Discussion of p-RfCs and p-RfDs for Candidate Critical Effects**

Tables 5-13–5-18 present the p-cRfCs and p-cRfDs developed using the PBPK internal dose-metrics, along with the cRfCs and cRfDs based on applied dose for comparison, for each health effect domain.

The greatest impact of using the PBPK model was, as expected, for kidney effects, since as discussed in Sections 3.3 and 3.5, some toxicokinetic data indicate substantially more GSH conjugation of TCE and subsequent bioactivation of GSH-conjugates in humans relative to rats or mice. In addition, as discussed in Sections 3.3 and 3.5, the available in vivo data indicate high interindividual variability in the amount of TCE conjugated with GSH. The overall impact is that the p-cRfCs and p-cRfDs based on the preferred dose-metric of bioactivated DCVC are 300–400-fold lower than the corresponding cRfCs and cRfDs based on applied dose. As shown in Figure 3-20 in Section 3.5, for this dose-metric there is about a 30–100-fold difference (depending on exposure route and level) between rats and humans in the “central estimates” of interspecies differences for the fraction of TCE that is bioactivated as DCVC. The uncertainty in the human central estimate is only on the order of 2-fold (in either direction), while that in the rat central estimate is substantially greater, about 10-fold (in either direction). In addition, the interindividual variability about the human median estimate is on the order of 10-fold (in either direction). However, as noted in Section 3.3.3.2, there are a number of discrepancies in estimates for the extent of GSH conjugation that may be related to different analytical methods, and it is possible that GSH conjugation data to which the PBPK model was calibrated overestimated the extent of DCVG formation by a substantial amount. Thus, there remain significant uncertainties in the human estimates of GSH conjugation derived from the PBPK model. Moreover, the estimates of the amount bioactivated are indirect, derived from the difference between overall GSH conjugation flux and NAcDCVC excretion (see Section 3.5.7.3.1). Therefore, while there is a high degree of confidence in the nephrotoxic hazard posed by TCE, there is less confidence in the p-cRfCs and p-RfDs derived using GSH conjugation dose-metrics for these effects.

In addition, in two cases in which BMD modeling was employed, using internal dose-metrics led to a sufficiently different dose-response shape so as to change the resulting reference value by greater than fivefold. For the Woolhiser et al. (2006) decreased PFC response, this occurred with the AUC of TCE in blood dose-metric, leading to a p-cRfC 17-fold higher than the

cRfC based on applied dose. However, the model fit for this effect using this metric was substantially worse than the fit using the preferred metric of Total oxidative metabolism. Moreover, whereas an adequate fit was obtained with applied dose only with the highest-dose group dropped, all of the dose groups were included when the total oxidative metabolism dose-metric was used while still resulting in a good model fit. Therefore, it appears that using this metric resolves some of the low-dose supralinearity in the dose-response curve. Nonetheless, the overall impact of the preferred metric was minimal, as the p-cRfC based on the Total oxidative metabolism metric was less than 1.4-fold larger than the cRfC based on applied dose. The second case in which BMD modeling based on internal doses changed the candidate reference value by more than fivefold was for resorptions reported by Narotsky et al. (1995). Here, the p-cRfDs were seven- to eightfold larger than the corresponding cRfD based on applied dose. However, for applied dose, there is substantial uncertainty in the low-dose curvature of the dose-response curve. This uncertainty persisted with the use of internal dose-metrics, so the BMD remains somewhat uncertain (see figures in Appendix F). In the remaining cases, which generally involved the “generic” dose-metrics of total metabolism and AUC of TCE in blood, the p-cRfCs and p-cRfDs were within fivefold of the corresponding cRfC or cRfD based on applied dose, with the vast majority within threefold. This suggests that the standard UFs for inter- and intraspecies pharmacokinetic variability are fairly accurate in capturing these differences for these TCE studies.

#### **5.1.4. Uncertainties in cRfCs and cRfDs**

##### **5.1.4.1. Qualitative Uncertainties**

An underlying assumption in deriving a reference value for a noncancer effect is that the dose-response relationship has a threshold. Thus, a fundamental uncertainty is the validity of that assumption. For some effects, in particular effects on very sensitive processes (e.g., developmental processes) or effects for which there is a nontrivial background level and even small exposures may contribute to background disease processes in more susceptible people, a practical threshold (i.e., a threshold within the range of environmental exposure levels of regulatory concern) may not exist.

Nonetheless, under the assumption of a threshold, the desired exposure level to have as a reference value is the maximum level at which there is no appreciable risk for an adverse effect in (nonnegligible) sensitive subgroups (of humans). However, because it is not possible to know what this level is, “uncertainty factors” are used to attempt to address quantitatively various aspects, depending on the data set, of qualitative uncertainty.

First there is uncertainty about the POD for the application of UFs. Conceptually, the POD should represent the maximum exposure level at which there is no appreciable risk for an adverse effect in the study population under study conditions (i.e., the threshold in the dose-response relationship). Then, the application of the relevant UFs is intended to convey that

exposure level to the corresponding exposure level for sensitive human subgroups exposed continuously for a lifetime. In fact, it is again not possible to know that exposure level even for a laboratory study because of experimental limitations (e.g., the power to detect an effect, dose spacing, measurement errors, etc.), and crude approximations like the NOAEL or a BMDL are used. If a LOAEL is used as the POD, then the LOAEL-to-NOAEL UF is applied as an adjustment factor to get a better approximation of the desired exposure level (threshold), but the necessary extent of adjustment is unknown.

If a BMDL is used as the POD, there are uncertainties regarding the appropriate dose-response model to apply to the data, but these should be minimal if the modeling is in the observable range of the data. There are also uncertainties about what BMR to use to best approximate the desired exposure level (threshold, see above). For continuous endpoints, in particular, it is often difficult to identify the level of change that constitutes the “cut-point” for an adverse effect. Sometimes, to better approximate the desired exposure level, a BMR somewhat below the observable range of the data is selected. In such cases, the model uncertainty is increased, but this is a trade-off to reduce the uncertainty about the POD not being a good approximation for the desired exposure level.

For each of these types of PODs, there are additional uncertainties pertaining to adjustments to the administered exposures (doses). Typically, administered exposures (doses) are converted to equivalent continuous exposures (daily doses) over the study exposure period under the assumption that the effects are related to concentration  $\times$  time, independent of the daily (or weekly) exposure regimen (i.e., a daily exposure of 6 hours to 4 ppm is considered equivalent to 24 hours of exposure to 1 ppm). However, the validity of this assumption is generally unknown, and, if there are dose-rate effects, the assumption of  $C \times t$  equivalence would tend to bias the POD downwards. Where there is evidence that administered exposure better correlates to the effect than equivalent continuous exposure averaged over the study exposure period (e.g., visual effects), administered exposure was not adjusted. For the PBPK analyses in this assessment, the actual administered exposures are taken into account in the PBPK modeling, and equivalent daily values (averaged over the study exposure period) for the dose-metrics are obtained (see above, Section 5.1.3.2). Additional uncertainties about the PBPK-based estimates include uncertainties about the appropriate dose-metric for each effect, although for some effects there was better information about relevant dose-metrics than for others (see Section 5.1.3.1). Furthermore, as discussed in Section 3.3.3.2, there remains substantial uncertainty in the extrapolation of GSH conjugation from rodents to humans due to limitations in the available data.

Second, there is uncertainty about the UFs. The human variability UF is to some extent an adjustment factor because, for more sensitive people, the dose-response relationship shifts to lower exposures. However, there is uncertainty about the extent of the adjustment required (i.e., about the distribution of human susceptibility). Therefore, in the absence of data on a more

sensitive population(s) or on the distribution of susceptibility in the general population, an UF of 10 is generally used, in part for pharmacokinetic variability and in part for pharmacodynamic variability. The PBPK analyses in this assessment attempt to account for the pharmacokinetic portion of human variability using human data on pharmacokinetic variability. A quantitative uncertainty analysis of the PBPK-derived dose-metrics used in the assessment is presented in Section 5.1.4.2. There is still uncertainty regarding the susceptible subgroups for TCE exposure and the extent of pharmacodynamic variability.

If the data used to determine a particular POD are from laboratory animals, an interspecies extrapolation UF is used. This UF is also to some extent an adjustment factor for the expected scaling for toxicologically-equivalent doses across species (i.e., according to body weight to the  $3/4$  power for oral exposure). However, there is also uncertainty about the true extent of interspecies differences for specific noncancer effects from specific chemical exposures. Often, the “adjustment” component of this UF has been attributed to pharmacokinetics, while the “uncertainty” component has been attributed to pharmacodynamics, but as discussed above in Section 5.1.3.1, this is not the only interpretation supported. For oral exposures, the standard value for the interspecies UF is 10, which can be viewed as breaking down (approximately) to a factor of three for the “adjustment” (nominally pharmacokinetics) and a factor of three for the “uncertainty” (nominally pharmacodynamics). For inhalation exposures, no adjustment across species is generally assumed for fixed air concentrations (ppm equivalence), and the standard value for the interspecies UF is 3, reflecting only “uncertainty” (nominally pharmacodynamics). The PBPK analyses in this assessment attempt to account for the “adjustment” portion of interspecies extrapolation using rodent pharmacokinetic data to estimate internal doses for various dose-metrics. With respect to the “uncertainty” component, quantitative uncertainty analyses of the PBPK-derived dose-metrics used in the assessment are presented in Section 5.1.4.2. However, these only address the pharmacokinetic uncertainties in a particular dose-metric, and there is still uncertainty regarding the true dose-metrics. Nor do the PBPK analyses address the uncertainty in either cross-species pharmacodynamic differences (i.e., about the assumption that equal doses of the appropriate dose-metric convey equivalent risk across species for a particular endpoint from a specific chemical exposure) or in cross-species pharmacokinetic differences not accounted for by the PBPK model dose-metrics (e.g., departures from the assumed interspecies scaling of clearance of the active moiety, in the cases where only its production is estimated). A value of 3 is typically used for the “uncertainty” about cross-species differences, and this generally represents true uncertainty because it is usually unknown, even after adjustments have been made to account for the expected interspecies differences, whether humans have more or less susceptibility, and to what degree, than the laboratory species in question.

If only subchronic data are available, the subchronic-to-chronic UF is to some extent an adjustment factor because, if the effect becomes more severe with increasing exposure, then

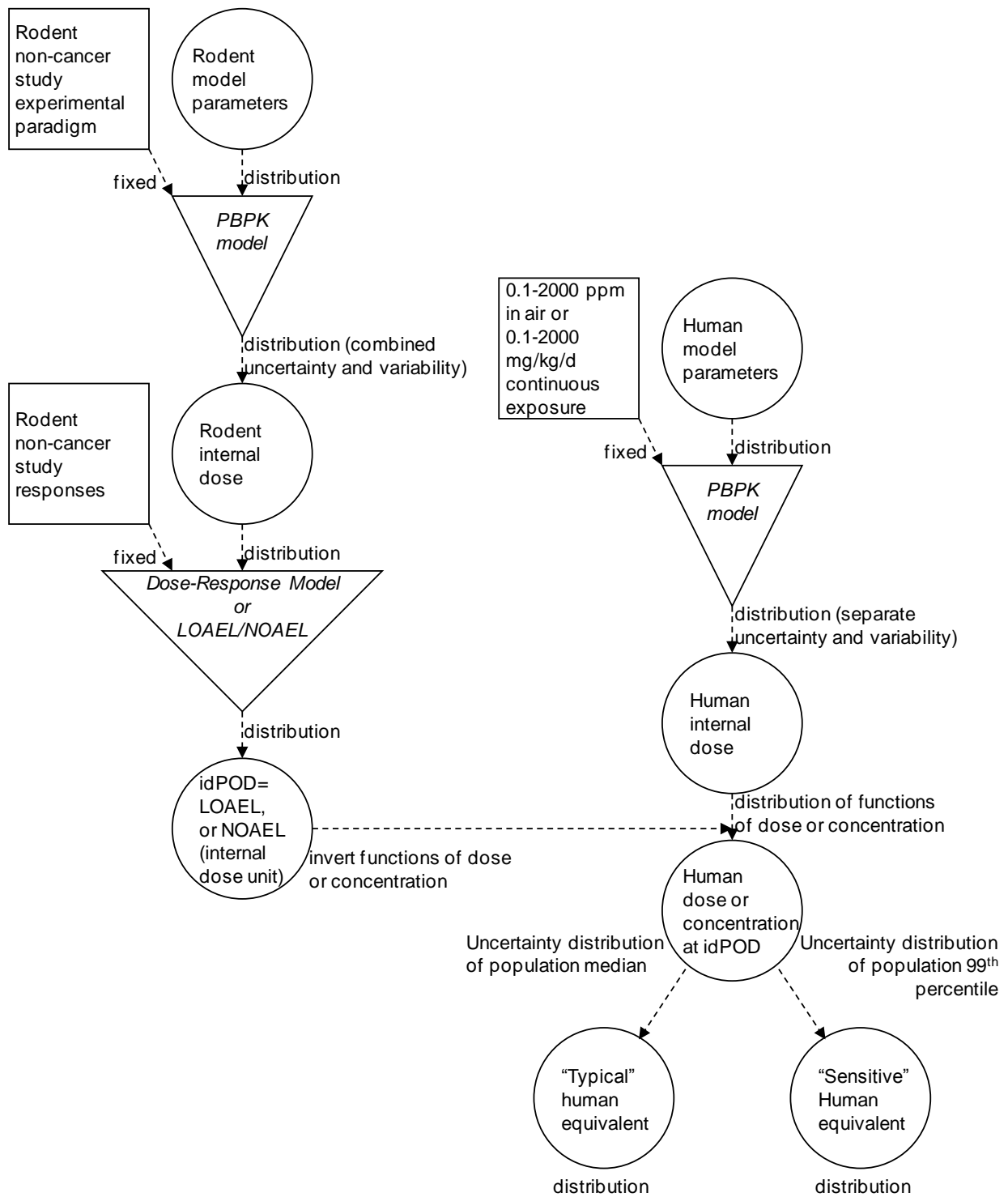
chronic exposure would shift the dose-response relationship to lower exposures. However, the true extent of the shift is unknown.

Sometimes a database UF is also applied to address limitations or uncertainties in the database. The overall database for TCE is quite extensive, with studies for many different types of effects, including two-generation reproductive studies, as well as neurological, immunological, and developmental immunological studies. In addition, there were sufficient data to develop a reliable PBPK model to estimate route-to-route extrapolated doses for some candidate critical effects for which data were only available for one route of exposure. Thus, there is a high degree of confidence that the TCE database was sufficient to identify sensitive endpoints.

#### **5.1.4.2. Quantitative Uncertainty Analysis of PBPK Model-Based Dose-metrics for LOAEL- or NOAEL-Based PODs**

The Bayesian analysis of the PBPK model for TCE generates distributions of uncertainty and variability in the internal dose-metrics that can be readily used for characterizing the uncertainty and variability in the PBPK model-based derivations of the HEC and HED. However, in the primary analysis, a number of simplifications are made including: (1) use of median estimates for rodent internal doses and (2) expressing the “sensitive human” HEC and HED in terms of combined uncertainty and variability. Therefore, a 2-dimensional quantitative uncertainty and variability analysis is performed, the objective of which is to characterize the impact of these assumptions.

As shown in Figure 5-4, the overall approach taken for the uncertainty analysis is similar to that used for the point estimates except for the carrying through of separate uncertainty and variability distributions throughout the analysis. In particular, to address simplification (1), above, the distribution of rodent internal dose estimates is carried through; and to address simplification (2), above, uncertainty and variability distributions in human internal dose estimates are kept distinct.



Square nodes indicate point values, circle nodes indicate distributions, and the inverted triangle indicates a (deterministic) functional relationship.

**Figure 5-4. Flow-chart for uncertainty analysis of HECs and HEDs derived using PBPK model-based dose-metrics.**

Because of a lack of tested software and limitations of time and resources, this analysis was not performed for idPODs based on BMD modeling, and was only performed for idPODs derived from a LOAEL or NOAEL. However, for those endpoints for which BMD modeling was performed, for the purposes of this uncertainty analysis, an alternative idPOD was used based on the study LOAEL or NOAEL.

In brief, the methodology involves an iterative process of sampling from three separate distributions—the uncertainty distribution of rodent PBPK model parameters, the uncertainty distribution of human population PBPK parameters, and the variability distribution of human individual PBPK model parameters—the latter two of which are related hierarchically. For a sample from the rodent parameter distribution, the corresponding idPOD is calculated. Then, an individual is sampled from a human population distribution, which itself is sampled from the uncertainty distribution of population parameters. For this individual, a human equivalent exposure (HEC or HED) corresponding to the idPOD is derived by interpolation. Taking multiple individuals from this population, a HEC or HED corresponding to the median and 99<sup>th</sup> percentile individuals is then derived. Repeating this process (starting again with a sample from the rodent distribution) results in two distributions (both reflecting uncertainty): one of “typical” individuals represented by the distribution of population medians, and one of “sensitive” individuals represented by the distribution of an upper percentile of the population (e.g., 99<sup>th</sup> percentile). This uncertainty reflects both uncertainty in the rodent internal dose and uncertainty in the human population parameters. Thus, for selected quantiles of the population and level of confidence (e.g., X<sup>th</sup> percentile individual at Y<sup>th</sup>% confidence), the interpretation is that at the resulting HEC or HED, there is Y% confidence that X% of the population has an internal dose less than that of the rodent in the toxicity study.

As shown in Tables 5-19–5-23, the HEC<sub>99</sub> and HED<sub>99</sub> derived using the rodent median dose-metrics and the combined uncertainty and variability in human dose-metrics is generally near (within 1.3-fold of) the median confidence level estimate of the HEC and HED for the 99<sup>th</sup> percentile individual. Therefore, the interpretation is that there is about 50% confidence that human exposure at the HEC<sub>99</sub> or HED<sub>99</sub> will, in 99% of the human population, lead to an internal dose less than or equal to that in the subjects (rodent or human) exposed at the POD in the corresponding study.

**Table 5-19. Comparison of “sensitive individual” HECs or HEDs for neurological effects based on PBPK modeled internal dose-metrics at different levels of confidence and sensitivity, at the NOAEL or LOAEL**

Candidate critical effect Candidate critical study <sup>a</sup> (species)	POD type	Ratio HEC/D <sub>50</sub> : HEC/D <sub>99</sub>	HEC <sub>x</sub> or HED <sub>x</sub> <sup>b</sup>			[Dose-metric]
			X = 99	X = 99, median	X = 99, 95lcb	
<b>Neurological</b>						
Trigeminal nerve effects Ruijten et al. (1991) (human)	HEC	2.62	5.4	5.4	2.6	[TotMetabBW34]
	HEC	1.68	8.3	8.3	4.9	[AUCCBld]
	HED	1.02	7.3	7.2	3.8	[TotMetabBW34] (rtr)
	HED	4.31	14	16	8.0	[AUCCBld] (rtr)
Demyelination in hippocampus Isaacson et al. (1990) (rat)	HED	1.02	9.21	9.20	7.39	[TotMetabBW34]
	HED	7.20	4.29	5.28	2.52	[AUCCBld]
	HEC	2.59	7.09	6.77	4.94	[TotMetabBW34] (rtr)
	HEC	1.68	2.29	2.42	0.606	[AUCCBld] (rtr)
Changes in wakefulness Arito et al. (1994) (rat)	HEC	2.65	4.79	4.86	2.37	[TotMetabBW34]
	HEC	1.67	9	9.10	4.63	[AUCCBld]
	HED	1.02	6.46	6.50	3.39	[TotMetabBW34] (rtr)
	HED	4.25	15.2	18.0	8.33	[AUCCBld] (rtr)
↓ Regeneration of sciatic nerve Kjellstrand et al. (1987) (rat)	HEC	2.94	93.1	93.6	38.6	[TotMetabBW34]
	HEC	1.90	257	266	114	[AUCCBld]
	HED	1.13	97.1	96.8	43.4	[TotMetabBW34] (rtr)
	HED	3.08	142	147	78.0	[AUCCBld] (rtr)
↓ Regeneration of sciatic nerve Kjellstrand et al. (1987) (mouse)	HEC	3.16	120	125	48.8	[TotMetabBW34]
	HEC	1.84	108	111	59.7	[AUCCBld]
	HED	1.21	120	121	57.0	[TotMetabBW34] (rtr)
	HED	2.13	75.8	79.1	53.4	[AUCCBld] (rtr)
Degeneration of dopaminergic neurons Gash et al. (2008) (rat)	HED	1.06	53	53.8	17.1	[TotMetabBW34]
	HED	2.98	192	199	94.7	[AUCCBld]
	HEC	2.70	46.8	47.9	14.2	[TotMetabBW34] (rtr)

<sup>a</sup>Shaded rows denote results for the primary dose-metric.

<sup>b</sup>HEC<sub>99</sub> = the 99<sup>th</sup> percentile of the combined human uncertainty and variability distribution of continuous exposure concentrations that lead to the (fixed) median estimate of the rodent internal dose at the POD; HEC<sub>99,median</sub> (or HEC<sub>99,95lcb</sub>) = the median (or 95<sup>th</sup> percentile lower confidence bound) estimate of the uncertainty distribution of continuous exposure concentrations for which the 99<sup>th</sup> percentile individual has an internal dose less than the (uncertain) rodent internal dose at the POD.

rtr = route-to-route extrapolation using PBPK model and the specified dose-metric

**Table 5-20. Comparison of “sensitive individual” HECs or HEDs for kidney and liver effects based on PBPK modeled internal dose-metrics at different levels of confidence and sensitivity, at the NOAEL or LOAEL**

Candidate critical effect Candidate critical study <sup>a</sup> (species)	POD type	Ratio HEC/D <sub>50</sub> : HEC/D <sub>99</sub>	HEC <sub>X</sub> or HED <sub>X</sub> <sup>b</sup>			[Dose-metric]
			X = 99	X = 99, median	X = 99, 95lcb	
<b>Kidney</b>						
Meganucleocytosis [NOAEL] <sup>c</sup> Maltoni et al. (1986) (rat inhalation)	HEC	7.53	0.0233	0.0260	0.00366	[ABioactDCVCBW34]
	HEC	7.70	0.0364	0.0411	0.00992	[AMetGSHBW34]
	HEC	2.57	8.31	7.97	4.03	[TotMetabBW34]
	HED	9.86	0.0140	0.0156	0.00216	[ABioactDCVCBW34] (rtr)
	HED	9.83	0.0223	0.0242	0.00597	[AMetGSHBW34] (rtr)
	HED	1.02	10.6	10.7	5.75	[TotMetabBW34] (rtr)
Toxic nephrosis NCI (1976) (mouse)	HED	9.51	0.30	0.32	0.044	[AMetGSHBW34]
	HED	1.05	48	48.9	16.2	[TotMetabBW34]
	HEC	7.78	0.50	0.514	0.0703	[AMetGSHBW34] (rtr)
	HEC	2.67	42	43.5	13.7	[TotMetabBW34] (rtr)
Toxic nephropathy [LOAEL] <sup>c</sup> NTP (1988) (rat)	HED	9.75	0.121	0.126	0.0177	[ABioactDCVCBW34]
	HED	9.64	0.193	0.210	0.0379	[AMetGSHBW34]
	HED	1.03	33.1	33.1	11.1	[TotMetabBW34]
	HEC	7.55	0.201	0.204	0.0269	[ABioactDCVCBW34] (rtr)
	HEC	7.75	0.314	0.353	0.0676	[AMetGSHBW34] (rtr)
	HEC	2.59	28.2	27.2	8.77	[TotMetabBW34] (rtr)
Meganucleocytosis [NOAEL] <sup>c</sup> Maltoni et al. (1986) (rat oral)	HED	9.85	0.0133	0.0145	0.00158	[ABioactDCVCBW34]
	HED	9.86	0.0214	0.0249	0.00366	[AMetGSHBW34]
	HED	1.02	8.7	8.57	4.95	[TotMetabBW34]
	HEC	7.55	0.022	0.0249	0.00256	[ABioactDCVCBW34] (rtr)
	HEC	7.71	0.0349	0.0424	0.00615	[AMetGSHBW34] (rtr)
	HEC	2.60	6.66	6.31	3.70	[TotMetabBW34] (rtr)
↑ Kidney/body weight ratio [NOAEL] <sup>c</sup> Kjellstrand et al. (1983a) (mouse)	HEC	7.69	0.111	0.103	0.00809	[AMetGSHBW34]
	HEC	2.63	34.5	33.7	13.5	[TotMetabBW34]
	HED	9.78	0.068	0.00641	0.00497	[AMetGSHBW34] (rtr)
	HED	1.03	39.9	39.2	17.9	[TotMetabBW34] (rtr)

**Table 5-20. Comparison of “sensitive individual” HECs or HEDs for kidney and liver effects based on PBPK modeled internal dose-metrics at different levels of confidence and sensitivity, at the NOAEL or LOAEL (continued)**

Candidate critical effect Candidate critical study (species)	POD type	Ratio HEC/D <sub>50</sub> : HEC/D <sub>99</sub>	HEC <sub>x</sub> or HED <sub>x</sub>			[Dose-metric]
			X = 99	X = 99, median	X = 99, 95lcb	
↑ Kidney/body weight ratio [NOAEL] <sup>c</sup> Woolhiser et al. (2006) (rat)	HEC	7.53	0.0438	0.0481	0.00737	[ABioactDCVCBW34]
	HEC	7.70	0.0724	0.0827	0.0179	[AMetGSHBW34]
	HEC	2.54	16.1	15.2	7.56	[TotMetabBW34]
	HED	9.84	0.0264	0.0282	0.00447	[ABioactDCVCBW34] (rtr)
	HED	9.81	0.0444	0.0488	0.0111	[AMetGSHBW34] (rtr)
	HED	1.02	19.5	19.2	10.5	[TotMetabBW34] (rtr)
<b>Liver</b>						
↑ Liver/body weight ratio [LOAEL] <sup>c</sup> Kjellstrand et al. (1983a) (mouse)	HEC	2.85	16.2	16.3	6.92	[AMetLiv1BW34]
	HEC	3.63	40.9	38.1	15.0	[TotOxMetabBW34]
	HED	1.16	14.1	14.1	5.85	[AMetLiv1BW34] (rtr)
	HED	1.53	40.1	39.4	17.9	[TotOxMetabBW34] (rtr)
↑ Liver/body weight ratio [NOAEL] <sup>c</sup> Woolhiser et al. (2006) (rat)	HEC	2.86	20.7	21.0	11.0	[AMetLiv1BW34]
	HEC	2.94	18.2	17.1	8.20	[TotOxMetabBW34]
	HED	1.20	17.8	17.7	9.94	[AMetLiv1BW34] (rtr)
	HED	1.21	19.6	19.3	10.5	[TotOxMetabBW34] (rtr)
↑ Liver/body weight ratio [LOAEL] <sup>c</sup> Buben and O'Flaherty (1985) (mouse)	HED	1.14	8.82	8.95	4.17	[AMetLiv1BW34]
	HED	1.14	9.64	9.78	5.28	[TotOxMetabBW34]
	HEC	2.80	10.1	9.97	4.83	[AMetLiv1BW34] (rtr)
	HEC	3.13	7.83	7.65	4.23	[TotOxMetabBW34] (rtr)

<sup>a</sup>Shaded rows denote results for the primary dose-metric.

<sup>b</sup>HEC<sub>99</sub> = the 99<sup>th</sup> percentile of the combined human uncertainty and variability distribution of continuous exposure concentrations that lead to the (fixed) median estimate of the rodent internal dose at the POD; HEC<sub>99,median</sub> (or HEC<sub>99,95lcb</sub>) = the median (or 95<sup>th</sup> percentile lower confidence bound) estimate of the uncertainty distribution of continuous exposure concentrations for which the 99<sup>th</sup> percentile individual has an internal dose less than the (uncertain) rodent internal dose at the POD.

<sup>c</sup>BMDL used for p-cRfC or p-cRfD, but LOAEL or NOAEL (as noted) used for uncertainty analysis.

rtr = route-to-route extrapolation using PBPK model and the specified dose-metric

**Table 5-21. Comparison of “sensitive individual” HECs or HEDs for immunological effects based on PBPK modeled internal dose-metrics at different levels of confidence and sensitivity, at the NOAEL or LOAEL**

Candidate critical effect Candidate critical study <sup>a</sup> (species)	POD type	Ratio HEC/D <sub>50</sub> : HEC/D <sub>99</sub>	HEC <sub>x</sub> or HED <sub>x</sub> <sup>b</sup>			[Dose-metric]
			X = 99	X = 99, median	X = 99, 95lcb	
<b>Immunological</b>						
Changes in immunoreactive organs—liver (including sporadic necrosis in hepatic lobules), spleen Kaneko et al. (2000) (mouse)	HEC	2.65	36.7	38.3	16.0	[TotMetabBW34]
	HEC	1.75	68.9	70.0	37.1	[AUCCBld]
	HED	1.04	42.3	43.3	21.3	[TotMetabBW34] (rtr)
	HED	3.21	56.5	59.0	39.8	[AUCCBld] (rtr)
↑ Anti-dsDNA and anti-ssDNA Abs (early markers for auto-immune disease); ↓ thymus weight Keil et al. (2009) (mouse)	HED	1.02	0.0482	0.0483	0.0380	[TotMetabBW34]
	HED	12.1	0.0161	0.0189	0.00363	[AUCCBld]
	HEC	2.77	0.0332	0.0337	0.0246	[TotMetabBW34] (rtr)
	HEC	1.69	0.00821	0.00787	0.00199	[AUCCBld] (rtr)
↓ PFC response [NOAEL] <sup>c</sup> Woolhiser et al. (2006) (rat)	HEC	2.54	16.1	15.2	7.56	[TotMetabBW34]
	HEC	1.73	59.6	60.1	26.2	[AUCCBld]
	HED	1.02	19.5	19.2	10.5	[TotMetabBW34] (rtr)
	HED	3.21	52	55.9	33.0	[AUCCBld] (rtr)
↓ Stem cell bone marrow recolonization; ↓ cell-mediated response to SRBC Sanders et al. (1982b) (mouse)	HED	1.02	2.48	2.48	1.94	[TotMetabBW34]
	HED	10.5	0.838	0.967	0.187	[AUCCBld]
	HEC	2.77	1.72	1.75	1.28	[TotMetabBW34] (rtr)
	HEC	1.68	0.43	0.412	0.103	[AUCCBld] (rtr)

<sup>a</sup>Shaded rows denote results for the primary dose-metric.

<sup>b</sup>HEC<sub>99</sub> = the 99<sup>th</sup> percentile of the combined human uncertainty and variability distribution of continuous exposure concentrations that lead to the (fixed) median estimate of the rodent internal dose at the POD; HEC<sub>99,median</sub> (or HEC<sub>99,95lcb</sub>) = the median (or 95<sup>th</sup> percentile lower confidence bound) estimate of the uncertainty distribution of continuous exposure concentrations for which the 99<sup>th</sup> percentile individual has an internal dose less than the (uncertain) rodent internal dose at the POD.

<sup>c</sup>BMDL used for p-cRfC or p-cRfD, but LOAEL or NOAEL (as noted) used for uncertainty analysis.

rtr = route-to-route extrapolation using PBPK model and the specified dose-metric

**Table 5-22. Comparison of “sensitive individual” HECs or HEDs for reproductive effects based on PBPK modeled internal dose-metrics at different levels of confidence and sensitivity, at the NOAEL or LOAEL**

Candidate critical effect Candidate critical study <sup>a</sup> (species)	POD type	Ratio HEC/D <sub>50</sub> : HEC/D <sub>99</sub>	HEC <sub>X</sub> or HED <sub>X</sub> <sup>b</sup>			[Dose-metric]
			X = 99	X = 99, median	X = 99, 95lcb	
<b>Reproductive</b>						
Hyperzoospermia Chia et al. (1996) (human)	HEC	2.78	0.50	0.53	0.25	[TotMetabBW34]
	HEC	1.68	0.83	0.83	0.49	[AUCCBld]
	HED	1.02	0.73	0.71	0.37	[TotMetabBW34] (rtr)
	HED	9.69	1.6	2.0	0.92	[AUCCBld] (rtr)
↓ Fertilization Xu et al. (2004) (mouse)	HEC	2.85	66.6	72.3	26.6	[TotMetabBW34]
	HEC	1.89	170	171	97.1	[AUCCBld]
	HED	1.09	73.3	76.9	32.9	[TotMetabBW34] (rtr)
	HED	3.11	104	109	67.9	[AUCCBld] (rtr)
Multiple sperm effects, testicular enzyme markers Kumar et al. (2001b; 2000b) (rat)	HEC	2.53	12.8	12.2	6.20	[TotMetabBW34]
	HEC	1.72	53.2	54.4	23.2	[AUCCBld]
	HED	1.02	15.8	15.7	8.60	[TotMetabBW34] (rtr)
	HED	3.21	48.8	52.6	30.6	[AUCCBld] (rtr)
↓ Ability of sperm to fertilize in vitro DuTeaux et al. (2004a) (rat)	HED	4.20	15.6	18.1	4.07	[AUCCBld]
	HED	1.57	41.7	41.9	32.0	[TotOxMetabBW34]
	HEC	1.67	9.3	10.1	2.09	[AUCCBld] (rtr)
	HEC	3.75	42.5	55.6	39.1	[TotOxMetabBW34] (rtr)
Effects on epididymis epithelium Forkert et al. (2002); Kan et al. (2007) (mouse)	HEC	2.85	66.6	72.3	26.6	[TotMetabBW34]
	HEC	1.89	170	171	97.1	[AUCCBld]
	HED	1.09	73.3	76.9	32.9	[TotMetabBW34] (rtr)
	HED	3.11	104	109	67.9	[AUCCBld] (rtr)
Testes effects Kumar et al. (2001b; 2000b) (rat)	HEC	2.53	12.8	12.2	6.20	[TotMetabBW34]
	HEC	1.72	53.2	54.4	23.2	[AUCCBld]
	HED	1.02	15.8	15.7	8.60	[TotMetabBW34] (rtr)
	HED	3.21	48.8	52.6	30.6	[AUCCBld] (rtr)
Delayed parturition Narotsky et al. (1995) (rat)	HED	1.06	44.3	43.9	15.1	[TotMetabBW34]
	HED	3.07	114	119	47.7	[AUCCBld]
	HEC	2.66	36.9	35.3	11.6	[TotMetabBW34] (rtr)
	HEC	1.91	190	197	48.1	[AUCCBld] (rtr)

**Table 5-22. Comparison of “sensitive individual” HECs or HEDs for reproductive effects based on PBPK modeled internal dose-metrics at different levels of confidence and sensitivity, at the NOAEL or LOAEL (continued)**

Candidate critical effect Candidate critical study (species)	POD type	Ratio HEC/D <sub>50</sub> : HEC/D <sub>99</sub>	HEC <sub>x</sub> or HED <sub>x</sub>			[Dose-metric]
			X = 99	X = 99, median	X = 99, 95lcb	
↓ Mating (both sexes exposed) George et al. (1986) (rat)	HED	1.10	77.4	77.1	34.2	[TotMetabBW34]
	HED	3.21	51.9	55.8	14.7	[AUCCBld]
	HEC	2.86	71.1	70.0	29.5	[TotMetabBW34] (rtr)
	HEC	1.73	59.5	63.3	8.14	[AUCCBld] (rtr)

<sup>a</sup>Shaded rows denote results for the primary dose-metric.

<sup>b</sup>HEC<sub>99</sub> = the 99<sup>th</sup> percentile of the combined human uncertainty and variability distribution of continuous exposure concentrations that lead to the (fixed) median estimate of the rodent internal dose at the POD; HEC<sub>99,median</sub> (or HEC<sub>99,95lcb</sub>) = the median (or 95<sup>th</sup> percentile lower confidence bound) estimate of the uncertainty distribution of continuous exposure concentrations for which the 99<sup>th</sup> percentile individual has an internal dose less than the (uncertain) rodent internal dose at the POD.

rtr = route-to-route extrapolation using PBPK model and the specified dose-metric

**Table 5-23. Comparison of “sensitive individual” HECs or HEDs for developmental effects based on PBPK modeled internal dose-metrics at different levels of confidence and sensitivity, at the NOAEL or LOAEL**

Candidate critical effect Candidate critical study <sup>a</sup> (species)	POD type	Ratio HEC/D <sub>50</sub> : HEC/D <sub>99</sub>	HEC <sub>x</sub> or HED <sub>x</sub> <sup>b</sup>			[Dose-metric]
			X = 99	X = 95, median	X = 95, 95lcb	
<b>Developmental</b>						
Resorptions Healy et al. (1982) (rat)	HEC	2.58	6.19	6.02	3.13	[TotMetabBW34]
	HEC	1.69	13.7	13.9	7.27	[AUCCBld]
	HED	1.02	8.5	8.50	4.61	[TotMetabBW34] (rtr)
	HED	3.68	19.7	22.4	11.5	[AUCCBld] (rtr)
Resorptions [LOAEL] <sup>c</sup> Narotsky et al. (1995) (rat)	HED	1.06	44.3	43.9	15.1	[TotMetabBW34]
	HED	3.07	114	119	47.7	[AUCCBld]
	HEC	2.66	36.9	35.3	11.6	[TotMetabBW34] (rtr)
	HEC	1.91	190	197	48.1	[AUCCBld] (rtr)
↓ Fetal weight; skeletal effects Healy et al. (1982) (rat)	HEC	2.58	6.19	6.02	3.13	[TotMetabBW34]
	HEC	1.69	13.7	13.9	7.27	[AUCCBld]
	HED	1.02	8.5	8.50	4.61	[TotMetabBW34] (rtr)
	HED	3.68	19.7	22.4	11.5	[AUCCBld] (rtr)
Heart malformations (pups) [LOAEL] <sup>c</sup> Johnson et al. (2003) (rat)	HED	1.02	0.012	0.012	0.0102	[TotOxMetabBW34]
	HED	11.6	0.00382	0.00476	0.00112	[AUCCBld]
	HEC	2.75	0.00848	0.00866	0.00632	[TotOxMetabBW34] (rtr)
	HEC	1.70	0.00216	0.00221	0.000578	[AUCCBld] (rtr)
↓ Rearing postexposure Fredriksson et al. (1993) (mouse)	HED	1.02	4.13	4.19	2.22	[TotMetabBW34]
	HED	7.69	3.46	4.21	0.592	[AUCCBld]
	HEC	2.71	2.96	2.96	1.48	[TotMetabBW34] (rtr)
	HEC	1.68	1.84	1.81	0.302	[AUCCBld] (rtr)
↑ Exploration postexposure Taylor et al. (1985) (rat)	HED	1.02	10.7	10.7	8.86	[TotMetabBW34]
	HED	7.29	4.11	5.08	1.16	[AUCCBld]
	HEC	2.57	8.36	7.94	5.95	[TotMetabBW34] (rtr)
	HEC	1.68	2.19	2.31	0.580	[AUCCBld] (rtr)

<sup>a</sup>Shaded rows denote results for the primary dose-metric.

<sup>b</sup>HEC<sub>99</sub> = the 99<sup>th</sup> percentile of the combined human uncertainty and variability distribution of continuous exposure concentrations that lead to the (fixed) median estimate of the rodent internal dose at the POD; HEC<sub>99,median</sub> (or HEC<sub>99,95lcb</sub>) = the median (or 95<sup>th</sup> percentile lower confidence bound) estimate of the uncertainty distribution of continuous exposure concentrations for which the 99<sup>th</sup> percentile individual has an internal dose less than the (uncertain) rodent internal dose at the POD.

<sup>c</sup>BMDL used for p-cRfC or p-cRfD, but LOAEL or NOAEL (as noted) used for uncertainty analysis.

rtr = route-to-route extrapolation using PBPK model and the specified dose-metric

In several cases, the uncertainty, as reflected in the ratio between the 95 and 50% confidence bounds on the 99<sup>th</sup> percentile individual, was rather high (e.g.,  $\geq 5$ -fold), and reflected primarily uncertainty in the rodent internal dose estimates, discussed previously in Section 3.5.7. The largest uncertainties (ratios between 95 to 50% confidence bounds of 8–10-fold) were for kidney effects in mice using the AMetGSHBW34 dose-metric ([Kjellstrand et al., 1983a](#); [NCI, 1976](#)). More moderate uncertainties (ratios between 95 to 50% confidence bounds of five- to eightfold) were evident in some oral studies using the AUCCBlD dose-metric ([Keil et al., 2009](#); [Fredriksson et al., 1993](#); [George et al., 1986](#); [Sanders et al., 1982b](#)), as well as in studies reporting kidney effects in rats in which the ABioactDCVCBW34 or AMetGSHBW34 dose-metrics were used ([Woolhiser et al., 2006](#); [NTP, 1988](#); [Maltoni et al., 1986](#)). Therefore, in these cases, a POD that is protective of the 99<sup>th</sup> percentile individual at a confidence level higher than 50% could be as much as an order of magnitude lower.

For comparison, Tables 5-19 and 5-23 also show the ratios of the overall 50<sup>th</sup> percentile to the overall 99<sup>th</sup> percentile HECs and HEDs, reflecting combined human uncertainty and variability at the median study/endpoint idPOD. The smallest ratios (up to 1.2-fold) are for total, oxidative, and hepatic oxidative metabolism dose-metrics from oral exposures, due to the large hepatic first-pass effect resulting in virtually all of the oral intake being metabolized before systemic circulation. Conversely, the large hepatic first-pass results in high variability in the blood concentration of TCE following oral exposures, with ratios up to 12-fold at low exposures (e.g., 90 vs. 99% first-pass would result in amounts metabolized differing by about 10% but TCE blood concentrations differing by about 10-fold). From inhalation exposures, there is moderate variability in these metrics, about two- to threefold. For GSH conjugation and bioactivated DCVC, however, variability is high (8–10-fold) for both exposure routes, which follows from the incorporation in the PBPK model analysis of the data from Lash et al. ([1999b](#)) showing substantial interindividual variability in GSH conjugation in humans.

Finally, it is important to emphasize that this analysis only addresses pharmacokinetic uncertainty and variability, so other aspects of extrapolation addressed in the UFs (e.g., LOAEL to NOAEL, subchronic to chronic, and pharmacodynamic differences), discussed above, are not included in the level of confidence.

### **5.1.5. Summary of Noncancer Reference Values**

#### **5.1.5.1. Preferred Candidate Reference Values (cRfCs, cRfD, p-cRfCs, and p-cRfDs) for Candidate Critical Effects**

The candidate critical effects that yielded the lowest p-cRfC or p-cRfD for each type of effect, based on the primary dose-metric, are summarized in Tables 5-24 (p-cRfCs) and 5-25 (p-cRfDs). These results are extracted from Tables 5-13 to 5-18. In cases where a route-to-route extrapolated p-cRfC (p-cRfD) is lower than the lowest p-cRfC (p-cRfD) from an inhalation

(oral) study, both values are presented in the table. In addition, if there is greater than usual uncertainty associated with the lowest p-cRfC or p-cRfD for a type of effect, then the endpoint with the next lowest value is also presented. Furthermore, given those selections, the same sets of critical effects and studies are displayed across both tables, with the exception of two oral studies for which route-to-route extrapolation was not performed. Tables 5-24 and 5-25 are further summarized in Tables 5-26 and 5-27 to present the overall preferred p-cRfC and p-cRfD for each type of noncancer effect. The purpose of these summary tables is to show the most sensitive endpoints for each type of effect and the apparent relative sensitivities (based on reference value estimates) of the different types of effects.

**Table 5-24. Lowest p-cRfCs or cRfCs for different effect domains**

Effect domain Effect type	Candidate critical effect (species/critical study)	p-cRfC or cRfC in ppm (composite UF)		
		Preferred dose-metric <sup>a</sup>	Default methodology	Alternative dose- metrics/studies (Tables 5-13–5-18)
<b>Neurologic</b>				
Trigeminal nerve effects	Trigeminal nerve effects (human/ <a href="#">Ruijten et al., 1991</a> )	0.54 (10)	0.47 (30)	0.83 (10)
Cognitive effects	Demyelination in hippocampus (rat/ <a href="#">Isaacson et al., 1990</a> )	0.0071 (1,000)	– [rtr]	0.0023 (1,000)
Mood/sleep changes	Changes in wakefulness (rat/ <a href="#">Arito et al., 1994</a> )	0.016 (300)	0.012 (1,000)	0.030 (300)
<b>Kidney</b>				
Histological changes	<i>Toxic nephropathy</i> (rat/ <a href="#">NTP, 1988</a> )	0.00056 (10)	– [rtr]	0.00087–1.3 (10–300)
	Toxic nephrosis (mouse/ <a href="#">NCI, 1976</a> )	0.0017 (300)	– [rtr]	
	Meganeucleocytosis (rat/ <a href="#">Maltoni et al., 1986</a> )	0.0025 (10)	– [rtr]	
↑ Kidney weight	↑ kidney weight (rat/ <a href="#">Woolhiser et al., 2006</a> )	0.0013 (10)	0.52 (30)	0.0022–2.1 (10–30)
<b>Liver</b>				
↑ Liver weight	↑ liver weight (mouse/ <a href="#">Kjellstrand et al., 1983a</a> )	0.91 (10)	0.72 (30)	0.83–2.5 (10–30)
<b>Immunologic</b>				
↓ Thymus weight	↓ <b>thymus weight</b> (mouse/ <a href="#">Keil et al., 2009</a> )	<b>0.00033</b> (100)	– [rtr]	0.000082 (100)
Immuno-suppression	↓ cell-mediated response to SRBC ↓ stem cell recolonization (mouse/ <a href="#">Sanders et al., 1982b</a> )	0.017 (100)	– [rtr]	0.0043–1.4 (100)
	Decreased PFC response (rat/ <a href="#">Woolhiser et al., 2006</a> )	0.11 (100)	0.083 (300)	
Autoimmunity	↑ anti-dsDNA and anti-ssDNA Abs (mouse/ <a href="#">Keil et al., 2009</a> )	0.0011 (30)	– [rtr]	0.00027–0.23 (30–300)
	Autoimmune organ changes (mouse/ <a href="#">Kaneko et al., 2000</a> )	0.12 (300)	0.070 (1,000)	

**Table 5-24. Lowest p-cRfCs or cRfCs for different effect domains (continued)**

Effect domain Effect type	Candidate critical effect (species/critical study)	p-cRfC or cRfC in ppm (composite UF)		
		Preferred dose-metric <sup>a</sup>	Default methodology	Alternative dose- metrics/studies (Tables 5-13–5-18)
<b>Reproductive</b>				
Effects on sperm and testes	↓ ability of sperm to fertilize (rat/ <a href="#">DuTeaux et al., 2004a</a> )	0.0093 (1,000)	– [rtr]	0.028–0.17 (30–1,000)
	Multiple effects (rat/ <a href="#">Kumar et al., 2001b, 2000b</a> )	0.013 (1,000)	0.015 (3,000)	
	Hyperzoospermia (human/ <a href="#">Chia et al., 1996</a> ) <sup>b</sup>	0.017 (30)	0.014 (100)	
<b>Developmental</b>				
Congenital defects	<b>Heart malformations</b> (rat/ <a href="#">Johnson et al., 2003</a> )	<b>0.00037</b> (10)	– [rtr]	0.000093 (10)
Developmental neurotoxicity	↓ rearing postexposure (rat/ <a href="#">Fredriksson et al., 1993</a> )	0.028 (300)	– [rtr]	0.0077–0.084 (100–300)
Pre/postnatal mortality/growth	Resorptions/↓ fetal weight/ skeletal effects (rat/ <a href="#">Healy et al., 1982</a> )	0.062 (100)	0.057 (300)	0.14–2.4 (10–100)

<sup>a</sup>The critical effects/studies and p-cRfCs used to derive the RfC are in **bold**; supporting effects/studies and p-cRfCs in *italics*.

<sup>b</sup>Greater than usual degree of uncertainty (see Section 5.1.2).

rtr = route-to-route extrapolated result

**Table 5-25. Lowest p-cRfDs or cRfDs for different effect domains**

Effect domain Effect type	Candidate critical effect (species/critical study)	p-cRfD or cRfD in mg/kg/d (composite UF)		
		Preferred dose-metric <sup>a</sup>	Default methodology	Alternative dose- metrics/studies (Tables 5-13–5-18)
<b>Neurologic</b>				
Trigeminal nerve effects	Trigeminal nerve effects (human/ <a href="#">Ruijten et al., 1991</a> )	0.73 (10)	– [rtr]	1.4 (10)
Cognitive effects	Demyelination in hippocampus (rat/ <a href="#">Isaacson et al., 1990</a> )	0.0092 (1,000)	0.0047 (10,000 <sup>b</sup> )	0.0043 (1,000)
Mood/sleep changes	Changes in wakefulness (rat/ <a href="#">Arito et al., 1994</a> )	0.022 (300)	– [rtr]	0.051 (300)
<b>Kidney</b>				
Histological changes	<i>Toxic nephropathy</i> (rat/ <a href="#">NTP, 1988</a> )	0.00034 (10)	0.0945 (100)	0.00053–1.9 (10–300)
	Toxic nephrosis (mouse/ <a href="#">NCI, 1976</a> )	0.0010 (300)		
	Meganucleocytosis (rat/ <a href="#">Maltoni et al., 1986</a> )	0.0015 (10)	0.34 (100)	
↑ Kidney weight	↑ <i>kidney weight</i> (rat/ <a href="#">Woolhiser et al., 2006</a> )	0.00079 (10)	– [rtr]	0.0013–2.5 (10)
<b>Liver</b>				
↑ Liver weight	↑ liver weight (mouse/ <a href="#">Kjellstrand et al., 1983a</a> )	0.79 (10)	– [rtr]	0.82–2.6 (10–100)
<b>Immunologic</b>				
↓ Thymus weight	↓ <b>thymus weight</b> (mouse/ <a href="#">Keil et al., 2009</a> )	<b>0.00048</b> (100)	0.00035 (1,000)	0.00016 (100)
Immuno-suppression	↓ cell-mediated response to SRBC ↓ stem cell recolonization (mouse/ <a href="#">Sanders et al., 1982b</a> )	0.025 (100)	0.018 (1000)	0.0084–0.91 (100)
	Decreased PFC response (rat/ <a href="#">Woolhiser et al., 2006</a> )	0.14 (100)	– [rtr]	
Autoimmunity	↑ anti-dsDNA and anti-ssDNA Abs (mouse/ <a href="#">Keil et al., 2009</a> )	0.0016 (30)	0.0012 (300)	0.00053–0.19 (30–300)
	Autoimmune organ changes (mouse/ <a href="#">Kaneko et al., 2000</a> )	0.14 (300)	– [rtr]	

**Table 5-25. Lowest p-cRfDs or cRfDs for different effect domains (continued)**

Effect domain Effect type	Candidate critical effect (species/critical study)	p-cRfD or cRfD in mg/kg/d (composite UF)		
		Preferred dose-metric <sup>a</sup>	Default methodology	Alternative dose- metrics/studies (Tables 5-13–5-18)
<b>Reproductive</b>				
Effects on sperm and testes	↓ Ability of sperm to fertilize (rat/ <a href="#">DuTeaux et al., 2004a</a> )	0.016 (1,000)	0.014 (10,000 <sup>b</sup> )	0.042–0.10 (30–1,000)
	Multiple effects (rat/ <a href="#">Kumar et al., 2001b, 2000b</a> )	0.016 (1,000)	– [rtr]	
	Hyperzoospermia (human/ <a href="#">Chia et al., 1996</a> ) <sup>c</sup>	0.024 (30)	– [rtr]	
<b>Developmental</b>				
Develop. immunotox.	↓ PFC, ↑ DTH (rat/ <a href="#">Peden-Adams et al., 2006</a> ) <sup>d</sup>	<b>0.00037</b> (1,000)	Same as preferred	–
Congenital defects	<b>Heart malformations</b> (rat/ <a href="#">Johnson et al., 2003</a> )	<b>0.00052</b> (10)	0.00021 (100)	0.00017 (10)
Develop. neurotox.	↓ Rearing postexposure (rat/ <a href="#">Fredriksson et al., 1993</a> ) <sup>d</sup>	0.016 (1,000)	Same as preferred	0.017–0.11 (100–3,000)
Pre/postnatal mortality/growth	Resorptions/↓ fetal weight/ skeletal effects (rat/ <a href="#">Healy et al., 1982</a> )	0.085 (100)	[rtr]	0.70–2.9 (10–100)

<sup>a</sup>The critical effects/studies and p-cRfDs or cRfDs used to derive the RfD are in **bold**; supporting effects/studies and p-cRfDs in *italics*.

<sup>b</sup>EPA's report on the RfC and RfD processes ([U.S. EPA, 2002b](#)) recommends not deriving reference values with a composite UF of >3,000; however, composite UFs exceeding 3,000 are considered here because the derivation of the cRfCs and cRfDs is part of a screening process and the application of the PBPK model for candidate critical effects reduces the values of some of the individual UFs for the p-cRfCs and p-cRfDs.

<sup>c</sup>Greater than usual degree of uncertainty (see Section 5.1.2).

<sup>d</sup>No PBPK model based analyses were done, so cRfD on the basis of applied dose only.

rtr = route-to-route extrapolated result (no value for default methodology)

**Table 5-26. Lowest p-cRfCs for candidate critical effects for different types of effect based on primary dose-metric**

Type of effect	Effect (primary dose-metric)	p-cRfC (ppm)
Neurological	Demyelination in hippocampus in rats (TotMetabBW34)	0.007 (rtr)
Kidney	Toxic nephropathy in rats (ABioactDCVCBW34)	0.0006 (rtr)
Liver	Increased liver weight in mice (AMetLiv1BW34)	0.9
Immunological	Decreased thymus weight in mice (TotMetabBW34)	0.0003 (rtr)
Reproductive	Decreased ability of rat sperm to fertilize (AUCCBld)	0.009 (rtr) <sup>a</sup>
Developmental	Heart malformations in rats (TotOxMetabBW34)	0.0004 (rtr)

<sup>a</sup>This value is supported by the p-cRfC value of 0.01 ppm for multiple testes and sperm effects from an inhalation study in rats.

rtr = route-to-route extrapolated result

**Table 5-27. Lowest p-cRfDs for candidate critical effects for different types of effect based on primary dose-metric**

Type of effect	Effect (primary dose-metric)	p-cRfD (mg/kg/d)
Neurological	Demyelination in hippocampus in rats (TotMetabBW34)	0.009
Kidney	Toxic nephropathy in rats (ABioactDCVCBW34)	0.0003
Liver	Increased liver weight in mice (AMetLiv1BW34)	0.8 (rtr)
Immunological	Decreased thymus weight in mice (TotMetabBW34)	0.0005
Reproductive	Decreased ability of rat sperm to fertilize (AUCCBld) and multiple testes and sperm effects (TotMetabBW34) <sup>a</sup>	0.02
Developmental	Heart malformations in rats (TotOxMetabBW34)	0.0005 <sup>b</sup>

<sup>a</sup>Endpoints from two different studies yielded the same p-cRfD value.

<sup>b</sup>This value is supported by the cRfD value of 0.0004 mg/kg/day derived for developmental immunotoxicity effects in mice ([Peden-Adams et al., 2006](#)); however, no PBPK analyses were done for this latter effect, so the value of 0.0004 mg/kg/day is based on applied dose.

rtr = route-to-route extrapolated result

For neurological, kidney, immunological, and developmental effects, the lowest p-cRfCs were derived from oral studies by route-to-route extrapolation. This appears to be a function of the lack of comparable inhalation studies for many effects studied via the oral exposure route, for

which there is a larger database of studies. For the liver and reproductive effects, inhalation studies yielded a p-cRfC lower than the lowest route-to-route extrapolated p-cRfC for that type of effect. Conversely, the lowest p-cRfDs were derived from oral studies with the exception of reproductive effects, for which route-to-route extrapolation from an inhalation study in humans also yielded among the lowest p-cRfDs. The only effect for which there were comparable studies for comparing a p-cRfC from an inhalation study with a p-cRfC estimated by route-to-route extrapolation from an oral study was increased liver weight in the mouse. The primary dose-metric of amount of TCE oxidized in the liver yielded similar p-cRfCs of 1.0 and 1.1 ppm for the inhalation result and the route-to-route extrapolated result, respectively (see Table 5-15).

As can be seen in these tables, the most sensitive types of effects (the types with the lowest p-cRfCs and p-cRfDs) appear to be developmental, kidney, and immunological (adult and developmental) effects, and then neurological and reproductive effects, in that order. Lastly, the liver effects have p-cRfC and p-cRfD values that are about 3.5 orders of magnitude higher than those for developmental, kidney, and immunological effects.

#### **5.1.5.2. RfC**

The goal is to select an overall RfC that is well supported by the available data (i.e., without excessive uncertainty given the extensive database) and protective for all of the candidate critical effects, recognizing that individual candidate RfC values are by nature somewhat imprecise. The lowest candidate RfC values within each health effect category span a 3,000-fold range from 0.0003 to 0.9 ppm (see Table 5-26). One approach to selecting an RfC would be to select the lowest calculated value of 0.0003 ppm for decreased thymus weight in mice. However, as can be seen in Table 5-24, three p-cRfCs are in the relatively narrow range of 0.0003–0.0006 ppm at the low end of the overall range. Given the somewhat imprecise nature of the individual candidate RfC values, and the fact that multiple effects/studies lead to similar candidate RfC values, the approach taken in this assessment is to select an RfC supported by multiple effects/studies. The advantages of this approach, which is only possible when there is a relatively large database of studies/effects and when multiple candidate values happen to fall within a narrow range at the low end of the overall range, are that it leads to a more robust RfC (less sensitive to limitations of individual studies) and that it provides the important characterization that the RfC exposure level is similar for multiple noncancer effects rather than being based on a sole explicit critical effect.

Tables 5-28 and 5-29 summarize the PODs and UFs for the two critical and one supporting studies/effects, respectively, corresponding to the p-cRfCs that have been chosen as the basis of the RfC for TCE noncancer effects. Each of these lowest candidate p-cRfCs, ranging from 0.0003 to 0.0006 ppm, for developmental, immunologic, and kidney effects, are values derived from route-to-route extrapolation using the PBPK model. The lowest p-cRfC estimate (for a primary dose-metric) from an inhalation study is 0.001 ppm for kidney effects, which is

higher than the route-to-route extrapolated p-cRfC from the most sensitive oral study. For each of the candidate RfCs, the PBPK model was used for inter- and intraspecies extrapolation, based on the preferred dose-metric for each endpoint.

**Table 5-28. Summary of critical studies, effects, PODs, and UFs used to derive the RfC**

For the database,  $UF_D = 1$  because there is minimal potential for deriving an underprotective toxicity value as a result of an incomplete characterization of TCE toxicity.

<p>Keil et al. (2009)—Decreased thymus weight in female B6C3F<sub>1</sub> mice exposed for 30 wks by drinking water.</p> <ul style="list-style-type: none"> <li>• idPOD = 0.139 mg TCE metabolized/kg<sup>3/4</sup>/d, which is the PBPK model-predicted internal dose at the applied dose LOAEL of 0.35 mg/kg/d (continuous) (no BMD modeling due to inadequate model fit caused by supralinear dose-response shape) (see Appendix F, Section F.6.3).</li> <li>• HEC<sub>99</sub> = 0.033 ppm (lifetime continuous exposure) derived from combined interspecies, intraspecies, and route-to-route extrapolation using PBPK model.</li> <li>• <math>UF_L = 10</math> because POD is a LOAEL for an adverse effect.</li> <li>• <math>UF_A = 3</math> because the PBPK model was used for interspecies extrapolation.</li> <li>• <math>UF_H = 3</math> because the PBPK model was used to characterize human toxicokinetic variability.</li> <li>• p-cRfC = 0.033/100 = 0.00033 ppm (2 µg/m<sup>3</sup>).</li> </ul>
<p>Johnson et al. (2003)—Fetal heart malformations in Sprague-Dawley rats exposed on GDs 1–22 by drinking water.</p> <ul style="list-style-type: none"> <li>• idPOD = 0.0142 mg TCE metabolized by oxidation/kg<sup>3/4</sup>/d, which is the BMDL from BMD modeling using PBPK model-predicted internal doses, with highest dose group (1,000-fold higher than next highest dose group) dropped, pup as unit of analysis, BMR = 1% (due to severity of defects, some of which could have been fatal), and a nested Log-logistic model to account for intralitter correlation (see Appendix F, Section F.6.4).</li> <li>• HEC<sub>99</sub> = 0.0037 ppm (lifetime continuous exposure) derived from combined interspecies, intraspecies, and route-to-route extrapolation using PBPK model.</li> <li>• <math>UF_A = 3</math> because the PBPK model was used for interspecies extrapolation.</li> <li>• <math>UF_H = 3</math> because the PBPK model was used to characterize human toxicokinetic variability.</li> <li>• p-cRfC = 0.0037/10 = 0.00037 ppm (2 µg/m<sup>3</sup>).</li> </ul>

**Table 5-29. Summary of supporting studies, effects, PODs, and UFs for the RfC**

For the database,  $UF_D = 1$  because there is minimal potential for deriving an underprotective toxicity value as a result of an incomplete characterization of TCE toxicity.

<p>NTP (1988)—Toxic nephropathy in female Marshall rats exposed for 104 wks by gavage (5 d/wk).</p> <ul style="list-style-type: none"> <li>• idPOD = 0.0132 mg DCVC bioactivated/kg<sup>3/4</sup>/d, which is the BMDL from BMD modeling using PBPK model-predicted internal doses, BMR = 5% (clearly toxic effect), and log-logistic model (see Appendix F, Section F.6.1).</li> <li>• HEC<sub>99</sub> = 0.0056 ppm (lifetime continuous exposure) derived from combined interspecies, intraspecies, and route-to-route extrapolation using PBPK model.</li> <li>• <math>UF_A = 3</math> because the PBPK model was used for interspecies extrapolation.</li> <li>• <math>UF_H = 3</math> because the PBPK model was used to characterize human toxicokinetic variability.</li> <li>• p-cRfC = 0.0056/10 = 0.00056 ppm (3 µg/m<sup>3</sup>).</li> </ul>
---

There is moderate confidence in the lowest p-cRfC for developmental effects (heart malformations) (see Section 5.1.2.8) and the lowest p-cRfC estimate for immunological effects

(see Section 5.1.2.5), and these are considered the critical effects used for deriving the RfC. For developmental effects, although the available study has important limitations, the overall weight of evidence supports an effect of TCE on cardiac development. For immunological effects, there is high confidence in the evidence for an immunotoxic hazard from TCE, but the available dose-response data preclude application of BMD modeling.

For kidney effects (see Section 5.1.2.2), there is high confidence in the evidence for a nephrotoxic hazard from TCE. Moreover, the lowest p-cRfC for kidney effects (toxic nephropathy) is derived from a chronic study and is based on BMD modeling. However, as discussed in Section 3.3.3.2, there remains substantial uncertainty in the extrapolation of GSH conjugation from rodents to humans due to limitations in the available data. In addition, the p-cRfC for toxic nephropathy had greater dose-response uncertainty since the estimation of its POD involved extrapolation from high response rates (>60%). Therefore, toxic nephropathy is considered supportive but is not used as a primary basis for the RfC. The other sensitive p-cRfCs for kidney effects in Table 5-19 were all within a factor of 5 of that for toxic nephropathy; however, these values similarly relied on the uncertain interspecies extrapolation of GSH conjugation.

As a whole, the estimates support an RfC of 0.0004 ppm (0.4 ppb or 2  $\mu\text{g}/\text{m}^3$ ). This value essentially reflects the midpoint between the similar p-cRfC estimates for the two critical effects (0.00033 ppm for decreased thymus weight in mice and 0.00037 ppm for heart malformations in rats), rounded to one significant figure. This value is also within a factor of 2 of the p-cRfC estimate of 0.0006 ppm for the supporting effect of toxic nephropathy in rats. Thus, there is robust support for an RfC of 0.0004 ppm provided by estimates for multiple effects from multiple studies. The estimates are based on PBPK model-based estimates of internal dose for interspecies, intraspecies, and route-to-route extrapolation, and there is sufficient confidence in the PBPK model and support from mechanistic data for one of the dose-metrics (TotOxMetabBW34 for the heart malformations). There is high confidence that ABioactDCVCBW34 and AMetGSHBW34 would be appropriate dose-metrics for kidney effects, but there is substantial uncertainty in the PBPK model predictions for these dose-metrics in humans (see Section 5.1.3.1). Note that there is some human evidence of developmental heart defects from TCE exposure in community studies (see Section 4.8.3.1.1) and of kidney toxicity in TCE-exposed workers (see Section 4.4.1).

In summary, the RfC is **0.0004 ppm** (0.4 ppb or 2  $\mu\text{g}/\text{m}^3$ ) based on route-to-route extrapolated results from oral studies for the critical effects of heart malformations (rats) and immunotoxicity (mice). This RfC value is further supported by route-to-route extrapolated results from an oral study of toxic nephropathy (rats).

### 5.1.5.3. RfD

As with the RfC determination above, the goal is to select an overall RfD that is well supported by the available data (i.e., without excessive uncertainty given the extensive database) and protective for all of the candidate critical effects, recognizing that individual candidate RfD values are by nature somewhat imprecise. The lowest candidate RfD values within each health effect category span a nearly 3,000-fold range from 0.0003 to 0.8 mg/kg/day (see Table 5-26). One approach to selecting an RfC would be to select the lowest calculated value of 0.0003 ppm for toxic nephropathy in rats. However, as can be seen in Table 5-25, multiple p-cRfDs or cRfDs from oral studies are in the relatively narrow range of 0.0003–0.0008 mg/kg/day at the low end of the overall range. Given the somewhat imprecise nature of the individual candidate RfD values, and the fact that multiple effects/studies lead to similar candidate RfD values, the approach taken in this assessment is to select an RfD supported by multiple effects/studies. The advantages of this approach, which is only possible when there is a relatively large database of studies/effects and when multiple candidate values happen to fall within a narrow range at the low end of the overall range, are that it leads to a more robust RfD (less sensitive to limitations of individual studies) and that it provides the important characterization that the RfD exposure level is similar for multiple noncancer effects rather than being based on a sole explicit critical effect.

Tables 5-30 and 5-31 summarize the PODs and UFs for the three critical and two supporting studies/effects, respectively, corresponding to the p-cRfDs or cRfDs that have been chosen as the basis of the RfD for TCE noncancer effects. Two of the lowest p-cRfDs for the primary dose-metrics—0.0008 mg/kg/day for increased kidney weight in rats and 0.0005 mg/kg/day for both heart malformations in rats and decreased thymus weights in mice—are derived using the PBPK model for inter- and intraspecies extrapolation, and a third—0.0003 mg/kg/day for increased toxic nephropathy in rats—is derived using the PBPK model for inter- and intraspecies extrapolation as well as route-to-route extrapolation from an inhalation study. The other of these lowest values—0.0004 mg/kg/day for developmental immunotoxicity (decreased PFC response and increased delayed-type hypersensitivity) in mice—is based on applied dose.

**Table 5-30. Summary of critical studies, effects, PODs, and UFs used to derive the RfD**

For the database,  $UF_D = 1$  because there is minimal potential for deriving an underprotective toxicity value as a result of an incomplete characterization of TCE toxicity.

<p>Keil et al. (2009)—Decreased thymus weight in female B6C3F<sub>1</sub> mice exposed for 30 wks by drinking water.</p> <ul style="list-style-type: none"> <li>• idPOD = 0.139 mg TCE metabolized/kg<sup>3/4</sup>/d, which is the PBPK model-predicted internal dose at the applied dose LOAEL of 0.35 mg/kg/d (continuous) (no BMD modeling due to inadequate model fit caused by supralinear dose-response shape) (see Appendix F, Section F.6.3).</li> <li>• HED<sub>99</sub> = 0.048 mg/kg/d (lifetime continuous exposure) derived from combined interspecies and intraspecies extrapolation using PBPK model.</li> <li>• UF<sub>L</sub> = 10 because POD is a LOAEL for an adverse effect.</li> <li>• UF<sub>A</sub> = 3 because the PBPK model was used for interspecies extrapolation.</li> <li>• UF<sub>H</sub> = 3 because the PBPK model was used to characterize human toxicokinetic variability.</li> <li>• p-cRfD = 0.048/100 = 0.00048 mg/kg/d.</li> </ul>
<p>Peden-Adams et al. (2006)—Decreased PFC response (3 and 8 wks), and increased delayed-type hypersensitivity (8 wks) in pups exposed from GDs 0–3- or 8 wks of age through drinking water (placental and lactational transfer, and pup ingestion).</p> <ul style="list-style-type: none"> <li>• POD = 0.37 mg/kg/d is the applied dose LOAEL (estimated daily dam dose) (no BMD modeling due to inadequate model fit caused by supralinear dose-response shape). No PBPK modeling was attempted due to lack of appropriate models/parameters to account for complicated fetal/pup exposure pattern (see Appendix F, Section F.6.5).</li> <li>• UF<sub>L</sub> = 10 because POD is a LOAEL for multiple adverse effects.</li> <li>• UF<sub>A</sub> = 10 for interspecies extrapolation because PBPK model was not used.</li> <li>• UF<sub>H</sub> = 10 for human variability because PBPK model was not used.</li> <li>• cRfD = 0.37/1,000 = 0.00037 mg/kg/d.</li> </ul>
<p>Johnson et al. (2003)—Fetal heart malformations in Sprague-Dawley rats exposed on GDs 1–22 by drinking water.</p> <ul style="list-style-type: none"> <li>• idPOD = 0.0142 mg TCE metabolized by oxidation/kg<sup>3/4</sup>/d, which is the BMDL from BMD modeling using PBPK model-predicted internal doses, with highest dose group (1,000-fold higher than next highest dose group) dropped, pup as unit of analysis, BMR = 1% (due to severity of defects, some of which could have been fatal), and a nested Log-logistic model to account for intralitter correlation (see Appendix F, Section F.6.4).</li> <li>• HED<sub>99</sub> = 0.0051 mg/kg/d (lifetime continuous exposure) derived from combined interspecies and intraspecies extrapolation using PBPK model.</li> <li>• UF<sub>A</sub> = 3 because the PBPK model was used for interspecies extrapolation.</li> <li>• UF<sub>H</sub> = 3 because the PBPK model was used to characterize human toxicokinetic variability.</li> <li>• p-cRfD = 0.0051/10 = 0.00051 mg/kg/d.</li> </ul>

**Table 5-31. Summary of supporting studies, effects, PODs, and UFs for the RfD**

For the database,  $UF_D = 1$  because there is minimal potential for deriving an underprotective toxicity value as a result of an incomplete characterization of TCE toxicity.

<p>NTP (1988)—Toxic nephropathy in female Marshall rats exposed for 104 wks by gavage (5 d/wk).</p> <ul style="list-style-type: none"> <li>• <math>idPOD = 0.0132 \text{ mg DCVC bioactivated/kg}^{3/4}/\text{d}</math>, which is the BMDL from BMD modeling using PBPK model-predicted internal doses, <math>BMR = 5\%</math> (clearly toxic effect), and Log-logistic model (see Appendix F, Section F.6.1).</li> <li>• <math>HED_{99} = 0.0034 \text{ mg/kg/d}</math> (lifetime continuous exposure) derived from combined interspecies and intraspecies extrapolation using PBPK model.</li> <li>• <math>UF_A = 3</math> because the PBPK model was used for interspecies extrapolation.</li> <li>• <math>UF_H = 3</math> because the PBPK model was used to characterize human toxicokinetic variability.</li> <li>• <math>p\text{-cRfD} = 0.0034/10 = 0.00034 \text{ mg/kg/d}</math>.</li> </ul>
<p>Woolhiser et al. (2006)—Increased kidney weight in female Sprague-Dawley rats exposed for 4 wks by inhalation (6 hrs/d, 5 d/wk).</p> <ul style="list-style-type: none"> <li>• <math>idPOD = 0.0309 \text{ mg DCVC bioactivated/kg}^{3/4}/\text{d}</math>, which is the BMDL from BMD modeling using PBPK model-predicted internal doses, <math>BMR = 10\%</math>, and Hill model with constant variance (see Appendix F, Section F.6.2).</li> <li>• <math>HED_{99} = 0.0079 \text{ mg/kg/d}</math> (lifetime continuous exposure) derived from combined interspecies and intraspecies extrapolation using PBPK model.</li> <li>• <math>UF_S = 1</math> because Kjellstrand et al. (1983a) reported that in mice, kidney effects after exposure for 120 d was no more severe than those after 30 d exposure.</li> <li>• <math>UF_A = 3</math> because the PBPK model was used for interspecies extrapolation.</li> <li>• <math>UF_H = 3</math> because the PBPK model was used to characterize human toxicokinetic variability.</li> <li>• <math>p\text{-cRfD} = 0.0079/10 = 0.00079 \text{ mg/kg/d}</math>.</li> </ul>

There is moderate confidence in the  $p\text{-cRfDs}$  for decreased thymus weights (see Section 5.1.2.5) and heart malformations (see Section 5.1.2.8) and the  $cRfD$  for developmental immunological effects (see Section 5.1.2.8), and these effects are considered the critical effects used for deriving the RfD. For heart malformations, although the available study has important limitations, the overall weight of evidence supports an effect of TCE on cardiac development. For adult and developmental immunological effects, there is high confidence in the evidence for an immunotoxic hazard from TCE. However, the available dose-response data for immunological effects preclude application of BMD modeling.

For kidney effects (see Section 5.1.2.2), there is high confidence in the evidence for a nephrotoxic hazard from TCE. Moreover, the two lowest  $p\text{-cRfDs}$  for kidney effects (toxic nephropathy and increased kidney weight) are both based on BMD modeling and one is derived from a chronic study. However, as discussed in Section 3.3.3.2, there remains substantial uncertainty in the extrapolation of GSH conjugation from rodents to humans due to limitations in the available data. In addition, the  $p\text{-cRfD}$  value for toxic nephropathy had greater dose-response uncertainty since the estimation of its POD involved extrapolation from high response rates (>60%). Therefore, kidney effects are considered supportive but are not used as a primary basis for the RfD.

As a whole, the estimates support an RfD of 0.0005 mg/kg/day. This value is within 20% of the estimates for the critical effects—0.0004 mg/kg/day for developmental immunotoxicity (decreased PFC and increased delayed-type hypersensitivity) in mice, and 0.0005 mg/kg/day for both heart malformations in rats and decreased thymus weights in mice. This value is also within approximately a factor of 2 of the supporting effect estimates of 0.0003 mg/kg/day for toxic nephropathy in rats and 0.0008 mg/kg/day for increased kidney weight in rats. Thus, there is strong, robust support for an RfD of 0.0005 mg/kg/day provided by the concordance of estimates derived from multiple effects from multiple studies. The estimates for kidney effects, thymus effects, and developmental heart malformations are based on PBPK model-based estimates of internal dose for interspecies and intraspecies extrapolation, and there is sufficient confidence in the PBPK model and support from mechanistic data for one of the dose-metrics (TotOxMetabBW34 for the heart malformations). There is high confidence that ABioactDCVCBW34 would be an appropriate dose-metric for kidney effects, but there is substantial uncertainty in the PBPK model predictions for this dose-metric in humans (see Section 5.1.3.1). Note that there is some human evidence of developmental heart defects from TCE exposure in community studies (see Section 4.8.3.1.1) and of kidney toxicity in TCE-exposed workers (see Section 4.4.1).

In summary, the RfD is **0.0005 mg/kg/day** based on the critical effects of heart malformations (rats), adult immunological effects (mice), and developmental immunotoxicity (mice), all from oral studies. This RfD value is further supported by results from an oral study for the effect of toxic nephropathy (rats) and route-to-route extrapolated results from an inhalation study for the effect of increased kidney weight (rats).

## **5.2. DOSE-RESPONSE ANALYSIS FOR CANCER ENDPOINTS**

This section describes the dose-response analysis for cancer endpoints. Section 5.2.1 discusses the analyses of data from chronic rodent bioassays. Section 5.2.2 discusses the analyses of human epidemiologic data. Section 5.2.3 discusses the choice of the preferred inhalation unit risk and oral slope factor estimates, as well as the application of ADAFs to the slope factor and unit risk estimates.

### **5.2.1. Dose-Response Analyses: Rodent Bioassays**

This section describes the calculation of cancer slope factor and unit risk estimates based on rodent bioassays. First, all of the available studies (i.e., chronic rodent bioassays) were considered, and those suitable for dose-response modeling were selected for analysis (see Section 5.2.1.1). Then dose-response modeling using the linearized multistage model was performed using applied doses (default dosimetry) as well as PBPK model-based internal doses (see Section 5.2.1.2). Bioassays for which time-to-tumor data were available were analyzed using poly-3 adjustment techniques and using a Multistage Weibull model. In addition, a cancer

potency estimate for different cancer types combined was derived from bioassays in which there was more than one type of tumor response in the same sex and species. Slope factor and unit risk estimates based on PBPK model-estimated internal doses were then extrapolated to human population slope factor and unit risk estimates using the human PBPK model. From these results (see Section 5.2.1.3), estimates from the most sensitive bioassay (i.e., that with the greatest slope factor or unit risk estimate) for each combination of administration route, sex, and species, based on the PBPK model-estimated internal doses, were considered as candidate slope factor or unit risk estimates for TCE. Uncertainties in the rodent-based dose-response analyses are described in Section 5.2.1.4.

#### **5.2.1.1. Rodent Dose-Response Analyses: Studies and Modeling Approaches**

The rodent cancer bioassays that were identified for consideration for dose-response analysis are listed in Tables 5-32 (inhalation bioassays) and 5-33 (oral bioassays) for each sex/species combination. The bioassays selected for dose-response analysis are marked with an asterisk; rationales for rejecting the bioassays that were not selected are provided in the “Comments” columns of the tables. For the selected bioassays, the tissues/organs that exhibited a TCE-associated carcinogenic response and for which dose-response modeling was performed are listed in the “Tissue/Organ” columns.

**Table 5-32. Inhalation bioassays**

Study	Strain	Tissue/organ	Comments
<b>Female mice</b>			
Fukuda et al. (1983) <sup>a</sup>	Crj:CD-1 (ICR)	Lung	
Henschler et al. (1980) <sup>a</sup>	Han:NMRI	Lymphoma	
Maltoni et al. (1986) <sup>a</sup>	B6C3F <sub>1</sub>	Liver, Lung	
Maltoni et al. (1986)	Swiss	–	No dose-response
<b>Male mice</b>			
Henschler et al. (1980)	Han:NMRI	–	No dose-response
Maltoni et al. (1986)	B6C3F <sub>1</sub>	Liver	Exp #BT306: excessive fighting
Maltoni et al. (1986)	B6C3F <sub>1</sub>	Liver	Exp #BT306bis. Results similar to Swiss mice
Maltoni et al. (1986) <sup>a</sup>	Swiss	Liver	
<b>Female rats</b>			
Fukuda et al. (1983)	Sprague-Dawley	–	No dose-response
Henschler et al. (1980)	Wistar	–	No dose-response
Maltoni et al. (1986)	Sprague-Dawley	–	No dose-response
<b>Male rats</b>			
Henschler et al. (1980)	Wistar	–	No dose-response
Maltoni et al. (1986) <sup>a</sup>	Sprague-Dawley	Kidney, Leydig cell, Leukemia	

<sup>a</sup>Selected for dose-response analysis.

“No dose-response” = no tumor incidence data suitable for dose-response modeling

**Table 5-33. Oral bioassays**

Study	Strain	Tissue/organ	Comments
<b>Female mice</b>			
Henschler et al. (1984)	Han:NMRI	–	Toxicity, no dose-response
NCI (1976) <sup>a</sup>	B6C3F <sub>1</sub>	Liver, lung, sarcomas and lymphomas	
NTP (1990)	B6C3F <sub>1</sub>	Liver, lung, lymphomas	Single dose
Van Duuren et al. (1979)	Swiss	Liver	Single dose, no dose-response
<b>Male mice</b>			
Anna et al. (1994)	B6C3F <sub>1</sub>	Liver	Single dose
Bull et al. (2002)	B6C3F <sub>1</sub>	Liver	Single dose
Henschler et al. (1984)	Han:NMRI	–	Toxicity, no dose-response
NCI (1976) <sup>a</sup>	B6C3F <sub>1</sub>	Liver	
NTP (1990)	B6C3F <sub>1</sub>	Liver	Single dose
Van Duuren et al. (1979)	Swiss	–	Single dose, no dose-response
<b>Female rats</b>			
NCI (1976)	Osborne-Mendel	–	Toxicity, no dose-response
NTP (1988)	ACI	–	No dose-response
NTP (1988) <sup>a</sup>	August	Leukemia	
NTP (1988)	Marshall	–	No dose-response
NTP (1988)	Osborne-Mendel	Adrenal cortex	Adenomas only
NTP (1990)	F344/N	–	No dose-response
<b>Male rats</b>			
NCI (1976)	Osborne-Mendel	–	Toxicity, no dose-response
NTP (1988)	ACI	–	No dose-response
NTP (1988) <sup>a</sup>	August	Subcutaneous tissue sarcomas	
NTP (1988) <sup>a</sup>	Marshall	Testes	
NTP (1988) <sup>a</sup>	Osborne-Mendel	Kidney	
NTP (1990) <sup>a</sup>	F344/N	Kidney	

<sup>a</sup>Selected for dose-response analysis.

“No dose-response” = no tumor incidence data suitable for dose-response modeling

The general approach used was to model each sex/species/bioassay tumor response to determine the most sensitive bioassay response (in terms of HEC or HED) for each sex/species combination. The various modeling approaches, model selection, and slope factor and unit risk derivation are discussed below. Modeling was done using the applied dose or exposure (default dosimetry) and several internal dose-metrics. The dose-metrics used in the dose-response modeling are discussed in Section 5.2.1.2. Because of the large volume of analyses and results, detailed discussions about how the data were modeled using the various dosimetry and modeling approaches and results for individual data sets are provided in Appendix G. The overall results are summarized and discussed in Section 5.2.1.3.

Most tumor responses were modeled using the multistage model in EPA's BMDS ([www.epa.gov/ncea/bmnds](http://www.epa.gov/ncea/bmnds)). The multistage model is a flexible model, capable of fitting most cancer bioassay data, and it is EPA's long-standing model for the modeling of such cancer data. The multistage model has the general form

$$P(d) = 1 - \exp\left[-q_0 + q_1d + q_2d^2 + \dots + q_kd^k\right]$$

where  $P(d)$  represents the lifetime risk (probability) of cancer at dose  $d$ , and parameters  $q_i \geq 0$ , for  $i = 0, 1, \dots, k$ . For each data set, the multistage model was evaluated for one stage and  $(n - 1)$  stages, where  $n$  is the number of dose groups in the bioassay. A detailed description of how the data were modeled, as well as tables of the dose-response input data and figures of the multistage modeling results, is provided in Appendix G.

Only models with acceptable fit ( $p > 0.05$ ) were considered.<sup>37</sup> If 1-parameter and 2-parameter models were both acceptable (in no case was there a 3-parameter model), then the more parsimonious model (i.e., the 1-parameter model) was selected unless the inclusion of the 2<sup>nd</sup> parameter resulted in a statistically significant<sup>38</sup> improvement in fit. If two different 1-parameter models were available (e.g., a 1-stage model and a 3-stage model with  $\beta_1$  and  $\beta_2$  both equal to 0), then the one with the best fit, as indicated by the lowest AIC value, was selected. If the AIC values were the same (to three significant figures), then the lower-stage model was selected. Visual fit and scaled  $\chi^2$  residuals were also considered for confirmation in model selection. For two data sets, the highest-dose group was dropped to improve the fit in the lower dose range.

From the selected model for each data set, the maximum likelihood estimate (MLE) for the dose corresponding to a specified level of risk (i.e., the BMD) and its 95% lower confidence bound (BMDL) were estimated.<sup>39</sup> In most cases, the risk level, or BMR, was 10% extra risk;<sup>40</sup> however, in a few cases with low response rates, a BMR of 5%, or even 1%, extra risk was used to avoid extrapolation above the range of the data. As discussed in Section 4.4, there is sufficient evidence to conclude that a mutagenic mode of action is operative for TCE-induced kidney tumors, so linear extrapolation from the BMDL to the origin was used to derive slope factor and unit risk estimates for this site. The weight of evidence also supports involvement of processes of cytotoxicity and regenerative proliferation in the carcinogenicity of TCE, although not with the extent of support as for a mutagenic mode of action. In particular, data linking TCE-induced

---

<sup>37</sup>When considering multiple types of model for noncancer effects,  $p > 0.10$  is used. For cancer, there is a prior preference for the multistage model, thus the  $p > 0.05$  (which increases the probability of accepting the preferred model).

<sup>38</sup>Using a standard criterion for nested models, that the difference in  $-2 \times \log$ -likelihood exceeds 3.84 (the 95th percentile of  $\chi^2$  [1]).

<sup>39</sup>BMDS estimates confidence intervals using the profile likelihood method.

<sup>40</sup>Extra risk over the background tumor rate is defined as  $[P(d) - P(0)] / [1 - P(0)]$ , where  $P(d)$  represents the lifetime risk (probability) of cancer at dose  $d$ .

proliferation to increased mutation or clonal expansion are lacking, as are data informing the quantitative contribution of cytotoxicity. Moreover, it is unlikely that any contribution from cytotoxicity leads to a non-linear dose-response relationship near the POD for rodent kidney tumors, since maximal levels of toxicity are reached before the onset of tumors. Finally, because any possible involvement of a cytotoxicity mode of action would be additional to mutagenicity, the dose-response relationship would nonetheless be expected to be linear at low doses. Therefore, the additional involvement of a cytotoxicity mode of action does not provide evidence against the use of linear extrapolation from the POD.

For all other cancer types, the available evidence supports the conclusion that the mode(s) of action for TCE-induced rodent tumors is unknown, as discussed in Sections 4.5–4.10 and summarized in Section 4.11.2.3. Therefore, linear extrapolation was also used based on the general principles outlined in EPA’s *Guidelines for Carcinogen Risk Assessment* ([U.S. EPA, 2005b](#)) and reviewed below in Section 5.2.1.4.1. Thus, for all TCE-associated rodent tumors, slope factor and unit risk estimates are equal to BMR/BMDL (e.g., 0.10/BMDL<sub>10</sub> for a BMR of 10%). See Section 5.2.1.3 for a summary of the slope factor and unit risk estimates for each sex/species/bioassay/tumor type.

Some of the bioassays exhibited differential early mortality across the dose groups, and, for three such male rat studies (identified with checkmarks in the “Time-to-tumor” column of Table 5-34), analyses that take individual animal survival times into account were performed. (For bioassays with differential early mortality occurring primarily before the time of the 1<sup>st</sup> tumor [or 52 weeks, whichever came first], the effects of early mortality were largely accounted for by adjusting the tumor incidence for animals at risk, as described in Appendix G, and the dose-response data were modeled using the regular multistage model, as discussed above, rather than approaches that account for individual animal survival times.)

Two approaches were used to take individual survival times into account. First, EPA’s Multistage Weibull (MSW) software<sup>41</sup> was used for time-to-tumor modeling. The Multistage Weibull time-to-tumor model has the general form:

$$P(d,t) = 1 - \exp\left[- q_0 + q_1d + q_2d^2 + \dots + q_kd^k \times (t-t_0)^z\right]$$

---

<sup>41</sup>This software is available on U.S. EPA’s BMDS Web site ([www.epa.gov/ncea/bmnds](http://www.epa.gov/ncea/bmnds)).

**Table 5-34. Specific dose-response analyses performed and dose-metrics used**

Bioassay	Strain	Endpoint	Applied dose	PBPK-based—primary dose-metric <sup>a</sup>	PBPK-based—alternative dose-metric(s) <sup>a</sup>	Time-to-tumor
<b>INHALATION</b>						
<b>Female mice</b>						
Fukuda et al. ( <a href="#">1983</a> )	Crj:CD-1 (ICR)	Lung adenomas and carcinomas	√	AMetLngBW34	TotOxMetabBW34 AUCCBld	
Henschler et al. ( <a href="#">1980</a> )	Han:NMRI	Lymphoma	√	TotMetabBW34	AUCCBld	
Maltoni et al. ( <a href="#">1986</a> )	B6C3F <sub>1</sub>	Liver hepatomas	√	AMetLiv1BW34	TotOxMetabBW34	
		Lung adenomas and carcinomas	√	AMetLngBW34	TotOxMetabBW34 AUCCBld	
		Combined risk	√			
<b>Male mice</b>						
Maltoni et al. ( <a href="#">1986</a> )	Swiss	Liver hepatomas	√	AMetLiv1BW34	TotOxMetabBW34	
<b>Female rats</b>						
None selected						
<b>Male rats</b>						
Maltoni et al. ( <a href="#">1986</a> )	Sprague-Dawley	Kidney adenomas and carcinomas	√	ABioactDCVCBW34	AMetGSHBW34 TotMetabBW34	
		Leydig cell tumors	√	TotMetabBW34	AUCCBld	
		Leukemias	√	TotMetabBW34	AUCCBld	
		Combined risk	√			

**Table 5-34. Specific dose-response analyses performed and dose-metrics used (continued)**

Bioassay	Strain	Endpoint	Applied dose	PBPK-based—primary dose-metric	PBPK-based—alternative dose-metric(s)	Time-to-tumor
<b>ORAL</b>						
<b>Female mice</b>						
NCI (1976)	B6C3F <sub>1</sub>	Liver carcinomas	√	AMetLiv1BW34	TotOxMetabBW34	
		Lung adenomas and carcinomas	√	AMetLngBW34	TotOxMetabBW34 AUCCBld	
		Multiple sarcomas/lymphomas	√	TotMetabBW34	AUCCBld	
		Combined risk	√			
<b>Male mice</b>						
NCI (1976)	B6C3F <sub>1</sub>	Liver carcinomas	√	AMetLiv1BW34	TotOxMetabBW34	
<b>Female rats</b>						
NTP (1988)	August	Leukemia	√	TotMetabBW34	AUCCBld	
<b>Male rats</b>						
NTP (1988)	August	Subcutaneous tissue sarcomas	√	TotMetabBW34	AUCCBld	
NTP (1988)	Marshall	Testicular interstitial cell tumors	√	TotMetabBW34	AUCCBld	√
NTP (1988)	Osborne-Mendel	Kidney adenomas and carcinomas	√	ABioactDCVCBW34	AMetGSHBW34 TotMetabBW34	√
NTP (1990)	F344/N	Kidney adenomas and carcinomas	√	ABioactDCVCBW34	AMetGSHBW34 TotMetabBW34	√

**<sup>a</sup>PBPK-based dose-metric abbreviations:**

ABioactDCVCBW34 = Amount of DCVC bioactivated in the kidney per unit body weight<sup>3/4</sup> (mg DCVC/kg<sup>3/4</sup>/week).

AMetGSHBW34 = Amount of TCE conjugated with GSH per unit body weight<sup>3/4</sup> (mg TCE/kg<sup>3/4</sup>/week).

AMetLiv1BW34 = Amount of TCE oxidized per unit body weight<sup>3/4</sup> (mg TCE/kg<sup>3/4</sup>/week).

AMetLngBW34 = Amount of TCE oxidized in the respiratory tract per unit body weight<sup>3/4</sup> (mg TCE/kg<sup>3/4</sup>/week).

AUCCBld = Area under the curve of the venous blood concentration of TCE (mg-hr/L/week).

TotMetabBW34 = Total amount of TCE metabolized per unit body weight<sup>3/4</sup> (mg TCE/kg<sup>3/4</sup>/week).

TotOxMetabBW34 = Total amount of TCE oxidized per unit body weight<sup>3/4</sup> (mg TCE/kg<sup>3/4</sup>/week).

where  $P(d,t)$  represents the probability of a tumor by age  $t$  for dose  $d$ , and parameters  $z \geq 1$ ,  $t_0 \geq 0$ , and  $q_i \geq 0$  for  $i = 0, 1, \dots, k$ , where  $k$  = the number of dose groups; the parameter  $t_0$  represents the time between when a potentially fatal tumor becomes observable and when it causes death. (All of our analyses used the model for incidental tumors, which has no  $t_0$  term.) Although the fit of the MSW model can be assessed visually using the plot feature of the MSW software, because there is no applicable goodness-of-fit statistic with a well-defined asymptotic distribution, an alternative survival-adjustment technique, “poly-3 adjustment,” was also applied ([Portier and Bailer, 1989](#)). This technique was used to adjust the tumor incidence denominators based on the individual animal survival times.<sup>42</sup> The adjusted incidence data then served as inputs for EPA’s BMDS multistage model, and model (i.e., stage) selection was conducted as already described above. Under both survival-adjustment approaches, BMDs and BMDLs were obtained and slope factor and unit risks were derived as discussed above for the standard multistage model approach. See Appendix G for a more detailed description of the MSW modeling and for the results of both the MSW and poly-3 approaches for the individual data sets. A comparison of the results for the three different data sets and the various dose-metrics used is presented in Section 5.2.1.3.

For bioassays that exhibited more than one type of tumor response in the same sex and species (these studies have a row for “combined risk” in the “Endpoint” column of Table 5-34), the cancer potency for the different cancer types combined was estimated, in accordance with EPA’s *Guidelines for Carcinogen Risk Assessment* ([U.S. EPA, 2005b](#)). The combined tumor risk estimate describes the risk of developing tumors for *any* (not all together) of the cancer types that exhibited a TCE-associated tumor response; this estimate then represents the total excess cancer risk. The model for the combined tumor risk is also multistage, with the sum of the stage-specific multistage coefficients from the individual tumor models serving as the stage-specific coefficients for the combined risk model (i.e., for each  $q_i$ ,  $q_{i[\text{combined}]} = q_{i1} + q_{i2} + \dots + q_{ik}$ , where the  $q_i$ s are the coefficients for the powers of dose and  $k$  is the number of cancer types being combined) ([NRC, 1994](#); [Bogen, 1990](#)). This model assumes that the occurrences of two or more cancer types are independent. Although the resulting model equation can be readily solved for a given BMR to obtain an MLE (BMD) for the combined risk, the confidence bounds for the combined risk estimate were not calculated by modeling software available during the development of this assessment. Therefore, the confidence bounds on the combined BMD were estimated using a Bayesian approach, computed using Markov chain Monte Carlo techniques and implemented using the freely available WinBugs software ([Spiegelhalter et al., 2003](#)). Use of WinBugs for derivation of a distribution of BMDs for a single multistage model has been demonstrated by Kopylev et al. ([2007](#)), and this approach can be straightforwardly generalized to

---

<sup>42</sup>Each tumorless animal is weighted by its fractional survival time (number of days on study divided by 728 days, the typical number of days in a 2-year bioassay) raised to the power of 3 to reflect the fact that animals are at greater risk of cancer at older ages. Animals with tumors are given a weight of 1. The sum of the weights of all of the animals in an exposure group yields the effective survival-adjusted denominator.

derive the distribution of BMDs for the combined tumor load. For further details on the implementation of this approach and for the results of the analyses, see Appendix G.

#### **5.2.1.2. Rodent Dose-Response Analyses: Dosimetry**

In modeling the applied doses (or exposures), default dosimetry procedures were applied to convert applied rodent doses to HEDs. Essentially, for inhalation exposures, “ppm equivalence” across species was assumed, consistent with the recommendations of U.S. EPA (1994a) for deriving a human equivalent concentration for a Category 3 gas for which the blood:air partition coefficient in laboratory animals is greater than that in humans (e.g., the posterior population median estimate for the TCE blood:air partition coefficient was 14 in the mouse [Table 3-37], 19 in the rat [Table 3-38], and 9.2 in the human [Table 3-39]). For oral doses,  $\frac{3}{4}$ -power body-weight scaling was used, with a default average human body weight of 70 kg. See Appendix G for more details on the default dosimetry procedures.

In addition to applied doses, several internal dose-metrics were used in the dose-response modeling for each tumor type. Use of internal dose-metrics in dose-response modeling is described here briefly. For more details on the PBPK modeling used to estimate the levels of the dose-metrics corresponding to different exposure scenarios in rodents and humans, as well as a qualitative discussion of the uncertainties and limitations of the model, see Section 3.5; for a more detailed discussion of how the dose-metrics were used in dose-response modeling, see Appendix G. Quantitative analyses of the uncertainties and their implications for dose-response assessment, utilizing the results of the Bayesian analysis of the PBPK model, are discussed separately in Section 5.2.1.4.2.

##### **5.2.1.2.1. Selection of dose-metrics for different cancer types**

One area of scientific uncertainty in cancer dose-response assessment is the appropriate scaling between rodent and human doses for equivalent responses. As discussed above, for applied dose, the standard dosimetry assumptions for equal lifetime carcinogenic risk are, for inhalation exposure, the same lifetime exposure concentration in air, and, for oral exposure, the same lifetime daily dose scaled by body weight to the  $\frac{3}{4}$  power. In this assessment, the cross-species scaling methodology, grounded in the principles of allometric variation of biologic processes, is used for describing pharmacokinetic equivalence (U.S. EPA, 1992, 2011a, 2005b; Allen and Fisher, 1993; Crump et al., 1989; Allen et al., 1987). Briefly, in the absence of adequate information to the contrary, the methodology determines pharmacokinetic equivalence across species through equal average lifetime concentrations or AUCs of the toxicant. Thus, in cases where the PBPK model can predict internal concentrations of the active moiety, equivalent daily AUCs are assumed to address cross-species pharmacokinetics. For cancer assessments, there is currently no adjustment for pharmacodynamic differences.

More detailed discussion of the cross-species scaling methodology, and its implications for dose-metric selection, was presented for the noncancer dose-response analyses in Section 5.1.3.1, and those details are not repeated here.

To summarize, the preferred dose-metric under this methodology is equivalent daily AUC of the active moiety (parent compound or metabolite). For metabolites, in cases where the rate of production, but not the rate of clearance, of the active moiety can be estimated, the preferred dose-metric is the rate of metabolism (through the appropriate pathway) scaled by body weight to the  $3/4$  power. If there are sufficient data to consider the active metabolite moiety(ies) “reactive” and cleared through nonbiological processes, then the preferred dose-metric is the rate of metabolism (through the appropriate pathway) scaled by the tissue mass. Finally, if local metabolism is thought to be involved but cannot be estimated with the available data, then the AUC of the parent compound in blood is considered an appropriate surrogate and thus the preferred dose-metric.

Generally, an attempt was made to use tissue-specific dose-metrics representing particular pathways or metabolites identified from available data as having a likely role in the induction of a tissue-specific cancer. Where insufficient information was available to establish particular metabolites or pathways of likely relevance to a tissue-specific cancer, more general “upstream” metrics representing either parent compound or total metabolism had to be used. In addition, the selection of dose-metrics was limited to metrics that could be adequately estimated by the PBPK model (see Section 3.5). The (PBPK-based) dose-metrics used for the different cancer types are listed in Table 5-34. For each tumor type, the “primary” dose-metric referred to in Table 5-34 is the metric representing the particular metabolite or pathway whose involvement in carcinogenicity has the greatest biological support, whereas “alternative” dose-metrics represent upstream metabolic pathways (or TCE distribution, in the case of AUCCBld) that may be more generally involved.

#### **5.2.1.2.1.1. Kidney**

As discussed in Sections 4.4.6–4.4.7, there is sufficient evidence to conclude that TCE-induced kidney tumors in rats are primarily caused by GSH-conjugation metabolites either produced in situ in or delivered systemically to the kidney. As discussed in Section 3.3.3.2, bioactivation of these metabolites within the kidney, either by beta-lyase, FMO, or P450s, produces reactive species. Therefore, multiple lines of evidence support the conclusion that renal bioactivation of DCVC is the preferred basis for internal dose extrapolations of TCE-induced kidney tumors. However, uncertainties remain as to the relative contributions from each bioactivation pathway, and quantitative clearance data necessary to calculate the concentration of each species are lacking. Moreover, the estimates of the amount bioactivated are indirect, derived from the difference between overall GSH conjugation flux and NAcDCVC excretion (see Section 3.5.7.3.1).

The rationales for the dose-metrics for kidney tumors are the same as for kidney noncancer toxicity, discussed above in Section 5.1.3.1.1, and not repeated here. The primary internal dose-metric for TCE-induced kidney tumors is the weekly rate of DCVC bioactivation per unit body weight to the  $3/4$  power (**ABioactDCVCBW34 [mg/kg<sup>3/4</sup>/week]**). Due to the larger relative kidney weight in rats as compared to humans, using the alternative scaling by kidney weight instead of body weight to the  $3/4$  power would only change the quantitative interspecies extrapolation by about twofold,<sup>43</sup> so the sensitivity of the results to the scaling choice is relatively small. An alternative dose-metric that also involves the GSH conjugation pathway is the amount of GSH conjugation scaled by the  $3/4$  power of body weight (**AMetGSHBW34 [mg/kg<sup>3/4</sup>/week]**). This dose-metric uses the total flux of GSH conjugation as the toxicologically-relevant dose, and, thus, incorporates any direct contributions from DCVG and DCVC, which are not addressed in the DCVC bioactivation metric. Another alternative dose-metric is the total amount of TCE metabolism (oxidation and GSH conjugation together) scaled by the  $3/4$  power of body weight (**TotMetabBW34 [mg/kg<sup>3/4</sup>/week]**). This dose-metric uses the total flux of TCE metabolism as the toxicologically relevant dose, and, thus, incorporates the possible involvement of oxidative metabolites, acting either additively or interactively, in addition to GSH conjugation metabolites in nephrocarcinogenicity (see Section 4.4.6). While there is no evidence that TCE oxidative metabolites can on their own induce kidney cancer, some nephrotoxic effects attributable to oxidative metabolites (e.g., peroxisome proliferation) may modulate the nephrocarcinogenic potency of GSH metabolites. However, this dose-metric is given less weight than those involving GSH conjugation because, as discussed in Sections 4.4.6 and 4.4.7, the weight of evidence supports the conclusion that GSH conjugation metabolites play a predominant role in nephrocarcinogenicity.

#### **5.2.1.2.1.2. Liver**

As discussed in Section 4.5.6, there is substantial evidence that oxidative metabolism is involved in TCE hepatocarcinogenicity, based primarily on noncancer and cancer effects similar to those observed with TCE being observed with a number of oxidative metabolites of TCE (e.g., CH, TCA, and DCA). While TCA is a stable, circulating metabolite, CH and DCA are relatively short-lived, although enzymatically cleared (see Section 3.3.3.1). As discussed in Sections 4.5.6 and 4.5.7, there is now substantial evidence that TCA does not adequately account for the hepatocarcinogenicity of TCE; therefore, unlike in previous dose-response analyses ([Clewell and Andersen, 2004](#); [Rhomberg, 2000](#)), the AUCs of TCA in plasma and in liver were not considered as dose-metrics. However, there are inadequate data across species to quantify the dosimetry of CH and DCA, and other intermediates of oxidative metabolism (such as TCE-oxide or

---

<sup>43</sup>The range of the difference is 2.1–2.4-fold using the posterior medians for the relative kidney weight in rats and humans from the PBPK model described in Section 3.5 (see Table 3-38) and body weights of 0.3–0.4 kg for rats and 60–70 kg for humans.

dichloroacetylchloride) also may be involved in carcinogenicity. Thus, due to uncertainties as to the active moiety(ies), but the strong evidence associating TCE liver effects with oxidative metabolism in the liver, hepatic oxidative metabolism is the preferred basis for internal dose extrapolations of TCE-induced liver tumors.

The rationales for the dose-metrics for liver tumors are the same as for liver noncancer toxicity, discussed above in Section 5.1.3.1.2, and not repeated here. The primary internal dose-metric for TCE-induced liver tumors is selected to be the weekly rate of hepatic oxidation per unit body weight to the  $3/4$  power (**AMetLiv1BW34 [mg/kg<sup>3/4</sup>/week]**). Due to the larger relative liver weight in mice as compared to humans, scaling by liver weight instead of body weight to the  $3/4$  power would only change the quantitative interspecies extrapolation by about fourfold,<sup>44</sup> so the sensitivity of the results to the scaling choice is relatively modest. The total amount of oxidative metabolism of TCE scaled by the  $3/4$  power of body weight (**TotOxMetabBW34 [mg/kg<sup>3/4</sup>/week]**) was selected as an alternative dose-metric (the justification for the body weight to the  $3/4$  power scaling is analogous to that for hepatic oxidative metabolism, above). This dose-metric accounts for the possible additional contributions of systemically delivered products of lung oxidation.

#### 5.2.1.2.1.3. Lung

As discussed in Section 4.7.3, in situ oxidative metabolism in the respiratory tract may be more important to lung toxicity than systemically delivered metabolites, at least as evidenced by acute pulmonary toxicity. While chloral was originally implicated as the active metabolite, based on either acute toxicity or mutagenicity of chloral and/or CH, more recent evidence suggests that other oxidative metabolites may also contribute to lung toxicity. These data include the identification of dichloroacetyl lysine adducts in Clara cells ([Forkert et al., 2006](#)), and the induction of pulmonary toxicity by TCE in CYP2E1-null mice, which may generate a different spectrum of oxidative metabolites as compared to wild-type mice (respiratory tract tissue also contains P450s from the CYP2F family). Overall, the weight of evidence supports the selection of respiratory tract oxidation of TCE as the preferred basis for internal dose extrapolations of TCE-induced lung tumors. However, uncertainties remain as to the relative contributions from different oxidative metabolites, and quantitative clearance data necessary to calculate the concentration of each species are lacking.

Under the cross-species scaling methodology, the rate of respiratory tract oxidation would be scaled by body weight to the  $3/4$  power. For chloral, as discussed in Section 4.7.3, the reporting of substantial TCOH but no detectable CH in blood following TCE exposure from experiments in isolated, perfused lungs ([Dalbey and Bingham, 1978](#)) support the conclusion that

---

<sup>44</sup>The range of the difference is 3.5–3.9-fold using the posterior medians for the relative liver weight in mice and humans from the PBPK model described in Section 3.5 (see Table 3-37) and body weights of 0.03–0.04 kg for mice and 60–70 kg for humans.

chloral does not leave the target tissue in substantial quantities, but that there is substantial clearance by enzyme-mediated biotransformation. DCAC is a relatively-short-lived intermediate from aqueous (nonenzymatic) decomposition of TCE-oxide that can be trapped with lysine or degrade further to form DCA, among other products (Cai and Guengerich, 1999). Cai and Guengerich (1999) reported a half-life of TCE-oxide under aqueous conditions of 12 s at 23°C, a time-scale that would be shorter at physiological conditions (37°C) and that includes formation of DCAC as well as its decomposition. Therefore, evidence for this metabolite suggests that its clearance both is sufficiently rapid so that it would remain at the site of formation and is nonenzymatically mediated so that its rate would be independent of body weight. Other oxidative metabolites may also play a role, but, because they have not been identified, no inferences can be made as to their clearance.

Therefore, because it is not clear what the contributions to TCE-induced lung tumors are from different oxidative metabolites produced in situ and the scaling by body weight to the  $\frac{3}{4}$  power is supported for at least one of the possible active moieties, it was decided here to scale the rate of respiratory tract tissue oxidation of TCE by body weight to the  $\frac{3}{4}$  power. The primary internal dose-metric for TCE-induced lung tumors is, thus, the weekly rate of respiratory tract oxidation per unit body weight to the  $\frac{3}{4}$  power (**AMetLngBW34 [mg/kg<sup>3/4</sup>/week]**). It should be noted that, due to the larger relative respiratory tract tissue weight in mice as compared to humans, scaling by tissue weight instead of body weight to the  $\frac{3}{4}$  power would change the quantitative interspecies extrapolation by less than twofold,<sup>45</sup> so the sensitivity of the results to the scaling choice is relatively small.

While there is substantial evidence that acute pulmonary toxicity is related to pulmonary oxidative metabolism, for carcinogenicity, it is possible that, in addition to locally produced metabolites, systemically-delivered oxidative metabolites also play a role. Therefore, total oxidative metabolism scaled by the  $\frac{3}{4}$  power of body weight (**TotOxMetabBW34 [mg/kg<sup>3/4</sup>/week]**) was selected as an alternative dose-metric (the justification for the body weight to the  $\frac{3}{4}$  power scaling is analogous to that for respiratory tract oxidative metabolism, above).

Another alternative dose-metric considered here is the AUC of TCE in blood (**AUCCBld [mg-hour/L/week]**). This dose-metric would account for the possibility that local metabolism is determined primarily by TCE delivered in blood via systemic circulation to pulmonary tissue (the flow rate of which scales as body weight to the  $\frac{3}{4}$  power), as assumed in previous PBPK models, rather than TCE delivered in air via diffusion to the respiratory tract, as is assumed in the PBPK model described in Section 3.5. However, as discussed in Section 3.5 and Appendix A, the available pharmacokinetic data provide greater support for the updated model structure. This dose-metric also accounts for the possible role of TCE itself in pulmonary

---

<sup>45</sup>The range of the difference is 1.6–1.8-fold using the posterior medians for the relative respiratory tract tissue weight in mice and humans from the PBPK model described in Section 3.5 (see Table 3-37), and body weights of 0.03–0.04 kg for mice and 60–70 kg for humans.

carcinogenicity (consistent with the assumption that the same average concentration of TCE in blood will lead to a similar lifetime cancer risk across species).

#### **5.2.1.2.1.4. Other sites**

For all other sites listed in Table 5-34, there is insufficient information for site-specific determinations of appropriate dose-metrics. While TCE metabolites and/or metabolizing enzymes have been reported in some of these tissues (e.g., male reproductive tract), their roles in carcinogenicity for these specific sites have not been established. Although “primary” and “alternative” dose-metrics are defined, they do not differ appreciably in their degrees of plausibility.

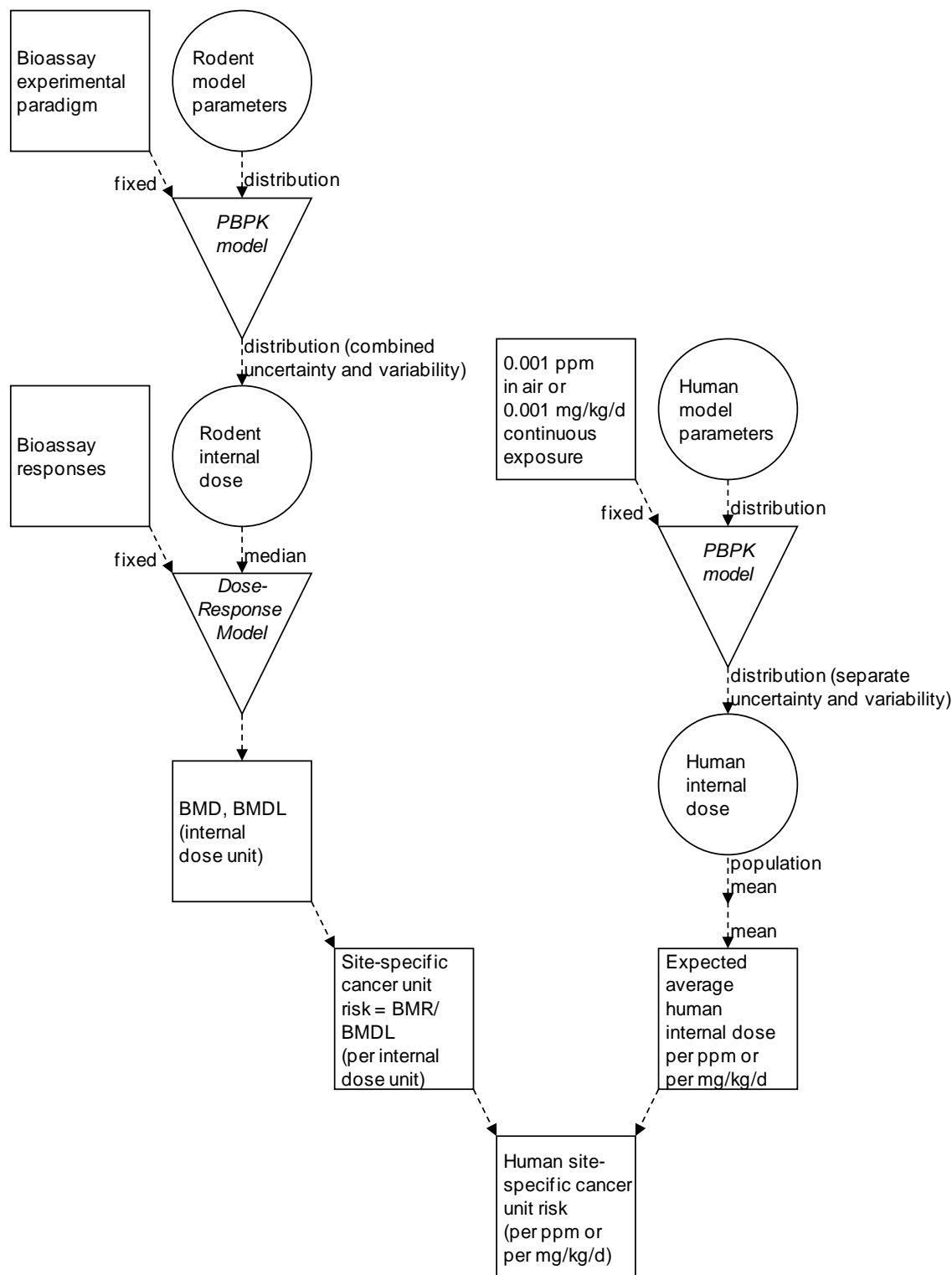
Given that the majority of the toxic and carcinogenic responses to TCE appear to be associated with metabolism, total metabolism of TCE scaled by the  $\frac{3}{4}$  power of body weight was selected as the primary dose-metric (**TotMetabBW34 [mg/kg<sup>3/4</sup>/week]**). This dose-metric uses the total flux of TCE metabolism as the toxicologically-relevant dose, and, thus, incorporates the possible involvement of any TCE metabolite in carcinogenicity.

An alternative dose-metric considered here is the AUC of TCE in blood. This dose-metric would account for the possibility that the determinant of carcinogenicity is local metabolism, governed primarily by TCE delivered in blood via systemic circulation to the target tissue (the flow rate of which scales as body weight to the  $\frac{3}{4}$  power). This dose-metric also accounts for the possible role of TCE itself in carcinogenicity (consistent with the assumption that the same average concentration of TCE in blood will lead to a similar lifetime cancer risk across species).

#### **5.2.1.2.2. Methods for dose-response analyses using internal dose-metrics**

As shown in Figure 5-5, the general approach taken for the use of internal dose-metrics in dose-response modeling was to first apply the rodent PBPK model to obtain rodent values for the dose-metrics corresponding to the applied doses in a bioassay. Then, dose-response modeling for a tumor response was performed using the internal dose-metrics and the multistage model or the survival-adjusted modeling approaches described above to obtain a BMD and BMDL in terms of the dose-metric. On an internal dose basis, humans and rodents are presumed to have similar lifetime cancer risks, and the relationship between human internal and external doses is essentially linear at low doses up to 0.1 mg/kg/day or 0.1 ppm, and nearly linear up to 10 mg/kg/day or 10 ppm. Therefore, the BMD and BMDL were then converted HEDs (or exposures) using conversion ratios estimated from the human PBPK model at 0.001 mg/kg/day or 0.001 ppm (see Table 5-35). Because the male and female conversions differed by <11%, the human BMDLs were derived using the mean of the sex-specific conversion factors (except for testicular tumors, for which only male conversion factors were used). Finally, a slope factor or unit risk estimate for that tumor response was derived from the human “BMDLs” as described

above (i.e., BMR/BMDL). Note that the converted “BMDs” and “BMDLs” are not actually human equivalent BMDs and BMDLs corresponding to the BMR because the conversion was not made in the dose range of the BMD; the converted BMDs and BMDLs are merely intermediaries to obtain a converted slope factor or unit risk estimate. In addition, it should be noted that median values of dose-metrics were used for rodents, whereas mean values were used for humans. Because the rodent population model characterizes study-to-study variation, animals of the same sex/species/strain combination within a study were assumed to be identical. Therefore, use of median dose-metric values for rodents can be interpreted as assuming that the animals in the bioassay were all “typical” animals and the dose-response model is estimating a “risk to the typical rodent.” In practice, the use of median or mean internal doses for rodents did not make much difference except when the uncertainty in the dose-metric was high (e.g., AMetLungBW34 dose-metric in mice). A quantitative analysis of the impact of the uncertainty in the rodent PBPK dose-metrics is included in Section 5.2.1.4.2. On the other hand, the human population model characterizes individual-to-individual variation. Because the quantity of interest is the human population mean risk, the expected value (averaging over the uncertainty) of the population mean (averaging over the variability) dose-metric was used for the conversion to human slope factor or unit risks. Therefore, the extrapolated slope factor or unit risk estimates can be interpreted as the expected “average risk” across the population based on rodent bioassays.



Square nodes indicate point values, circular nodes indicate distributions, and the inverted triangles indicate a (deterministic) functional relationship.

**Figure 5-5. Flow-chart for dose-response analyses of rodent bioassays using PBPK model-based dose-metrics.**

**Table 5-35. Mean PBPK model predictions for weekly internal dose in humans exposed continuously to low levels of TCE via inhalation (ppm) or orally (mg/kg/day)**

Dose-metric <sup>a</sup>	0.001 ppm		0.001 mg/kg/d	
	Female	Male	Female	Male
ABioactDCVCBW34	0.00324	0.00324	0.00493	0.00515
AMetGSHBW34	0.00200	0.00200	0.00304	0.00318
AMetLiv1BW34	0.00703	0.00683	0.0157	0.0164
AMetLngBW34	0.00281	0.00287	$6.60 \times 10^{-5}$	$6.08 \times 10^{-5}$
AUCCBld	0.00288	0.00298	0.000411	0.000372
TotMetabBW34	0.0118	0.0117	0.0188	0.0196
TotOxMetabBW34	0.00984	0.00970	0.0157	0.0164

<sup>a</sup>See note to Table 5-34 for dose-metric abbreviations. Values represent the mean of the (uncertainty) distribution of population means for each sex and exposure scenario, generated from Monte Carlo simulation of 500 populations of 500 individuals each.

### 5.2.1.3. Rodent Dose-Response Analyses: Results

A summary of the PODs and slope factor and unit risk estimates for each sex/species/bioassay/tumor type is presented in Tables 5-36 (inhalation studies) and 5-37 (oral studies). The PODs for individual cancer types were extracted from the modeling results in the figures in Appendix G. For the applied dose (default dosimetry) analyses, the POD is the BMDL from the male human (“M”) BMDL entry at the top of the figure for the selected model; male results were extracted because the default weight for males in the PBPK modeling is 70 kg, which is the overall human weight in EPA’s default dosimetry methods (for inhalation, male and female results are identical). As described in Section 5.2.1.2, for internal dose-metrics, male and female results were averaged, and the converted human “BMDLs” are not true BMDLs because they were converted outside the linear range of the PBPK models. It can be seen in Appendix G that the male and female results were similar for all of the dose-metrics.

**Table 5-36. Summary of PODs and unit risk estimates for each sex/species/bioassay/tumor type (inhalation)**

Study	Tumor type	BMR	PODs (ppm, in HECs) <sup>a</sup>							
			Applied dose	AUC CBId	TotMetab BW34	TotOxMetab BW34	AMetLng BW34	AMetLiv1 BW34	AMetGSH BW34	ABioact DCVCBW34
<b>Female mouse</b>										
Fukuda et al. (1983)	Lung adenoma + carcinoma	0.1	26.3	55.5		31.3	38.8			
Henschler et al. (1980)	Lymphoma	0.1	11.0 <sup>b</sup>	– <sup>b</sup>	9.84					
Maltoni et al. (1986)	Lung adenoma + carcinoma	0.1	44.6	96.6		51.4	55.7			
	Liver	0.05	37.1			45.8		41.9		
	Combined	0.05	15.7			20.7				
<b>Male mouse</b>										
Maltoni et al. (1986)	Liver	0.1	34.3			51		37.9		
<b>Male rat</b>										
Maltoni et al. (1986)	Leukemia	0.05	28.2 <sup>c</sup>	– <sup>b</sup>	28.3					
	Kidney adenoma + carcinoma	0.01	22.7		13.7			0.197	0.121	
	Leydig cell	0.1	18.6 <sup>c</sup>	– <sup>d</sup>	18.1					
	Combined	0.01	1.44		1.37					
Study	Tumor type	Applied dose	Unit risk estimate (ppm <sup>-1</sup> ) <sup>e</sup>							
			AUC CBId	TotMetab BW34	TotOxMetab BW34	AMetLng BW34	AMetLiv1 BW34	AMetGSH BW34	ABioact DCVCBW34	
<b>Female mouse</b>										
Fukuda et al. (1983)	Lung adenoma + carcinoma	$3.8 \times 10^{-3}$	$1.8 \times 10^{-3}$		$3.2 \times 10^{-3}$	$2.6 \times 10^{-3}$				
Henschler et al. (1980)	Lymphoma	$9.1 \times 10^{-3}$		$1.0 \times 10^{-2}$						
Maltoni et al. (1986)	Lung adenoma + carcinoma	$2.2 \times 10^{-3}$	$1.0 \times 10^{-3}$		$1.9 \times 10^{-3}$	$1.8 \times 10^{-3}$				
	Liver	$1.3 \times 10^{-3}$			$1.1 \times 10^{-3}$		$1.2 \times 10^{-3}$			
	Combined	$3.2 \times 10^{-3}$			$2.4 \times 10^{-3}$					

**Table 5-36. Summary of PODs and unit risk estimates for each sex/species/bioassay/tumor type (inhalation) (continued)**

Study	Tumor type	Unit risk estimate (ppm <sup>-1</sup> ) <sup>e</sup>							
		Applied dose	AUC CBld	TotMetab BW34	TotOxMetab BW34	AMetLng BW34	AMetLiv1 BW34	AMetGSH BW34	ABioact DCVCBW34
<b>Male mouse</b>									
Maltoni et al. (1986)	Liver	2.9 × 10 <sup>-3</sup>			2.0 × 10 <sup>-3</sup>		2.6 × 10 <sup>-3</sup>		
<b>Male rat</b>									
Maltoni et al. (1986)	Leukemia	1.8 × 10 <sup>-3</sup>		<b>1.8 × 10<sup>-3</sup></b>					
	Kidney adenoma + carcinoma	4.4 × 10 <sup>-4</sup>		7.3 × 10 <sup>-4</sup>				5.1 × 10 <sup>-2</sup>	<b>8.3 × 10<sup>-2</sup></b>
	Leydig cell	5.4 × 10 <sup>-3</sup>		<b>5.5 × 10<sup>-3</sup></b>					
	Combined	7.0 × 10 <sup>-3</sup>		7.3 × 10 <sup>-3</sup>					

<sup>a</sup>For the applied doses, the PODs are BMDLs. However, for the internal dose-metrics, the PODs are not actually human equivalent BMDLs corresponding to the BMR because the interspecies conversion does not apply to the dose range of the BMDL; the converted BMDLs are merely intermediaries to obtain a converted unit risk estimate. The calculation that was done is equivalent to using linear extrapolation from the BMDLs in terms of the internal dose-metric to get a unit risk estimate for low-dose risk in terms of the internal dose-metric and then converting that estimate to a unit risk estimate in terms of human equivalent exposures. The PODs reported here are what one would get if one then used the unit risk estimate to calculate the human exposure level corresponding to a 10% extra risk, but the unit risk estimate is not intended to be extrapolated upward out of the low-dose range, e.g., above 10<sup>-4</sup> risk. In addition, for the internal dose-metrics, the PODs are the average of the male and female human “BMDL” results presented in Appendix G.

<sup>b</sup>Inadequate fit to control group, but the primary metric, TotMetabBW34, fits adequately.

<sup>c</sup>Dropped highest-dose group to improve model fit.

<sup>d</sup>Inadequate overall fit.

<sup>e</sup>Unit risk estimate = BMR/POD. Results for the primary dose-metric are in bold.

**Table 5-37. Summary of PODs and slope factor estimates for each sex/species/bioassay/tumor type (oral)**

Study	Tumor type	BMR	PODs (mg/kg/d, in HEDs) <sup>a</sup>							
			Applied dose	AUC CBld	TotMetab BW34	TotOxMetab BW34	AMetLng BW34	AMetLiv1 BW34	AMetGSH BW34	ABioact DCVCBW34
<b>Female mouse</b>										
NCI (1976)	Liver carcinoma	0.1	26.5			17.6		14.1		
	Lung adenoma + carcinoma	0.1	41.1	682		24.7	757			
	Leukemias + sarcomas	0.1	43.1	733	20.6					
	Combined	0.05	7.43			5.38				
<b>Male mouse</b>										
NCI (1976)	Liver carcinoma	0.1	8.23			4.34		3.45		
<b>Female rat</b>										
NTP (1988)	Leukemia	0.05	72.3	3,220	21.7					
<b>Male rat</b>										
NTP (1990) <sup>c</sup>	Kidney adenoma + carcinoma	0.1	32		11.5				0.471	0.292
NTP (1988)										
Marshall <sup>d</sup>	Testicular	0.1	3.95	167	1.41					
August	Subcutaneous sarcoma	0.05	60.2	2,560	21.5					
Osborne-Mendel <sup>c</sup>	Kidney adenoma + carcinoma	0.1	41.5		14.3				0.648	0.402
<b>Female mouse</b>										
NCI (1976)	Liver carcinoma		$3.8 \times 10^{-3}$			$5.7 \times 10^{-3}$		$7.1 \times 10^{-3}$		
	Lung adenoma + carcinoma		$2.4 \times 10^{-3}$	$1.5 \times 10^{-4}$		$4.0 \times 10^{-3}$	$1.3 \times 10^{-4}$			
	Leukemias + sarcomas		$2.3 \times 10^{-3}$	$1.4 \times 10^{-4}$	$4.9 \times 10^{-3}$					
	Combined		$6.7 \times 10^{-3}$			$9.3 \times 10^{-3}$				

**Table 5-37. Summary of PODs and slope factor estimates for each sex/species/bioassay/tumor type (oral)  
(continued)**

Study	Tumor type	Slope factor estimate (mg/kg/d) <sup>-1b</sup>							
		Applied dose	AUC CBld	TotMetab BW34	TotOxMetab BW34	AMetLng BW34	AMetLiv1 BW34	AMetGSH BW34	ABioact DCVCBW34
<b>Male mouse</b>									
NCI (1976)	Liver carcinoma	$1.2 \times 10^{-2}$			$2.3 \times 10^{-2}$			$2.9 \times 10^{-2}$	
<b>Female rat</b>									
NTP (1988)	Leukemia	$6.9 \times 10^{-4}$	$1.6 \times 10^{-5}$	<b><math>2.3 \times 10^{-3}</math></b>					
<b>Male rat</b>									
NTP (1990) <sup>c</sup>	Kidney adenoma + carcinoma	$1.6 \times 10^{-3}$		$4.3 \times 10^{-3}$				$1.1 \times 10^{-1}$	<b><math>1.7 \times 10^{-1}</math></b>
NTP (1988)									
Marshall <sup>d</sup>	Testicular	$2.5 \times 10^{-2}$	$6.0 \times 10^{-4}$	<b><math>7.1 \times 10^{-2}</math></b>					
August	Subcutaneous sarcoma	$8.3 \times 10^{-4}$	$2.0 \times 10^{-5}$	<b><math>2.3 \times 10^{-3}</math></b>					
Osborne-Mendel <sup>c</sup>	Kidney adenoma + carcinoma	$2.4 \times 10^{-3}$		$7.0 \times 10^{-3}$				$1.5 \times 10^{-1}$	<b><math>2.5 \times 10^{-1}</math></b>

<sup>a</sup>For the applied doses, the PODs are BMDLs. However, for the internal dose-metrics, the PODs are not actually human equivalent BMDLs corresponding to the BMR because the interspecies conversion does not apply to the dose range of the BMDL; the converted BMDLs are merely intermediaries to obtain a converted slope factor estimate. The calculation that was done is equivalent to using linear extrapolation from the BMDLs in terms of the internal dose-metric to get a slope factor estimate for low-dose risk in terms of the internal dose-metric and then converting that estimate to a slope factor estimate in terms of HEDs. The PODs reported here are what one would get if one then used the slope factor estimate to calculate the human dose level corresponding to a 10% extra risk, but the slope factor estimate is not intended to be extrapolated upward out of the low-dose range, e.g., above  $10^{-4}$  risk. In addition, for the internal dose-metrics, the PODs are the average of the male and female human “BMDL” results presented in Appendix G.

<sup>b</sup>Slope factor estimate = BMR/POD. Results for the primary dose-metric are in bold.

<sup>c</sup>Using MSW adjusted incidences (see text and Table 5-38).

<sup>d</sup>Using poly-3 adjusted incidences (see text and Table 5-38).

For two data sets, the highest dose (exposure) group was dropped to get a better fit when using applied doses. This technique can improve the fit when the response tends to plateau with increasing dose. Plateauing typically occurs when metabolic saturation alters the pattern of metabolite formation or when survival is impacted at higher doses, and it is assumed that these high-dose responses are less relevant to low-dose risk. The highest-dose group was not dropped to improve the fit for any of the internal dose-metrics because it was felt that if the dose-metric was an appropriate reflection of internal dose of the reactive metabolite(s), then use of the dose-metric should have ameliorated the plateauing in the dose-response relationship (note that survival-impacted data sets were addressed using survival adjustment techniques). For a 3<sup>rd</sup> data set (Henschler lymphomas), it might have helped to drop the highest exposure group, but there were only two exposure groups, so this was not done. As a result, the selected model, although it had an adequate fit overall, did not fit the control group very well (the model estimated a higher background response than was observed); thus, the BMD and BMDL were likely overestimated and the risk underestimated. The estimates from the NCI (1976) oral male mouse liver cancer data set are also somewhat more uncertain because the response rate was extrapolated down from a response rate of about 50% extra risk to the BMR of 10% extra risk.

Some general patterns can be observed in Tables 5-36 and 5-37. For inhalation, the unit risk estimates for different dose-metrics were generally similar (within about 2.5-fold) for most cancer types. The exception was for kidney cancer, where the estimates varied by over 2 orders of magnitude, with the AMetGSHBW34 and ABioactDCVCBW34 metrics yielding the highest estimates. This occurs because pharmacokinetic data indicate, and the PBPK model predicts, substantially more GSH conjugation (as a fraction of intake), and hence subsequent bioactivation, in humans relative to rats. The range of the risk estimates for individual cancer types overall (across cancer types and dose-metrics) was encompassed by the range of estimates across the dose-metrics for kidney cancer in the male rat, which was from  $4.4 \times 10^{-4}$  per ppm (applied dose) to  $8.3 \times 10^{-2}$  per ppm (ABioactDCVCBW34).

For oral exposure, the slope factor estimates are more variable across dose-metrics because of first-pass effects in the liver (median estimates for the fraction of TCE metabolized in *one* pass through the liver in mice, rats, and humans are >0.8). Here, the exception is for the risk estimates for cancer of the liver itself, which are also within about a 2.5-fold range, because the liver gets the full dose of all of the metrics during that “first pass.” For the other cancer types, the range of estimates across dose-metrics varies from about 30-fold to over 2 orders of magnitude, with the estimates based on AUCCBld and AMetLngBW34 being at the low end and those based on AMetGSHBW34 and ABioactDCVCBW34 again being at the high end. For AUCCBld, the PBPK model predicted the blood concentrations to scale more closely to body weight rather than the  $\frac{3}{4}$  power of body weight, so the extrapolated human unit risks using this dose-metric are smaller than those obtained by applied dose or other dose-metrics that included  $\frac{3}{4}$  power body weight scaling. For AMetLngBW34, pharmacokinetic data indicate, and the

PBPK model predicts, that the human respiratory tract metabolizes a lower fraction of total TCE intake than the mouse respiratory tract, so the extrapolated risk to humans based on this metric is lower than that obtained using applied dose or other dose-metrics. Overall, the oral slope factor estimates for individual cancer types ranged from  $1.6 \times 10^{-5}$  per mg/kg/day (female rat leukemia, AUCCB1d) to  $2.5 \times 10^{-1}$  per mg/kg/day (male Osborne-Mendel rat kidney, ABioactDCVCBW34), a range of over 4 orders of magnitude. It must be recognized, however, that not all dose-metrics are equally credible, and, as will be presented below, the slope factor estimates for total cancer risk for the most sensitive bioassay response for each sex/species combination using the primary (preferred) dose-metrics fall within a very narrow range.

Results for survival-adjusted analyses are summarized in Table 5-38. For the time-independent (BMDS) multistage model, the risk estimates using poly-3 adjustment are higher than those without poly-3 adjustment. This is to be expected because the poly-3 adjustment decreases denominators when accounting for early mortality, and, for these data sets, the higher-dose groups had greater early mortality. The difference was fairly modest for the kidney cancer data sets (about 30% higher) but somewhat larger for the testicular cancer data set (about 150% higher).

**Table 5-38. Comparison of survival-adjusted results for three oral male rat data sets<sup>a</sup>**

Dose-metric	Adjustment method	BMR	POD (mg/kg/d)	BMD:BMDL	Slope factor estimate (per mg/kg/d)
<b>NTP (1990) F344 rat kidney adenoma + carcinoma</b>					
Applied dose	unadj BMDS	0.05	56.9	1.9	$8.8 \times 10^{-4}$
	poly-3 BMDS	0.1	89.2	1.9	$1.1 \times 10^{-3}$
	MSW	0.05	32.0	2.6	$1.6 \times 10^{-3}$
TotMetabBW34	unadj BMDS	0.05	20.2	2.1	$2.5 \times 10^{-3}$
	poly-3 BMDS	0.1	31.8	1.7	$3.1 \times 10^{-3}$
	MSW	0.05	11.5	3.1	$4.3 \times 10^{-3}$
AMetGSHBW34	unadj BMDS	0.05	0.841	1.9	$5.9 \times 10^{-2}$
	poly-3 BMDS	0.1	1.32	1.9	$7.6 \times 10^{-2}$
	MSW	0.05	0.471	2.4	$1.1 \times 10^{-1}$
ABioactDCVCBW34	unadj BMDS	0.05	0.522	1.9	$9.6 \times 10^{-2}$
	poly-3 BMDS	0.1	0.817	1.9	$1.2 \times 10^{-1}$
	MSW	0.05	0.292	2.4	<b><math>1.7 \times 10^{-1}</math></b>

**Table 5-38. Comparison of survival-adjusted results for three oral male rat data sets<sup>a</sup>**

Dose-metric	Adjustment method	BMR	POD (mg/kg/d)	BMD:BMDL	Slope factor estimate (per mg/kg/d)
<b>NTP (1988) Osborne-Mendel rat kidney adenoma + carcinoma</b>					
Applied dose	unadj BMDS	0.1	86.6	1.7	$1.2 \times 10^{-3}$
	poly-3 BMDS	0.1	65.9	1.7	$1.5 \times 10^{-3}$
	MSW	0.1	41.5	2.0	$2.4 \times 10^{-3}$
TotMetabBW34	unadj BMDS	0.1	30.4	1.7	$3.3 \times 10^{-3}$
	poly-3 BMDS	0.1	23.1	1.7	$4.3 \times 10^{-3}$
	MSW	0.1	14.3	2.0	$7.0 \times 10^{-3}$
AMetGSHBW34	unadj BMDS	0.1	1.35	1.7	$7.4 \times 10^{-2}$
	poly-3 BMDS	0.1	1.03	1.7	$9.7 \times 10^{-2}$
	MSW	0.1	0.648	2.0	$1.5 \times 10^{-1}$
ABioactDCVCBW34	unadj BMDS	0.1	0.835	1.7	$1.2 \times 10^{-1}$
	poly-3 BMDS	0.1	0.636	1.7	$1.6 \times 10^{-1}$
	MSW	0.1	0.402	2.0	<b><math>2.5 \times 10^{-1}</math></b>
<b>NTP (1988) Marshall rat testicular tumors</b>					
Applied dose	unadj BMDS	0.1	9.94	1.4	$1.0 \times 10^{-2}$
	poly-3 BMDS	0.1	3.95	1.5	$2.5 \times 10^{-2}$
	MSW	0.1	1.64	5.2	$6.1 \times 10^{-2}$
AUCCBld	unadj BMDS	0.1	427	1.4	$2.3 \times 10^{-4}$
	poly-3 BMDS	0.1	167	1.6	$6.0 \times 10^{-4}$
	MSW	0.1	60.4	2.6	$1.7 \times 10^{-3}$
TotMetabBW34	unadj BMDS	0.1	3.53	4.3	$2.8 \times 10^{-2}$
	poly-3 BMDS	0.1	1.41	1.5	<b><math>7.1 \times 10^{-2}</math></b>
	MSW	0.1	0.73	9.4	$1.4 \times 10^{-1}$

<sup>a</sup>For the applied doses, the PODs are BMDLs. However, for the internal dose-metrics, the PODs are not actually human equivalent BMDLs corresponding to the BMR because the interspecies conversion does not apply to the dose range of the BMDL; the converted BMDLs are merely intermediaries to obtain a converted slope factor estimate. Results for the primary dose-metric are in bold.

In addition, the MSW time-to-tumor model generated higher risk estimates than the poly-3 adjustment technique. The MSW results were about 40% higher for the NTP F344 rat kidney cancer data sets and about 60% higher for the NTP Osborne-Mendel rat kidney cancer data sets. For the NTP Marshall rat testicular cancer data set, the discrepancies were greater; the results ranged from about 100 to 180% higher for the different dose-metrics. As discussed in Section 5.2.1.1, these two approaches differ in the way they take early mortality into account. The poly-3 technique merely adjusts the tumor incidence denominators, using a constant power 3 of time, to reflect the fact that animals are at greater risk of cancer at older ages. The MSW model estimates risk as a function of time (and dose), and it estimates the power (of time)

parameter for each data set.<sup>46</sup> For the NTP F344 rat kidney cancer and NTP Marshall rat testicular cancer data sets, the estimated power parameter was close to 3 in each case, ranging from 3.0 to 3.7; for the NTP Osborne-Mendel rat kidney cancer data sets, however, the estimated power parameter was about 10 for each of the dose-metrics, presumably reflecting the fact that these were late-occurring tumors (the earliest occurred at 92 weeks). Using a higher power parameter than 3 in the poly-3 adjustment would give even less weight to nontumor-bearing animals that die early and would, thus, increase the adjusted incidence even more in the highest-dose groups where the early mortality is most pronounced, increasing the slope factor estimate. Nonetheless, as noted above, the MSW results were only about 60% higher for the NTP Osborne-Mendel rat kidney cancer data sets for which MSW estimated a power parameter of about 10.

In general, the risk estimates from the MSW model would be preferred because, as discussed above, this model incorporates more information (e.g., tumor context) and estimates the power parameter rather than using a constant value of three. From Table 5-38, it can be seen that the results from MSW yielded higher BMD:BMDL ratios than the results from the poly-3 technique. These ratios were only slightly higher and not unusually large for MSW model analyses of the NTP ([1990](#), [1988](#)) kidney tumor estimates, and this, along with the adequate fit (assessed visually) of the MSW model, supports using the slope factor estimates from the MSW modeling of rat kidney tumor incidence. On the other hand, the BMD:BMDL ratio was relatively large for the applied dose analysis and, in particular, for the preferred dose-metric analysis (9.4-fold) of the NTP Marshall rat testicular tumor data set. Therefore, for this endpoint, the poly-3-adjusted results were used, although they may underestimate risk somewhat as compared to the MSW model.

In addition to the results from dose-response modeling of individual cancer types, the results of the combined tumor risk analyses for the three bioassays in which the rodents exhibited increased risks at multiple sites are also presented in Tables 5-36 and 5-37, in the rows labeled “combined” under the column heading “Tumor Type.” These results were extracted from the detailed results in Appendix G. Note that, because of the computational complexity of the combined tumor analyses, dose-response modeling was only done using applied dose and a common upstream internal dose-metric, rather than using the different preferred dose-metrics for each tumor type within a combined tumor analysis.

For the Maltoni et al. ([1986](#)) female mouse inhalation bioassay, the combined tumor risk estimates are bounded by the highest individual tumor risk estimates and the sums of the individual tumor risks estimates (the risk estimates are upper bounds, so the combined risk estimate (i.e., the upper bound on the sum of the individual central tendency estimates) should be

---

<sup>46</sup>Conceptually, the approaches differ most when different tumor contexts (incidental or fatal) are considered, because the poly-3 technique only accounts for time of death, while the MSW model can account for the tumor context and attempt to estimate an induction time (t<sub>0</sub>), although this was not done for any of the data sets in this assessment.

less than the sum of the individual upper bound estimates), as one would expect. The common upstream internal dose-metric used for the combined analysis was TotOxMetabBW34, which is not the primary metric for either of the individual cancer types. For the liver tumors, the primary metric was AMetLiv1BW34, but as can be seen in Table 5-36, it yields results similar to those for TotOxMetabBW34. Likewise, for the lung tumors, the primary metric was AMetLngBW34, which yields a unit risk estimate slightly smaller than for TotOxMetabBW34. Thus, the results of the combined analysis using TotOxMetabBW34 as a common metric is not likely to substantially over- or underestimate the combined risk based on preferred metrics for each of the cancer types.

For the Maltoni et al. (1986) male rat inhalation bioassay, the combined risk estimates are also reasonably bounded, as expected. The common upstream internal dose-metric used for the combined analysis was TotMetabBW34, which is the primary metric for two of the three individual cancer types. However, as can be seen in Table 5-36, the risk estimate for the preferred dose-metric for the third tumor type, ABioactDCVCBW34 for the kidney tumors, is substantially higher than the risk estimates for the primary dose-metrics for the other two cancer types and would dominate a combined tumor risk estimate across primary dose-metrics; thus, the ABioactDCVCBW34-based kidney tumor risk estimate alone can reasonably be used to represent the total cancer risk for the bioassay using preferred internal dose-metrics, although it would underestimate the combined risk to some extent (e.g., the kidney-based estimate is  $8.3 \times 10^{-2}$  per ppm; the combined estimate would be about  $9 \times 10^{-2}$  per ppm, rounded to one significant figure).

For the third bioassay [NCI (1976) female mouse oral bioassay], the combined tumor risk estimates are once again reasonably bounded. The common upstream internal dose-metric used for the combined analysis was TotOxMetabBW34, which is not the primary metric for any of the three individual cancer types but was considered to be the most suitable metric to apply as a basis for combining risk across these different cancer types. The slope factor estimate for the lung based on the primary dose-metric for that site becomes negligible compared to the estimates for the other two cancer types (see Table 5-37). However, the slope factor estimates for the remaining two cancer types are both somewhat underestimated using the TotOxMetabBW34 metric rather than the primary metrics for those tumors (the TotOxMetabBW34-based estimate for leukemias + sarcomas, which is not presented in Table 5-30 because, in the absence of better mechanistic information, more upstream metrics were used for that individual tumor type, is  $4.1 \times 10^{-3}$  per mg/kg/day). Thus, overall, the combined estimate based on TotOxMetabBW34 is probably a reasonable estimate for the total tumor risk in this bioassay, although it might overestimate risk slightly.

The most sensitive sex/species results are extracted from Tables 5-29 and 5-30 and presented in Tables 5-39 (inhalation) and 5-40 (oral). The BMD:BMDL ratios for all of the results corresponding to the slope factor and unit risk estimates based on the preferred dose-

metrics ranged from 1.3 to 2.1. For inhalation, the most sensitive bioassay responses based on the preferred dose-metrics ranged from  $2.6 \times 10^{-3}$  to  $8.3 \times 10^{-2}$  per ppm across the sex/species combinations (with the exception of the female rat, which exhibited no apparent TCE-associated response in the 3 available bioassays). For oral exposure, the most sensitive bioassay responses based on the preferred dose-metrics ranged from  $2.3 \times 10^{-3}$  to  $2.5 \times 10^{-1}$  per mg/kg/day across the sex/species combinations. For both routes of exposure, the most sensitive sex/species response was (or was dominated by, in the case of the combined tumors in the male rat by inhalation) male rat kidney cancer based on the preferred dose-metric of ABioactDCVCBW34.

**Table 5-39. Inhalation: most sensitive bioassay for each sex/species combination<sup>a</sup>**

Sex/species	Endpoint (study)	Unit risk per ppm		
		Preferred dose-metric	Default methodology	Alternative dose-metrics, studies, or endpoints
Female mouse	Lymphoma ( <a href="#">Henschler et al., 1980</a> )	$1.0 \times 10^{-2}$	$9.1 \times 10^{-3}$	$1 \times 10^{-3} \sim 4 \times 10^{-3}$
Male mouse	Liver hepatoma ( <a href="#">Maltoni et al., 1986</a> )	$2.6 \times 10^{-3}$	$2.9 \times 10^{-3}$	$2 \times 10^{-3}$
Female rat	–	–	–	–
Male rat	Leukemia+ Kidney adenoma and carcinoma+ Leydig cell tumors ( <a href="#">Maltoni et al., 1986</a> )	$8.3 \times 10^{-2}$	$7.0 \times 10^{-3}$	$4 \times 10^{-4} \sim 5 \times 10^{-2}$ [individual site results]

<sup>a</sup>Results extracted from Table 5-36.

**Table 5-40. Oral: most sensitive bioassay for each sex/species combination<sup>a</sup>**

Sex/species	Endpoint (study)	Unit risk per mg/kg/d		
		Preferred dose-metric	Default methodology	Alternative dose-metrics, studies, or endpoints
Female mouse	Liver carcinoma+ lung adenoma and carcinoma+ sarcomas + leukemias ( <a href="#">NCI, 1976</a> )	$9.3 \times 10^{-3}$	$6.7 \times 10^{-3}$	$1 \times 10^{-4} \sim 7 \times 10^{-3}$ [individual site results]
Male mouse	Liver carcinoma ( <a href="#">NCI, 1976</a> )	$2.9 \times 10^{-2}$	$1.2 \times 10^{-2}$	$2 \times 10^{-2}$
Female rat	Leukemia ( <a href="#">NTP, 1988</a> )	$2.3 \times 10^{-3}$	$6.9 \times 10^{-4}$	$2 \times 10^{-5}$
Male rat	Kidney adenoma + carcinoma ( <a href="#">NTP, 1988, Osborne-Mendel</a> )	$2.5 \times 10^{-1}$	$2.4 \times 10^{-3}$ <sup>b</sup>	$2 \times 10^{-5} \sim 2 \times 10^{-1}$

<sup>a</sup>Results extracted from Table 5-37.

<sup>b</sup>Most sensitive male rat result using default methodology is  $2.5 \times 10^{-2}$  per mg/kg/day for NTP ([1988](#)) Marshall rat testicular tumors.

## **5.2.1.4. Uncertainties in Dose-Response Analyses of Rodent Bioassays**

### **5.2.1.4.1. Qualitative discussion of uncertainties**

All risk assessments involve uncertainty, as study data are extrapolated to make inferences about potential effects in humans from environmental exposure. The largest sources of uncertainty in the TCE rodent-based cancer risk estimates are interspecies extrapolation and low-dose extrapolation. Some limited human (occupational) data from which to estimate human cancer risk are available, and cancer risk estimates based on these data are developed in Section 5.2.2 below. In addition, some quantitative uncertainty analyses of the interspecies differences in pharmacokinetics were conducted and are presented in Section 5.2.1.4.2.

The rodent bioassay data offer conclusive evidence of carcinogenicity in both rats and mice, and the available epidemiologic and mechanistic data support the relevance to humans of the TCE-induced carcinogenicity observed in rodents. The epidemiologic data provide sufficient evidence that TCE is “carcinogenic to humans” (see Section 4.11). There is even some evidence of site concordance with the rodent findings, although site concordance is not essential to human relevance and, in fact, is not observed across TCE-exposed rats and mice. The strongest evidence in humans is for TCE-induced kidney tumors, with fairly strong evidence for lymphomas and some lesser support for liver tumors; each of these cancer types has also been observed in TCE rodent bioassays. Furthermore, the mechanistic data are supportive of human relevance because, while the exact reactive species associated with TCE-induced cancers are not known, the metabolic pathways for TCE are qualitatively similar for rats, mice, and humans (see Section 3.3). The impact of uncertainties with respect to quantitative differences in TCE metabolism is discussed in Section 5.2.1.4.2.

Typically, the cancer risk estimated is for the total cancer burden from all sites that demonstrate an increased tumor incidence for the most sensitive experimental species and sex. It is expected that this approach is protective of the human population, which is more diverse but is exposed to lower exposure levels.

For the inhalation unit risk estimates, the preferred estimate from the most sensitive species and sex was the estimate of  $8.3 \times 10^{-2}$  per ppm for the male rat, which was based on multiple tumors observed in this sex/species but was dominated by the kidney tumor risk estimated with the dose-metric for bioactivated DCVC. This estimate was the high end of the range of estimates (see Table 5-39) but was within an order of magnitude of other estimates, such as the preferred estimate for the female mouse and the male rat kidney estimate based on the GSH conjugation dose-metric, which provide additional support for an estimate of this magnitude. The preferred estimate for the male mouse was about an order of magnitude and a half lower. The female rat showed no apparent TCE-associated tumor response in the three available inhalation bioassays; however, this apparent absence of response is inconsistent with the observations of increased cancer risk in occupationally exposed humans and in female rats in

oral bioassays. In Section 5.2.2.2, an inhalation unit risk estimate based on the human data is derived and can be compared to the rodent-based estimate.

For the oral slope factor estimate, the preferred estimate from the most sensitive species and sex was the estimate of  $2.5 \times 10^{-1}$  per mg/kg/day, again for the male rat, based on the kidney tumor risk estimated with the dose-metric for bioactivated DCVC. This estimate was at the high end of the range of estimates (see Table 5-40) but was within an order of magnitude of other estimates, such as the preferred male mouse estimate and the male rat kidney estimate based on the GSH conjugation dose-metric, which provide additional support for an estimate of this magnitude. The preferred estimates for the female mouse and the female rat were about another order of magnitude lower. Some of the oral slope factor estimates based on the alternative dose-metric of AUC for TCE in the blood were as much as three orders of magnitude lower, but these estimates were considered less credible than those based on the preferred dose-metrics. In Section 5.2.2.3, an oral slope factor estimate based on the human (inhalation) data is derived using the PBPK model for route-to-route extrapolation; this estimate can be compared to the rodent-based estimate.

Furthermore, the male rat kidney tumor estimates from the inhalation ([Maltoni et al., 1986](#)) and oral ([NTP, 1988](#)) studies were consistent on the basis of internal dose using the dose-metric for bioactivated DCVC. In particular, the linearly extrapolated slope (i.e., the BMR/BMDL) per unit of internal dose derived from Maltoni et al. ([1986](#)) male rat kidney tumor data was  $2.4 \times 10^{-1}$  per weekly mg DCVC bioactivated per unit body weight<sup>3/4</sup>, while the analogous slope derived from NTP ([1988](#)) male rat kidney tumor data was  $9.3 \times 10^{-2}$  per weekly mg DCVC bioactivated per unit body weight<sup>3/4</sup> (MSW-modeled results), a difference of less than threefold.<sup>47</sup> These results also suggest that differences between routes of administration are adequately accounted for by the PBPK model using this dose-metric.

Regarding low-dose extrapolation, a key consideration in determining what extrapolation approach to use is the mode(s) of action. However, mode-of-action data are lacking or limited for each of the cancer responses associated with TCE exposure, with the exception of the kidney tumors (see Section 4.11). For the kidney tumors, the weight of the available evidence supports the conclusion that a mutagenic mode of action is operative (see Section 4.4); this mode of action supports linear low-dose extrapolation. The weight of evidence also supports involvement of processes of cytotoxicity and regenerative proliferation in the carcinogenicity of TCE, although not with the extent of support as for a mutagenic mode of action. In particular, data linking

---

<sup>47</sup>For the Maltoni et al. ([1986](#)) male rat kidney tumors, the unit risk estimate of  $8.3 \times 10^{-2}$  per ppm using the ABioactDCVCBW34 dose metric, from Table 5-36, is divided by the average male and female internal doses at 0.001 ppm (0.0034/0.001) from Table 5-35, to yield a unit risk in internal dose units of  $2.4 \times 10^{-2}$ . For the NTP ([1988](#)) male rat kidney tumors, the unit risk estimate of  $2.5 \times 10^{-1}$  per mg/kg/day using the ABioactDCVCBW34 dose metric, from Table 5-37, is divided by the average male and female internal doses at 0.001 mg/kg/day (0.0027/0.001) from Table 5-35, to yield a unit risk in internal dose units of  $9.3 \times 10^{-2}$ . Note that the original BMDLs and unit risks from BMD modeling were in internal dose units that were then converted to applied dose units using the values in Table 5-35, so this calculation reverses that conversion.

TCE-induced proliferation to increased mutation or clonal expansion are lacking, as are data informing the quantitative contribution of cytotoxicity. Moreover, it is unlikely that any contribution from cytotoxicity leads to a non-linear dose-response relationship near the POD for rodent kidney tumors, since maximal levels of toxicity are reached before the onset of tumors. Finally, because any possible involvement of a cytotoxicity mode of action would be additional to mutagenicity, the dose-response relationship would nonetheless be expected to be linear at low doses. Therefore, the additional involvement of a cytotoxicity mode of action does not provide evidence against the use of linear extrapolation from the POD.

For the other TCE-induced cancers, the mode(s) of action is unknown. When the mode(s) of action cannot be clearly defined, EPA generally uses a linear approach to estimate low-dose risk ([U.S. EPA, 2005b](#)), based on the following general principles:

- A chemical's carcinogenic effects may act additively to ongoing biological processes, given that diverse human populations are already exposed to other agents and have substantial background incidences of various cancers.
- A broadening of the dose-response curve (i.e., less rapid fall-off of response with decreasing dose) in diverse human populations and, accordingly, a greater potential for risks from low-dose exposures ([Lutz et al., 2005](#); [Zeise et al., 1987](#)) is expected for two reasons: First, even if there is a “threshold” concentration for effects at the cellular level, that threshold is expected to differ across individuals. Second, greater variability in response to exposures would be anticipated in heterogeneous populations than in inbred laboratory species under controlled conditions (due to, e.g., genetic variability, disease status, age, nutrition, and smoking status).
- The general use of linear extrapolation provides reasonable upper-bound estimates that are believed to be health-protective ([U.S. EPA, 2005b](#)) and also provides consistency across assessments.

Additional uncertainties arise from the specific dosimetry assumptions, the model structures and parameter estimates in the PBPK models, the dose-response modeling of data in the observable range, and the application of the results to potentially sensitive human populations. As discussed in Section 5.2.1.2.1, one uncertainty in the tissue-specific dose-metrics used here is whether to scale the rate of metabolism by tissue mass or body weight to the  $\frac{3}{4}$  in the absence of specific data on clearance; however, in the cases where this is an issue (the lung, liver, and kidney), the impact of this choice is relatively modest (less than twofold to about fourfold). An additional dosimetry assumption inherent in this analysis is that equal concentrations of the active moiety over a lifetime yield equivalent lifetime risk of cancer across species, and the extent to which this is true for TCE is unknown. Furthermore, it should be noted that use of tissue-specific dosimetry inherently presumes site concordance of tumors across species.

With respect to uncertainties in the estimates of internal dose themselves, a quantitative analysis of the uncertainty and variability in the PBPK model-predicted dose-metric estimates and their impacts on cancer risk estimates is presented in Section 5.2.1.4.2. Additional uncertainties in the PBPK model were discussed in Section 3.5. Furthermore, this assessment examined a variety of dose-metrics for the different cancer types using PBPK models for rats, mice, and humans, so the impact of dose-metric selection can be assessed. As discussed in Section 5.2.1.2.1, there is strong support for the primary dose-metrics selected for kidney, liver, and, to a lesser extent, lung. For the other tumor sites, there is more uncertainty about dose-metric selection. The cancer slope factor and unit risk estimates obtained using the preferred dose-metrics were generally similar (within about threefold) to those derived using default dosimetry assumptions (e.g., equal risks result from equal cumulative equivalent exposures or doses), with the exception of the bioactivated DCVC dose-metric for rat kidney tumors and the metric for the amount of TCE oxidized in the respiratory tract for mouse lung tumors occurring from oral exposure (see Tables 5-39 and 5-40). The higher risk estimates for kidney tumors based on the bioactivated DCVC dose-metric are to be expected because pharmacokinetic data indicate, and the PBPK model predicts, substantially more GSH conjugation (as a fraction of intake), and hence subsequent bioactivation, in humans relative to rats. Nonetheless, there is substantial uncertainty in the quantitative extrapolation of GSH conjugation from rodents to humans due to limitations in the available data. The lower risk estimates for lung tumors from oral TCE exposure based on the metric for the amount of TCE oxidized in the respiratory tract are because there is a greater first-pass effect in human liver relative to mouse liver following oral exposure and because the gavage dosing used in rodent studies leads to a large bolus dose that potentially overwhelms liver metabolism to a greater extent than a more graded oral exposure. Both of these effects result in relatively more TCE being available for metabolism in the lung for mice than for humans. In addition, mice have greater respiratory metabolism relative to humans. However, because oxidative metabolites produced in the liver may contribute to respiratory tract effects, using respiratory tract metabolism alone as a dose-metric may underestimate lung tumor risk. The slope factor or unit risk estimates obtained using the alternative dose-metrics were also generally similar to those derived using default dosimetry assumptions, with the exception of the metric for the amount of TCE conjugated with GSH for rat kidney tumors, again because humans have greater GSH conjugation, and the AUC of TCE in blood for all of the cancer types resulting from oral exposure, again because of first-pass effects.

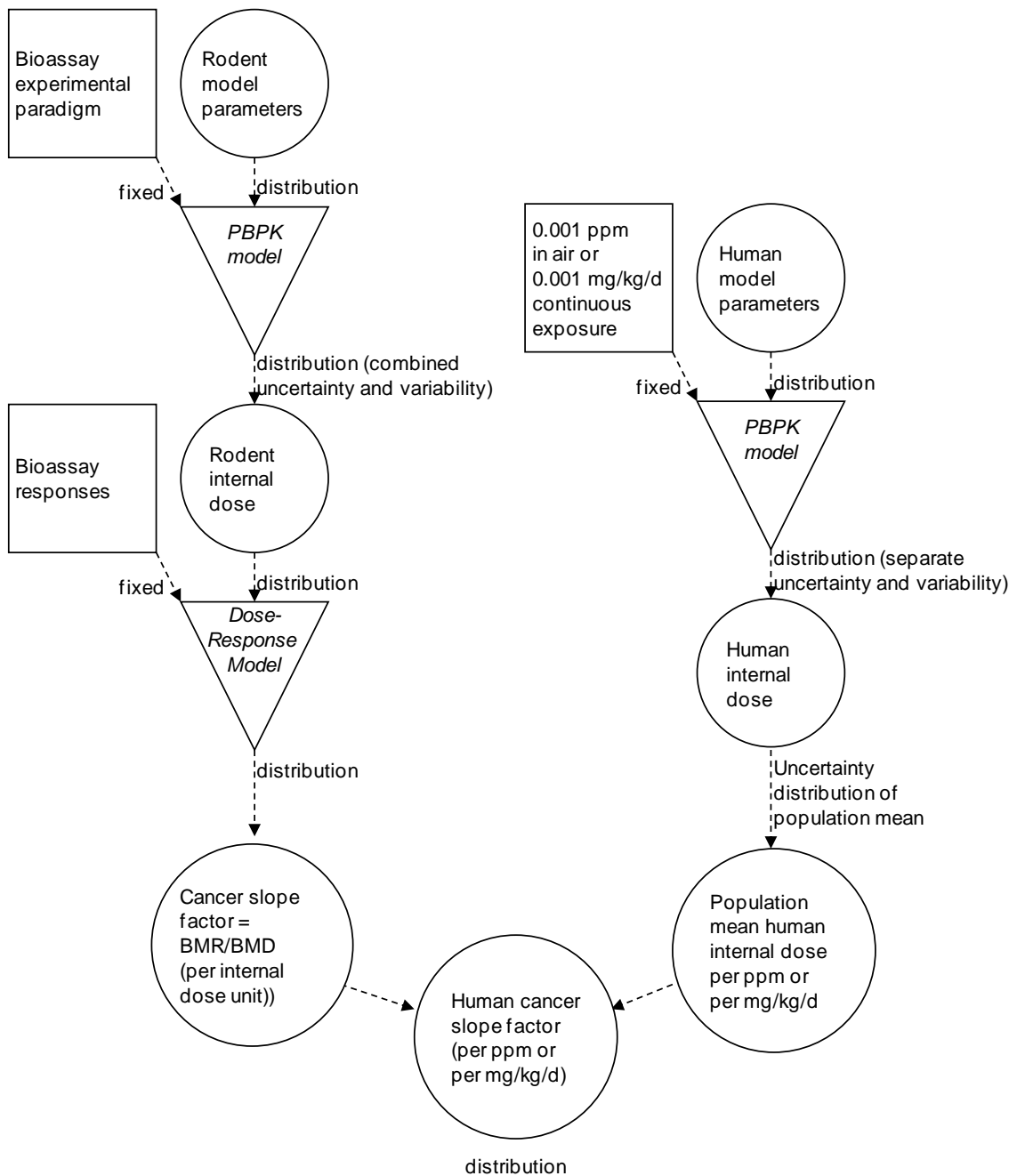
With respect to uncertainties in the dose-response modeling, the two-step approach of modeling only in the observable range, as put forth in EPA's cancer assessment guidelines ([U.S. EPA, 2005b](#)), is designed in part to minimize model dependence. The ratios of the BMDs to the BMDLs give some indication of the statistical uncertainties in the dose-response modeling. These ratios did not exceed a value of 2.5 for any of the primary analyses used in this assessment. Thus, overall, modeling uncertainties in the observable range are considered to be

minimal. Some additional uncertainty is conveyed by uncertainties in the survival adjustments made to some of the bioassay data; however, their impact is also believed to be minimal relative to the uncertainties already discussed (i.e., interspecies and low-dose extrapolations).

Regarding the cancer risks to potentially sensitive human populations or lifestages, pharmacokinetic data on 42 individuals were used in the Bayesian population analysis of the PBPK model discussed in Section 3.5. The impacts of these data on the predicted population mean are incorporated in the quantitative uncertainty analyses presented in Section 5.2.1.4.2. These data do not, however, reflect the full range of metabolic variability in the human population (they are all from healthy, mostly male, volunteers) and do not address specific potentially sensitive subgroups (see Section 4.10). Moreover, there is inadequate information about disease status, co-exposures, and other factors that make humans vary in their responses to TCE. It will be a challenge for future research to quantify the differential risk indicated by different risk factors or exposure scenarios.

#### **5.2.1.4.2. Quantitative uncertainty analysis of PBPK model-based dose-metrics**

The Bayesian analysis of the PBPK model for TCE generates distributions of uncertainty and variability in the internal dose-metrics than can be readily fed into dose-response analysis. As shown in Figure 5-6, the overall approach taken for the uncertainty analysis is similar to that used for the point estimates except that distributions are carried through the analysis rather than median or expected values. In particular, the PBPK model-based rodent internal doses are carried through to a distribution of BMDs (which also includes sampling variance from the number of responding and at risk animals in the bioassay). This distribution of BMDs generates a distribution of cancer slope factors based on internal dose, which then is combined with the (uncertainty) distribution of the human population mean conversion to applied dose or exposure. The resulting distribution for the human population mean risk per unit dose or exposure accounts for uncertainty in the PBPK model parameters (rodent and human) and the binomial sampling error in the bioassays. These distributions can then be compared with the point estimates, based on median rodent dose-metrics and mean human population dose-metrics, reported in Tables 5-36 and 5-37. Details of the implementation of this uncertainty analysis, which used the WinBugs software in conjunction with the R statistical package, are reported in Appendix G.



Square nodes indicate point values, circular nodes indicate distributions, and the inverted triangles indicate a (deterministic) functional relationship.

**Figure 5-6. Flow-chart for uncertainty analysis of dose-response analyses of rodent bioassays using PBPK model-based dose-metrics.**

Overall, as shown in Tables 5-41 and 5-42, the 95% confidence upper bound of the distributions for the linearly extrapolated risk per unit dose or exposure ranged from one- to eightfold higher than the point slope factors and unit risks derived using the BMDLs reported in Tables 5-36 and 5-37. The largest differences, up to fourfold, for rat kidney tumors and

eightfold for mouse lung tumors, primarily reflect the substantial uncertainty in the internal dose-metrics for rat kidney DCVC and GSH conjugation and for mouse lung oxidation (see Section 3.5). Additionally, despite the differences in the degree of uncertainty due to the PBPK model across endpoints and dose-metrics, the only case where the choice of the most sensitive bioassay for each sex/species combination would change based on the 95% confidence upper bounds reported in Tables 5-41 and 5-42 would be for female mouse inhalation bioassays. Even in this case, the difference between slope factor or unit risk estimate for the most sensitive and next most sensitive study/endpoint was only twofold.

**Table 5-41. Summary of PBPK model-based uncertainty analysis of unit risk estimates for each sex/species/bioassay/tumor type (inhalation)**

Study	Tumor type	BMR	Dose-metric	Unit risk estimates (ppm) <sup>-1</sup>				
				From	Summary statistics of unit risk distribution			
				Table 5-36	Mean	5% lower bound	Median	95% upper bound
<b>Female mouse</b>								
Fukuda et al. (1983)	Lung adenoma + carcinoma <sup>a</sup>	0.1	<b>AMetLngBW34</b>	<b>2.6 × 10<sup>-3</sup></b>	5.65 × 10 <sup>-3</sup>	2.34 × 10 <sup>-4</sup>	1.49 × 10 <sup>-3</sup>	2.18 × 10 <sup>-2</sup>
			TotOxMetabBW34	3.2 × 10 <sup>-3</sup>	1.88 × 10 <sup>-3</sup>	3.27 × 10 <sup>-4</sup>	1.52 × 10 <sup>-3</sup>	4.59 × 10 <sup>-3</sup>
			AUCCBld	1.8 × 10 <sup>-3</sup>	1.01 × 10 <sup>-3</sup>	1.54 × 10 <sup>-4</sup>	8.36 × 10 <sup>-4</sup>	2.44 × 10 <sup>-3</sup>
Henschler et al. (1980)	Lymphoma <sup>b</sup>	0.1	<b>TotMetabBW34</b>	<b>1.0 × 10<sup>-2</sup></b>	4.38 × 10 <sup>-3</sup>	6.06 × 10 <sup>-4</sup>	3.49 × 10 <sup>-3</sup>	1.11 × 10 <sup>-2</sup>
Maltoni et al. (1986)	Lung adenoma + carcinoma <sup>a</sup>	0.1	<b>AMetLngBW34</b>	<b>1.8 × 10<sup>-3</sup></b>	3.88 × 10 <sup>-3</sup>	1.48 × 10 <sup>-4</sup>	1.04 × 10 <sup>-3</sup>	1.52 × 10 <sup>-2</sup>
			TotOxMetabBW34	1.9 × 10 <sup>-3</sup>	1.10 × 10 <sup>-3</sup>	3.73 × 10 <sup>-4</sup>	9.52 × 10 <sup>-4</sup>	2.32 × 10 <sup>-3</sup>
			AUCCBld	1.0 × 10 <sup>-3</sup>	5.25 × 10 <sup>-4</sup>	1.63 × 10 <sup>-4</sup>	4.64 × 10 <sup>-4</sup>	1.10 × 10 <sup>-3</sup>
	Liver	0.05	<b>AMetLiv1BW34</b>	<b>1.2 × 10<sup>-3</sup></b>	6.27 × 10 <sup>-4</sup>	2.18 × 10 <sup>-4</sup>	5.39 × 10 <sup>-4</sup>	1.32 × 10 <sup>-3</sup>
			TotOxMetabBW34	1.1 × 10 <sup>-3</sup>	5.98 × 10 <sup>-4</sup>	1.81 × 10 <sup>-4</sup>	5.07 × 10 <sup>-4</sup>	1.31 × 10 <sup>-3</sup>
<b>Male mouse</b>								
Maltoni et al. (1986)	Liver	0.1	<b>AMetLiv1BW34</b>	<b>2.6 × 10<sup>-3</sup></b>	1.35 × 10 <sup>-3</sup>	4.28 × 10 <sup>-4</sup>	1.16 × 10 <sup>-3</sup>	2.93 × 10 <sup>-3</sup>
			TotOxMetabBW34	2.0 × 10 <sup>-3</sup>	1.23 × 10 <sup>-3</sup>	4.24 × 10 <sup>-4</sup>	1.06 × 10 <sup>-3</sup>	2.60 × 10 <sup>-3</sup>
<b>Male rat</b>								
Maltoni et al. (1986)	Leukemia <sup>b</sup>	0.05	<b>TotMetabBW34</b>	<b>1.8 × 10<sup>-3</sup></b>	9.38 × 10 <sup>-4</sup>	1.26 × 10 <sup>-4</sup>	7.86 × 10 <sup>-4</sup>	2.25 × 10 <sup>-3</sup>
	Kidney adenoma + carcinoma	0.01	<b>ABioactDCVCBW34</b>	<b>8.3 × 10<sup>-2</sup></b>	9.07 × 10 <sup>-2</sup>	3.66 × 10 <sup>-3</sup>	3.64 × 10 <sup>-2</sup>	3.21 × 10 <sup>-1</sup>
			AMetGSHBW34	5.1 × 10 <sup>-2</sup>	3.90 × 10 <sup>-2</sup>	2.71 × 10 <sup>-3</sup>	2.20 × 10 <sup>-2</sup>	1.30 × 10 <sup>-1</sup>
			TotMetabBW34	7.3 × 10 <sup>-4</sup>	3.94 × 10 <sup>-4</sup>	8.74 × 10 <sup>-5</sup>	3.42 × 10 <sup>-4</sup>	8.74 × 10 <sup>-4</sup>
Leydig cell <sup>b</sup>	0.1	<b>TotMetabBW34</b>	<b>5.5 × 10<sup>-3</sup></b>	4.34 × 10 <sup>-3</sup>	1.99 × 10 <sup>-3</sup>	3.98 × 10 <sup>-3</sup>	7.87 × 10 <sup>-3</sup>	

<sup>a</sup>WinBUGS dose-response analyses did not adequately converge for the AMetLngBW34 dose-metric using the 3<sup>rd</sup>-order multistage model (used for results in Table 5-36), but did converge when the 2<sup>nd</sup>-order model was used. Summary statistics reflect results of 2<sup>nd</sup>-order model calculations.

<sup>b</sup>Poor dose-response fits in point estimates for AUCCBld, so not included in uncertainty analysis.

**Table 5-42. Summary of PBPK model-based uncertainty analysis of slope factor estimates for each sex/species/bioassay/tumor type (oral)**

Study	Tumor type	BMR	Dose-metric	Slope factor estimates (mg/kg/d) <sup>-1</sup>				
				From	Summary statistics of slope factor distribution			
				Table 5-37 or 5-38	Mean	5% lower bound	Median	95% upper bound
<b>Female mouse</b>								
NCI (1976)	Liver carcinoma	0.1	AMetLiv1BW34	$7.1 \times 10^{-3}$	$3.26 \times 10^{-3}$	$9.35 \times 10^{-4}$	$2.44 \times 10^{-3}$	$8.35 \times 10^{-3}$
			TotOxMetabBW34	$5.7 \times 10^{-3}$	$2.63 \times 10^{-3}$	$8.76 \times 10^{-4}$	$2.01 \times 10^{-3}$	$6.60 \times 10^{-3}$
	Lung adenoma + carcinoma <sup>a</sup>	0.1	AMetLngBW34	$1.3 \times 10^{-4}$	$1.28 \times 10^{-4}$	$6.73 \times 10^{-6}$	$4.12 \times 10^{-5}$	$4.62 \times 10^{-4}$
			TotOxMetabBW34	$4.0 \times 10^{-3}$	$1.84 \times 10^{-3}$	$5.29 \times 10^{-4}$	$1.39 \times 10^{-3}$	$4.73 \times 10^{-3}$
			AUCCBld	$1.5 \times 10^{-4}$	$7.16 \times 10^{-5}$	$4.40 \times 10^{-6}$	$3.39 \times 10^{-5}$	$2.18 \times 10^{-4}$
	Leukemias + sarcomas	0.1	TotMetabBW34	$4.9 \times 10^{-3}$	$1.60 \times 10^{-3}$	$1.42 \times 10^{-4}$	$1.13 \times 10^{-3}$	$4.65 \times 10^{-3}$
AUCCBld			$1.4 \times 10^{-4}$	$6.36 \times 10^{-5}$	$3.10 \times 10^{-6}$	$2.90 \times 10^{-5}$	$1.94 \times 10^{-4}$	
<b>Male mouse</b>								
NCI (1976)	Liver carcinoma	0.1	AMetLiv1BW34	$2.9 \times 10^{-2}$	$1.65 \times 10^{-2}$	$4.70 \times 10^{-3}$	$1.25 \times 10^{-2}$	$4.25 \times 10^{-2}$
			TotOxMetabBW34	$2.3 \times 10^{-2}$	$1.32 \times 10^{-2}$	$4.41 \times 10^{-3}$	$1.01 \times 10^{-2}$	$3.29 \times 10^{-2}$
<b>Female rat</b>								
NTP (1988)	Leukemia	0.05	TotMetabBW34	$2.3 \times 10^{-3}$	$1.89 \times 10^{-3}$	$5.09 \times 10^{-4}$	$1.43 \times 10^{-3}$	$4.69 \times 10^{-3}$
			AUCCBld	$1.6 \times 10^{-5}$	$1.56 \times 10^{-5}$	$3.39 \times 10^{-6}$	$1.07 \times 10^{-5}$	$3.98 \times 10^{-5}$
<b>Male rat</b>								
NTP (1990)	Kidney adenoma + carcinoma <sup>b</sup>	0.1	ABioactDCVCBW34	$1.2 \times 10^{-1}$	$1.40 \times 10^{-1}$	$5.69 \times 10^{-3}$	$5.24 \times 10^{-2}$	$5.18 \times 10^{-1}$
			AMetGSHBW34	$7.6 \times 10^{-2}$	$6.18 \times 10^{-2}$	$4.00 \times 10^{-3}$	$3.27 \times 10^{-2}$	$2.11 \times 10^{-1}$
			TotMetabBW34	$3.1 \times 10^{-3}$	$2.49 \times 10^{-3}$	$7.14 \times 10^{-4}$	$1.96 \times 10^{-3}$	$5.96 \times 10^{-3}$

**Table 5-42. Summary of PBPK model-based uncertainty analysis of slope factor estimates for each sex/species/bioassay/tumor type (oral) (continued)**

Study	Tumor type	BMR	Dose-metric	Slope factor estimates (mg/kg/d) <sup>-1</sup>				
				From	Summary statistics of slope factor distribution			
				Table 5-37 or 5-38	Mean	5% lower bound	Median	95% upper bound
NTP (1988)								
Marshall	Testicular <sup>b</sup>	0.1	TotMetabBW34	$7.1 \times 10^{-2}$	$6.18 \times 10^{-2}$	$1.92 \times 10^{-2}$	$4.89 \times 10^{-2}$	$1.45 \times 10^{-1}$
			AUCCBld	$6.0 \times 10^{-4}$	$5.45 \times 10^{-4}$	$1.18 \times 10^{-4}$	$3.70 \times 10^{-4}$	$1.44 \times 10^{-3}$
August	Subcut sarcoma	0.05	TotMetabBW34	$2.3 \times 10^{-3}$	$1.65 \times 10^{-3}$	$4.58 \times 10^{-4}$	$1.27 \times 10^{-3}$	$4.04 \times 10^{-3}$
			AUCCBld	$2.0 \times 10^{-5}$	$1.35 \times 10^{-5}$	$1.53 \times 10^{-6}$	$8.34 \times 10^{-6}$	$3.73 \times 10^{-5}$
Osborne-Mendel	Kidney adenoma + carcinoma <sup>b</sup>	0.1	ABioactDCVCBW34	$1.6 \times 10^{-1}$	$1.61 \times 10^{-1}$	$5.45 \times 10^{-3}$	$6.35 \times 10^{-2}$	$6.02 \times 10^{-1}$
			AMetGSHBW34	$9.7 \times 10^{-2}$	$7.47 \times 10^{-2}$	$3.90 \times 10^{-3}$	$3.85 \times 10^{-2}$	$2.54 \times 10^{-1}$
			TotMetabBW34	$4.3 \times 10^{-3}$	$2.73 \times 10^{-3}$	$5.40 \times 10^{-4}$	$2.10 \times 10^{-3}$	$6.89 \times 10^{-3}$

<sup>a</sup>WinBUGS dose-response analyses did not adequately converge for AMetLngBW34 dose-metric using the 3<sup>rd</sup>-order multistage model (used for results in Table 5-37), but did converge when the 2<sup>nd</sup>-order model was used. Summary statistics reflect results of 2<sup>nd</sup>-order model calculations.

<sup>b</sup>Using poly-3 adjusted incidences from Table 5-38 (software for WinBUGS-based analyses using the MSW model was not developed).

## 5.2.2. Dose-Response Analyses: Human Epidemiologic Data

Of the epidemiological studies of TCE and cancer, only two had sufficient exposure-response information for potential dose-response analysis. The two studies, Charbotel et al. (2006) and Moore et al. (2010), were both case-control studies of TCE and kidney cancer, and both had quantitative cumulative exposure estimates for the individual subjects. In the study by Moore et al. (2010), however, the cumulative exposure estimates were assessed by experts based on categorical metrics for frequency and intensity of exposure and not continuous measures. Moore et al. (2010) also used a categorical confidence-of-exposure metric to classify different jobs because of the potential for exposure misclassification from this approach. While the detailed approach used by Moore et al. (2010) should be fairly reliable for general rankings, the resulting estimates are not expected to be as quantitatively accurate as those in the Charbotel et al. (2006) study, which relied on a task-exposure matrix based on decades of measurements from the Arve Valley workshops (Fevotte et al., 2006; see also Section 4.4 for more discussion of the exposure assessments). Thus, the Charbotel et al. (2006) study was selected as the sole basis for the derivation of an inhalation unit risk estimate for kidney cancer (see Section 5.2.2.1). Other epidemiological studies were used in Section 5.2.2.2 below to provide information for a comparison of RR estimates across cancer types. These epidemiologic data were used to derive an adjusted inhalation unit risk estimate for the combined risk of developing kidney cancer, NHL, or liver cancer. The human PBPK model was then used to perform route-to-route extrapolation to derive an oral slope factor estimate for the combined risk of kidney cancer, NHL, or liver cancer (see Section 5.2.2.3).

### 5.2.2.1. Inhalation Unit Risk Estimate for RCC Derived from Charbotel et al. (2006) Data

The Charbotel et al. (2006) case-control study of 86 incident RCC cases and 316 age- and sex-matched controls, with individual cumulative exposure estimates for TCE for each subject, provides a sufficient human data set for deriving quantitative cancer risk estimates for RCC in humans. The study is a high-quality study that used a detailed exposure assessment (Fevotte et al., 2006) and took numerous potential confounding factors, including exposure to other chemicals, into account (see Section 4.4). A significant dose-response relationship was reported for cumulative TCE exposure and RCC (Charbotel et al., 2006).

The derivation of an inhalation unit risk estimate, defined as the plausible upper bound lifetime risk of cancer from chronic inhalation of TCE per unit of air concentration, for RCC incidence in the U.S. population, based on results of the Charbotel et al. (2006) case-control study, is presented in the following subsections.

### 5.2.2.1.1. RCC results from the Charbotel et al. (2006) study

Charbotel et al. (2006) analyzed their data using conditional logistic regression, matching on sex and age, and reported results (ORs) for cumulative TCE exposure categories, adjusted for tobacco smoking and BMI (Charbotel et al., 2006, Table 6). The exposure categories were constructed as tertiles based on the cumulative exposure levels in the exposed control subjects. The results are summarized in Table 5-43, with mean exposure levels kindly provided by Dr. Charbotel (2008).

For additional details and discussion of the Charbotel et al. (2006) study, see Section 4.4 and Appendix B.

**Table 5-43. Results from Charbotel et al. (2006) on relationship between TCE exposure and RCC**

Cumulative exposure category	Mean cumulative exposure (ppm × yrs)	Adjusted OR (95% CI)
Nonexposed		1
Low	62.4	1.62 (0.75, 3.47)
Medium	253.2	1.15 (0.47, 2.77)
High	925.0	2.16 (1.02, 4.60)

### 5.2.2.1.2. Prediction of lifetime extra risk of RCC incidence from TCE exposure

The categorical results summarized in Table 5-43 were used for predicting the extra risk of RCC incidence from continuous environmental exposure to TCE. Extra risk is defined as:

$$\text{Extra risk} = (R_x - R_o)/(1 - R_o),$$

where  $R_x$  is the lifetime risk in the exposed population and  $R_o$  is the lifetime risk in an unexposed population (i.e., the background risk). Because kidney cancer is a rare event, the ORs in Table 5-43 can be used as estimates of the RR ratio =  $R_x/R_o$  (Rothman and Greenland, 1998). A weighted linear regression model was used to model the dose-response data in Table 5-43 to obtain a slope estimate (regression coefficient) for RR of RCC versus cumulative exposure, under the commonly employed assumption that exposure was measured without error. Use of a linear model in the observable range of the data is often a good general approach for epidemiological data because such data are frequently too limited (i.e., imprecise), as is the case here, to clearly identify an alternate model (U.S. EPA, 2005b). This linear dose-response function was then used to calculate lifetime extra risks in an actuarial program (life-table analysis) that accounts for age-specific rates of death and background disease, under the common

assumption that the RR is independent of age.<sup>48</sup> In addition, it is generally assumed that RR estimates transfer across populations, independent of background disease rates—in this case, the RR estimates based on the Charbotel et al. (2006) study, which was conducted in France, are assumed to apply to the U.S. population.<sup>49</sup>

For the weighted linear regression, the weights used for the RR estimates were the inverses of the variances, which were calculated from the CIs. Using this approach,<sup>50</sup> a linear regression coefficient of 0.001205 per ppm × year (SE = 0.0008195 per ppm × year) was obtained from the categorical results.

For the life-table analysis, U.S. age-specific all-cause mortality rates for 2004 for both sexes and all race groups combined (CDC, 2007) were used to specify the all-cause background mortality rates in the actuarial program. Because the goal is to estimate the unit risk for extra risk of cancer incidence, not mortality, and because the Charbotel et al. (2006) data are incidence data, RCC incidence rates were used for the cause-specific background “mortality” rates in the life-table analysis.<sup>51</sup> SEER 2001–2005 cause-specific background incidence rates for RCC were obtained from the SEER public-use database.<sup>52</sup> SEER collects good-quality cancer incidence data from a variety of geographical areas in the United States. The incidence data used here are from SEER 17, a registry of 17 states, cities, or regions covering about 26% of the United States population (<http://seer.cancer.gov>). The risks were computed up to age 85 years for continuous exposures to TCE.<sup>53</sup> Conversions between occupational TCE exposures and continuous environmental exposures were made to account for differences in the number of days exposed per year (240 vs. 365 days) and in the amount of air inhaled per day (10 vs. 20 m<sup>3</sup>; U.S. EPA, 1994a). The SE for the regression coefficient from the weighted linear regression calculation described above was used to compute the 95% upper confidence limit (UCL) for the slope estimate, and this value was used to derive 95% UCLs for risk estimates (or 95% lower

---

<sup>48</sup>This program is an adaptation of the approach previously used by the Committee on the Biological Effects of Ionizing Radiation (BEIR, 1988). The same methodology was also used in U.S. EPA’s 1,3-butadiene health risk assessment (U.S. EPA, 2002d). A spreadsheet illustrating the extra risk calculation for the derivation of the LEC<sub>01</sub> for RCC incidence is presented in Appendix H.

<sup>49</sup>In any event, background kidney cancer rates between the United States and France are similar, with estimated age-adjusted incidence rates of 14.1 per 100,000 in the United States (Surveillance, Epidemiology, and End Results: <http://seer.cancer.gov/statfacts/html/kidrp.html>) and 10.4 per 100,000 in France (European Cancer Observatory: <http://eu-cancer.iarc.fr/cancer-19-kidney.html.en>).

<sup>50</sup>Equations for this weighted linear regression approach are presented in Rothman (1986) and summarized in Appendix H.

<sup>51</sup>No adjustment was made for using RCC incidence rates rather than mortality rates to represent cause-specific mortality in the actuarial program because the RCC incidence rates are negligible in comparison to the all-cause mortality rates. Otherwise, all-cause mortality rates for each age interval would have been adjusted to reflect people dying of a cause other than RCC or being diagnosed with RCC.

<sup>52</sup>In accordance with the “SEER Program Coding and Staging Manual 2007”

([http://seer.cancer.gov/manuals/2007/SPCSM\\_2007\\_AppendixC\\_p6.pdf](http://seer.cancer.gov/manuals/2007/SPCSM_2007_AppendixC_p6.pdf)), pages C-831 to C-833, RCC was specified as ICD-0-3 histological types coded 8312, 8260, 8310, 8316-8320, 8510, 8959, and 8255 (mixed types).

<sup>53</sup>Rates above age 85 years are not included because cause-specific disease rates are less stable for those ages. Note that 85 years is not employed here as an average lifespan but, rather, as a cut-off point for the life-table analysis, which uses actual age-specific mortality rates.

confidence limits [LCLs] for corresponding exposure estimates), based on a normal approximation.

Point estimates and one-sided 95% UCLs for the extra risk of RCC incidence associated with varying levels of environmental exposure to TCE based on linear regression of the Charbotel et al. (2006) categorical results were determined by the actuarial program; the results are presented in Section 5.2.1.3. The models based on cumulative exposure yield extra risk estimates that are fairly linear for exposures up to approximately 1 ppm.

Consistent with EPA's *Guidelines for Carcinogen Risk Assessment* (U.S. EPA, 2005b), the same data and methodology were also used to estimate the exposure level ( $EC_x$ : "effective concentration corresponding to an extra risk of  $x\%$ ") and the associated 95% lower confidence limit of the effective concentration corresponding to an extra risk of 1% ( $LEC_x$  [lowest effective concentration],  $x = 0.01$ ). A 1% extra risk level is commonly used for the determination of the POD for epidemiological data. Use of a 1% extra risk level for these data is supported by the fact that, based on the actuarial program, the risk ratio (i.e.,  $R_x/R_0$ ) for an extra risk of 1% for RCC incidence is 1.9, which is in the range of the ORs reported by Charbotel et al. (see Table 5-43). Thus, 1% extra risk was selected for determination of the POD, and, consistent with the *Guidelines for Carcinogen Risk Assessment*, the LEC value corresponding to that risk level was used as the actual POD. For the linear model that was selected, the unit risk is independent of the benchmark risk level used to determine the POD (at low exposures/risk levels; see Table 5-44); however, selection of a benchmark risk level is generally useful for comparisons across models.

**Table 5-44. Extra risk estimates for RCC incidence from various levels of lifetime exposure to TCE, using linear cumulative exposure model**

Exposure concentration (ppm)	MLE of extra risk	95% UCL on extra risk
0.001	$2.603 \times 10^{-6}$	$5.514 \times 10^{-6}$
0.01	$2.603 \times 10^{-5}$	$5.514 \times 10^{-5}$
0.1	$2.602 \times 10^{-4}$	$5.512 \times 10^{-4}$
1.0	$2.598 \times 10^{-3}$	$5.496 \times 10^{-3}$
10.0	$2.562 \times 10^{-2}$	$5.333 \times 10^{-2}$

As discussed in Section 4.4, there is sufficient evidence to conclude that a mutagenic mode of action is operative for TCE-induced kidney tumors, which supports the use of linear low-dose extrapolation from the POD. The  $EC_{01}$ ,  $LEC_{01}$ , and inhalation unit risk estimates for RCC incidence using the linear cumulative exposure model are presented in Table 5-45. Converting the units,  $5.49 \times 10^{-3}$  per ppm corresponds to a unit risk of  $1.02 \times 10^{-6}$  per  $\mu\text{g}/\text{m}^3$  for RCC incidence.

**Table 5-45. EC<sub>01</sub>, LEC<sub>01</sub>, and unit risk estimates for RCC incidence, using linear cumulative exposure model**

EC <sub>01</sub> (ppm)	LEC <sub>01</sub> (ppm)	unit risk (per ppm) <sup>a</sup>
3.87	1.82	5.49 × 10 <sup>-3</sup>

<sup>a</sup>Unit risk = 0.01/LEC<sub>01</sub>.

### 5.2.2.1.3. Uncertainties in the RCC unit risk estimate

The two major sources of uncertainty in quantitative cancer risk estimates are generally interspecies extrapolation and high-dose to low-dose extrapolation. The unit risk estimate for RCC incidence derived from the Charbotel et al. (2006) results is not subject to interspecies uncertainty because it is based on human data. A major uncertainty remains in the extrapolation from occupational exposures to lower environmental exposures. There was some evidence of a contribution to increased RCC risk from peak exposures; however, there remained an apparent dose-response relationship for RCC risk with increasing cumulative exposure without peaks, and the OR for exposure with peaks compared to exposure without peaks was not significantly elevated (Charbotel et al., 2006). Although the actual exposure-response relationship at low exposure levels is unknown, the conclusion that a mutagenic mode of action is operative for TCE-induced kidney tumors supports the linear low-dose extrapolation that was used (U.S. EPA, 2005b). The weight of evidence also supports involvement of processes of cytotoxicity and regenerative proliferation in the carcinogenicity of TCE, although not with the extent of support as for a mutagenic mode of action. In particular, data linking TCE-induced proliferation to increased mutation or clonal expansion are lacking, as are data informing the quantitative contribution of cytotoxicity. Because any possible involvement of a cytotoxicity mode of action would be additional to mutagenicity, the dose-response relationship would nonetheless be expected to be linear at low doses. Therefore, the additional involvement of a cytotoxicity mode of action does not provide evidence against the use of linear extrapolation from the POD.

Another notable source of uncertainty in the cancer unit risk estimate is the dose-response model used to model the study data to estimate the POD. A weighted linear regression across the categorical ORs was used to obtain a slope estimate; use of a linear model in the observable range of the data is often a good general approach for human data because epidemiological data are frequently too limited (i.e., imprecise) to clearly identify an alternate model (U.S. EPA, 2005b). The Charbotel et al. (2006) study is a relatively small case-control study, with only 86 RCC cases, 37 of which had TCE exposure; thus, the dose-response data upon which to specify a model are indeed limited.

In accordance with EPA's *Guidelines for Carcinogen Risk Assessment*, the lower bound on the EC<sub>01</sub> is used as the POD; this acknowledges some of the uncertainty in estimating the POD from the available dose-response data. In this case, the statistical uncertainty associated with the EC<sub>01</sub> is relatively small, as the ratio between the EC<sub>01</sub> and the LEC<sub>01</sub> is about twofold.

The inhalation unit risk estimate of  $5.49 \times 10^{-3}$  per ppm presented above, which is calculated based on a linear extrapolation from the POD ( $LEC_{01}$ ), is expected to provide an upper bound on the risk of cancer incidence. However, for certain applications, such as benefit-cost analyses, estimates of “central tendency” for the risk below the POD are desired. Because a linear dose-response model was used in the observable range of the human data and the POD was within the low-dose linear range for extra risk as a function of exposure, linear extrapolation below the  $LEC_{01}$  has virtually the same slope as the 95% UCL on the actual (linear) dose-response model in the low-dose range (i.e., below the POD). This is illustrated in Table 5-44, where the 95% UCL on extra risk for RCC incidence predicted by the dose-response model is about  $5.51 \times 10^{-3}$  per ppm for exposures at or below about 0.1 ppm, which is virtually equivalent to the unit risk estimate of  $5.49 \times 10^{-3}$  per ppm derived from the  $LEC_{01}$  (see Table 5-45). The same holds for the central tendency (weighted least squares) estimates of the extra risk from the (linear) dose-response model (i.e., the dose-response model prediction of  $2.60 \times 10^{-3}$  per ppm from Table 5-44 is virtually identical to the value of  $2.58 \times 10^{-3}$  per ppm obtained from linear extrapolation below the  $EC_{01}$ , i.e., by dividing 0.01 extra risk by the  $EC_{01}$  of 3.87 from Table 5-45). In other words, because the dose-response model that was used to model the data in the observable range is already low-dose linear near the POD, if one assumes that the same linear model is valid for the low-dose range, one can use the central tendency (weighted least squares) estimate from the model to derive a statistical “best estimate” of the slope rather than relying on an extrapolated risk estimate ( $0.01/EC_{01}$ ). (The extrapolated risk estimates are not generally central tendency estimates in any statistical sense because once risk is extrapolated below the  $EC_{01}$  using the formulation  $0.01/EC_{01}$ , it is no longer a function of the original model that generated the  $EC_{01}$  and  $LEC_{01}$  estimates.)

An important source of uncertainty in the underlying Charbotel et al. (2006) study is the retrospective estimation of TCE exposures in the study subjects. This case-control study was conducted in the Arve Valley in France, a region with a high concentration of workshops devoted to screw cutting, which involves the use of TCE and other degreasing agents. Since the 1960s, occupational physicians of the region have collected a large quantity of well-documented measurements, including TCE air concentrations and urinary metabolite levels (Fevotte et al., 2006). The study investigators conducted a comprehensive exposure assessment to estimate cumulative TCE exposures for the individual study subjects, using a detailed occupational questionnaire with a customized task-exposure matrix for the screw-cutting workers and a more general occupational questionnaire for workers exposed to TCE in other industries (Fevotte et al., 2006). The exposure assessment even attempted to take dermal exposure from hand-dipping practices into account by equating it with an equivalent airborne concentration based on biological monitoring data. Despite the appreciable effort of the investigators, considerable uncertainty associated with any retrospective exposure assessment is inevitable, and some exposure misclassification is unavoidable. Such exposure misclassification was most likely for

the 19 deceased cases and their matched controls, for which proxy respondents were used, and for exposures outside the screw-cutting industry (295 of 1,486 identified job periods involved TCE exposure; 120 of these were not in the screw-cutting industry).

Although the exposure estimates from Moore et al. (2010) were not considered to be as quantitatively accurate as those of Charbotel et al. (2006), as discussed at the beginning of Section 5.2.2, it is worth noting, in the context of uncertainty in the exposure assessment, that the exposure estimates in Moore et al. (2010) are substantially lower than those of Charbotel et al. (2006) for comparable OR estimates. For example, for all subjects and high-confidence assessments only, respectively, Moore et al. (2010) reported OR estimates of 1.19 and 1.77 for cumulative exposures  $<1.58 \text{ ppm} \times \text{years}$  and 2.02 and 2.23 for cumulative exposures  $\geq 1.58 \text{ ppm} \times \text{years}$ . Charbotel et al. (2006), on the other hand, reported OR estimates for all subjects of 1.62, 1.15, and 2.16 for mean cumulative exposures of 62.4, 253.2, and 925.0  $\text{ppm} \times \text{years}$ , respectively. If the exposure estimates for Charbotel et al. (2006) are overestimated, as suggested by the exposure estimates from Moore et al. (2010), then the slope of the linear regression model, and hence the unit risk estimate, would be correspondingly underestimated.

Another noteworthy source of uncertainty in the Charbotel et al. (2006) study is the possible influence of potential confounding or modifying factors. This study population, with a high prevalence of metal-working, also had relatively high prevalences of exposure to petroleum oils, cadmium, petroleum solvents, welding fumes, and asbestos (Fevotte et al., 2006). Other exposures assessed included other solvents (including other chlorinated solvents), lead, and ionizing radiation. None of these exposures was found to be significantly associated with RCC at a  $p = 0.05$  significance level. Cutting fluids and other petroleum oils were associated with RCC at a  $p = 0.1$  significance level; however, further modeling suggested no association with RCC when other significant factors were taken into account (Charbotel et al., 2006). Moreover, a review of other studies suggested that potential confounding from cutting fluids and other petroleum oils is of minimal concern (see Section 4.4.2.3). Nonetheless, a sensitivity analysis was conducted using the OR estimates further adjusted for cutting fluids and other petroleum oils from the unpublished report by Charbotel et al. (2005), and an essentially identical unit risk estimate of  $5.46 \times 10^{-3}$  per ppm was obtained.<sup>54</sup> In addition, the medical questionnaire included familial kidney disease and medical history, such as kidney stones, infection, chronic dialysis, hypertension, and use of antihypertensive drugs, diuretics, and analgesics. BMI was also calculated, and lifestyle information such as smoking habits and coffee consumption was collected. Univariate analyses found high levels of smoking and BMI to be associated with

---

<sup>54</sup>The OR estimates further adjusted for cutting fluids and other petroleum oils were 1.52 (95% CI: 0.66, 3.49), 1.07 (0.39, 2.88), and 1.96 (0.71, 5.37) for the low, medium, and high cumulative exposure groups, respectively (Charbotel et al., 2005). For the linear regression model, these OR estimates yielded a shallower slope estimate of 0.0009475 per  $\text{ppm} \times \text{year}$  but a larger SE of 0.0009709 per  $\text{ppm} \times \text{year}$ . In the lifetable analysis, these latter estimates in turn yielded a slightly higher  $\text{EC}_{01}$  estimate (4.92 versus 3.87 ppm), because of the shallower slope estimate, but an essentially identical  $\text{LEC}_{01}$ , because of the larger SE.

increased odds of RCC, and these two variables were included in the conditional logistic regressions. Thus, although impacts of other factors are possible, this study took great pains to attempt to account for potential confounding or modifying factors.

Some other sources of uncertainty associated with the epidemiological data are the dose-metric and lag period. As discussed above, there was some evidence of a contribution to increased RCC risk from peak TCE exposures; however, there appeared to be an independent effect of cumulative exposure without peaks. Cumulative exposure is considered a good measure of total exposure because it integrates exposure (levels) over time. If there is a contributing effect of peak exposures, not already taken into account in the cumulative exposure metric, the linear slope may be overestimated to some extent. Sometimes, cancer data are modeled with the inclusion of a lag period to discount more recent exposures not likely to have contributed to the onset of cancer. In an unpublished report, Charbotel et al. (2005) also present the results of a conditional logistic regression with a 10-year lag period, and these results are very similar to the unlagged results reported in their published paper, suggesting that the lag period might not be an important factor in this study.

Some additional sources of uncertainty are not so much inherent in the exposure-response modeling or in the epidemiologic data themselves but, rather, arise in the process of obtaining more general Agency risk estimates from the epidemiologic results. EPA cancer risk estimates are typically derived to represent an upper bound on increased risk of cancer incidence for all sites affected by an agent for the general population. From experimental animal studies, this is accomplished by using tumor incidence data and summing across all of the tumor sites that demonstrate significantly increased incidences, customarily for the most sensitive sex and species, to attempt to be protective of the general human population. However, in estimating comparable risks from the Charbotel et al. (2006) epidemiologic data, certain limitations are encountered. For one thing, these epidemiology data represent a geographically limited (Arve Valley, France), and likely not very diverse, population of working adults. Thus, there is uncertainty about the applicability of the results to a more diverse general population. Additionally, the Charbotel et al. (2006) study was a study of RCC only, and so the risk estimate derived from it does not represent all of the tumor sites that may be affected by TCE. The issue of cancer risk at other sites is addressed in the next section (see Section 5.2.2.2).

#### **5.2.2.1.4. Conclusions regarding the RCC unit risk estimate**

An EC<sub>01</sub> of 3.9 ppm was calculated using a life-table analysis and linear modeling of the categorical conditional logistic regression results for RCC incidence reported in a high-quality case-control study. Linear low-dose extrapolation from the LEC<sub>01</sub> yielded a lifetime extra RCC incidence unit risk estimate of  $5.5 \times 10^{-3}$  per ppm ( $1.0 \times 10^{-6}$  per  $\mu\text{g}/\text{m}^3$ ) of continuous TCE exposure. The assumption of low-dose linearity is supported by the conclusion that a mutagenic mode of action is operative for TCE-induced kidney tumors.

The inhalation unit risk estimate is expected to provide an upper bound on the risk of RCC incidence; however, this is just the risk estimate for RCC. A risk estimate for total cancer risk to humans would need to include the risk for other potential TCE-associated cancers.

#### **5.2.2.2. Adjustment of the Inhalation Unit Risk Estimate for Multiple Sites**

Human data on TCE exposure and cancer risk sufficient for dose-response modeling are only available for RCC, yet human and rodent data suggest that TCE exposure increases the risk of other cancers as well. In particular, there is evidence from human (and rodent) studies for increased risks of NHL and liver cancer (see Section 4.11). Therefore, the inhalation unit risk estimate derived from human data for RCC incidence was adjusted to account for potential increased risk of those cancer types. To make this adjustment, a factor accounting for the relative contributions to the extra risk for cancer incidence from TCE exposure for these three cancer types combined versus the extra risk for RCC alone was estimated, and this factor was applied to the unit risk estimate for RCC to obtain a unit risk estimate for the three cancer types combined (i.e., lifetime extra risk for developing *any* of the three types of cancer). This estimate is considered a better estimate of total cancer risk from TCE exposure than the estimate for RCC alone.

Although only the Charbotel et al. (2006) study was found adequate for direct estimation of inhalation unit risks, the available epidemiologic data provide sufficient information for estimating the *relative* potency of TCE across tumor sites. In particular, the relative contributions to extra risk (for cancer incidence) were calculated from two different data sets to derive the adjustment factor for adjusting the unit risk estimate for RCC to a unit risk estimate for the three types of cancers (RCC, NHL, and liver) combined. The first calculation is based on the results of the meta-analyses of human epidemiologic data for the three cancer types (see Appendix C); the second calculation is based on the results of the Raaschou-Nielsen et al. (2003) study, the largest single human epidemiologic study by far with RR estimates for all three cancer types. The approach for each calculation was to use the RR estimates and estimates of the lifetime background risk in an unexposed population,  $R_o$ , to calculate the lifetime risk in the exposed population,  $R_x$ , where  $R_x = RR \times R_o$ , for each tumor type. Then, the extra risk from TCE exposure for each tumor type could be calculated using the equation in Section 5.2.2.1.2. Finally, the extra risks were summed across the three cancer types and the ratio of the sum of the extra risks to the extra risk for RCC was derived. For the first calculation, the  $RR_m$  estimates from the meta-analyses for NHL, kidney cancer, and liver (and biliary) cancer were used as the RR estimates. For the second calculation, the SIR estimates from the Raaschou-Nielsen et al. (2003) study were used. For both calculations,  $R_o$  for RCC was taken from the life-table analysis described in Section 5.2.2.1.2 and presented in Appendix H, which estimated a lifetime risk for RCC incidence up to age 85 years. For  $R_o$  values for the other two sites, SEER statistics for the lifetime risk of developing cancer were used

(<http://seer.cancer.gov/statfacts/html/nhl.html> and <http://seer.cancer.gov/statfacts/html/livibd.html>).

In both cases, an underlying assumption in deriving the relative potencies is that the relative values of the age-specific background incidence risks for the person-years from the epidemiologic studies for each tumor type approximate the relative values of the lifetime background incidence risks for those cancer types. In other words, at least on a proportional basis, the lifetime background incidence risks (for the U.S. population) for each site approximate the age-specific background incidence risks for the study populations. A further assumption is that the lifetime risk of RCC up to 85 years is an adequate approximation to the full lifetime risk, which is what was used for the other two cancer types. The first calculation, based on the results of the meta-analyses for the three cancer types, has the advantage of being based on a large data set, incorporating data from many different studies. However, this calculation relies on a number of additional assumptions. First, it is assumed that the RR<sub>m</sub> estimates from the meta-analyses, which are based on different groups of studies, reflect similar overall TCE exposures (i.e., that the overall TCE exposures are similar across the different groups of studies that went into the different meta-analyses for the three cancer types). Second, it is assumed that the RR<sub>m</sub> estimates, which incorporate RR estimates for both mortality and incidence, represent good estimates for cancer incidence risk from TCE exposure. In addition, it is assumed that the RR<sub>m</sub> for kidney cancer, for which RCC estimates from individual studies were used when available, is a good estimate for the overall RR for RCC and that the RR<sub>m</sub> estimate for NHL, for which different studies used different classification schemes, is a good estimate for the overall RR for NHL. The second calculation, based on the results of the Raaschou-Nielsen et al. (2003) study, the largest single study with RR estimates for all three cancer types, has the advantage of having RR estimates that are directly comparable. In addition, the Raaschou-Nielsen et al. study provided data for the precise cancer types of interest for the calculation (i.e., RCC, NHL, and liver [and biliary] cancer).

The input data and results of the calculations are presented in Table 5-46. The value for the ratio of the sum of the extra risks to the extra risk for RCC alone was 3.28 in calculation #1 and 4.36 in calculation #2, which together suggest that 4 is a reasonable factor to use to adjust the inhalation unit risk estimate based on RCC for multiple sites to obtain a total cancer unit risk estimate.<sup>55</sup> Using this factor to adjust the unit risk estimate based on RCCs entails the further fundamental assumption that the dose-response relationships for the other two cancer types (NHL and liver cancer) are similarly linear (i.e., that the relative potencies are roughly maintained at lower exposure levels). This assumption is consistent with EPA's *Guidelines for Carcinogen Risk Assessment* (U.S. EPA, 2005b), which recommends low-dose linear extrapolation in the absence of sufficient evidence to support a nonlinear mode of action.

---

<sup>55</sup>Both the geometric and arithmetic means of the two values for the ratio are 3.8, which rounds to 4, in keeping with the imprecise nature of the adjustment factor. The factor of 4 is within 25% of either calculated ratio.

**Table 5-46. Relative contributions to extra risk for cancer incidence from TCE exposure for multiple cancer types**

	RR	Ro	Rx	Extra risk	Ratio to kidney value
<b>Calculation #1: using RR estimates from the meta-analyses</b>					
Kidney (RCC)	1.27	0.0107	0.01359	0.002920	1
NHL	1.23	0.0202	0.02485	0.004742	1.62
Liver (and biliary) cancer	1.29	0.0066	0.008514	0.001927	0.66
			<b>sum</b>	0.009589	<b>3.28</b>
Kidney + NHL only			<b>sum</b>	0.007662	2.62
<b>Calculation #2: using RR estimates from Rasschou-Nielsen et al. (2003)</b>					
Kidney (RCC)	1.20	0.0107	0.01284	0.002163	1
NHL	1.24	0.0202	0.02505	0.004948	2.29
Liver (and biliary) cancer	1.35	0.0066	0.008910	0.002325	1.07
			<b>sum</b>	0.009436	<b>4.36</b>
Kidney + NHL only			<b>sum</b>	0.007111	3.29

Applying the factor of 4 to the lifetime extra RCC incidence unit risk estimate of  $5.49 \times 10^{-3}$  per ppm ( $1.0 \times 10^{-6}$  per  $\mu\text{g}/\text{m}^3$ ) of continuous TCE exposure yields a cancer unit risk estimate of  $2.2 \times 10^{-2}$  per ppm ( $4.1 \times 10^{-6}$  per  $\mu\text{g}/\text{m}^3$ ). Table 5-46 also presents calculations for just kidney and NHL extra risks combined, because the strongest human evidence is for those two cancer types. For those two cancer types, the calculations support a factor of 3.<sup>56</sup> Applying this factor to the RCC unit risk estimate yields an estimate of  $1.6 \times 10^{-2}$  per ppm, which results in the same estimate as for the three cancer types combined when finally rounded to one significant figure (i.e.,  $2 \times 10^{-2}$  per ppm [or  $3 \times 10^{-6}$  per  $\mu\text{g}/\text{m}^3$ , which is still similar to the three-tumor-type estimate in those units]).

In addition to the uncertainties in the underlying RCC estimate, there are uncertainties related to the assumptions inherent in these calculations for adjusting to multiple sites, as detailed above. Nonetheless, the fact that the calculations based on two different data sets yielded comparable values for the adjustment factor (both within 25% of the selected factor of 4) provides more robust support for the use of the factor of 4. Additional uncertainties pertain to the weight of evidence supporting the association of TCE exposure with increased risk of cancer for the three cancer types. As discussed in Section 4.11.2, it was found that the weight of evidence for kidney cancer was sufficient to classify TCE as “carcinogenic to humans.” It was also concluded that there was strong evidence that TCE causes NHL as well, although the evidence for liver cancer was more limited. In addition, the rodent studies demonstrate clear

<sup>56</sup>The geometric and mean of the two values for the ratio, 2.62 and 3.29, is 2.96, and the arithmetic mean is 2.94, which both round to 3, in keeping with the imprecise nature of the adjustment factor. The factor of 3 is within 15% of either calculated ratio.

evidence of multisite carcinogenicity, with cancer types including those for which associations with TCE exposure are observed in human studies (i.e., liver and kidney cancers and NHLs). Overall, the evidence was found to be sufficiently persuasive to support the use of the adjustment factor of 4 based on these three cancer types, resulting in a cancer inhalation unit risk estimate of  $2.2 \times 10^{-2}$  per ppm ( $4.1 \times 10^{-6}$  per  $\mu\text{g}/\text{m}^3$ ). Alternatively, if one were to use the factor based only on the two cancer types with the strongest human evidence, the cancer inhalation unit risk estimate would be only slightly reduced (25%).

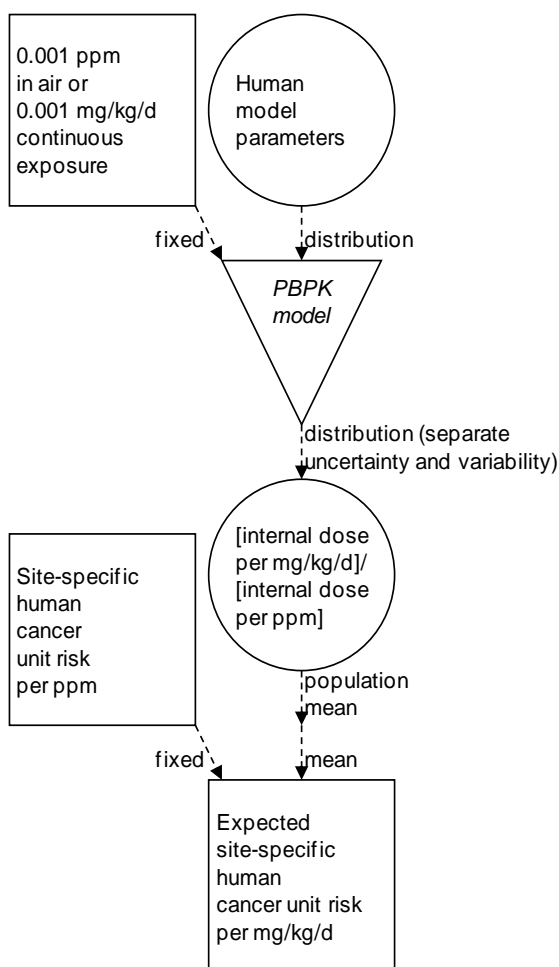
### 5.2.2.3. Route-to-Route Extrapolation Using PBPK Model

Route-to-route extrapolation of the inhalation unit risk estimate was performed using the PBPK model described in Section 3.5. The (partial) unit risk estimates for NHL and liver cancer were derived as for the total cancer inhalation unit risk estimate in Section 5.2.2.2, except that the ratios of extra risk for the individual cancer types relative to kidney cancer were used as adjustment factors rather than the ratio of the sum. As presented in Table 5-46, for NHL, the ratios from the two different calculations were 1.62 and 2.29, so a factor of 2 was used; for liver cancer, the ratios were 0.66 and 1.07, so a factor of 1 was used. (With the ratio of 1 for kidney cancer itself, the combined adjustment factor is 4, reproducing the factor of 4 used to estimate the total cancer unit risk from the multiple sites in Section 5.2.2.2)

Because different internal dose-metrics are preferred for each target tissue site, a separate route-to-route extrapolation was performed for each site-specific unit risk estimate calculated in Sections 5.2.2.1 and 5.2.2.2. As shown in Figure 5-7, the approach taken to apply the human PBPK model in the low-dose range where external and internal doses are linearly related to derive a conversion that is the ratio of internal dose per mg/kg/day to internal dose per ppm. The expected value of the population mean for this conversion factor (in ppm per mg/kg/day) was used to extrapolate each inhalation unit risk in units of risk per ppm to an oral slope factor in units of risk per mg/kg/day. Note that this conversion is the *mean of the ratio* of internal dose predictions, and is not the same as taking the *ratio of the mean* of internal dose predictions in Table 5-35.<sup>57</sup>

---

<sup>57</sup>For route-to-route extrapolation based on dose-response analysis performed on internal dose, as is the case for rodent bioassays, it would be appropriate to use the values in Table 5-35 to first “unconvert” the unit risk based on one route, and then recover to a unit risk based on the other route.



Square nodes indicate point values, circle nodes indicate distributions, and the inverted triangle indicates a (deterministic) functional relationship.

**Figure 5-7. Flow-chart for route-to-route extrapolation of human site-specific cancer inhalation unit risks to oral slope factors.**

Table 5-47 shows the results of this route-to-route extrapolation for the “primary” and “alternative” dose-metrics. For reference, route-to-route extrapolation based on total intake (i.e., ventilation rate  $\times$  air concentration = oral dose  $\times$  body weight) using the parameters in the PBPK model would yield an expected population average conversion of 0.95 ppm per mg/kg/day. For TotMetabBW34, TotOxMetabBW34, and AMetLiv1BW34, the conversion is 2.0–2.8 ppm per mg/kg/day, greater than that based on intake. This is because of the greater metabolic first pass in the liver, which leads to a higher percentage of intake being metabolized via oral exposure relative to inhalation exposure for the same intake. Conversely, for the AUC in blood, the conversion is 0.14 ppm per mg/kg/day, less than that based on intake—the greater first pass in the liver means lower blood levels of parent compound via oral exposure relative to inhalation for the same intake. The conversion for the primary dose-metric for the kidney, ABioactDCVCBW34, is 1.7 ppm per mg/kg/day, less than that for total, oxidative, or liver

oxidative metabolism. This is because the majority of metabolism in first pass through the liver is via oxidation, whereas with inhalation exposure, more parent compound reaches the kidney, in which metabolism is via GSH conjugation.

**Table 5-47. Route-to-route extrapolation of site-specific inhalation unit risks to oral slope factors**

	<b>Kidney</b>	<b>NHL</b>	<b>Liver</b>
Inhalation unit risk (risk per ppm)	$5.49 \times 10^{-3}$	$1.10 \times 10^{-2}$	$5.49 \times 10^{-3}$
Primary dose-metric	ABioactDCVCBW34 <sup>a</sup>	TotMetabBW34	AMetLiv1BW34
ppm per mg/kg/d <sup>b</sup>	1.70	1.97	2.82
Oral slope factor (risk per mg/kg/d)	$9.33 \times 10^{-3}$	$2.16 \times 10^{-2}$	$1.55 \times 10^{-2}$
Alternative dose-metric	TotMetabBW34	AUCCBld	TotOxMetabBW34
ppm per mg/kg/d <sup>b</sup>	1.97	0.137	2.04
Oral slope factor (risk per mg/kg/d)	$1.08 \times 10^{-2}$	$1.50 \times 10^{-3}$	$1.12 \times 10^{-2}$

<sup>a</sup>The AMetGSHBW34 dose-metric gives the same route-to-route conversion because there is no route dependence in the pathway between GSH conjugation and DCVC bioactivation.

<sup>b</sup>Average of expected population mean of males and females. Male and female estimates differed by <1% for ABioactDCVCBW34; TotMetabBW34, AMetLiv1BW34, and TotOxMetabBW34, and <15% for AUCCBld. Uncertainty on the population mean route-to-route conversion, expressed as the ratio between the 97.5% quantile the 2.5% quantile, is about 2.6-fold for ABioactDCVCBW34, 1.5-fold for TotMetabBW34, AMetLiv1BW34, and TotOxMetabBW34, and about 3.4-fold for AUCCBld.

When one sums the oral slope factor estimates based on the primary (preferred) dose-metrics for the three individual cancer types shown in Table 5-47, the resulting total cancer oral slope factor estimate is  **$4.64 \times 10^{-2}$  per mg/kg/day**. In the case of the oral route-extrapolated results, the ratio of the risk estimate for the three cancer types combined to the risk estimate for kidney cancer alone is 5.0. This value differs from the factor of 4 used for the total cancer inhalation unit risk estimate because of the different dose-metrics used for the different cancer types when the route-to-route extrapolation is performed. If only the kidney cancer and NHL results, for which the evidence is strongest, were combined, the resulting total cancer oral slope factor estimate would be  $3.09 \times 10^{-2}$  per mg/kg/day, and the ratio of this risk estimate to that for kidney cancer alone would be 3.3.

If one were to use some of the risk estimates based on alternative dose-metrics in Table 5-40, the total cancer risk estimate would vary depending on for which tumor type(s) an alternative metric was used. The most extreme difference would occur when the alternative metric is used for NHL and liver tumors; in that case, the resulting total cancer oral slope factor estimate would be  $2.20 \times 10^{-2}$  per mg/kg/day, and the ratio of this risk estimate to that for kidney cancer alone (based on the primary dose-metric of ABioactDCVCBW34) would be 2.4.

The uncertainties in these conversions are relatively modest. As discussed in the note to Table 5-47, the 95% confidence range for the route-to-route conversions at its greatest spans 3.4-fold. The greatest uncertainty is in the selection of the dose-metric for NHL, since the use of the alternative dose-metric of AUCCBI<sub>d</sub> yields a converted oral slope factor that is 14-fold lower than that using the primary dose-metric of TotMetabBW<sub>34</sub>. However, for the other two tumor sites, the range of conversions is tighter, and lies within threefold of the conversion based solely on intake.

### 5.2.3. Summary of Unit Risk Estimates

#### 5.2.3.1. Inhalation Unit Risk Estimate

The inhalation unit risk for TCE is defined as a plausible upper bound lifetime extra risk of cancer from chronic inhalation of TCE per unit of air concentration. The preferred estimate of the inhalation unit risk for TCE is  $2.20 \times 10^{-2}$  per ppm ( **$2 \times 10^{-2}$  per ppm [ $4 \times 10^{-6}$  per  $\mu\text{g}/\text{m}^3$ ]** rounded to one significant figure), based on human kidney cancer risks reported by Charbotel et al. (2006) and adjusted for potential risk for NHL and liver cancer. This estimate is based on good-quality human data, thus avoiding the uncertainties inherent in interspecies extrapolation.

This value is supported by inhalation unit risk estimates from multiple rodent bioassays, the most sensitive of which range from  **$1 \times 10^{-2}$  to  $2 \times 10^{-1}$  per ppm [ $2 \times 10^{-6}$  to  $3 \times 10^{-5}$  per  $\mu\text{g}/\text{m}^3$ ]**. From the inhalation bioassays selected for analysis in Section 5.2.1.1, and using the preferred PBPK model-based dose-metrics, the inhalation unit risk estimate for the most sensitive sex/species is  $8 \times 10^{-2}$  per ppm [ $2 \times 10^{-5}$  per  $\mu\text{g}/\text{m}^3$ ], based on kidney adenomas and carcinomas reported by Maltoni et al. (1986) for male Sprague-Dawley rats. Leukemias and Leydig cell tumors were also increased in these rats, and, although a combined analysis for these cancer types that incorporated the different site-specific preferred dose-metrics was not performed, the result of such an analysis is expected to be similar, about  $9 \times 10^{-2}$  per ppm [ $2 \times 10^{-5}$  per  $\mu\text{g}/\text{m}^3$ ]. The next most sensitive sex/species from the inhalation bioassays is the female mouse, for which lymphomas were reported by Henschler et al. (1980); these data yield a unit risk estimate of  $1.0 \times 10^{-2}$  per ppm [ $2 \times 10^{-6}$  per  $\mu\text{g}/\text{m}^3$ ]. In addition, the 90% CIs reported in Table 5-41 for male rat kidney tumors from Maltoni et al. (1986) and female mouse lymphomas from Henschler et al. (1980), derived from the quantitative analysis of PBPK model uncertainty, both included the estimate based on human data of  $2 \times 10^{-2}$  per ppm. Furthermore, PBPK model-based route-to-route extrapolation of the results for the most sensitive sex/species from the oral bioassays, kidney tumors in male Osborne-Mendel rats and testicular tumors in Marshall rats (NTP, 1988), leads to inhalation unit risk estimates of  $2 \times 10^{-1}$  per ppm [ $3 \times 10^{-5}$  per  $\mu\text{g}/\text{m}^3$ ] and  $4 \times 10^{-2}$  per ppm [ $8 \times 10^{-6}$  per  $\mu\text{g}/\text{m}^3$ ], respectively, with the preferred estimate based on human data falling within the route-to-route extrapolation of the 90%

CI reported in Table 5-42.<sup>58</sup> Finally, for all of these estimates, the ratios of BMDs to the BMDLs did not exceed a value of 3, indicating that the uncertainties in the dose-response modeling for determining the POD in the observable range are small.

Although there are uncertainties in these various estimates, as discussed in Sections 5.2.1.4, 5.2.2.1.3, and 5.2.2.2, confidence in the proposed inhalation unit risk estimate of  $2 \times 10^{-2}$  per ppm [ $4 \times 10^{-6}$  per  $\mu\text{g}/\text{m}^3$ ], based on human kidney cancer risks reported by Charbotel et al. (2006) and adjusted for potential risk for NHL and liver cancer (as discussed in Section 5.2.2.2), is further increased by the similarity of this estimate to estimates based on multiple rodent data sets.

### 5.2.3.2. Oral Slope Factor Estimate

The oral slope factor for TCE is defined as a plausible upper bound lifetime extra risk of cancer from chronic ingestion of TCE per mg/kg/day oral dose. The preferred estimate of the oral slope factor is  $4.64 \times 10^{-2}$  per mg/kg/day ( **$5 \times 10^{-2}$  per mg/kg/day** rounded to one significant figure), resulting from PBPK model-based route-to-route extrapolation of the inhalation unit risk estimate based on the human kidney cancer risks reported in Charbotel et al. (2006) and adjusted for potential risk for NHL and liver cancer. This estimate is based on good-quality human data, thus avoiding uncertainties inherent in interspecies extrapolation. In addition, uncertainty in the PBPK model-based route-to-route extrapolation is relatively low (Chiu, 2006; Chiu and White, 2006). In this particular case, extrapolation using different dose-metrics yielded expected population mean risks within about a twofold range, and, for any particular dose-metric, the 95% CI for the extrapolated population mean risks for each site spanned a range of no more than about threefold.

This value is supported by oral slope factor estimates from multiple rodent bioassays, the most sensitive of which range from  **$3 \times 10^{-2}$  to  $3 \times 10^{-1}$  per mg/kg/day**. From the oral bioassays selected for analysis in Section 5.2.1.1, and using the preferred PBPK model-based dose-metrics, the oral slope factor estimate for the most sensitive sex/species is  $3 \times 10^{-1}$  per mg/kg/day, based on kidney tumors in male Osborne-Mendel rats (NTP, 1988). The oral slope factor estimate for testicular tumors in male Marshall rats (NTP, 1988) is somewhat lower at  $7 \times 10^{-2}$  per mg/kg/day. The next most sensitive sex/species result from the oral studies is for male mouse liver tumors (NCI, 1976), with an oral slope factor estimate of  $3 \times 10^{-2}$  per mg/kg/day. In addition, the 90% CIs reported in Table 5-42 for male Osborne-Mendel rat kidney tumors (NTP,

---

<sup>58</sup>For oral-to-inhalation extrapolation of NTP (1988) male rat kidney tumors, the unit risk estimate of  $2.5 \times 10^{-1}$  per mg/kg/day using the ABioactDCVCBW34 dose metric, from Table 5-37, is divided by the average male and female internal doses at 0.001 mg/kg/day, (0.00504/0.001), and then multiplied by the average male and female internal doses at 0.001 ppm (0.00324/0.001), both from Table 5-35, to yield a unit risk of  $1.6 \times 10^{-1}$  [ $3.0 \times 10^{-5}$  per  $\mu\text{g}/\text{m}^3$ ]. For oral-to-inhalation extrapolation of NTP (1988) male rat testicular tumors, the unit risk estimate of  $7.1 \times 10^{-2}$  per mg/kg/day using the TotMetabBW34 dose metric, from Table 5-37, is divided by the male internal dose at 0.001 mg/kg/day, (0.0192/0.001), and then multiplied by the male internal doses at 0.001 ppm (0.0118/0.001), both from Table 5-35, to yield a unit risk of  $4.4 \times 10^{-2}$  [ $8.1 \times 10^{-6}$  per  $\mu\text{g}/\text{m}^3$ ].

[1988](#)), male F344 rat kidney tumors ([NTP, 1990](#)), and male Marshall rat testicular tumors ([NTP, 1988](#)), derived from the quantitative analysis of PBPK model uncertainty, all included the estimate based on human data of  $5 \times 10^{-2}$  per mg/kg/day, while the upper 95% confidence bound for male mouse liver tumors from NCI ([1976](#)) was slightly below this value at  $4 \times 10^{-2}$  per mg/kg/day. Furthermore, PBPK model-based route-to-route extrapolation of the most sensitive endpoint from the inhalation bioassays, male rat kidney tumors from Maltoni et al. ([1986](#)), leads to an oral slope factor estimate of  $1 \times 10^{-1}$  per mg/kg/day, with the preferred estimate based on human data falling within the route-to-route extrapolation of the 90% CI reported in Table 5-41.<sup>59</sup> Finally, for all of these estimates, the ratios of BMDs to the BMDLs did not exceed a value of 3, indicating that the uncertainties in the dose-response modeling for determining the POD in the observable range are small.

Although there are uncertainties in these various estimates, as discussed in Sections 5.2.1.4, 5.2.2.1.3, 5.2.2.2, and 5.2.2.3, confidence in the proposed oral slope factor estimate of  $5 \times 10^{-2}$  per mg/kg/day, resulting from PBPK model-based route-to-route extrapolation of the inhalation unit risk estimate based on the human kidney cancer risks reported in Charbotel et al. ([2006](#)) and adjusted for potential risk for NHL and liver cancer (as discussed in Section 5.2.2.2), is further increased by the similarity of this estimate to estimates based on multiple rodent data sets.

### **5.2.3.3. Application of ADAFs**

When there is sufficient weight of evidence to conclude that a carcinogen operates through a mutagenic mode of action, and in the absence of chemical-specific data on age-specific susceptibility, EPA's *Supplemental Guidance for Assessing Susceptibility from Early-Life Exposure to Carcinogens* ([U.S. EPA, 2005e](#)) advises that increased early-life susceptibility be assumed and recommends that default ADAFs be applied to adjust for this potential increased susceptibility from early-life exposure. As discussed in Section 4.4, there is sufficient evidence to conclude that a mutagenic mode of action is operative for TCE-induced kidney tumors. The weight of evidence also supports involvement of processes of cytotoxicity and regenerative proliferation in the carcinogenicity of TCE, although not with the extent of support as for a mutagenic mode of action. In particular, data linking TCE-induced proliferation to increased mutation or clonal expansion are lacking, as are data informing the quantitative contribution of cytotoxicity. Because any possible involvement of a cytotoxicity mode of action would be additional to mutagenicity, the mutagenic mode of action would be expected to dominate at low doses. Therefore, the additional involvement of a cytotoxicity mode of action does not provide evidence against the application of ADAFs. In addition, as described in Section 4.10, TCE-

---

<sup>59</sup>For the Maltoni et al. ([1986](#)) male rat kidney tumors, the unit risk estimate of  $8.3 \times 10^{-2}$  per ppm using the ABioactDCVCBW34 dose metric, from Table 5-36, is divided by the average male and female internal doses at 0.001 ppm (0.00324/0.001) and then multiplied by the average male and female internal doses at 0.001 mg/kg/day, (0.00504/0.001), both from Table 5-35, to yield a unit risk of  $1.3 \times 10^{-1}$  per mg/kg/day.

specific data are inadequate for quantification of early-life susceptibility to TCE carcinogenicity. Therefore, as recommended in the *Supplemental Guidance*, the default ADAFs are applied.

See the *Supplemental Guidance* for detailed information on the general application of these adjustment factors. In brief, the *Supplemental Guidance* establishes ADAFs for three specific age groups. The current ADAFs and their age groupings are 10 for <2 years, 3 for 2–<16 years, and 1 for  $\geq 16$  years ([U.S. EPA, 2005e](#)). For risk assessments based on specific exposure assessments, the 10- and 3-fold adjustments to the slope factor or unit risk estimates are to be combined with age-specific exposure estimates when estimating cancer risks from early-life (<16-years-of-age) exposure. Currently, due to lack of appropriate data, no ADAFs are used for other lifestages, such as the elderly. However, the ADAFs and their age groups may be revised over time. The most current information on the application of ADAFs for cancer risk assessment can be found at [www.epa.gov/cancerguidelines](http://www.epa.gov/cancerguidelines).

In the case of TCE, the inhalation unit risk and oral slope factor estimates reflect lifetime risk for cancer at multiple sites, and a mutagenic mode of action has been established for one of these sites, the kidney. The following subsections illustrate how one might apply the default ADAFs to the *kidney-cancer component* of the inhalation unit risk and oral slope factor estimates for TCE. These are **sample calculations**, and individual risk assessors should use exposure-related parameters (e.g., age-specific water ingestion rates) that are appropriate for their particular risk assessment applications.

In addition to the uncertainties discussed above for the inhalation and oral total cancer unit risk or slope factor estimates, there are uncertainties in the application of ADAFs to adjust for potential increased early-life susceptibility. For one thing, the adjustment is made only for the kidney cancer component of total cancer risk because that is the tumor type for which the weight of evidence was sufficient to conclude that TCE-induced carcinogenesis operates through a mutagenic mode of action. However, it may be that TCE operates through a mutagenic mode of action for other cancer types as well or that it operates through other modes of action that might also convey increased early-life susceptibility. Additionally, the ADAFs are general default factors, and it is uncertain to what extent they reflect increased early-life susceptibility for exposure to TCE, if increased early-life susceptibility occurs.

Furthermore, the assumption of increased early-life susceptibility, invoked by the finding of a mutagenic mode of action for kidney cancer, is in contradiction to the assumption that RR is independent of age that was used to derive the unit risk estimates in the life-table analysis. In some other assessments faced with a similar situation, a small modification has been made to the derivation of the unit risk estimate to avoid the contradictory assumptions (by calculating an adult-exposure-only unit risk estimate for the application of ADAFs). This has the effect of slightly reducing the unit risk estimate to which the ADAFs are applied. Because there are multiple cancer types for TCE but the finding of a mutagenic mode of action applies to only one of them, and because under these circumstances application of the ADAFs already has a minimal

impact on the total risk for most exposure scenarios, as discussed with respect to the examples in Sections 5.2.3.3.1 and 5.2.3.3.2 below, no attempt was made to modify the kidney cancer unit risk estimate for this assessment. Such a modification would have substantially increased the complexity of the calculations, which are already more elaborate than the standard ADAF applications, without having much quantitative impact on the final risk estimates.

#### **5.2.3.3.1. Example application of ADAFs for inhalation exposures.**

A calculation template for application of the ADAFs is provided in Table 5-48, with an Excel spreadsheet version available on the HERO database ([U.S. EPA, 2011e](#)). In the example provided, it is assumed that an individual is exposed to  $1 \mu\text{g}/\text{m}^3$  in air from birth through age 70 years. Using the template, risk estimates for different exposure scenarios can be obtained by changing the exposure concentrations (including possibly zero for some age groups). The steps in the calculation are as follows:

- (1) Separate the kidney cancer contribution from the NHL + liver cancer contribution to the inhalation unit risk estimate. From Section 5.2.2.1.4, the kidney lifetime unit risk is  $1.0 \times 10^{-6}$  per  $\mu\text{g}/\text{m}^3$  in air. Subtracting this from the total lifetime unit risk of  $4.1 \times 10^{-6}$  per  $\mu\text{g}/\text{m}^3$  from Section 5.2.2.2 results in the estimated contribution of NHL + liver cancer being  $3.1 \times 10^{-6}$  per  $\mu\text{g}/\text{m}^3$ .
- (2) Assign a lifetime unit risk estimate for each age group. The template shows the recommended age groupings from U.S. EPA (2005c) in Column A (augmented by additional age groups from U.S. EPA, 2008c, and for assessing 30 year exposures), along with the age group duration (Column D), and the fraction of lifetime each age group represents (Column E; used as a duration adjustment). For each age group, the (unadjusted) lifetime unit risk estimates for kidney cancer, total cancer, and NHL + liver cancer are shown in Column F, I, and J, respectively.
- (3) For each age group, the kidney cancer inhalation unit risk estimate (Column F) is multiplied by the risk per  $\mu\text{g}/\text{m}^3$  equivalence (Column B), the exposure concentration (Column C), the duration adjustment (Column E), and the ADAF (Column G), to obtain the partial risk from exposure during those ages (Column H). For inhalation exposures, a “risk per  $\mu\text{g}/\text{m}^3$  equivalence” of 1 is assumed across age groups (i.e., equivalent risk from equivalent exposure levels in air, independent of body size), as shown in Column B. In this calculation, a unit lifetime exposure of  $1 \mu\text{g}/\text{m}^3$  is assumed, as shown in Column C.
- (4) For each age group, the NHL + liver cancer unit risk estimate (Column J) is multiplied by the risk per  $\mu\text{g}/\text{m}^3$  equivalence (Column B), the exposure concentration (Column C), and the duration adjustment (Column E), to obtain the partial risk from exposure during those ages (Column K).
- (5) For each age group, the ADAF-adjusted partial risk for kidney cancer (Column H) is added to the partial risk for NHL + liver cancer (Column K), resulting in the total partial risk (Column L).

(6) The age-group-specific partial risks are added together to obtain the estimated total lifetime risk (bottom of Column L).

**Table 5-48. Sample calculation for total lifetime cancer risk based on the kidney unit risk estimate, potential risk for NHL and liver cancer, and potential increased early-life susceptibility, assuming a constant lifetime exposure to 1 µg/m<sup>3</sup> of TCE in air**

Column A	Column B	Column C	Column D	Column E	Column F	Column G	Column H	Column I	Column J	Column K	Column L	
	Exposure scenario parameters				Dose-response assessment calculations							
Units:		(µg/m <sup>3</sup> )	yr	-	(µg/m <sup>3</sup> ) <sup>-1</sup>	-		(µg/m <sup>3</sup> ) <sup>-1</sup>	(µg/m <sup>3</sup> ) <sup>-1</sup>			
Age group	Risk per µg/m <sup>3</sup> air equivalence	Exposure concentration	Age group duration	Duration adjustment (Column D/70 yr)	Kidney cancer unadjusted lifetime unit risk (see Section 5.2.2.1.4)	Default ADAF	<b>Kidney cancer ADAF-adjusted partial risk (Column B × Column C × Column E × Column F × Column G)</b>	Kidney cancer+NHL+ liver cancer unadjusted lifetime unit risk (see Section 5.2.2.2)	NHL+ liver cancer lifetime unit risk (Column I – Column F)	<b>NHL and liver cancer partial risk (Column B × Column C × Column E × Column J)</b>	<b>Total partial risk (Column H + Column K)</b>	
Birth to <1 mo	1	1.000	0.083	0.0012	1 × 10 <sup>-6</sup>	10	<b>1.2 × 10<sup>-8</sup></b>	4.1 × 10 <sup>-6</sup>	3.1 × 10 <sup>-6</sup>	<b>3.7 × 10<sup>-9</sup></b>	<b>1.6 × 10<sup>-8</sup></b>	
1–<3 mo	1	1.000	0.167	0.0024	1 × 10 <sup>-6</sup>	10	<b>2.4 × 10<sup>-8</sup></b>	4.1 × 10 <sup>-6</sup>	3.1 × 10 <sup>-6</sup>	<b>7.4 × 10<sup>-9</sup></b>	<b>3.1 × 10<sup>-8</sup></b>	
3–<6 mo	1	1.000	0.250	0.0036	1 × 10 <sup>-6</sup>	10	<b>3.6 × 10<sup>-8</sup></b>	4.1 × 10 <sup>-6</sup>	3.1 × 10 <sup>-6</sup>	<b>1.1 × 10<sup>-8</sup></b>	<b>4.7 × 10<sup>-8</sup></b>	
6–<12 mo	1	1.000	0.500	0.0071	1 × 10 <sup>-6</sup>	10	<b>7.1 × 10<sup>-8</sup></b>	4.1 × 10 <sup>-6</sup>	3.1 × 10 <sup>-6</sup>	<b>2.2 × 10<sup>-8</sup></b>	<b>9.4 × 10<sup>-8</sup></b>	
1–<2 yrs	1	1.000	1.000	0.0143	1 × 10 <sup>-6</sup>	10	<b>1.4 × 10<sup>-7</sup></b>	4.1 × 10 <sup>-6</sup>	3.1 × 10 <sup>-6</sup>	<b>4.4 × 10<sup>-8</sup></b>	<b>1.9 × 10<sup>-7</sup></b>	
2–<3 yrs	1	1.000	1.000	0.0143	1 × 10 <sup>-6</sup>	3	<b>4.3 × 10<sup>-8</sup></b>	4.1 × 10 <sup>-6</sup>	3.1 × 10 <sup>-6</sup>	<b>4.4 × 10<sup>-8</sup></b>	<b>8.7 × 10<sup>-8</sup></b>	
3–<6 yrs	1	1.000	3.000	0.0429	1 × 10 <sup>-6</sup>	3	<b>1.3 × 10<sup>-7</sup></b>	4.1 × 10 <sup>-6</sup>	3.1 × 10 <sup>-6</sup>	<b>1.3 × 10<sup>-7</sup></b>	<b>2.6 × 10<sup>-7</sup></b>	
6–<11 yrs	1	1.000	5.000	0.0714	1 × 10 <sup>-6</sup>	3	<b>2.1 × 10<sup>-7</sup></b>	4.1 × 10 <sup>-6</sup>	3.1 × 10 <sup>-6</sup>	<b>2.2 × 10<sup>-7</sup></b>	<b>4.4 × 10<sup>-7</sup></b>	
11–<16 yrs	1	1.000	5.000	0.0714	1 × 10 <sup>-6</sup>	3	<b>2.1 × 10<sup>-7</sup></b>	4.1 × 10 <sup>-6</sup>	3.1 × 10 <sup>-6</sup>	<b>2.2 × 10<sup>-7</sup></b>	<b>4.4 × 10<sup>-7</sup></b>	
16–<18 yrs	1	1.000	2.000	0.0286	1 × 10 <sup>-6</sup>	1	<b>2.9 × 10<sup>-8</sup></b>	4.1 × 10 <sup>-6</sup>	3.1 × 10 <sup>-6</sup>	<b>8.9 × 10<sup>-8</sup></b>	<b>1.2 × 10<sup>-7</sup></b>	
18–<21	1	1.000	3.000	0.0429	1 × 10 <sup>-6</sup>	1	<b>4.3 × 10<sup>-8</sup></b>	4.1 × 10 <sup>-6</sup>	3.1 × 10 <sup>-6</sup>	<b>1.3 × 10<sup>-7</sup></b>	<b>1.8 × 10<sup>-7</sup></b>	
21–<30	1	1.000	9.000	0.1286	1 × 10 <sup>-6</sup>	1	<b>1.3 × 10<sup>-7</sup></b>	4.1 × 10 <sup>-6</sup>	3.1 × 10 <sup>-6</sup>	<b>4.0 × 10<sup>-7</sup></b>	<b>5.3 × 10<sup>-7</sup></b>	
30–70 yrs	1	1.000	40.000	0.5714	1 × 10 <sup>-6</sup>	1	<b>5.7 × 10<sup>-7</sup></b>	4.1 × 10 <sup>-6</sup>	3.1 × 10 <sup>-6</sup>	<b>1.8 × 10<sup>-6</sup></b>	<b>2.3 × 10<sup>-6</sup></b>	
										<b>Total unit risk</b>	<b>4.8 × 10<sup>-6</sup></b>	

From the example calculation, based on continuous exposure to  $1 \mu\text{g}/\text{m}^3$  from birth to age 70, the estimated total lifetime risk is  $4.8 \times 10^{-6}$ , which corresponds to a lifetime unit risk estimate of  $4.8 \times 10^{-6}$  per  $\mu\text{g}/\text{m}^3$ . The risk-specific air concentrations at risk levels of  $10^{-6}$ ,  $10^{-5}$ , and  $10^{-4}$  are 0.21, 2.1, and  $21 \mu\text{g}/\text{m}^3$ , respectively.

This total cancer unit risk estimate of  $4.8 \times 10^{-6}$  per  $\mu\text{g}/\text{m}^3$  ( $2.6 \times 10^{-2}$  per ppm), adjusted for potential increased early-life susceptibility, is only minimally (17.5%) increased over the unadjusted total cancer unit risk estimate because the kidney cancer risk estimate that gets adjusted for potential increased early-life susceptibility is only part of the total cancer risk estimate. Thus, foregoing the ADAF adjustment in the case of full lifetime calculations will not seriously impact the resulting risk estimate. For less-than-lifetime exposure calculations, the impact of applying the ADAFs will increase as the proportion of time at older ages decreases. The maximum impact will be when exposure is for only the first 2 years of life, in which case, the partial lifetime total cancer risk estimate for exposure to  $1 \mu\text{g}/\text{m}^3$  adjusted for potential increased early-life susceptibility is  $10 \times (1 \mu\text{g}/\text{m}^3) \times (1.0 \times 10^{-6} \text{ per } \mu\text{g}/\text{m}^3) \times (2 / 70)$  for the kidney cancer risk +  $(1 \mu\text{g}/\text{m}^3) \times (3.1 \times 10^{-6} \text{ per } \mu\text{g}/\text{m}^3) \times (2 / 70)$  for the NHL and liver cancer, or  $3.7 \times 10^{-7}$ , which is over 3 times greater than the unadjusted partial lifetime total cancer risk estimate for exposure to  $1 \mu\text{g}/\text{m}^3$  of  $(1 \mu\text{g}/\text{m}^3) \times (4.1 \times 10^{-6} \text{ per } \mu\text{g}/\text{m}^3) \times (2 / 70)$ , or  $1.2 \times 10^{-7}$ .

#### **5.2.3.3.2. Example application of ADAFs for oral drinking water exposures**

For oral exposures, the calculation of risk estimates adjusted for potential increased early-life susceptibility is complicated by the fact that for a constant exposure level (e.g., a constant concentration of TCE in drinking water) doses will vary by age because of different age-specific uptake rates (e.g., drinking water consumption rates). Different EPA Program or Regional Offices may have different default age-specific uptake rates that they use for risk assessments for specific exposure scenarios, and the calculations presented below are merely to illustrate the general approach to applying ADAFs for oral TCE exposures, using exposure to  $1 \mu\text{g}/\text{L}$  of TCE in drinking water from birth through age 70 years as an example. Using the template, risk estimates for different exposure scenarios can be obtained by changing the intake rates and exposure concentrations (including possibly zero for some age groups). The steps in the calculation, illustrated in the template in Table 5-49 (available as an Excel spreadsheet version on the HERO database, [U.S. EPA, 2011e](#)), are as follows:

- (1) Separate the kidney cancer contribution from the NHL + liver cancer contribution to the oral slope factor estimate. From Section 5.2.2.3, the kidney lifetime oral slope factor is  $9.3 \times 10^{-3}$  per mg/kg/day. Subtracting this from the total lifetime oral slope factor of  $4.6 \times 10^{-2}$  per mg/kg/day from Section 5.2.2.3 results in an estimated contribution from NHL + liver cancer of  $3.7 \times 10^{-2}$  per mg/kg/day.

- (2) Assign a lifetime oral slope factor estimate for each age group. The template shows the recommended age groupings from U.S. EPA (2005c) in Column A (augmented by additional age groups from U.S. EPA, 2008c, and for assessing 30 year exposures), along with the age group duration (Column D), and the fraction of lifetime each age group represents (Column E; used as a duration adjustment). For each age group, the (unadjusted) lifetime oral slope factor estimates for kidney cancer, total cancer, and NHL + liver cancer are shown in Columns F, I, and J, respectively.
- (3) For each age group, the kidney cancer oral slope factor estimate (Column F) is multiplied by the drinking water ingestion rate (Column B), the exposure concentration (Column C), the duration adjustment (Column E), and the ADAF (Column G), to obtain the partial risk from exposure during those ages (Column H). Age-specific water ingestion rates in L/kg/day, taken from the EPA Office of Water Policy Document *Age Dependent Adjustment Factor (ADAF) Application* are shown in Column B.<sup>60</sup> In this calculation, a lifetime unit exposure of 1 µg/L is assumed, as shown in Column C.
- (4) For each age group, the NHL + liver cancer oral slope factor estimate (Column J) is multiplied by the drinking water ingestion rate (Column B), the exposure concentration (Column C), and the duration adjustment (Column E), to obtain the partial risk from exposure during those ages (Column K).
- (5) For each age group, the ADAF-adjusted partial risk for kidney cancer (Column H) is added to the partial risk for NHL + liver cancer (Column K), resulting in the total partial risk (Column L).
- (6) The age-group-specific partial risks are added together to obtain the estimated total lifetime risk (bottom of Column L).

---

<sup>60</sup>Values for the 90<sup>th</sup> percentile were taken from Table 3-19 of U.S. EPA (2008a) (consumers-only estimates of combined direct and indirect water ingestion from community water) and U.S. EPA (2004) (Table A1). The 90<sup>th</sup> percentile was based on the policy in the U.S. EPA Office of Water for determining risk through direct and indirect consumption of drinking water (U.S. EPA, 2011f). Community water was used in the illustration because U.S. EPA only regulates community water sources and not private wells and cisterns or bottled water. Data for “consumers only” (i.e., excluding individuals who did not ingest community water) were used because formula-fed infants (as opposed to breast-fed infants, who consume very little community water), children, and young adolescents are often the population of concern with respect to water consumption.

**Table 5-49. Sample calculation for total lifetime cancer risk based on the kidney cancer slope factor estimate, potential risk for NHL and liver cancer, and potential increased early-life susceptibility, assuming a constant lifetime exposure to 1 µg/L of TCE in drinking water**

Column A	Column B	Column C	Column D	Column E	Column F	Column G	Column H	Column I	Column J	Column K	Column L	
	Exposure scenario parameters				Dose-response assessment calculations							
<b>Units:</b>	L water/kg/d	mg/L water	yr	-	(mg/kg/d) <sup>-1</sup>	-	-	(mg/kg/d) <sup>-1</sup>	(mg/kg/d) <sup>-1</sup>	-	-	
<b>Age group</b>	Ingestion rate	Exposure concentration	Age group duration	Duration adjustment (Column D/ 70 yr)	Kidney cancer unadjusted lifetime slope factor (see Table 5-40)	Default ADAF	<b>Kidney cancer ADAF adjusted partial risk (Column B × Column C × Column E × Column F × Column G)</b>	Kidney cancer+NHL+ liver cancer unadjusted lifetime unit risk (see Section 5.2.2.3)	NHL+ liver cancer lifetime unit risk (Column I – Column F)	<b>NHL and liver cancer partial risk (Column B × Column C × Column E × Column J)</b>	<b>Total partial risk (Column H + Column K)</b>	
<b>Birth to &lt;1 mo</b>	0.235	0.001	0.083	0.0012	$9.3 \times 10^{-3}$	10	$2.6 \times 10^{-8}$	$4.6 \times 10^{-2}$	$3.7 \times 10^{-2}$	$1.0 \times 10^{-8}$	$3.6 \times 10^{-8}$	
<b>1–&lt;3 mo</b>	0.228	0.001	0.167	0.0024	$9.3 \times 10^{-3}$	10	$5.0 \times 10^{-8}$	$4.6 \times 10^{-2}$	$3.7 \times 10^{-2}$	$2.0 \times 10^{-8}$	$7.0 \times 10^{-8}$	
<b>3–&lt;6 mo</b>	0.148	0.001	0.250	0.0036	$9.3 \times 10^{-3}$	10	$4.9 \times 10^{-8}$	$4.6 \times 10^{-2}$	$3.7 \times 10^{-2}$	$1.9 \times 10^{-8}$	$6.9 \times 10^{-8}$	
<b>6–&lt;12 mo</b>	0.112	0.001	0.500	0.0071	$9.3 \times 10^{-3}$	10	$7.4 \times 10^{-8}$	$4.6 \times 10^{-2}$	$3.7 \times 10^{-2}$	$2.9 \times 10^{-8}$	$1.0 \times 10^{-7}$	
<b>1–&lt;2 yrs</b>	0.056	0.001	1.000	0.0143	$9.3 \times 10^{-3}$	10	$7.4 \times 10^{-8}$	$4.6 \times 10^{-2}$	$3.7 \times 10^{-2}$	$2.9 \times 10^{-8}$	$1.0 \times 10^{-7}$	
<b>2–&lt;3 yrs</b>	0.052	0.001	1.000	0.0143	$9.3 \times 10^{-3}$	3	$2.1 \times 10^{-8}$	$4.6 \times 10^{-2}$	$3.7 \times 10^{-2}$	$2.7 \times 10^{-8}$	$4.8 \times 10^{-8}$	
<b>3–&lt;6 yrs</b>	0.049	0.001	3.000	0.0429	$9.3 \times 10^{-3}$	3	$5.9 \times 10^{-8}$	$4.6 \times 10^{-2}$	$3.7 \times 10^{-2}$	$7.7 \times 10^{-8}$	$1.4 \times 10^{-7}$	
<b>6–&lt;11 yrs</b>	0.035	0.001	5.000	0.0714	$9.3 \times 10^{-3}$	3	$7.0 \times 10^{-8}$	$4.6 \times 10^{-2}$	$3.7 \times 10^{-2}$	$9.2 \times 10^{-8}$	$1.6 \times 10^{-7}$	
<b>11–&lt;16 yrs</b>	0.026	0.001	5.000	0.0714	$9.3 \times 10^{-3}$	3	$5.2 \times 10^{-8}$	$4.6 \times 10^{-2}$	$3.7 \times 10^{-2}$	$6.8 \times 10^{-8}$	$1.2 \times 10^{-7}$	
<b>16–&lt;18 yrs</b>	0.024	0.001	2.000	0.0286	$9.3 \times 10^{-3}$	1	$6.4 \times 10^{-9}$	$4.6 \times 10^{-2}$	$3.7 \times 10^{-2}$	$2.8 \times 10^{-8}$	$3.2 \times 10^{-8}$	
<b>18–&lt;21 yrs</b>	0.029	0.001	3.000	0.0429	$9.3 \times 10^{-3}$	1	$1.2 \times 10^{-8}$	$4.6 \times 10^{-2}$	$3.7 \times 10^{-2}$	$4.6 \times 10^{-8}$	$5.7 \times 10^{-8}$	
<b>21–&lt;30 yrs</b>	0.032	0.001	9.000	0.1286	$9.3 \times 10^{-3}$	1	$3.8 \times 10^{-8}$	$4.6 \times 10^{-2}$	$3.7 \times 10^{-2}$	$1.5 \times 10^{-7}$	$1.9 \times 10^{-7}$	
<b>30–70 yrs</b>	0.032	0.001	40.000	0.5714	$9.3 \times 10^{-3}$	1	$1.7 \times 10^{-7}$	$4.6 \times 10^{-2}$	$3.7 \times 10^{-2}$	$6.7 \times 10^{-7}$	$8.4 \times 10^{-7}$	
										<b>Total unit risk:</b>	$2.0 \times 10^{-6}$	

Because the TCE intake is not constant across age groups, one does not calculate a lifetime unit risk estimate in terms of risk per mg/kg/day adjusted for potential increased early-life susceptibility. One could calculate a unit risk estimate for TCE in drinking water in terms of  $\mu\text{g/L}$  from the result in Table 5-49, but this is dependent on the water ingestion rates used. Based on the example calculation assuming continuous exposure to  $1 \mu\text{g/L}$  of TCE in drinking water from birth to age 70 years and using the drinking water intake rates shown, estimated total lifetime risk is  $2.0 \times 10^{-6}$ , which corresponds to a lifetime drinking water unit risk estimate of  $2.0 \times 10^{-6}$  per  $\mu\text{g/L}$ . The corresponding risk-specific drinking water concentrations at risk levels of  $10^{-6}$ ,  $10^{-5}$ , and  $10^{-4}$  are 0.51, 5.1, and 51  $\mu\text{g/L}$ , respectively. For different exposure and intake parameters, the risk-specific drinking water concentrations would need to be recalculated.

As with the adjusted inhalation risk estimate in Section 5.2.3.3.1, the lifetime total cancer risk estimate of  $2.0 \times 10^{-6}$  calculated for lifetime exposure to  $1 \mu\text{g/L}$  of TCE in drinking water adjusted for potential increased early-life susceptibility is only minimally (25%) increased over the unadjusted total cancer unit risk estimate. (This calculation is not shown, but if one omits the ADAFs for each of the age groups in Table 5-49, the resulting total lifetime risk estimate is  $1.6 \times 10^{-6}$ .) Unlike with inhalation exposure under the assumption of ppm equivalence, which is generally assumed to extend across age groups as well as species, the oral intake rates are higher in the potentially more susceptible younger age groups. This would tend to yield a larger relative impact of adjusting for potential increased early-life susceptibility for oral risk estimates compared to inhalation risk estimates. In the case of TCE, however, this impact is partially offset by the lesser proportion of the total oral cancer risk that is accounted for by the kidney cancer risk, which is the component of total risk that is being adjusted for potential increased early-life susceptibility, based on the primary dose-metrics (1/5 vs. 1/4 for inhalation). Thus, as with lifetime inhalation risk, foregoing the ADAF adjustment in the case of full lifetime calculations will not seriously impact the resulting risk estimate. For less-than-lifetime exposure calculations, the impact of applying the ADAFs will increase as the proportion of time at older ages decreases. The maximum impact will be when exposure is for only the first 2 years of life, in which case the partial lifetime total cancer risk estimate for exposure to  $1 \mu\text{g/L}$  adjusted for potential increased early-life susceptibility is  $3.8 \times 10^{-7}$  (adding partial risks from Table 5-49 for the appropriate ages groups), which is almost 3 times greater than the unadjusted partial lifetime total cancer risk estimate for exposure to  $1 \mu\text{g/L}$  of  $5 \times (0.001 \text{ mg/L}) \times (0.103 \text{ L/kg/day}) \times (9.33 \times 10^{-3} \text{ per mg/kg/day}) \times (2/70)$ , or  $1.4 \times 10^{-7}$ , where 5 is the factor for the multiple cancer types for oral exposure, 0.103 L/kg/day is the time-weighted ingestion rate for the 1<sup>st</sup> two years of life using the rates in Table 5-49,  $9.33 \times 10^{-3}$  per mg/kg/day is the unadjusted oral slope factor estimate for kidney cancer, and 2/70 is the duration adjustment.

### 5.3. KEY RESEARCH NEEDS FOR TCE DOSE-RESPONSE ANALYSES

For noncancer dose-response assessment, key research that would substantially improve the accuracy or utility of TCE noncancer risk estimates includes:

- Research to obtain toxicokinetic data to better quantify the amount of bioactivation of DCVC to toxic moiety(ies) in rats and humans, including data on human variability in DCVC bioactivation.
- Research to obtain mechanistic data that would identify the active moiety(ies) for TCE-induced immunological effects and developmental cardiac defects. As a corollary, data on human variability pharmacokinetics of the active moiety after TCE exposure would also be informative.
- Research to obtain mechanistic data that would quantitatively inform the pharmacodynamic factors that would make individuals more or less susceptible to kidney, immunological, and developmental cardiac defects induced by TCE.
- Research to obtain TCE dose-response data on kidney effects, immunological effects, and developmental cardiac defects at a larger number of doses at and below the current LOAELs, so as to better describe the dose-response shape at low effect levels. Ideally, studies would be based on human epidemiologic data with good quantitative exposure assessment. Studies in laboratory animals would need to address the limitations in the currently available studies. For example, studies of cardiac defects would need to address limitations of the Johnson et al. (2003) study described in Section 4.8.3.3.2.
- Development of a probabilistic approach to noncancer dose-response analysis that would enable calculation of a risk-specific dose for noncancer effects, while capturing uncertainty and variability quantitatively.

For cancer dose-response assessment, key research that would substantially improve the accuracy or utility of TCE cancer risk estimates includes:

- Research to obtain toxicokinetic data to better quantify the amount of bioactivation of DCVC to toxic moiety(ies) in humans, including data on human variability in DCVC bioactivation.
- Research to obtain mechanistic data that would identify the active moiety(ies) for TCE-induced liver tumors and NHL. As a corollary, data on human variability pharmacokinetics of the active moiety after TCE exposure would also be informative.
- Research to obtain mechanistic data that would quantitatively inform the pharmacodynamic factors that would make individuals more or less susceptible to kidney tumors, liver tumors, and NHL induced by TCE. This includes data on life-stage-specific susceptibility that would replace the default ADAFs for kidney tumors and the assumption of no life-stage-specific susceptibility for liver tumors and NHL.

- Research to obtain human epidemiologic dose-response data on TCE-induced kidney tumors, liver tumors, and NHL with good quantitative exposure assessment.
- Research to obtain additional human epidemiologic data on TCE exposure and other tumors, so as to better estimate the total risk of cancer from TCE exposure.
- Development of a probabilistic approach to cancer dose-response analysis that would enable calculation of a differential susceptibility to carcinogenic effects, while capturing uncertainty and variability quantitatively.